the ENERGY lab

Office of Fossil Energy
Advanced Turbine Program

2009 Annual Report

Turbines for Coal Based Power Systems that Capture Carbon

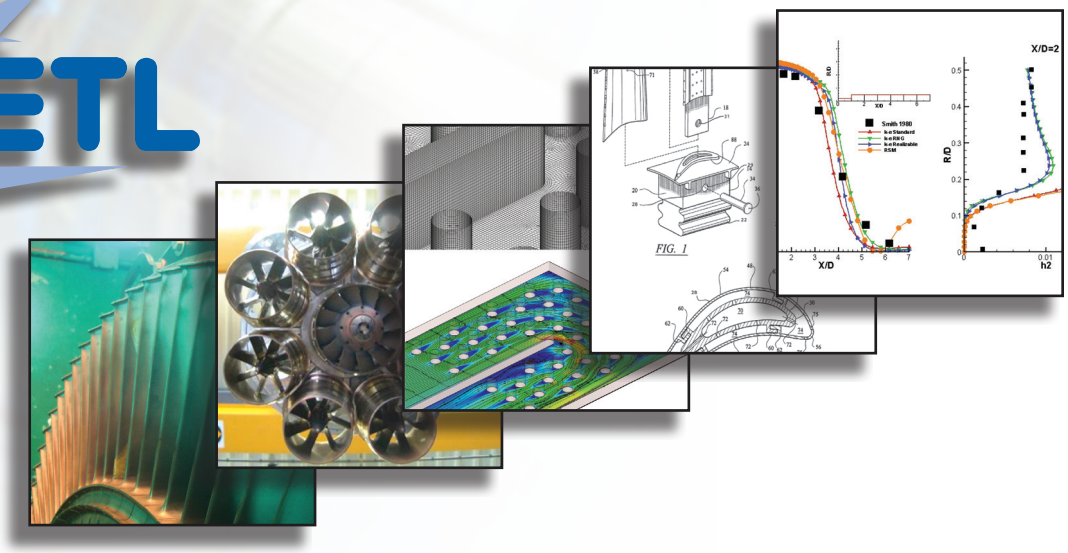

U.S. DEPARTMENT OF ENERGY

DOE/NETL-2009/1378

OFFICE OF FOSSIL ENERGY ADVANCED TURBINE PROGRAM 2009 ANNUAL REPORT

November 2009

Disclaimer

This report was prepared as an account of work sponsored by an agency of the United States Government. Neither the United States Government nor any agency thereof, nor any of their employees, makes any warranty, express or implied, or assumes any legal liability or responsibility for the accuracy, completeness, or usefulness of any information, apparatus, product, or process disclosed, or represents that its use would not infringe privately owned rights. Reference therein to any specific commercial product, process, or service by trade name, trademark, manufacturer, or otherwise does not necessarily constitute or imply its endorsement, recommendation, or favoring by the United States Government or any agency thereof. The views and opinions of authors expressed therein do not necessarily state or reflect those of the United States Government or any agency thereof.

Table of Contents

I. INTRODUCTION . . . 1

II. HYDROGEN TURBINES FOR NEAR-ZERO EMISSION SYSTEMS . . . 13

1 GE Energy: DOE Advanced IGCC/H_2 Gas Turbine Development . . . 15

2 Siemens Energy, Inc.: Advanced Hydrogen Turbine Development . . . 18

3 Gas Technology Institute: Partial Oxidation Gas Turbine for Power and Hydrogen Co-Production from Coal-Derived Fuel in Industrial Applications . . . 21

4 GE Global Research: Fuel-Flexible Combustion System for Co-Production Plant Applications. . . . 30

5 Lawrence Berkeley National Laboratory: Low-Swirl Burners for Hydrogen Gas Turbines in Near-Zero Emissions Clean Coal Power Plants . . . 33

6 National Energy Technology Laboratory: Combustion and Aerothermal Research for Hydrogen Energy Systems . . . 37

7 Parker Hannifin Corporation: Micro-Mixing Lean-Premix System for Ultra-Low Emission Hydrogen/Syngas Combustion . . . 42

8 Precision Combustion, Inc.: Catalytic Combustion for Ultra-Low NOx Hydrogen Turbines . . . 46

III. ADVANCED OXY-FUEL TURBINES . . . 49

1 Siemens Energy, Inc.: Zero Emissions Coal Syngas-Oxygen Turbo Machinery . . . 51

2 Clean Energy Systems, Inc.: Coal-Based Oxy-Fuel System Evaluation and Combustor Development . . . 55

IV. ADVANCED RESEARCH . . . 59

1 Ames Laboratory: Analysis of Gas Turbine Thermal Performance . . . 61

2 Case Western Reserve University: Development of Comprehensive Detailed and Reduced Reaction Mechanisms for Syngas and Hydrogen Combustion . . . 64

3 CFD Research Corporation: Practical Multi-Step Turbulent-Combustion Model for Fuel-Flexible Gas Turbine Combustor Analysis . . . 68

4 Faraday Technology, Inc.: Faradayic ElectroPhoretic Deposition of YSZ for Use in Thermal Barrier Coatings . . . 71

5 Florida Turbine Technologies, Inc.: High Temperature Capability and Innovative Cooling with a Spar and Shell Turbine Blade . . . 75

6 Georgia Institute of Technology: Prediction of Combustion Stability and Flashback in Turbines with High-Hydrogen Fuel . . . 78

7 National Energy Technology Laboratory: Materials and Component Development for Advanced Turbine Systems . . . 82

8 National Energy Technology Laboratory: Materials Performance in Oxy-Fuel Turbine Environments . . . 93

9 National Institute of Standards and Technology: Data for Thermophysical Properties of Humid Gases in Power Cycles . . . 96

10 Princeton University: Reduced and Validated Kinetic Mechanisms for Hydrogen-CO-Air Combustion in Gas Turbines . . . 100

11 Precision Combustion, Inc.: Compact and Streamlined Oxy-Syngas Reheat Combustor . . . 104

V. UNIVERSITY TURBINE SYSTEMS RESEARCH 107

A. AERO-HEAT TRANSFER 107

1 Brigham Young University: Deposition of Alternative (Syngas) Fuels on Turbine Blades with Film Cooling. 109

2 Ohio State University: Designing Turbine Endwalls for Deposition Resistance with 1,400°C Combustor Exit Temperatures and Syngas Water Vapor Levels 113

3 University of Pittsburgh: Effects of Coating Blockage and Deposits on Film Cooling Effectiveness and Heat Transfer 117

4 University of Texas at Austin: Simulating Particle Deposition and Mitigating Deposition Degradation Effects in Film-Cooled Turbine Sections. 123

5 Virginia Polytechnic Institute and State University: Syngas Particulate Deposition and Erosion at the Leading Edge of a Turbine Blade with Film Cooling. 127

B. COMBUSTION 131

1 Georgia Institute of Technology: Turbulent Flame Speed Measurements and Modeling of Syngas Fuels 133

2 Massachusetts Institute of Technology: Fundamental Studies in Syngas Premixed Combustion Dynamics. 136

3 The Pennsylvania State University: Autoignition Studies of Syngas and Hydrogen (SGH) Fuels. 139

4 The Pennsylvania State University: Combustion Dynamics in Multi-Nozzle Combustors Operating on High-Hydrogen Fuels 143

5 University of California, Irvine: Numerical and Experimental Study of Mixing Processes Associated with Hydrogen and High Hydrogen Content Fuels. 146

6 University of Colorado at Boulder: High Pressure Kinetics of Syngas and Nearly Pure Hydrogen Fuels 150

C. MATERIALS 155

1 Ohio State University: Degradation of Thermal Barrier Coatings from Deposits and Its Mitigation 157

2 University of California, Santa Barbara: Evaluating Coatings for Current and Future Service. 160

3 University of Pittsburgh: Materials for Oxy-Fuel Turbomachine Conditions. 165

VI. ACRONYMS AND ABBREVIATIONS 169

VII. PRIMARY CONTACT INDEX 173

VIII. ORGANIZATION INDEX. 175

IX. CONTRACT NUMBER INDEX 177

I. INTRODUCTION

I. Introduction

On behalf of the Office of Fossil Energy (FE), the Advanced Turbine Program is pleased to present the Fiscal Year 2009 Advanced Turbine Program Annual Report. This report summarizes current progress towards developing turbines that help to achieve power production from coal that is clean, efficient, less costly, and minimizes carbon dioxide emissions (CO_2).

Background and Technology Status

Turbines are a proven technology for power generation, which is typified by the shear number of turbines in use today. Turbines find use in a wide range of applications: turbines for propulsion in the aviation industry, steam turbines in pulverized coal combustion boilers, megawatt (MW)-scale turbines for shaft work and electric power, compressors, micro-turbines and gas turbines in simple and combined cycle (CC) applications. Turbine technology is responsible for the vast majority of power production in the U.S. and the world. For the past 25 years, increases in power generation, in terms of added capacity, have been dominated by natural gas turbines in the CC configuration (a natural gas and steam turbine coupled together). This growth in natural gas CC applications is due to unprecedented performance in terms of cost, efficiency, emissions and power density when compared to any other utility-scale power generation system.

Gas turbine technology for electric power generation continues to advance in response to ever more demanding performance requirements. This advancement has been achieved in part because of cost-shared research and development (R&D) partnerships between industry and the government. These partnerships strive to advance turbine technology and performance beyond what the industry is expected to achieve on its own in terms of efficiency, emissions and cost. This advanced performance with accelerated availability to the marketplace has direct and tangible benefits to the public in terms of lower cost of electricity and reduced emissions of criteria pollutants.

The Department of Energy is committed to using coal in ways that are cleaner and more efficient. The technological progress of recent years has created a new opportunity for coal. Aggressive goals have been developed to lead the industry to a new, affordable breed of coal plant – a near-zero emissions plant that generates power and produces high-value fuels such as hydrogen with minimal impact on the environment.

Advanced turbines are an essential component of this new breed of coal plant. With gas turbines these new power plants will produce electricity and hydrogen from coal while capturing and sequestering the produced CO_2. To realize the full potential of these coal plants in meeting the nation's energy goals, progress must be made on hydrogen-fueled turbine performance to reduce emissions, increase efficiency and reduce cost.

There are significant scientific and engineering challenges associated with meeting increasing demands on turbine technology when using hydrogen fuels derived from coal. For example:

- Hydrogen-fueled combustor performance is being optimized for low oxides of nitrogen (NOx) and high stability operation. Simultaneously, turbine inlet temperatures are being increased to realize higher efficiency, creating the need to protect the turbine's hot gas path components from heat damage.
- Combustion research is exploring the fundamental science of low-NOx hydrogen combustion.
- Hydrogen combustor concepts that use physical mixing, catalysts and diluents are being engineered to minimize flame flashback, flame holding, instability and NOx production.
- Differences in the properties of the working fluids produced by hydrogen-air or syngas-oxygen combustion will also require new technologies related to turbine components, in the areas of materials as well as cooling.

To meet these challenges, the Advanced Turbine Program is implementing a research program to develop turbines for integrated gasification combined cycle (IGCC) systems that capture CO_2.

Office of Fossil Energy and Advanced Turbine Program Goals

The U.S. Department of Energy's Office of FE manages a portfolio of research programs directed to demonstrate advanced coal-based electric power generation with near-zero emissions. These programs are designed to provide low-cost technological solutions to high-level Presidential initiatives. Programs managed by the Office of FE's Office of Clean Coal are depicted in the figure below.

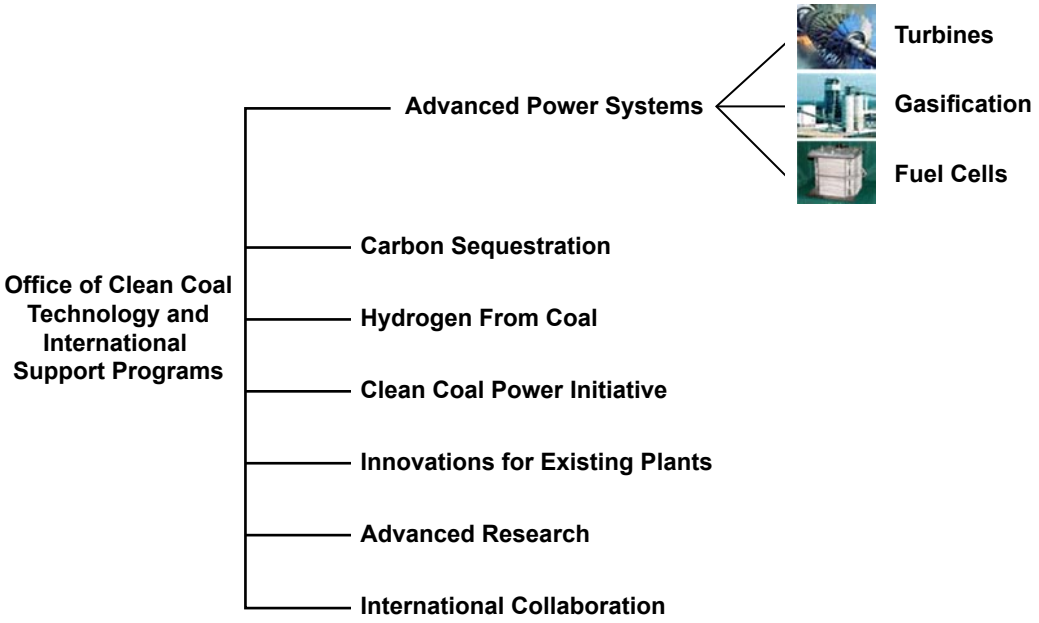

In response to these Presidential initiatives, the Office of FE Office of Clean Coal has developed a strategic plan that lays out goals for three distinct time horizons. These goals include:

1. By 2010, develop advanced coal-based power systems capable of 45–50 percent efficiency at <$1,000/kW (in 2002 dollars).
2. By 2012, develop technologies for capture and sequestration of CO_2 that result in less than 10 percent increase in the cost of electricity in an IGCC-based plant and less than 35 percent increase in the cost of electricity for pulverized coal boilers.
3. By 2015, demonstrate coal-based energy plants that offer near-zero emissions (including CO_2) with multi-product production.

The Advanced Turbine Program is organized into three areas: hydrogen-fueled turbines for IGCC applications, oxy-fuel turbines for IGCC applications, and advanced research. Included in the advanced research area is the National Energy Technology Laboratory's (NETL's) University Turbine Systems Research Program. This annual report presents the status of projects addressing these topic areas and progress towards the goals and objective outlined above.

Advanced Turbine Program's Objectives

The Advanced Turbine Program will contribute to the 2010 goal above by meeting the following objectives:

- Efficiency: Demonstrate 2–3 percentage points improvement above the baseline[1] for CC performance for an IGCC syngas-fueled system.

[1] Baseline efficiency is defined in "Development of Baseline Performance Values for Turbines in Existing IGCC Applications," Richard A. Dennis, Walter W. Shelton, and Patrick Le, Proceedings of GT2007, May, 2007.

- Cost: Demonstrate a 20–30 percent reduction (below the baseline) in CC capital cost, plus enhanced value for lower cost of electricity.
- Emissions: Demonstrate combustor emissions with 2 ppm NOx (at 15 percent oxygen, O_2) in simple cycle exhaust.

It is expected that the contributions to the 2010 goals will carry over and contribute to the 2012 goal for IGCC-based power systems that capture carbon. The main challenge here is that the machine will now be fueled by pure hydrogen (100 percent of the turbine energy input from hydrogen).

The Advanced Turbine Program will provide a turbine with the latest advances made through pursuing the 2010, 2012, and 2015 goals. It is envisioned that this turbine could be installed with a pre-planned technology improvement philosophy. This approach would allow the machine to be optimized in the field for combustion, firing temperature and other performance-enhancing components or subsystems. This approach would allow for a machine fueled with 100 percent hydrogen to operate with the highest efficiency and lowest NOx emissions and to validate Advanced Turbine Program contributions to 2010 and 2012 goals.

The Advanced Turbine Program will contribute to the 2015 goal above by meeting the following objectives:

Efficiency:

- Hydrogen-fueled CC turbine with 3-5 percentage points improvement (total above baseline).
- Oxy-fuel turbine-based IGCC system with competitive efficiency and nearly 100 percent CO_2 capture.

Cost:

- Competitive cost of electricity for near-zero emission systems.

Emissions:

- Hydrogen-fueled IGCC demonstrated with 2 ppm NOx (@15 percent O_2).
- Oxy-fuel turbine-based IGCC with near-zero emissions (>99 percent turbine exhaust captured and sequestered implying near-zero emissions of CO_2 and criteria pollutants).

Multiple Products:

- Hydrogen-fueled IGCC with higher capacity gasification to allow balancing between power and fuels production.
- Oxy-fuel turbine-based IGCC operating on hydrogen-depleted syngas producing power with hydrogen as a by-product.

2009 Annual Accomplishments

At the inception of the Advanced Turbine Program, system studies were used to baseline turbine and IGCC performance. Power plants with advanced turbines have since been modeled by hydrogen turbine developers, holding the balance of plant constant between the baseline plant and the advanced plant unless there was an obvious change required to make the balance of plant compatible with the advanced turbine. These system simulation studies with advanced hydrogen turbines show that the Program's efficiency and cost goals are attainable, assuming that the R&D pathways (combustion, materials, aerodynamics, heat transfer, and systems) being pursued by the Program are successfully implemented. The project highlights below and 2009 accomplishment outlined in the body of this report present the key results accomplished along these R&D pathways.

Over the past year, the Advanced Turbine Program has continued to improve turbine performance while reducing cost. In addition, the ability to effectively use hydrogen fuels at high temperature with low NOx production, a requirement essential for IGCC with CO_2 capture, has been demonstrated at the component scale.

In FY 2009, the advanced turbine program issued a funding opportunity announcement (FOA) for university-based research. This FOA was designed to solicit applied research for hydrogen-fueled turbines. Research proposals were sought in three topic areas: 1) Assessment of Fundamental Combustion Mechanisms in High Hydrogen Content Fuels for Advanced Gas Turbines, 2) Aero/Heat Transfer, and 3) Turbine Materials. Through a merit-based selection process, the three projects listed below were selected for award.

- The Pennsylvania State University, *An Experimental and Chemical Kinetics Study of the Combustion of Syngas and High Hydrogen Content Fuels*
- Texas A&M University, *Aerodynamics & Heat Transfer Studies of Parameters Specific to the IGCC Requirements: High Mass Flow Endwall Contouring, Leading Edge Filleting and Blade Tip Ejection under Rotating Turbine Conditions*
- University of Texas at El Paso, *Novel Hafnia-Based Nanostructured Thermal Barrier Coatings for Advanced Hydrogen Turbine Technology*

This and other university-based research is managed through the University Turbine Systems Research Program, a sub-element of the Advanced Turbine Program.

Project Highlights

The following projects highlight progress made in the Advanced Turbine Program during FY 2009.

Hydrogen Turbines for Near-Zero Emission Systems

At GE Energy in Schenectady, New York, a novel bucket concept was successfully tested for mechanical stability at conditions that could enable higher turbine performance levels to be achieved. By simulating actual operating conditions through the use of a highly instrumented test, the team was able to demonstrate the ability of the bucket design to provide increased capability relative to baseline technology. The data collection capability afforded by the test facility allowed the team to collect high quality information that is being used to improve predictive models and expand the operating window even farther in future design iterations.

Researchers in NETL's Fundamental Combustion Laboratory recently demonstrated that reducing NOx emissions in a high-hydrogen diffusion flame gas turbine combustor is better achieved by diluting the fuel stream rather than the air stream, which is currently a common industrial practice. Although air-side dilution minimizes the fuel manifold modifications required in gas turbines burning high-hydrogen fuels, NETL's results show that for all lean diffusion flame combustor types, including swirl-stabilized combustors, flame temperatures are always minimized with dilution of the fuel stream, leading to lower NOx emissions. In addition, NETL's experimental results show that for non-swirl combustor types, such as lean direct injection combustors, flame stability margins are improved and NOx formation times are reduced for fuel-side dilution vs. air-side dilution, which has important ramifications on how future high-hydrogen combustors are designed for low-NOx performance.

The fabrication and assembly of a test module for use in turbine aerothermal research in NETL's High Pressure Combustion Facility has been completed. Advanced land-based gas turbine systems for hydrogen or oxy-fueled applications will likely operate at higher operating temperatures than current systems. This new test capability is a key part of a larger collaborative effort through the NETL-Institute for Advanced Energy Solutions program (University of Pittsburgh). The new test rig will enable the detailed study of heat transfer and cooling mechanisms, turbine blade materials, and thermal barrier coatings in a controlled, but representative, gas turbine environment. It is anticipated that the data produced will enable the development of turbine blades with enhanced cooling and ultimately improve the overall cycle efficiency of future power plants.

Parker Hannifin Corporation, in collaboration with the University of California, Irvine Combustion Laboratory and operating under a cooperative agreement with the NETL, has tested innovative micro-mixing lean-premix fuel injectors for hydrogen and syngas fuels, demonstrating ultra-low emissions and flame stability. The micro-mixing fuel injectors consist of multiple small mixing cups, 6-12 mm in diameter, each with two fuel circuits and multiple fuel injection points to achieve rapid mixing of fuel and air. The injectors are built from etched metal plates that are bonded together using state-of-the-art diffusion bonding processes to form an integral structure, complete with air and fuel passages. An early cup design, optimized for superior mixing performance, demonstrated exceptional emissions performance, achieving 5 ppm NOx and lower at adiabatic flame temperature of 1,750 K (2,690°F) and pressures up to 5 atm, with 1 ppm NOx being generated at atmospheric condition. Flame imaging showed compact detached flames stabilized about one-half cup diameter downstream of the cup exit. A second generation of cups, designed to achieve superior flashback robustness, was tested in a multi-cup injector configuration at pressures up to 8 atm and demonstrated NOx emissions of 5 ppm at the target 1,750 K flame temperature when operating on hydrogen with less than 20 percent nitrogen dilution. Superior operability was also demonstrated, with the injector operating on 100 percent hydrogen fuel without flashback at pressure up to 8 atm (limit of the rig) and adiabatic flame temperatures up to 2,000 K. Overall, the micro-mixing fuel injectors show great promise for use in future gas turbine engines operating on hydrogen, syngas or other fuel mixtures of various compositions.

Advanced Oxy-Fuel Turbines

At Siemens Energy, one of the goals of the turbine development project for oxy-fuel conditions is to quantify the life of superalloy/thermal barrier coating (TBC) systems in an environment of steam and CO_2. This is important because originally, these systems were designed for operation in a regular gas turbine with products of combustion of natural gas in air. Siemens made significant progress towards understanding the material behavior in steam/CO_2 atmosphere. Baseline TBC spallation data from thermal cycling were generated, and studies were conducted to understand the oxidation effects of the environment on the microstructure underneath the TBC. Machined low-cycle fatigue specimens were exposed to steam/CO_2 atmosphere in order to prepare these specimens for tests and quantify the effects of the exposure on low-cycle fatigue properties. When completed, this work will allow an estimation of the expected life of blades and vanes in the selected Siemens SGT-900 turbine modified for oxy-fuel combustion conditions.

Clean Energy Systems, Inc. (CES) has completed fabrication and assembly of a prototype reheat combustor test rig designed to demonstrate the feasibility of increasing power plant efficiency by reheating the drive gas (primarily steam and CO_2) in a turbine "train" between the high and intermediate pressure turbines (HPT/IPT). Studies have shown that oxy-fuel plant efficiency can be increased by 10 percentage points by taking advantage of the higher temperature capabilities of modern IPTs and increasing the temperature of the drive gas exhausting from the HPT to optimal inlet temperature for the following IPT. CES will use a single "can" from a J79 GE turbine, instrumented and modified by Florida Turbine Technologies, Inc., to develop operating parameters, confirm combustion patterns, and demonstrate material compatibilities. The J79 combustor was previously "cold flowed" to analyze flow patterns, an oxy-fuel reheat design finished, and two J79 reheat combustors fabricated.

Advanced Research

A collaborative research effort that involves researchers from Case Western Reserve University, University of Southern California, and University of Michigan aims to provide an experimental database of high fidelity and develop comprehensive and computationally efficient reaction mechanisms for facilitating the design of syngas and hydrogen (SGH) fuel combustors. Mixtures of CO, H_2, and H_2O are used for simulating SGH fuels to experimentally obtain fundamental combustion data, including laminar flame speeds, ignition delay times, and extinction limits, with parametric variations of mixture composition, preheat temperature, and pressure. Recent experiments investigated the effect of moisture content on the ignition delay of syngas at elevated pressures using a rapid compression machine, demonstrating a complex behavior. For H_2-rich cases, the ignition delay shows a non-monotonic

response with water addition – it first increases with small amount of water addition, but with further water addition the ignition delay decreases. For CO-rich cases with a small amount of water addition, the ignition delay response is temperature dependent – while at higher temperatures the ignition delay increases, at lower temperatures the ignition delay decreases, when compared to the corresponding dry case. As the amount of water addition is further increased, the ignition delay becomes shorter for the CO-rich cases, throughout the range of temperatures studied. The present experimental results provide an extensive database for the understanding of combustion characteristics at varying syngas compositions. The resulting experimental database will be of practical use in determining the desired syngas compositions for optimal operation, as well as improving the design of advanced combustors fueled by syngas and hydrogen.

NETL, in collaboration with CFD Research Corporation, is developing an innovative, practical turbulent combustion model named the Modified Global Mechanism (MGM) model for premixed combustion in gas turbine combustors. A highly successful Phase I of the project was completed in 2009. A new turbulent combustion model proof-of-concept was developed and validated. The model included important features such as (1) accounting for differential (preferential) diffusion of light species and (2) utilizing highly accurate and computationally efficient global reaction mechanisms for prescribed operating conditions. The model will be extended to incorporate the effects of 3-dimensional grid-resolution on subgrid scale turbulence-chemistry interactions, and new models to enable computational fluid dynamics (CFD) of fuel-flexible combustors will be developed. These features will enable accurate large eddy simulations of practical engineering problems requiring tens of millions of grid cells, in reasonable turn-around times.

Researchers at Faraday Technology, Inc. are developing a pulse/pulse reverse electrophoretic deposition (EPD) process for the application of TBCs to hot section components of gas turbines. The new manufacturing process utilizes pulsed electric fields to induce migration of charged particles in suspension to uniformly deposit the TBCs. After binder burnout and sintering processing steps, a porous ceramic coating is formed on the turbine component. The non-line-of sight nature of the process makes it suitable for coating complex shaped components, such as turbine vanes and blades that are difficult to uniformly coat using the industrially practiced techniques of plasma spray or electron beam physical vapor deposition, and it's applicable to conventional and newly developed low conductivity TBCs that will enable higher temperatures in natural gas and synthesis gas environments. Recent experiments at Faraday Technology, Inc. have shown that the TBCs deposited by the pulse/pulse reverse EPD process have exhibited decreased roughness and enhanced uniformity when compared with TBCs deposited by conventional EPD, and exhibit favorable results in preliminary thermal cycling tests. In addition to the technical benefits, the enabling manufacturing process equipment will be affordable and relatively simple to operate.

At Florida Turbine Technologies, patented Spar-Shell Airfoil technology is being developed to provide significant efficiency improvements in advanced power systems, such as proposed turbomachinery using high hydrogen and alternative synthetic fuels. Feasibility of the technology has been demonstrated through conceptual design studies. Spar-Shell Airfoil technology can be retrofit into existing power plants worldwide to create up to 15 percent more power from the same plants with no additional fuel.

The development of innovative power cycles such as IGCC and oxy-fuel is hindered by the lack of validated data for thermodynamic and transport properties of the gaseous mixtures in the turbines and other parts of these cycles. Approaches such as ideal-gas thermodynamics are inaccurate for such systems, primarily due to the presence of water. Research at the National Institute of Standards and Technology is developing alternative modeling approaches, supplemented by selected high-temperature experimental measurements. First-principles molecular modeling is being used to provide accurate thermodynamic properties, with the key water-CO_2 interaction being added in 2009. One-of-a-kind apparatus have been designed for high-temperature measurements (extending up to 500°C) of density and thermal conductivity for mixtures of water with CO_2 and with nitrogen. The thermal conductivity apparatus has been completed, and high-temperature data have been obtained on pure water, CO_2, and nitrogen and on the water-nitrogen mixture. The density apparatus has been constructed and should start producing high-accuracy data in the second half of 2009.

At Princeton University, flame speeds and burning rates of syngas mixtures were measured over a significant range of typical syngas turbine conditions, employing a parametric approach by individually varying pressure from 1 to 25 atm, flame temperature from 1,500 to 1,800 K, equivalence ratio from 0.85 to 2.5, CO fuel fraction from 0 to 90 percent, and CO_2 dilution fraction from 0 to 40 percent. These measurements mapped the pressure dependence of $H_2/CO/CO_2$ burning rates, indicating the existence of *negative pressure dependence* in the burning rate at high pressure, low flame temperature conditions, which results in atypical engine stability behavior. Two state-of-the-art models were validated against burning rate data up to 10 atm for low flame temperature conditions. However, this study indicates that significant improvements to the models must be made to predict burning rates above 15 atm or with CO_2 dilution. In order to improve model performance, the key kinetic pathways and causes of the modeling difficulties under these conditions were identified. Efforts to improve model performance are underway with collaborators in the elementary reaction kinetics field. Additionally, strategies that reduce computational time in combustion calculations by over an order of magnitude were formulated and validated.

NETL's University Turbine Systems Research

Although filters are installed in gas turbine systems to remove flyash from synfuels, small concentrations of fine particles pass through the filters and reach the turbine surfaces, even if the filters are well maintained. Deposits build up over a year or two of operation and cause operational problems. Brigham Young University (BYU) is studying synfuel flyash deposition on representative film-cooled turbine blade surfaces that include TBCs, with the goal of determining the magnitude of deposition, erosion, and corrosion for the application of alternative fuels in modern gas turbines. During the past year, the deposition patterns and surface temperatures of small subbituminous coal flyash particles on coupons with film cooling holes were measured in the BYU Turbine Accelerated Deposition Facility. Gas temperatures were 1,183°C flowing at Mach 0.25. Effects of particle size, blowing ratio, and film cooling hole spacing were examined both with and without TBCs. Scale models of deposits were used to determine how deposits affect film cooling effectiveness and convective heat transfer coefficients. A computational flow model of deposition was developed as a user-defined function in Fluent.

A combined experimental/computational research effort was initiated in October 2008 to explore the possibility of modifying turbine endwall geometries to both increase their aerodynamic performance and reduce the potential for degradation due to deposition. The experimental work is divided between two reacting flow turbine test facilities: one at BYU and the other at Ohio State University (OSU). The facility at BYU has been modified for high temperature deposition experiments up to 1,400°C with film cooling capability. This facility will eventually be adapted to allow elevated diluent (water vapor) concentrations as well. The OSU facility provides the capability to test actual turbine vane flowpaths at operating temperatures with film cooling. The final fabrication and assembly of this facility was completed in June 2009. Deposition testing is now underway with actual industrial nozzle guide vane sectors from GE – operating at representative gas and coolant temperatures. Experimental data from both facilities will provide critical validation for computational models of deposition that have been developed under this same research effort.

The University of Pittsburgh is systematically exploring the transport processes associated with film-hole partial blockage and surface deposits on the film cooling performance. One of the key results gained from this study is the development of shaped film holes with advanced concepts. These new concepts may be realized by controlling the TBC to create desirable surface topology. New approaches explored in this project include: (1) flow-aligned blockers, (2) upstream ramp, and (3) transverse trench. CFD simulations have led the concept developments by revealing detailed flow structure and transport phenomena. Experiments based on an infrared thermal imaging technique have not only provided data validation for CFD but also fully characterized the spatial distribution of film effectiveness and heat transfer coefficient for all the new cooling concepts. While most of the new approaches explored in this project have shown promising features, one of the key accomplishments in 2009 was a direct comparison among the three approaches, based on film effectiveness, heat transfer coefficient ratio and reduced heat flux. Results obtained from both experimental measurement and computational simulation suggest that upstream ramps with an inclined angle of 20-25° show improved performance

in the region downstream to the film cooling hole. Transverse trench is an effective approach for film cooling enhancement over a wide range of blowing ratios. The collective information gained from this research could further provide guidelines for advanced film cooling strategies in future turbine engines.

At Virginia Polytechnic Institute and State University, syngas ash deposition dynamics was investigated in a three-row film-cooled leading edge with blowing ratios ranging from 0.5 to 2.0 and ash particle sizes of 5 and 7 microns (Stokes numbers 0.25, 0.49, respectively) using large eddy simulations. It was demonstrated that the stagnation row cooling is quite effective in protecting the blade surface locally from deposition by blowing away ash particles as well as cooling the particles below their deposition temperature. Detailed deposition profiles were obtained from these studies. It was demonstrated that particle Stokes number is an important parameter for deposition. Experiments also demonstrated that low melting point polyvinyl chloride and Teflon® particles behave similarly to ash particles in their scaling with free-stream and surface temperature. These results are significant because low temperature experiments can be used to study deposition at engine conditions.

Combustion dynamics is one of the biggest technical challenges in efficient, low-emission gas turbines. High frequency, transverse modes are particularly dangerous and can cause severe structural damage within seconds. A synergistic research approach is used at The Pennsylvania State University to understand the underlying physics of the coupling mechanism between catastrophic acoustic resonances and the flame dynamics that fuel them. The use of a multiple-nozzle experimental facility recreates the flow conditions in an actual gas turbine and allows for specific attention to be paid to the complicated interactions between flames that can aggravate the combustion dynamics problem. To date, this research has focused on understanding the fluid instabilities and flame dynamics in a single nozzle, as a building block to understanding dynamics in the multi-nozzle combustors that are used in actual power generation turbines. Strong evidence of a coupling between the transverse acoustic field and axial velocity motions has been established. These axial velocity perturbations create large vortices that deform the flame and cause bursts of heat release that feed back into the acoustic field. Understanding the vortex dynamics is also important in the multi-nozzle problem, since the paths of the convecting vortices of each nozzle intersect, allowing for vortex and flame interaction. This phenomenon has been seen at several operating conditions and acoustic frequencies, showing that this problem can be pervasive in several different gas turbine geometries and operating conditions. The knowledge garnered in this phase of the investigation will allow for better understanding of this important problem.

At the University of California, Irvine, an investigation of the mixing behavior of hydrogen and high-hydrogen fuels is being carried out using a parallel experimental and numerical approach. The work is motivated by the challenges associated with both simulation and measurement of hydrogen in gas turbine-type premixers. Thus far, a set of carefully made premixer hardware has been developed which mimics key features found in practice, including multipoint gas injection, swirl, and accelerating flow at the mixer exit. A systematic combination of geometries and conditions is being studied to establish a preferred strategy for simulation of hydrogen mixing. Due to the low density and high diffusivity of hydrogen, application of many modeling approaches has proven unsuccessful for simulation. Yet to aid in design screening, an efficient, reasonably accurate tool is required. Limited results obtained for a 2-dimensional axisymmetric coflowing geometry indicate that, even when following "best practices" for CFD gridding and simulation, the modeling approach selected can lead to errors approaching 300 percent in simulating the concentration of hydrogen in even a very simple configuration. The detailed data being obtained will serve as a database for others exercising current or developing simulation methodologies. A total of 48 different conditions will be examined and analyzed.

Power plant engines operating with coal-derived fuels have different types of TBC degradation compared to engines functioning in aerospace applications. OSU has examined fly ash samples collected from power plants with coal sources from different geographical regions to determine their composition and elucidate TBC degradation mechanisms. Two fly ash samples, namely Powder River Basin and lignite, have been found to contain large quantities of iron oxides along with calcium-magnesium-alumino-silicates and other elements in trace quantities using X-ray fluorescence spectroscopy. Ternary phase diagrams with these fly ash compositions have revealed a glassy intermediate psuedowollastonite-gehlenite-anorthite phase for lignite and Ca_2SiO_4-$Ca_2Si_3O_7$-$CaAl_2O_4$-

$Ca_2Al_2SiO_7$ phase for Powder River Basin, which would drift through the coatings. The fly ash samples, when heat treated in contact with 7 weight percent Y_2O_3 stabilized ZrO_2 air-plasma-sprayed TBCs at elevated temperatures, have been shown to diffuse through the TBCs. These observations demand an alternative TBC that can arrest the advancement of the glassy deposits. New TBC compositions, such as $Gd_2Zr_2O_7$, are being studied to mitigate the attack by these glassy deposits.

The University of Pittsburgh has obtained René N5, IN 738, and GTD 111 alloy specimens and coated them with a platinum aluminide coating. Specimens of NiCoCrAlY have also been obtained. An apparatus has been constructed whereby coupon specimens can be exposed to gas mixtures containing 85% H_2O-15% CO_2 at temperatures from 700°C to 1,100°C. Oxidation data existing in the literature for the alloys and coatings being studied in this project have been tabulated to compare with results generated in this project. Specimens of René N5, IN 738, GTD 111, and platinum aluminide coated René N5 have been exposed in dry air, 10% H_2O-90% air and 85% H_2O-15% CO_2 at 900°C and 950°C. Severe attack of these alloys and coatings was not observed in any of these gas environments. Such results indicate that these alloys will not be severely degraded in the high steam and CO_2 levels expected in coal-based oxy-fuel systems.

The remainder of this report contains brief status summaries for the projects managed through the Advanced Turbine Program. Each summary includes the scope, objectives, status and accomplishments of the project. The Advanced Turbine Program is encouraged by the technical progress made this year, and the prospects for continued advancements in the coming year are good, paving the way to achievement of the goals.

II. HYDROGEN TURBINES FOR NEAR-ZERO EMISSION SYSTEMS

II.1 DOE Advanced IGCC/H_2 Gas Turbine Development

Reed Anderson
GE Energy
1 River Road, 55-211
Schenectady, NY 12345
Phone: (518) 385-5689; Fax: (518) 385-8796
E-mail: reed.anderson@ge.com

DOE Project Manager: Robin Ames
Phone: (304) 285-0978
E-mail: Robin.Ames@netl.doe.gov

Subcontractors:
- GE Global Research Center, Niskayuna, NY
- GE Aviation, Cincinnati, OH

Contract Number: 42643

Start Date: October 1, 2005
End Date: September 30, 2012

FY 2009 Objectives

- Develop technology advancements necessary for an advanced integrated gasification combined cycle (IGCC), fuel flexible (coal-derived hydrogen and syngas), gas turbine to meet the DOE program goals of:
  - Improve IGCC efficiency (+3-5 points combined cycle efficiency).
  - Reduce NOx emissions to 2 ppm NOx at 15% O_2.
  - Contribute to capital cost reductions.

Accomplishments

- Continued excellent progress in the development of pre-mixed combustion technology for syngas and hydrogen by conducting extensive megawatt-scale, full head end testing on leading concept and completing design and hardware procurement activities for the next generation prototype.
- Conducted mechanical testing on initial advanced bucket design achieving desirable performance characteristics.
- Completed characterization of novel film cooling configurations, achieving targeted increases in cooling effectiveness.
- Completed process optimization trials for next iteration thermal barrier coatings (TBCs) and initiated testing to support a final down selection.

Introduction

Coal is this nation's most abundant domestic energy resource and is used to produce about 50% of the nation's electricity needs. Its continued use is an important part of realizing an "energy secure" United States. The challenge is to produce electricity in a cleaner and more efficient manner while significantly reducing carbon emissions. The goal of this project is to advance gas turbine technologies so that future coal-based IGCC power generation plants, including CO_2 capture, can be accomplished with higher efficiency, lower cost, and reduced emissions. The gas turbine has a significant influence on the performance of the IGCC power plant. The inherent performance penalties associated with CO_2 capture are driving a renewed focus on gas turbine technology advancement as a means to minimize the penalty.

In an IGCC power plant, syngas produced from the coal is cleanly burned in a heavy-duty gas turbine. With pre-combustion CO_2 capture, the resulting fuel burned in the gas turbine is hydrogen. GE's advanced gas turbine technology project addresses key technology developments required to achieve specific DOE performance goals relative to emissions, efficiency, and capital cost. The project is comprised of two phases. Phase I, which ran from October 2005 to September 2007, was focused on conceptual design and technology identification. The output of Phase I was a down selection of key technologies that are currently being further applied and developed in Phase II. The Phase II effort started in October 2007 and is focused on technology development and validation at a component level.

Approach

This gas turbine technology advancement project is comprised of three main technology areas (combustion, turbine/aero, and materials) plus a systems level activity.

- The combustion element of the project is focused on improving combustion technology to achieve the emissions target of 2 ppm NOx at the higher temperatures necessary to achieve the targeted efficiency improvement. Work in this area addresses the challenges of developing a combustion system that can burn both syngas and high hydrogen fuels to produce extremely low NOx emissions while avoiding flameholding, flashback, and dynamics issues.

- The turbine/aero element of the project drives technology improvements to address the efficiency targets. Examples include improved aerodynamic characteristics and better flow management.
- The materials portion of the project is focused on applying materials technology to enable the turbine to operate reliably at higher firing temperatures in the harsher IGCC environment. This includes evaluation of advanced alloys and coatings, including targeted use of ceramic matrix composites with environmental barrier coatings.
- The systems level approach translates the integration of technology improvements into plant performance and investigates the various system trade-offs and their impact on overall plant performance.

In summary, this comprehensive project addresses the technology development needs for advanced gas turbines for IGCC applications while targeting the specific goals identified by the DOE relative to emissions, efficiency, and capital cost.

Results

Government Fiscal Year (GFY) 2009 was the second year of Phase II of the project, and as such, advanced analysis tools and rig testing continued to be used extensively in the process of developing and characterizing performance improvements from each technology area.

The leading combustion concept was tested extensively in a full can configuration with component sizes approaching full-scale. Testing was conducted with pure hydrogen, natural gas, and hydrogen-nitrogen fuels. A picture of testing in progress is shown in Figure 1. The concept demonstrated operability consistent with that observed in earlier tests using a smaller-scale single-nozzle, even while local flame temperatures exceeded F-class requirements for long periods of time. The team incorporated lessons learned from the testing into a next generation design that at the time of writing, was about to be tested.

Mechanical response information was obtained for the first advanced bucket concept to be evaluated under the project. The data were obtained from a test facility where anticipated operational conditions were simulated via excitation of the rotating buckets. The test rig, shown in Figure 2, has proven to be an effective method to evaluate the bucket design and retire risks. The concept performed well, and will provide valuable insights to be used in the design of an optimized concept later in the program.

Building on the extensive screening test results from 2008, optimized designs for the best performing novel film cooling configurations were created and characterized in 2009. Figure 3 shows representative test results, which were in line with the level of improvement being targeted.

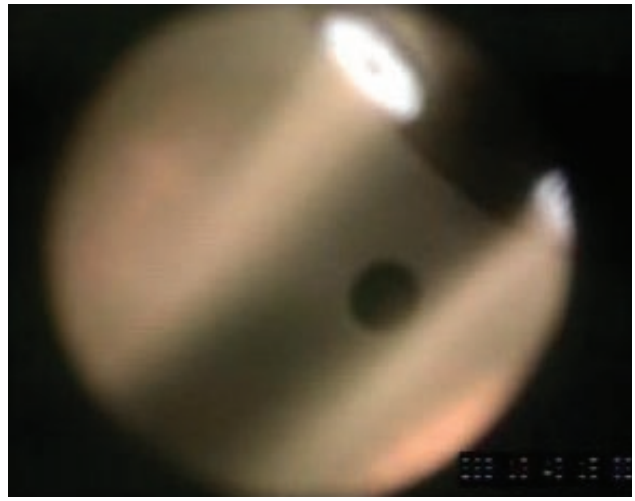

FIGURE 1. Full Head End Combustion Testing in Progress

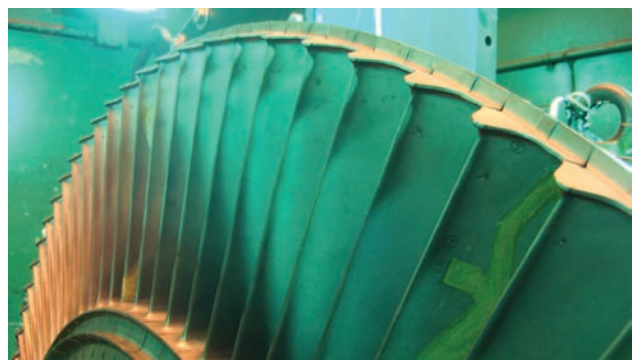

FIGURE 2. Test Facility Used to Evaluate New Bucket Concept

Process optimization studies on the down selected TBCs from 2008 were completed and testing in support of a final down selection is underway. Leading metallic coatings were prepared for evaluation in an upgraded test rig that better simulates the anticipated operating environment. Similar to the TBC coatings, testing of the candidate coatings is underway with results and a final down selection to follow.

The systems function continues to perform studies necessary to quantify the plant level performance and cost impact of the various technology development efforts, as well as guide component design decisions.

Conclusions and Future Directions

Phase II (technology development and validation) of this project is a continuation from Phase I (technology identification and conceptual design) which was completed on time, within budget, and

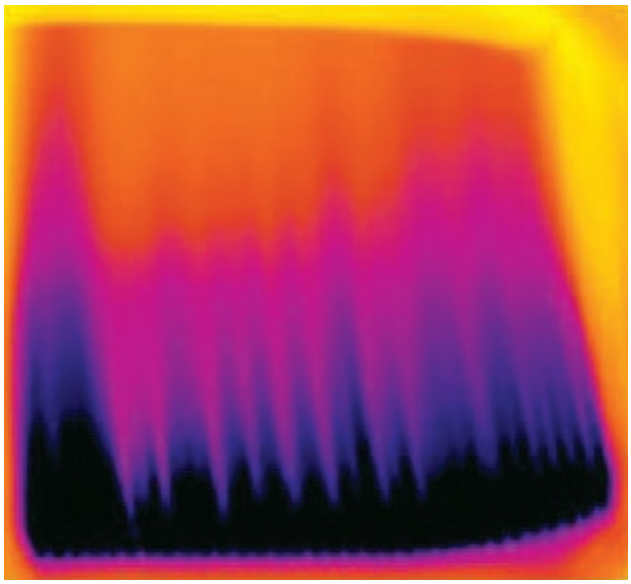

FIGURE 3. Film Effectiveness Map for a Novel Cooling Concept

with all major milestones achieved. In GFY 2009, the second year of the Phase II project was completed. Results to date in Phase II have been positive and continued to indicate that project progress is on track relative to available funding. Building on work performed in GFY 2009, future years will continue unfinished efforts from this year and initiate remaining areas of the project. Looking ahead, some of the specific technology areas are:

- Combustion technology will continue to be matured, as the project will conclude basic technology demonstration and move into the technology transition phase. In this phase there will be an increased focus on alternate construction/geometry to make the technology more reliable, affordable, easier to manufacture/service, and/or better integrated with other components/systems.
- Optimized designs for several sealing locations will be completed and their improvement levels validated through rig testing. Results from cooling and aero tests will be used for qualification of advanced design tools and optimization of next generation component designs.
- Testing of second iteration metallic and TBC materials will be completed and a final down selection will be made. This will be followed by a detailed characterization and process optimization phase.

Special Recognitions & Awards/Patents Issued

1. 45 U.S. patent filings have occurred, with another 12 in various stages of the filing process.

FY 2009 Publications/Presentations

1. Warren Nelson et al., "TBC Changes Due to Elevated Temperature Exposures," TSS Aerospace Coatings Symposium, October 2008.

2. Raymond Chupp, "Update on DOE Advanced IGCC/H_2 Gas Turbine," 2008 NASA Seal/Secondary Air System Workshop, November 2008.

3. Roger Schonewald, "Turbine and System Developments for Syngas/Hydrogen Gas Turbine Technology," ICEPAG 2009, February 2009.

4. Roger Schonewald, "Combustion Developments for Syngas/Hydrogen Gas Turbine Technology," ICEPAG 2009, February 2009.

5. Terry Raddings, Robert Jones and Jeffrey Goldmeer, "Syngas and Alternative Fuels Solutions – Meeting Energy Security and Climate Challenges," PowerGen Europe, May 2009.

II.2 Advanced Hydrogen Turbine Development

Joseph Fadok (Primary Contact), Tim Bradley
Siemens Energy, Inc.
4400 Alafaya Trail
Orlando, FL 32826
Phone: (407) 736-2361; Fax: (407) 736-5633
E-mail: joseph.fadok@siemens.com,
tim.bradley@siemens.com

DOE Project Manager: Robin Ames
Phone: (304) 285-0978
E-mail: Robin.Ames@netl.doe.gov

Subcontractors:

- Florida Turbine Technologies, Jupiter, FL
- Agillis, Jupiter, FL
- University of Central Florida, Orlando, FL
- University of Florida, Gainesville, FL
- Georgia Institute of Technology, Atlanta, GA
- Princeton University, Princeton, NJ
- Texas A&M University, College Station, TX
- Virginia Polytechnic Institute and State University, Blacksburg, VA

Contract Number: 42644

Start Date: October 1, 2005
End Date: September 30, 2012

FY 2009 Objectives

- Advance the overall technology readiness level of the various concepts necessary to meet the DOE 2010 and 2015 project goals.
- Select the turbine aerodynamic and sealing configurations for sub-scale testing in collaboration with universities and external partners.
- Complete manufacture of the turbine high turning aerodynamic test rig in preparation for sub-scale testing.
- Further develop advanced materials systems for the hydrogen turbine and complete oxidation studies for multi-component bond coat testing and compare to baseline.
- Complete first series of pilot rig performance verification of novel selective catalytic reduction (SCR) with commercial size samples in simulated integrated gasification combined cycle (IGCC) gas turbine exhaust.
- Progress the premix combustion technology with syngas by completing the second series of syngas and hydrogen testing of the improved premix combustor.

Accomplishments

- Materials verification testing was completed including thermal barrier coatings, bond coats, and modified superalloys. Figure 1 shows the results of modified bond coat testing where one modified system demonstrated a 40% improvement in coating life [1,2].
- The turbine aerodynamic test rig was manufactured and the first series of testing of high turning airfoils was completed. Figure 2 shows the high turning rig and complimentary analysis of a turbine blade.
- The Siemens premixed combustion design shown in Figure 3 has been adapted for syngas operation. An improved design has been developed which can operate at elevated temperatures with 100% syngas in all of the fuel stages [1].
- The activation process for the H_2-SCR catalyst has been developed in order to achieve NOx removal efficiency above 90% in the simulated IGCC exhaust with high water and sulfur content.

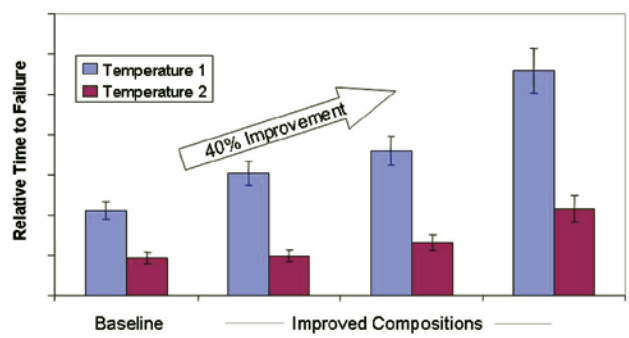

FIGURE 1. Improved Coating Life with Modified Bondcoats

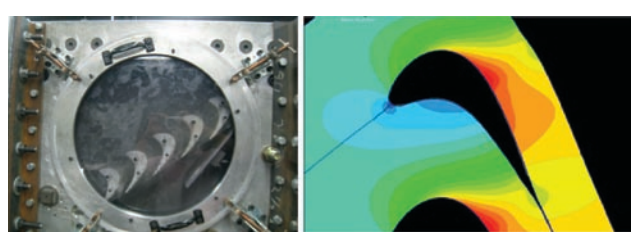

FIGURE 2. High Turning Turbine Aerodynamic Test Rig

FIGURE 3. Premix Syngas Combustor Nozzle

Introduction

Siemens Energy, Inc. was awarded a contract by the United States Department of Energy (DOE) for Phases 1 and 2 of the Advanced Hydrogen Turbine Development Program in October, 2005. The DOE Advanced Power Systems overall goal is to conduct research and development necessary to produce CO_2 sequestration ready coal-based IGCC power systems with high efficiency, near zero emissions and competitive capital cost.

Fiscal Year 2009 activities focused on the testing of component level technologies and systems required to meet the 2010 and 2015 project objectives, executing validation test plans for systems and components, performing validation testing of component technologies, and demonstrating the ability to attain the 2010 and 2015 Turbine Program performance goals. Additionally cost and performance models were utilized to evaluate technology changes and their associated impact on each.

Approach

Siemens has developed an overall project strategy that supports the DOE Program goals and future commercialization. The path forward is a stepped approach which ensures the DOE intermediate (2010) and long-term (2015) goals are addressed. Phase 2 includes advanced technologies development, down selection and validation, as well as basic component designs. In Phase 3, if awarded, the final product manufacturing specifications will be completed and the engine will be manufactured and installed in an IGCC plant for validation testing to demonstrate the project's commercial viability and that the DOE Program goals have been achieved.

Results

Significant progress has been made in characterization of materials needed for the advanced hydrogen turbine. The results of bond coat oxidation testing gave valuable insight to future direction of the project. Several improvements were identified and are being developed for future testing. The high temperature thermal barrier coatings are being testing at the Siemens test facility to quantify the material capability. Coupled with the success of the modified superalloys project, the combined system will offer superior performance to the baseline materials system.

The initial cost estimate for the 2010 syngas case indicates that a significant increase in power is necessary to achieve the 20-30% cost reduction goal. The reduction of the power block cost, combined with this increase in power will enable the target to be met.

The improved premix syngas design was successfully operated at the targeted temperature to meet the 2010 performance goals on 100% syngas. Even with increased hydrogen content in the syngas, successful operation without flashback was confirmed above the baseline conditions. Further temperature capability was demonstrated with the advanced premix system with some dilution needed [1].

Recent lab tests show that the Siemens Polyfunctional Emissions Reduction Catalytic system with the latest improved formulation allows achieving 90+% NOx reduction efficiency in the presence of water (up to 20%) and sulfur dioxide, and can be reliably operated at the temperature range 110-135°C which is 30-40°C above the acid dew point under IGCC gas turbine exhaust conditions. The catalyst demonstrates a high NOx removal efficiency in the IGCC simulated gas turbine exhaust after conducting a special pre-treatment - an activation process that includes contacting of the developed catalyst with the gaseous stream containing NO, H_2, H_2O, O_2, and inert gas such as N_2.

The high turning airfoil cascade rig assembly was completed and experimental results for blade loadings at 20%, mid-span, and 80% span at various mach numbers and inlet angles were obtained for the first airfoil set. There is good agreement between the 1-dimensional and 2-dimensional computational fluid dynamics (CFD) and test data for mid-span loss/wake shape.

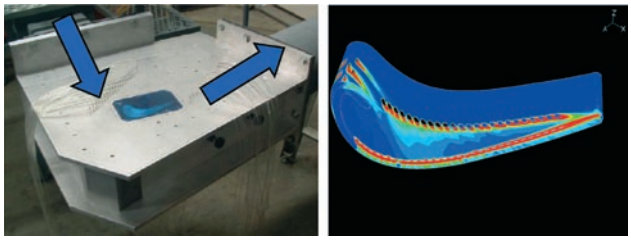

FIGURE 4. Turbine Blade Test Rig

Multiple blade tip configurations are being tested using a cascade rig (Figure 4). CFD analysis is used to predict the results. In FY 2009, calibration to the computational results was completed.

Conclusions and Future Directions

The development effort thus far has focused on engine cycles, combustion technology development and testing, turbine aerodynamics/cooling, modular component technology, materials/coatings technologies and engine system integration/flexibility considerations. Each component has to deal with specific challenges in order to meet the project goals. Rig tests, studies, CFD and scale lab test are demonstrating that each area is on track to achieving their targets. Through system studies the compressor has shown it is able to produce the increased pressure ratios required. The advanced and premix combustors have undergone several rig tests to show that the high firing temperature and decreased NOx emissions can be achieved. Material lab tests are showing an increase in spallation and thermal barrier coating life. Additionally novel manufacturing concepts, increased cooling effectiveness and increased efficiency are allowing the turbine to meet its goals as well.

The program has set specific goals for 2010 and 2015. In order to meet these goals Siemens is following a stepped approach. Future directions will include demonstrating component level technologies and systems required to meet the 2010 goals, and executing validation plans to meet the 2015 project objectives.

Special Recognitions & Awards/Patents Issued

1. More than 50 patent disclosures have been submitted on the new technologies being investigated in this project.

FY 2009 Publications/Presentations

1. DOE 08Q4 Quarterly Review Presentation, November 2008.

2. IGCC Needs Assessment Presentation, Powergen Conference, December 2008.

3. DOE 09Q1 Quarterly Review Presentation, February 2009.

4. ICEPAG Conference Presentation, January 2009.

5. DOE 09Q2 Quarterly Review Presentation, May 2009.

6. Turbo Expo Conference Paper and Presentation, June 2009.

References

1. T. Bradley and J. Fadok, Advanced Hydrogen Turbine Development Update, ASME GT-2009-59105.

2. J. Fadok and I. Diakunchak, Advanced Hydrogen Turbine Development Update, International Pittsburgh Coal Conference, 2008.

II.3 Partial Oxidation Gas Turbine for Power and Hydrogen Co-Production from Coal-Derived Fuel in Industrial Applications

Joseph Rabovitser, GTI (Primary Contact) and Dennis Horazak, Siemens Energy
Gas Technology Institute (GTI)
1700 S. Mount Prospect Rd.
Des Plaines, IL 60018
Phone: (847) 768-0548; Fax: (847) 768-0600
E-mail: joseph.rabovitser@gastechnology.org

DOE Project Manager: Charles Alsup
Phone: (304) 285-5432
E-mail: Charles.Alsup@netl.doe.gov

Subcontractors:
- Siemens Energy, Orlando, FL
- Solar Turbines, San Diego, CA
- Oak Ridge National Laboratory (ORNL), Oak Ridge, TN
- Georgia Institute of Technology (Georgia Tech), Atlanta, GA

Contract Number: 42649

Start Date: October 1, 2005
End Date: June 30, 2009

FY 2009 Objectives

- Develop a feasibility design for retrofitting a conventional gas turbine for partial oxidation duty in the industrial power plant.
- Produce a conceptual integrated gasification combined cycle (IGCC) plant design (systems study) that integrates the retrofitted turbine design.
- Conduct a preliminary market study that projects demand for the IGCC plant for industrial applications.

Accomplishments

- Finally, three candidate turbines for design study of retrofit conversion to a partial oxidation gas turbine (POGT) have been selected: SGT-800, SGT-400 and SGT-100 from Siemens with power output in the range from 5 to 100 MW. In addition, POGT performance evaluation was performed for a SGT6-6000G from Siemens with power output 350 MW in POGT mode.
- Retrofit design study is completed and detailed plans including schedule and budget have been developed for the SGT-800, SGT-400 and SGT-100: replacing the combustor with the partial oxidation reactor (POR), compressor downsizing for about 50% design flow rate, generator replacement with 60-90% power output increase, and overall unit integration.
- POGT performance for three selected turbines have been calculated. More detailed calculations were performed for the SGT-800. Detailed calculations of the SGT-400 and SGT-100 in POGT mode are also completed. In addition, gas turbine and POGT performance was calculated for the SGT6-6000G. With a POGT as the topping cycle for power generation systems, the power output from the POGT could be increased up to 90% compared to the conventional engine keeping hot section temperatures, pressures and volumetric flows practically identical.
- An advanced POGT-based IGCC detailed scheme has been developed and major components have been identified. A fuel-flexible fluid bed gasifier with moderate product gas temperature, ~1,800°F (~980°C), and novel POGT unit are the key components of the 100 MW IGCC plant for co-producing electricity, hydrogen and/or syngas.
- Gasifier performance has been calculated for bituminous coal in both air-blown and oxygen-blown versions. The oxygen-blown gasifier and a cryogenic air separation unit (ASU) have been selected for the study. Two versions of gas cooling and cleaning systems have been considered, and the more advanced warm system has been selected.
- Performance calculations were conducted for several IGCC-POGT systems with different power/hydrogen or power/syngas ratios. Results for four versions are presented in Table 1.
- Several POGT-based systems for co-production of electricity and hydrogen from natural gas were developed. Performance calculations for three versions of these systems were conducted and results are presented in Table 4.
- Preliminary market assessment was performed, and recommendations for POGT system applications in the oil industry were defined.
- ORNL has completed one series testing for POGT hot section materials in a reducing atmosphere. A total of 25 samples from Siemens and Solar have been tested. Processing and analyses of the test data have been performed and reported.
- Study of combustion instabilities in the POR has been completed by Georgia Tech, and the final report has been submitted.

Introduction

There are two main features that distinguish a POGT from a conventional gas turbine: the design arrangement and the operational thermodynamics. One design specific is utilization of a non-catalytic POR in place of a regular combustor. An important secondary design distinction is that a much smaller compressor is required, one that typically supplies less than half of the air flow required in a conventional gas turbine. From thermodynamic specifics, the turbine working fluid provided by the POR (a H_2-rich fuel gas) has higher specific heat than complete combustion products. This allows much higher energy per unit mass of fluid to be extracted by the POGT expander than in the conventional case. A POGT thus produces two products: power and secondary fuel that usually is a H_2-rich fuel gas.

GTI has been advancing the POGT concept since 1995. Siemens with GTI's participation has performed technical feasibility and cost analysis studies of the partial oxidation power cycle. GTI, Solar, Alturdyne and Tritek have designed, built and successfully tested a 200 kW POGT consisting of a non-catalytic POR integrated with the retrofitted 200 kW gas turbine. The experimental studies were completed for the 200 kW POGT solely, and for a combined heat and power unit consisting of the POGT and a boiler with modified burner. The results are positive; a detailed report has been issued including recommendation for retrofit conversion of a conventional gas turbine to POGT duty.

Under the ongoing DOE project, the team has evaluated POGT applications for co-production of power and hydrogen/syngas from coal-derived fuel or natural gas, and conducted a design study to retrofit conventional gas turbines with power output 5-100 MWe to POGT operation.

This report for DOE project 42649 was prepared by GTI and Siemens.

Approach

The project approach includes analytical, modeling and design studies of turbine performance and POGT-based systems, retrofit design study for conversion of a conventional turbine to a POGT, combustion instabilities study in the POR, and experimental study of materials for hot sections of the turbines in a reducing atmosphere. The following steps have been taken: selection of gas turbine candidates for retrofit to POGT duty; evaluation of the POGT performance for the retrofitted turbines and comparison with performance of conventional turbines; identification of the IGCC and power plant schemes for industrial applications; preparation of an Aspen-based model for POGT and plant studies; definition of specifications for retrofit design of the selected turbines to POGT; fulfillment of the feasibility retrofit design for the selected three turbines; development of a conceptual design of a IGCC-POGT plant and selection of the major units; conducting performance analysis to form the basis for decision making to build POGTs and new power plants offering a mix of multiple products (electricity, syngas and/or hydrogen, steam) for industrial high efficiency and low emission operations.

Results

After evaluation of two systems of the IGCC-POGT plants with air-blown and oxygen-blown gasifiers, the oxygen-blown IGCC-POGT unit has been selected for the detailed study, Figures 1 and 2. Using the developed Aspen-Plus model, performance calculations of the IGCC key components, gasifier and POGT, have been completed during the reporting period. Syngas recirculation was used for the oxygen-blown fluid-bed gasifier to maintain the required gasifier performance. Selection of syngas recycle compressors that can accommodate syngas upstream from syngas cleaning and supply to the gasifier has been performed. Schematics and equipment for the ASU have been reviewed, and a cryogenic ASU has been selected for application in the IGCC-POGT plant.

Gasifier performance for bituminous coal in both air-blown and oxygen-blown versions has been calculated, and product gas and clean syngas compositions as well as all required parameters have been defined. Based on gas turbine standards for gaseous fuel contaminant levels, the impurity requirements have been also calculated to set the basis for the clean-up system evaluation. Two versions of the gas cooling and cleaning system have been considered, and the more advanced warm system has been selected for future evaluations.

In this reporting period, work was conducted on calculations of hydrogen production using H_2 separation membranes for the IGCC-POGT plant with an oxygen-blown gasifier. Four locations of the separation units were evaluated. The first is just at the gasifier exit where the syngas temperature is the highest. The second is in the syngas recycling stream where the gases are partially cleaned and cooled. The third location is after the cleaning and cooling system before the POGT. In the fourth, the H_2 membrane separator is located in the exhaust stream after the POGT. Because of the low partial pressure of hydrogen, an additional H_2 compressor is required to bring the hydrogen pressure to a level similar to other separation units. Schematics of the IGCC-POGT plants are presented in Figures 1 and 2. All four options have been evaluated in detail, and

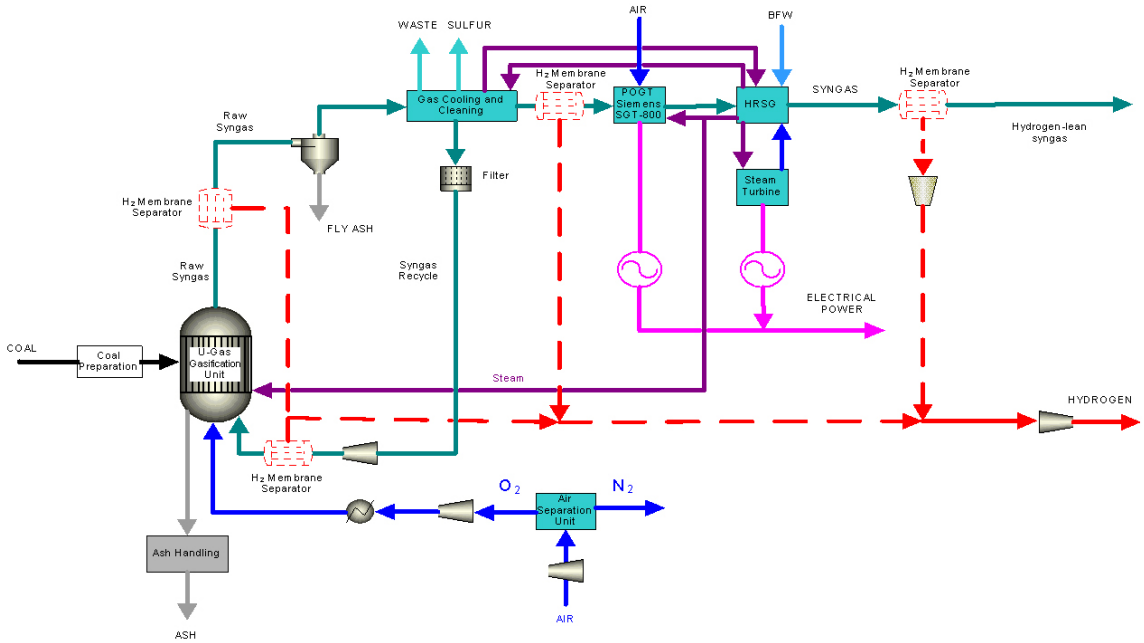

FIGURE 1. IGCC-POGT Plant Schematic with H_2 Membrane-Separators for Co-Production of Electricity, Hydrogen and Syngas

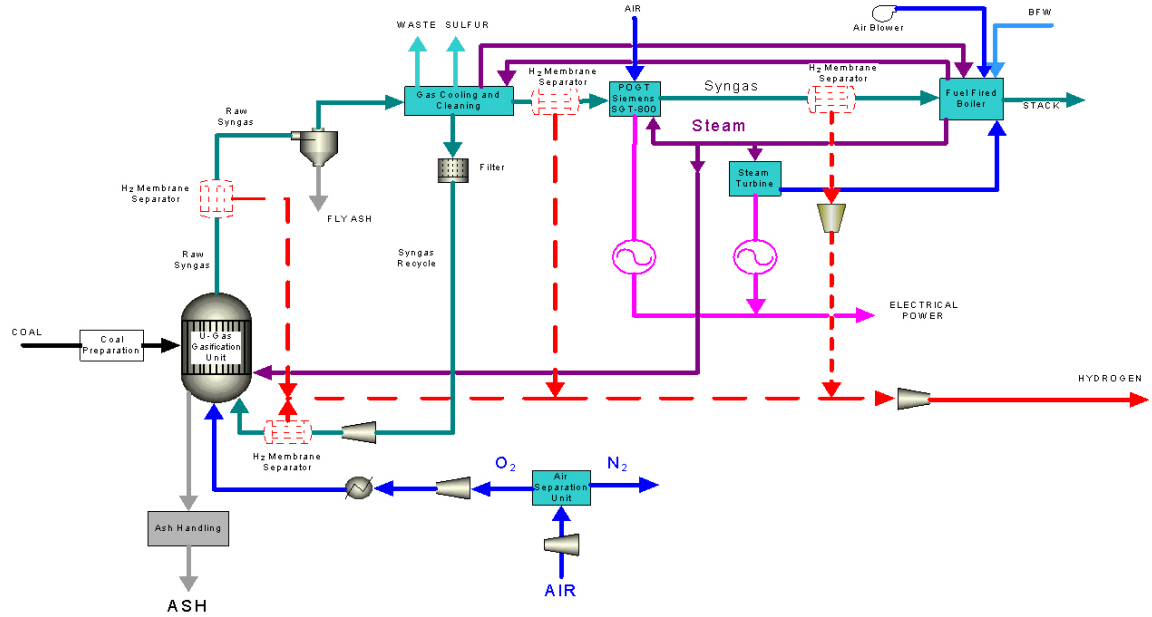

FIGURE 2. IGCC-POGT Plant Schematic with H_2 Membrane-Separators for Co-Production of Electricity and Hydrogen

hydrogen production rate and syngas composition and performance after the hydrogen separators were calculated. The IGCC-POGT plant schematic in Figure 1 is considered for a relatively moderate or low hydrogen production rate. In this case, the exhaust from the POGT still has potential for utilization as a syngas for different applications. Another version of the IGCC-POGT plant is presented in Figure 2. In this case, the hydrogen production rate could be high, and depleted syngas after the POGT is combusted in a fuel-fired boiler to produce high temperature/high pressure superheated steam mostly for electricity production as well as for use in the IGCC plant. Modeling results for four versions of the IGCC-POGT plant with co-production of power and hydrogen/syngas are presented in Table 1.

TABLE 1. IGCC-POGT Units Aspen Modeling Results

Version 1: High Hydrogen with Syngas			**Version 2: Low Hydrogen with Syngas**	
Chemical energy input	100%		Chemical energy input	100%
Compressor work required	7%		Compressor work required	6%
POGT unit work produced	13%		POGT unit work produced	13%
Hydrogen energy produced	39%		Hydrogen energy produced	19%
Syngas energy produced	13%		Syngas energy produced	23%
Total heat produced	23%		Total heat produced	31%
Hydrogen and syngas sensible heat	3%		Hydrogen and syngas sensible heat	2%
FFB exhaust heat	3%		FFB exhaust heat	5%
Heat losses	12%		Heat losses	12%
Electricity production through bottoming steam cycle	10%		Electricity production through bottoming steam cycle	13%
Total electricity production	16%		Total electricity production	20%
Total energy production	68%		Total energy production	62%
Version 3: High Hydrogen w/o Syngas			**Version 4: Low Hydrogen w/o Syngas**	
Chemical energy input	100%		Chemical energy input	100%
Compressor work required	7%		Compressor work required	6%
POGT unit work produced	13%		POGT unit work produced	13%
Hydrogen energy produced	39%		Hydrogen energy produced	19%
Syngas energy produced	0%		Syngas energy produced	0%
Total heat produced	35%		Total heat produced	51%
Hydrogen and syngas sensible heat	1%		Hydrogen and syngas sensible heat	0%
FFB exhaust heat	6%		FFB exhaust heat	10%
Heat losses	12%		Heat losses	12%
Electricity production through bottoming steam cycle	15%		Electricity production through bottoming steam cycle	21%
Total electricity production	21%		Total electricity production	29%
Total energy production	60%		Total energy production	48%

POGT performance calculations were conducted for four Siemens gas turbines, SGT-100, SGT-400, SGT-800 and SGT6-6000G. For SGT-800, POGT performance was defined for both coal-derived fuel and natural gas. For SGT-100, SGT-400, and SGT6-6000G, POGT performance was identified with natural gas as a main fuel. The procedure for performance calculation was developed by GTI and Siemens, and is briefly described below for the SGT6-6000G.

Siemens has provided design-point data for these turbines, including mass flows, volumetric flows, pressures, and temperatures for the compressors, burners, and expanders. GTI has produced the Aspen-Plus models for SGT6-6000G, for operation in conventional and POGT modes. Four models were actually generated. In the first step, GTI has calculated the performance for both engines in conventional mode with the goal to match as close as possible the major parameters, such as power output, turbine inlet temperature and pressure ratios for compressor and expander, and mass and volumetric flow rates. The results of calculations were sent to Siemens, and after approval of the matching parameters, GTI has conducted calculation of the POGT mode for the SGT6-6000G. Siemens has reviewed the results of the first Aspen run trials and sent comments and required steam flows to provide the needed blade path temperatures and cooling capacities. The resulting Aspen-Plus model schematic is shown for POGT-SGT6-6000G in Figure 3. The finally calculated POGT and gas turbine performance for the four engines, SGT-100, SGT-400, SGT-800 and SGT6-6000G, is presented in Table 2. It is notable that in POGT mode turbine net power could be increased by about 40 to 80%, and the POGT specific power (turbine net power per lb expander exhaust mass flow) is twice the value of the conventional turbine, Figure 4.

POGT feasibility design was completed for conversion of three conventional gas turbines, SGT-100, SGT-400 and SGT-800 to POGT mode operation. A schematic for the SGT-800 gas turbines is shown in Figure 5.

The basic development approach for the POGT is to use existing SGT-engine components as much as possible, making whatever modifications are necessary to meet specified performance requirements. A heat transfer analysis supported by Aspen-Plus calculations was used to identify the cooling stream flows to provide the required cooling capacity for the turbine expander. The design conditions for the compressor and expander for the POGT are within the capabilities of existing commercial technology, but the equipment is physically different from commercially available equipment. Therefore, a certain amount of development effort would be needed to produce a POGT.

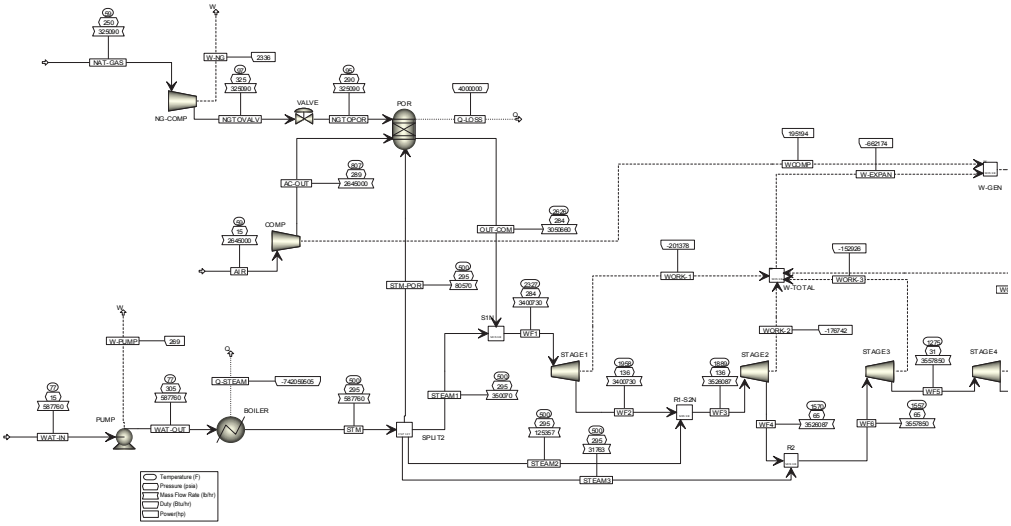

FIGURE 3. Aspen-Plus Schematics for SGT6-6000G Converted to a POGT, Version 3

TABLE 2. Conventional Turbine and POGT Performance for SGT-100, SGT-400, SGT-800 and SGT6-6000G

Conventional Turbine and POGT Performances for SGT-100, SGT- 400, SGT-800 and SGT6- 6000G									
		SGT-100	POGT SGT-100	SGT-400	POGT SGT-400	SGT-800	POGT SGT-800	SGT6-6000G	POGT SGT6-6000G
Compressor inlet flow rate	lb / h	162,865	95,700	307,310	171,000	1,013,760	490,000	4,513,877	2,645,000
Compressor inlet temperature	° F	59	59	59	59	59	59	59	59
Compressor inlet pressure	psia	14.7	14.7	14.7	14.7	14.7	14.7	14.7	14.7
Compressor exit flow rate	lb / h	128,663	95,700	233,556	171,000	1,013,760	490,000	3,435,407	2,645,000
Compressor exit temperature	° F	759	759	785	785	874.3	833.5	806.9	806.9
Compressor exit pressure	psia	215.3	215.3	245.9	245.9	280.8	280.8	289.5	289.5
Compressor power	MW	8.36	4.91	16.39	9.12	61.1	28	248.4	145.56
Expander inlet flow rate	lb / h	154,074	125920	271,232	217,730	947,030	791,000	4,171,125	3,400,730
Expander inlet temperature	° F	2038	1965	2300	2280	2318	2287	2415	2327.2
Expander inlet pressure	psia	211	211	241	241	275	275	283.71	283.71
Expander exhaust flow rate	lb / h	165,703	130,500	313,345	235,850	1,033,200	841,000	4,613,297	3,557,850
Expander exhaust temperature	° F	980	924	1024	1023	1004	1079	1035	1024.8
Expander exhaust pressure	psia	14.8	14.8	14.8	14.8	14.6	14.6	14.8	14.8
Expander power	MW	13.61	14.88	29.34	30.01	105.4	111.3	493.49	493.78
Turbine net power	MW	5.25	9.96	12.95	20.89	44.4	83.4	245.09	348.23
Turbine specific power	kW / pps	114.1	274.8	148.8	318.9	154.7	357.0	191.3	352.4

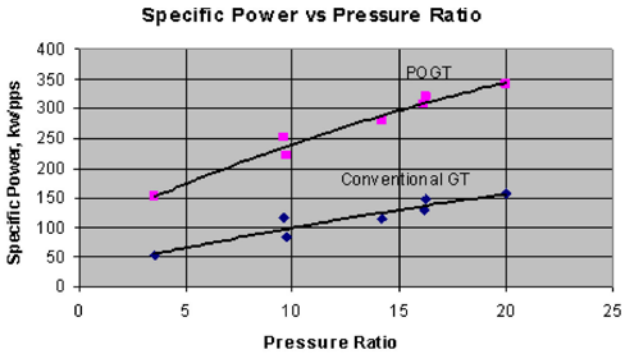

FIGURE 4. Specific Power Output vs. Pressure Ratio for Conventional Gas Turbine and POGT

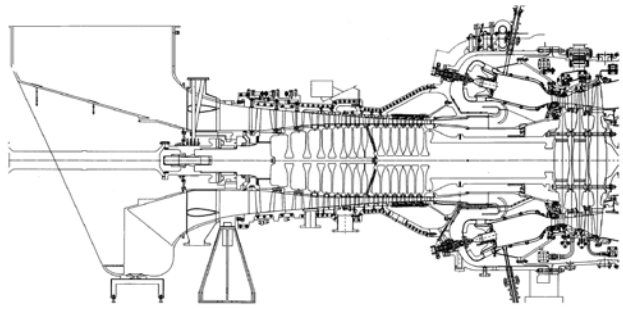

FIGURE 5. SGT-800 Gas Turbine Schematic

Siemens has completed the work on a feasibility design for conversion of the three engines, SGT-100, SGT-400 and SGT-800 to POGT duty, and two draft reports, one for SGT-100 and SGT-400, and another for SGT-800 are completed and submitted. The titles and tables of contents for both reports are presented.

Partial Oxidation Gas Turbine (POGT) Feasibility Design Based on Siemens SGT-100 and SGT-400 Gas Turbines

1. Summary ... 1
2. Introduction ... 1
3. Project Objectives ... 2
4. SGT-100 and SGT-400 Gas Turbines ... 2
5. Technical Issues and Feasibility Designs ... 4
   5.1 Compressor Modifications ... 4
      Option A - Redesign Compressor Blade Path ... 5
      Option B - Smaller Siemens Gas Turbine Compressor ... 5
      Option C - Separate Compressor, Same Shaft ... 6
      Option D - Separate Compressor, Separate Shaft ... 7
      Best Options ... 7
   5.2 POR-POGT Interface ... 8
      Option A: Circumferentially Distributed PORs ... 8
      Option B: Single POR with Volute Expander Inlet ... 8
   5.3 Expander Modifications ... 9
      5.3.1 POGT-400 Blade Path Re-Design ... 9
      5.3.2 Expander Inlet and Exhaust ... 10
      5.3.3 Expander Materials ... 10
      5.3.4 Expander Cooling ... 10
   5.4 Generator Modifications ... 11
   5.5 Reduction Gear Modifications ... 12
   5.6 Rotor and Bearing Modifications ... 13
6. Turbine Retrofit Conversion Plan ... 13
7. Conclusions ... 13

Partial Oxidation Gas Turbine (POGT) Feasibility Design Based on the Siemens SGT-800 Gas Turbine

1. Summary ... 1
2. Introduction ... 2
3. Project Objectives ... 3
4. Candidate Retrofit Turbines ... 3
5. Technical Issues and Feasibility Design ... 5
   5.1 Expander Modifications ... 7
      5.1.1 Expander Inlet and Exhaust ... 7
      5.1.2 Expander Materials ... 8
      5.1.3 Expander Cooling ... 8
   5.2 Compressor Modifications ... 8
      Option 1: New Compressor ... 9
      Option 2: Compressor from Another Engine ... 9
      Option 3: Connect Separate Compressor to Generator ... 11
      Option 4: Separate Compressor Branch from Drive Train ... 11
      Option 5: Compressor-Expander-Generator Arrangement ... 12
      Best Option ... 12
   5.3 POR-POGT Interface ... 13
      Option 1: Circumferentially Distributed PORs ... 13
      Option 2: Single POR with Volute Expander Inlet ... 14
      Better Option ... 14
   5.4 Generator Modifications ... 14
   5.5 Reduction Gear Modifications ... 16
   5.6 Rotor and Bearing Modifications ... 18
6. Turbine Retrofit Conversion Plan ... 18
7. Conclusions ... 19
Appendix A - POGT Stream Properties ... 20
Appendix B - Commercial Air Compressors ... 22

When the conventional gas turbine is converted to a POGT about 50% less compressor power is required and 60-90% more net power output is produced while the expander power is maintained practically the same. In Figure 6, the expander, compressor, and net power for the three engines, both conventional turbines and POGTs, are presented.

The defined effort and time needed for POGT conversion of the three engines, POGT-100, POGT-400 and POGT-800 are shown in Table 3. The effort for the POGT-800 is considered for 100%.

Several versions of system configuration for POGT-based co-production of power and hydrogen

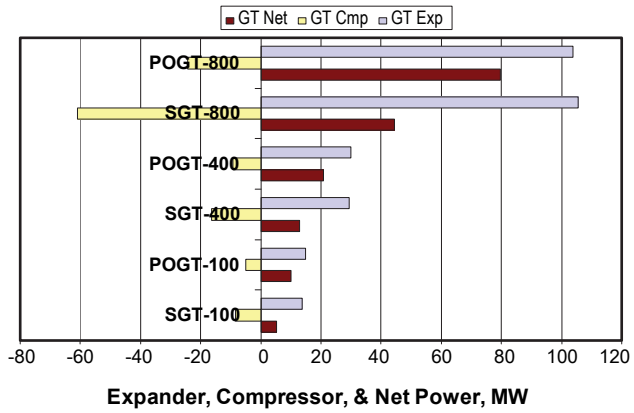

FIGURE 6. Expander, Compressor and Net Power Output for POGT- and SGT-100, -400, -800

from natural gas have been developed and an Aspen-Plus model has been created. In Figure 7, a schematic of one version is presented for co-production of power and syngas where syngas from the POGT exhaust is used as a fuel gas for a conventional steam-methane reformer (SMR) for hydrogen production. Another version of a POGT-based natural gas-fired system is presented in Figure 8. Electricity and hydrogen from natural gas in a POGT-based combined cycle are co-produced. Hydrogen production is considered via dense membranes installed inside the two-staged POR and the POGT exhaust. Several versions of the system shown in Figure 8 have been calculated, and modeling results for three versions with co-production of electricity and hydrogen from natural gas are presented in Table 4.

In the reporting period, there was no actual work conducted by ORNL for the project. In the 2008 Annual Report, however, the results and analysis were presented for one series of testing for POGT hot sections materials operated in a reducing atmosphere.

Summary of the major results of the ORNL testing are presented below.

- Samples of 25 different base material/coating combinations were exposed to a simulated POGT environment produced by the partial oxidation of natural gas with air. The samples were selected and supplied by Siemens and Solar.
- Most coatings did not provide an improvement on the corrosion resistance.
- The alumina forming alloys generally showed smaller weight gains than the majority of chromia forming alloys.

Study of combustion instabilities in a POR has been completed by Georgia Tech. A final report titled "Assessment of Combustion Instability of Partial Oxidation Gas Turbine Combustion Chambers" has

TABLE 3. Relative Development Efforts for POGT Retrofit Conversion

		POGT-100	POGT-400	POGT-800
Expander	Re-design HP & LP flow fields	-	7%	-
	Modify inlet and exhaust, Design airfoils, modify cooling	7%	7%	7%
	Blade vibration test, Rig test (Aero/Ht.Tr.), Film cooling rig test, Heat Transfer Test, High-Temp Rotating Rig Test	28%	37%	28%
Compressor	Use separate commercially available compressor	Purch	Purch	-
	Shorten blades and vanes, Blade vibration test	-	-	3%
	Design (scaled for rig test) Rig test	-	-	7%
Generator	Use larger model	Purch	Purch	Purch
Reduction Gears	Design new reduction gears	Purch	Purch	13%
Rotor & Bearings	Larger rotor, different bearings	10%	10%	10%
Tooling	Tooling Development	3%	3%	3%
	Tooling Manufacture	8%	8%	8%
Engine Testing	Engine initial test, Thermal paint test	21%	21%	21%
	Totals	**77%**	**92%**	**100%**
	Development Time (Years)	6	7	6

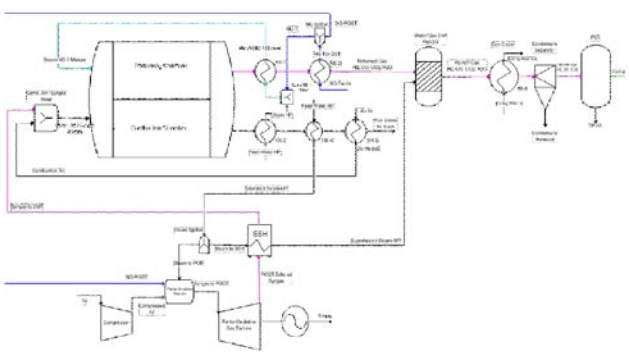

FIGURE 7. POGT for Co-Production of Power and Syngas in Combination with SMR

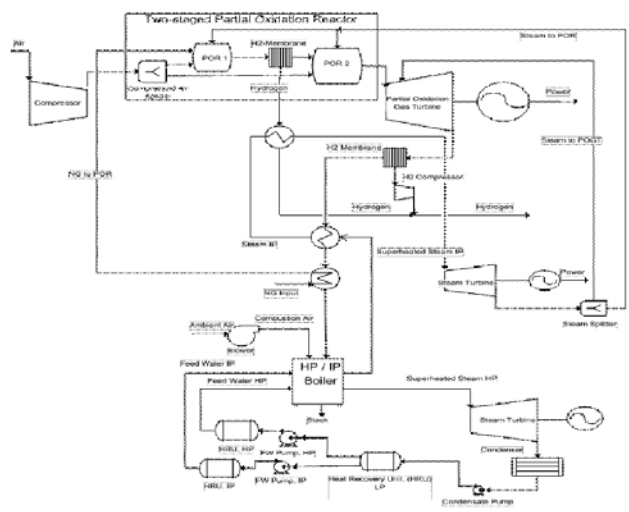

FIGURE 8. POGT Combined Cycle for Co-Production of Power and Hydrogen

been submitted. In the reporting period, there was no actual work conducted by Georgia Tech for the project. The work at Georgia Tech evaluated the response of rich, premixed combustion systems to acoustic oscillations.

There are two key mechanisms that must be considered in rich systems: the response of the flame to velocity oscillations (such as due to vortex shedding), and fuel/air ratio oscillations. In the recent WebEx project review, Georgia Tech has summarized the implications for POGT instability mitigation as following:

- Velocity coupled response of rich and lean premixed flames are very similar, so experience derived from dry low NOx (DLN) systems carry over directly to POGT systems.
- Fuel/air ratio coupled response of POGT and DLN premixed flames are very different from each other. The gain of POGT systems is less than that of DLN systems at low St_2; POGT systems are 180° out of phase from DLN systems operating at the same s_L; POGT systems are stable wherever DLN systems unstable; and fuel peg locations should be shifted.

TABLE 4. POGT Based Cycles for Co-Production of Electricity and Hydrogen from Natural Gas; Modeling Results

Version 1			**Version 3**	
Chemical energy input	100%		Chemical energy input	100%
Net electricity produced in POGT	24%		Net electricity produced in POGT	28%
Hydrogen energy produced	47%		Hydrogen energy produced	38%
Total unused heat and losses	0.9%		Total unused heat and losses	0.7%
Hydrogen sensible heat	0.2%		Hydrogen sensible heat	0.1%
FFB exhaust heat	28%		FFB exhaust heat	32%
Total energy production	71%		Total energy production	66%
Version 2			**Version 1: H2 membranes in POR and**	
Chemical energy input	100%		**POGT exhaust**	
Net electricity produced in POGT	25%			
Hydrogen energy produced	44%		**Version 2: H2 membranes in POR only**	
Total unused heat and losses	0.3%			
Hydrogen sensible heat	0.2%		**Version 3: H2 membranes in**	
FFB exhaust heat	30%		**POGT exhaust only**	
Total energy production	69%			

The key conclusion that has been drawn from the study is that rich premixed systems are certainly not more susceptible to these instabilities than lean systems, and are possibly less prone to instability.

Conclusions and Future Directions

Three candidate turbines, SGT-100, SGT-400 and SGT-800, were finally selected for design study of retrofit conversion to POGTs. The work on feasibility designs for conversion of the three engines to POGT duty has been practically completed, and two draft reports, one for SGT-100 and SGT-400, and another for SGT-800 are completed and submitted. The required effort and time needed for POGT development and testing of each of the three engines, POGT-100, POGT-400 and POGT-800, are defined and presented in the reports.

Aspen-Plus models were developed and detailed POGT performance was defined and compared with performance of conventional GTs for the three selected turbines. In addition, POGT and GT performance was indentified for the SGT6-6000G. In POGT mode, the engine power output is increased by 60-90% compared to a conventional gas turbine, and specific power (power output per pound of mass flow through the expander) is twice or more compared to a conventional turbine.

A POGT-based advanced IGCC process has been developed and all major components have been identified. Oxygen blown fuel-flexible fluid bed gasifier and a novel POGT unit are the key components of the IGCC plant for co-producing electricity, hydrogen and/or syngas in industrial applications.

The IGCC-POGT system study was completed. ASU and warm cleaning systems were selected and incorporated into the Aspen model. Hydrogen separation membranes were used for hydrogen production in the IGCC-POGT plant. Performance of the updated IGCC-POGT plant was calculated for several versions with co-production of electricity, hydrogen and syngas.

Study of POGT-based systems for co-production of power and hydrogen from natural gas was completed. Aspen-Plus models have been developed and calculations are completed for several versions with co-production of electricity and hydrogen.

One series of testing for POGT hot section materials operated in a reducing atmosphere was completed and results of the experimental data were presented.

A study of combustion instabilities in a POGT was completed, and the key conclusion is that rich premixed systems are certainly not more susceptible to these instabilities than lean systems, and are possibly less prone to instability.

The main future direction is to complete POGT-based natural gas-fired systems studies, and complete performance analyses to create the basis for development of a commercial POGT prototype. Another direction is to evaluate POGT-based combined cycles for electricity production only and for co-production of power and gas-to-liquid, and with optional separation and capture of CO_2.

FY 2009 Publications/Presentations

1. Four Quarterly Progress Reports, DOENT 42649-11, 12, 13 and 14.

2. "Partial Oxidation Gas Turbine for Power and Hydrogen Co-Production," WebEx Project Review, February 26, 2009.

3. J. Rabovitser, et.al., "Experimental Study of a 200 kW Partial Oxidation Gas Turbine (POGT) for Co-Production of Power and Hydrogen-Enriched Fuel Gas," ASME Turbo Expo 2009.

II.4 Fuel-Flexible Combustion System for Co-Production Plant Applications

Dr. Joel M. Haynes, Willy Ziminsky, Ben Lacy, William York, and Dr. Ertan Yilmaz
GE Global Research
1 Research Circle
Niskayuna, NY 12309
Phone: (518) 387-5813; Fax: (518) 387-7258
E-mail: haynes@ge.com

DOE Project Manager: Robin Ames
Phone: (304) 285-0978
E-mail: Robin.Ames@netl.doe.gov

Subcontractors:
- Prof. Tim Lieuwen, Prof. Suresh Menon, Prof. Jerry Seitzman
  Georgia Institute of Technology, Atlanta, GA
- GE Energy, Greenville, SC

Contract Number: 41776

Start Date: May 12, 2003
End Date: December 31, 2008

FY 2009 Objectives

- Design swirl-based combustion nozzles for high-hydrogen syngas combustion.
- Evaluate performance of swirl-based combustion nozzle designs, Prototype-1*, in a single nozzle configuration at realistic full-load operating conditions.
- Demonstrate performance of swirl-based combustion nozzles in a full-can configuration with high-reactivity syngas.

Accomplishments

- Completed swirl-based combustion nozzle design for high-hydrogen syngas operation.
- Demonstrated flameholding performance improvements on full-scale swirl-based nozzle compared to baseline.
- Demonstrated full operability for Prototype-1* nozzles.
- Extended the operability margin over baseline swirl stabilized nozzle on high-hydrogen fuels.

Introduction

Future high-efficiency, low-emissions generation plants that produce electric power, transportation fuels, and/or chemicals from fossil fuel feedstocks require a new class of fuel-flexible combustors. In this project, a validated combustor approach is being developed which will enable single-digit NOx operation of future generation plants with low-Btu off-gas and high-hydrogen fuels, with the flexibility of process-independent backup with both natural gas and liquid fuels. This combustion technology will overcome the limitations of current syngas gas turbine combustion systems, which are designed on a site-by-site basis, and enable improved future co-generation plant designs. In this capacity, a fuel-flexible combustor will enhance the efficiency and productivity of future co-production plants.

Approach

In the initial phase, the project characterized a variety of fuel-flexible combustion architectures and down-selected the most promising concepts for experimental evaluation. At the plant level, existing processes and resulting off-gas stream compositions were characterized to define fuel specifications from existing processes. Improvements in plant design were forecast and their impact on fuel stream compositions was modeled.

Characterization of syngas flames was pursued to improve syngas combustion modeling. Flame extinction limits, as a function of fuel composition were measured, and reduced order sub-models for computational fluid dynamic design tools were generated.

Two combustor prototypes incorporating emerging technologies were developed and tested for extended fuel performance range. In the final phase of the project, the focus has been on demonstrating high-hydrogen syngas performance of novel fuel nozzle designs. Several swirl-based designs were evaluated. A preferred design was selected and scaled-up to a full-can demonstration with high-hydrogen syngas.

Results

In the final year of the project a swirl stabilized fuel nozzle was developed with increased operability margin with high-hydrogen fuels. A prototype fuel nozzle was evaluated at various cycle conditions.

Detailed measurements of emissions and flame holding propensity were conducted at engine operating conditions in a high-pressure and temperature test rig.

The first prototype demonstrated lower NOx emissions with high-hydrogen syngas than the natural gas baseline. However, the operability of this prototype was limited to lower firing temperatures. The second swirl stabilized prototype, Prototype-1*, had the best operability with syngas at engine realistic operating conditions, but the NOx emissions rose slightly. The emission profile for the second prototype is shown in Figure 1.

Full-can multi-nozzle combustion tests were planned as a result of the successful demonstration of Prototype-1*. Full-can premixed syngas combustion experiments were conducted at GE's Gas Turbine Technology Laboratory in Greenville, South Carolina. The tests established a milestone for the first full-premixed syngas can combustor demonstration at realistic engine conditions. The test produced a complete set of operating data on emissions, dynamics, and operability. Video of the premixer during premixed operation was also obtained.

Testing of the full head end was conducted with high-reactivity syngas, consisting of H_2 and CO, with no operability difficulties such as combustion dynamics or flashback (at normal conditions). A fraction of the syngas fuel was sent to the new premixer, while the rest was sent to the existing premix system of the dry low-NOx (DLN) combustor.

A single stable emissions point, plotted in Figure 2, was acquired at the design point with the reaction zone temperature just below F-class levels. Emissions were only slightly above the entitlement data (perfectly premixed) for a high-hydrogen syngas fuel obtained in a previous experiment. This is notable, since the head end was run with a non-uniform fuel split, and locally elevated temperatures would be expected to lead to higher NOx than a uniform head end temperature. For reference, the NOx data for methane from Leonard and Stegmaier [1] is included on the plot.

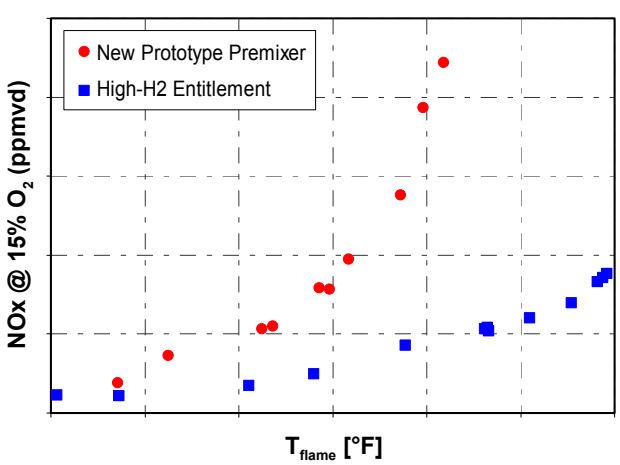

FIGURE 1. NOx Emissions on Hydrogen Fuel for Prototype-1*

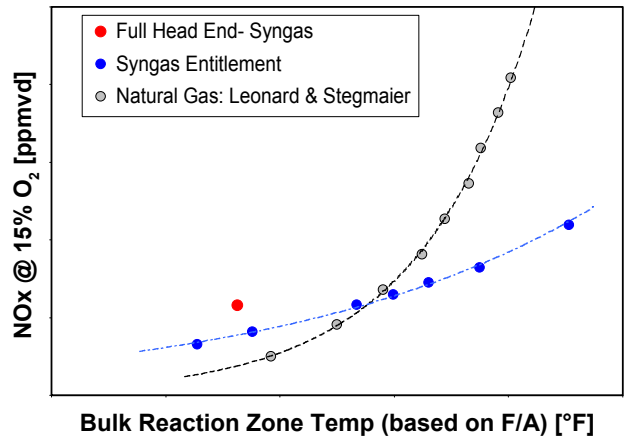

FIGURE 2. Can Combustion with Premixed Syngas and Entitlement Data

This combustion system with new premixer was designed for fuel-flexibility, meaning it should be able to operate with natural gas, syngas, and blends of these fuels. The experimental project included testing the new hardware with natural gas fuel. Combustion dynamic pressures were the same, or even slightly lower in amplitude, than the baseline hardware and were not a difficulty in normal operation. NOx emissions with natural gas were only marginally higher than the baseline.

Conclusions

A new combustor head end design was successfully operated with syngas fuel in a DLN (fully premixed) mode. NOx emissions were only slightly above entitlement levels. The head end (reaction zone) temperature was just below F-class levels. The new premixer exhibited excellent flashback margin at the design condition and at higher temperatures. To demonstrate the fuel-flexibility of the new premixer/combustor, operation on natural gas was obtained with a very small NOx penalty over the baseline (fielded) design, and no significant combustion dynamics were observed.

Special Recognitions & Awards/Patents Issued

1. Combustor nozzle for a fuel flexible combustion system (Patent pending).

References

1. G. Leonard and J. Stegmaier, "Development of an Aeroderiative Gas Turbine Dry Low Emissions Combustion System," ASME Paper 93-GT-288, Turbo-Expo 1993, Cincinnati, 1993.

II.5 Low-Swirl Burners for Hydrogen Gas Turbines in Near-Zero Emissions Clean Coal Power Plants

Robert K. Cheng (Primary Contact) and David Littlejohn
Lawrence Berkeley National Laboratory (LBNL)
MS 70-108B, 1 Cyclotron Road
Berkeley, CA 94720
Phone: (510) 486-5438; Fax: (510) 486-7303
E-mail: RKCheng@lbl.gov

DOE Project Manager: Robin Ames
Phone: (304) 285-0978
E-mail: Robin.Ames@netl.doe.gov

Subcontractor:
University of Iowa, Iowa City, IA

Contract Number: 678402

Start Date: October 1, 2007
End Date: September 30, 2009

FY 2009 Objectives

- Develop a dry, low-NO_x (DLN) combustion technology for the gas turbines in near-zero emissions clean coal integrated gasification combined cycle (IGCC) power plants that burn coal-derived syngases and hydrogen.
- Adapt LBNL's patented low-swirl combustion method for operation with natural gas, syngases and hydrogen fuels.
- Establish scaling rules and engineering guidelines for low-swirl burners (LSBs) to operate with natural gas, syngases and hydrogen.
- Seek gas turbine manufacturer/s to develop LSBs for the IGCC gas turbine combustors.
- Demonstrate and commercialize a LSB for utility-size gas turbines that meet the cost and performance targets of DOE Fossil Energy's Advanced Turbine Program.

Accomplishments

- Redesigned the LSB nozzle geometry to mitigate the influences of shear and corner recirculation on the hydrogen flames.
- Continued scaling-up of LSBs for F-frame engines in collaboration with a gas turbine manufacturer.
- Finalized a benchmark LSB configuration for evaluation at gas turbine conditions with natural gas and hydrogen.
- Formed an original equipment manufacturer (OEM)/national lab/university collaborative working group to develop new computational design tools for the LSB.

Introduction

This goal of this project is to develop a cost-effective and robust combustion system for the gas turbines in near-zero emissions IGCC coal power plants that burn high hydrogen fuel (80%+) and syngases derived from coal gasification. The DOE Fossil Energy Advanced Turbine Program sets a very aggressive emissions goal of less than 2 ppm NOx for these turbines. Current DLN combustion technologies that have been developed for burning of natural gas may not be readily adaptable to accommodate the fast burning and dynamic characteristics of the high hydrogen fueled flames. Some gas turbine manufacturers are considering reverting to the conventional and more polluting combustion methods that require treatment of the exhaust stream with expensive "tail-pipe" catalytic cleanup methods to reduce NOx to the targeted level.

All DLN combustion methods operate on the principle of lean premixed combustion where NOx formation can be reduced by burning of highly diluted lean fuel/air mixtures. These lean turbulent premixed flames are dynamic in nature and behave as self-propagating waves. They burn faster or slower according to the combustion properties of the fuel, and the thermal and fluid mechanical conditions of the fuel/air mixture, i.e. the initial temperature and pressure, flow velocity, and the type and intensity of turbulence. The complex coupling of the flame with turbulence dictates its dynamic behaviors and is the crux of the challenges in designing and engineering of DLN combustion systems for gas turbines. The conventional DLN approach is to hold the fast moving premixed turbulent flames within intensely swirling flows. The low-swirl combustion concept conceived at LBNL takes an opposite approach. It enables the premixed flame to propagate freely and burn in a divergent flow generated at the core of a weakly swirling flow.

Approach

The LSB was originally conceived for basic research. Laboratory studies and analysis have

provided the scientific foundation to facilitate the transfer of this emerging clean combustion technology to gas turbines. To adapt the LSB for the large-frame >200 MW hydrogen-fueled engines, the strategy is to optimize the basic LSB nozzle developed for a 7 MW natural gas engine to burn hydrogen, and collaborate with a gas turbine manufacturer to scale the design to larger sizes. The heart of the LSB is a patented swirler (Figure 1) engineered to produce the divergent flow. This design is capable of supporting stable turbulent lean premixed flames under a wide range of operating conditions. The characteristic signature of the LSB is a lifted flame that does not touch any part of the burner nozzle (Figure 2 photo insert). The LSB swirler can be adjusted to accommodate the changes in the combustion properties of various fuels. This is done by reconfiguring the swirler components to change the swirl intensity.

The development of an LSB for IGCC gas turbines starts with laboratory studies to optimize the configuration for burning of lean hydrogen flames whose NOx emissions are below 2 ppm. The experiments also provide turbulent flame speed data and quantitative information on the LSB flowfield to support the development of an analytical model that can be used to design gas turbines hardware. Testing of the LSB at simulated gas turbine conditions verifies its operability and indicates improvement needs. Scaling of the LSB to large capacities and adaptation to different engine configurations requires the development of new computational design tools. This is accomplished by detail experimental and computational studies in collaboration with researchers from national laboratories, universities and OEMs. Joint developments of the analytical model for hydrogen flames and the state-of-the-art computational methods are the essential steps to resolve issues on combustion intensity, dynamics, emissions, flashback, blowoff and auto-ignition. The designs of the LSB for different engines are led by the OEMs to configure hardware that meets specific engine and system operation requirements.

FIGURE 1. The swirler developed as a benchmark for experiments and computational studies has features that are amenable for adaptation to heavy-frame gas turbines.

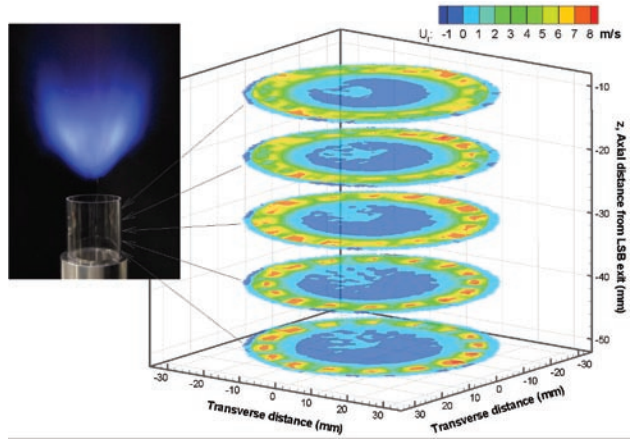

FIGURE 2. A transparent nozzle enables the measurements of the velocity inside the LSB to provide data needed for the development of computational design tools. Shown here are the contour plots of the tangential velocity component, u_t, at five locations. At the lowest positions, the red/orange contours show the pronounced imprint of the annulus swirl vane structure while the blue contours in the center indicate a non-swirling core. Correct prediction of the interaction between the swirled and the unswirled flows is deemed to be an important metric of the CFD methods for the LSB.

Results

The experiments conducted at the National Energy Technology Laboratory's (NETL's) SimVal high-pressure combustion facility in Fiscal Year 2007 and the analysis completed in FY 2008 have confirmed the LSB's potential to meet the DOE Fossil Energy goal of <2 ppm NOx at combustion temperatures of $2{,}500 < T_1 < 2{,}650$°F. Due to the high reactivity and diffusivity of H_2 molecules, the H_2 flames are very sensitive to the shear layer generated by the swirler, and to the large recirculation zone formed at the entrance corners of the combustion chamber. To mitigate these influences, the exit geometry of the LSB nozzle has been redesigned to retard the shear layer and to shield the flame from the corner recirculation zone. The effectiveness of the new nozzle with a diffuser cone was investigated by testing several prototypes with different cone angles and geometries. The atmospheric experiments showed that the new nozzle suppressed flame noise and the flame's propensity to oscillate. However, the shear layer effects could not be eliminated completely and showed the need to further optimize the aerodynamic profile of the nozzle to mitigate the shear intensity.

To continue the development for hydrogen operation, the LSB swirler has been modified to incorporate features that are amenable for adaptation to heavy-frame gas turbines. Based on the input from gas turbine OEMs, this LSB swirler (Figure 1) features 16 aerodynamically shaped thick vanes and a center channel with thick wall tapered to a thin trailing edge to reduce shear. It is sized for NETL's SimVal facility where the next round of experiments at simulated gas turbine conditions will be performed. The LSB with the new swirler has been evaluated through a series of experiments with methane, hydrogen and methane/hydrogen fuel blends at atmospheric condition. Its functionality and performance were found to be consistent with earlier versions of the LSB.

The collaboration with an OEM to scale the LSB to the utility-size gas turbines is progressing. A second round of tests in a combustion chamber of a 200 MW natural gas-fueled turbine is scheduled for June 2009. Our OEM collaborators consider the lack of high-fidelity computational fluid dynamics (CFD) design tools for the LSB to be a potential impediment for its adaptation. In response, a workshop group among researchers from OEMs, national laboratories and universities has been formed to facilitate the development of new CFD tools. The LSB with the new thick-vane swirler was designated as a benchmark for the working group members to use in laboratory studies and computations. It has already been scaled to different sizes to fit the various experimental facilities. Our experimental measurements on this new LSB have focused on detailed measurements of the flowfields of methane and hydrogen flames in quartz enclosures for validation of the computational results. To provide a complete set of data as requested by the CFD developers, the flowfields inside the LSB were measured by the use of a transparent nozzle (Figure 2). These data have already been shared with the OEMs for improving the fidelity of Reynolds averaged Navier-Stokes (RANS) tools and with the developers of large eddy simulations (LES).

On a fundamental level, the basic structures of turbulent H_2 flames were investigated by OH planar laser induced fluorescence (OH-PLIF). Due to the high diffusivity of H_2 molecules, the interaction of H_2 premixed flames with turbulence generates features that are not found in hydrocarbon flames (Figure 3). This is confirmed by high-fidelity direct numerical simulation (DNS) of the LSB H_2 flames conducted by computational research at LBNL that shows intense burning in local hot spots. Consequently, current turbulent flame models assuming slightly non-uniform heat releases is not applicable. The goal of our collaboration with the computational researchers is to characterize the features of H_2 flames to support the development of robust flame models that can be used in LES and RANS. The high-fidelity DNS employs detailed chemical kinetics scheme and transport coefficient to provide 3-dimensional time-dependent information that cannot be easily obtained by experiments. The synergistic computational effort, supported by the DOE Office of Mathematics Information and Computational Sciences, will contribute to the scientific foundation of

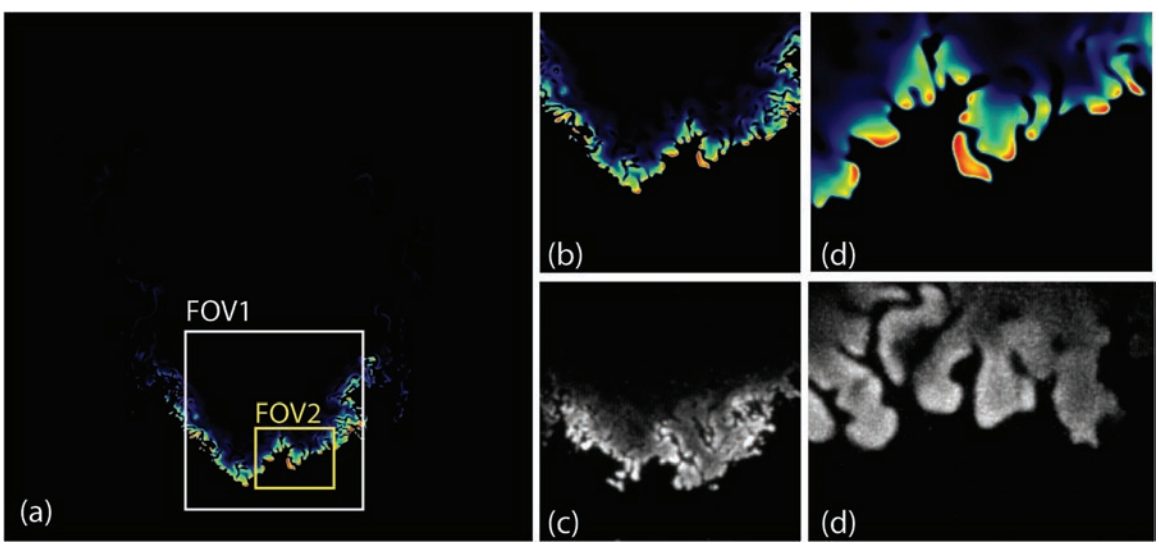

FIGURE 3. Experiments and high fidelity DNS helps to characterize the distinct features of H_2 flames. A Typical slice of OH concentration from the simulation is shown in (a) where red indicates high OH values that are correlated with the flame front. The boxes FOV1 and FOV2 represent the fields of view of OH-PLIF measurements of approximately 50 mm and 26 mm respectively. (b) and (d) are zooms of the simulation over FOV1 and FOV2, (c) and (e) are the corresponding OH-PLIF images. Both simulation and measurement show that H_2 flames are "discontinuous" and burn with local intense hot-spots. Such information is invaluable to help gain a better understanding of the fundamental mechanisms controlling the reaction rates and emissions.

H_2 combustion for LSB development as well as for the other H_2 projects in Fossil Energy's Advanced Turbine Program.

Conclusions and Future Directions

Laboratory experiments has shown that a DLN method conceived at LBNL called a low-swirl burner is a promising technology for the H_2 and syngases-fueled gas turbines in near-zero emissions IGCC coal power plants. The LSB nozzle has been redesigned to mitigate some side effects associated with the fast burning and diffusive nature of H_2. Scale-up of the LSB for utility size gas turbines with an OEM partner continues with new efforts on the development of CFD tools. Collaboration with computational research has shown that the CFD tools will need new turbulent flame models for H_2 to characterize their high non-uniform structures.

The focus of future work is on developing the basic layout of an LSB that is capable of operating with natural gas, unshifted syngases, and high hydrogen fuels hydrogen with provisions to address burner/combustor issues such as premixing, flashback and auto-ignition. The development of a scale-up LSB for natural gas utility-size gas turbine will be guided by the results from the second round of full-scale tests. Laboratory studies at atmospheric and simulated gas turbine conditions will support the developments of hardware, CFD and H_2 flame model.

- Initiated a feasibility study of a "three fuel" LSB, i.e., natural gas, unshifted syngases, and high hydrogen fuels for gas turbines.
- Test benchmark LSB at NETL Morgantown's SimVal facility with natural gas and hydrogen.
- Continue scale up of LSB to the size for utility gas turbines.
- Share the results of "three fuel" feasibility study with OEMs.

FY 2009 Publications/Presentations

1. R.K. Cheng and D. Littlejohn, "Development of a Low-Swirl Burner for Syngas and H_2 Gas Turbines," Paper presented at the Pittsburgh Coal Conference on September 30, 2008.

2. R.K. Cheng, "Low-Swirl Combustion – An Ultra-low Emissions Technology for Industrial Heating and Power Generation and Its Prospects for Fuel-Flexible Turbines," Seminar presented at Siemens Turbomachinery, Lincoln, United Kingdom on October 10, 2008.

3. R.K. Cheng, "Fundamental Issues of Lean Premixed Combustion for Fuel-Flexible Low-Swirl Burner for IGCC Gas Turbines," Seminar presented at the Technical University Eindhoven, the Netherlands, October 13, 2008.

4. R.K. Cheng, "Laboratory Investigations of Low-Swirl Burner Operating with Syngases and CH_4/H_2 Fuel Blends," Presented to Fuel-Flexible Working Group Meeting of the European Turbine Network, Brussels, Belgium, October 14, 2008.

5. R.K. Cheng and D. Littlejohn, "Adaptation of the Low-Swirl Combustion Technology to Syngas and H_2 Gas Turbines," Paper presented at the European Turbine Network 4th International Conference, Brussels, Belgium, October 15, 2008.

6. R.K. Cheng and D. Littlejohn, "Low-Swirl Burner for H_2 Gas Turbines in Near-Zero Emissions Clean Coal Power Plants," Web-based review presentation to NETL, December 2, 2008.

7. R.K. Cheng, "Laboratory Research on Fuel-Flexible Low-Swirl Burner," Paper presented at the Western Cost Section Meeting of the Air and Waste Management Association, Diamond Bar, California, January 29, 2009.

8. R.K. Cheng, D. Littlejohn, D.R. Noble, and T. Lieuwen, "Laboratory Investigations of Low-Swirl Injectors Operating with Syngases," To appear in the Journal of Engineering for Gas Turbine and Power.

9. R.K. Cheng, "Turbulent Combustion Properties of Premixed Syngases," To appear as Chapter 5 in Synthesis Gas Combustion: Fundamentals and Application, Taylor and Francis 2009.

II.6 Combustion and Aerothermal Research for Hydrogen Energy Systems

Kent H. Casleton (Primary Contact),
Don Ferguson, Todd Sidwell, Pete Strakey,
Doug Straub, Nathan Weiland,
Mary Anne Alvin
U.S. Department of Energy
National Energy Technology Laboratory (NETL)
3610 Collins Ferry Rd., P.O. Box 880
Morgantown, WV 26507-0880
Phone: (304) 285-4573; Fax: (304) 285-0903
E-mail: Kent.Casleton@netl.doe.gov

DOE Project Manager: George Richards
Phone: (304) 285-4458
E-mail: George.Richards@netl.doe.gov

Subcontractors:
- M. Chyu and S. Siw, RDS, LLC, Morgantown, WV
- Gilles Eggenspieler and Gautham Krishnamoorthy, ANSYS/Fluent, Morgantown, WV and Canonsburg, PA

Contract Number: 220623-3

Start Date: October 1, 2008
End Date: September 30, 2009

FY 2009 Objectives

- Develop and test a low-swirl injector (LSI) for use with high-hydrogen fuels. Developmental efforts are to be performed at Lawrence Berkeley National Laboratory (LBNL) with high-pressure testing to be performed at NETL in the SimVal combustor. Primary goal is to collect OH planar laser induced fluorescence data for model validation and for understanding basic physical phenomenon. Emissions data and some flashback data are to be collected as well.
- Design and test an "array" style injector for H_2 dilute diffusion studies. Testing will be conducted in SimVal at pressures up to 16 atm. NOx and unburned H_2 will be measured as a function of pressure, air preheat and flow rates.
- Modify the NETL High Pressure Combustion Facility in order to explore aerothermal protection and material issues related to future hydrogen and oxy-fuel turbines. This will enable detailed study of heat transfer and cooling mechanisms, turbine blade materials, and thermal barrier coatings in a controlled but realistic gas turbine environment.

Accomplishments

- An improved LSI with aerofoil-based swirler blades has been developed at LBNL and testing in the SimVal High Pressure Combustion Facility is planned for early Fiscal Year 2010.
- Fuel stream dilution has been found to be more effective than air-side dilution for high-hydrogen diffusion combustors for reduced NOx emissions and improved stability margins.
- A new scaling law has been developed that relates the flame's NOx emissions to its initial velocity, composition, and geometric conditions.
- Aerothermal test rig has been fabricated and installed in the refurbished high pressure combustion facility.
- A review article on issues for aerothermal heat transfer based on potentially new power cycles that can reduce CO_2 emissions was completed.

Introduction

The DOE Turbine Program goals include an emission goal of less than 2 ppmv NOx at target turbine inlet temperatures that are higher than for the current fleet of engines. The NOx emissions goal is 3-5 times lower than the current state-of-the-art gas turbine combustors. The highly variable fuel compositions of high-hydrogen fuels are expected to significantly impact the development and operation of future gas turbine combustors. Some issues that are likely to be of significant concern for the use of fuels with high H_2 contents in gas turbines include flashback, combustion dynamics, flame blowoff, NOx formation, and heat transfer.

This project, "Combustion and Aerothermal Research for Systems for Hydrogen Energy Systems" supports the NETL Turbines program and addresses these critical needs in the following tasks by

- Collaborating with LBNL to evaluate the characteristics and performance of the LSI in hydrogen-fueled applications at high pressure.
- Investigating an innovative diffusion combustion concept to assess combustor stability and NOx emission limits.
- Collaborating with the University of Pittsburgh to design, fabricate and begin testing of a high pressure test rig for aerothermal heat transfer studies appropriate for hydrogen and oxy-combustion turbines.

The overall goal of this project is to support ongoing research and development in gas turbines, with specific emphasis on hydrogen premixed burner concepts (LBNL low-swirl burner), hydrogen dilute diffusion concepts, and aerothermal/heat transfer studies.

Approach

This work supports the long-range goal of developing turbine combustors capable of NOx performance of 2 ppm at 15% oxygen using coal syngas or H_2. The overall approach involves a variety of laboratory-scale [1,2], atmospheric pressure bench-scale, and high pressure larger-scale test rigs [3] to study a variety of possible combustion alternatives for hydrogen turbine applications. These facilities are used to evaluate and test novel combustor designs to assess their applicability for low NOx operation with high hydrogen fuels.

An experimental aero-thermal test facility has been developed in collaboration with the University of Pittsburgh to explore aerothermal cooling of airfoils for use in advanced, land-based, turbine applications.

Results

LSI Testing

The LSI [4,5] is based on a flame stabilization concept developed for basic studies that has been adapted to industrial heaters [6]. Recent tests of a 7 MW gas turbine with a set of LSIs showed it to be a promising method to attain <5 ppm NOx for natural gas operation. The LSI has also been evaluated with fuels of a wide range of Wobbe indices and the results show it to be a fuel-flexible design [6].

The heart of the LSI is a swirler with an open center-channel that allows a portion of reactants to remain unswirled (see Figure 1). The non-swirling center flow inhibits vortex breakdown and promotes flow divergence that is the key aerodynamic feature for the low-swirl flame stabilization method. While most of the previous studies of the LSI focused on methane as a fuel, there has been very little work with high-hydrogen fuels. The goal of this study was to characterize the LSI in terms of flame shape, flashback and NOx emissions over a wide range of operating conditions including pressure, preheat temperature, inflow velocity and fuel type.

Developmental work is in progress at LBNL with aerofoil-based swirler blades and a reduced blade angle in an effort to optimize the design for hydrogen use. Testing at LBNL has included particle image velocimetry (PIV) and flame imaging at atmospheric pressure. Tests with a conical section or quarl in the combustor have also been conducted. Tests show that the configuration labeled "SV7" (Figure 1) which has 16 airfoil vanes with a 37° discharge angle and a center plate of the Lund/Darmstadt design performed better on hydrogen than SV8 which had a slightly larger hole size in the center plate. Further testing at LBNL included cross-plane PIV under non-reacting conditions and hot-fire testing using hydrogen with and without an exit quarl to characterize flame attachment and flame noise. Testing at NETL was scheduled for Q3/Q4 – FY 2009. However, upgrades to some site infrastructure facilities as well as upgrades to some of the high pressure combustion facility systems have pushed back this testing into FY 2010.

FIGURE 1. LSI Configuration SV7

Hydrogen Dilute Diffusion Experiments

In gas turbines operating on high-hydrogen fuels, diffusion flame combustion is preferred to avoid the risk of flashback and auto-ignition in premixed combustors. IGCC plant designs can create this high-hydrogen fuel with a water-gas shift reactor and subsequent separation and storage of the CO_2, while producing a roughly equal volume of byproduct nitrogen in the gasifier's air separation unit to help reduce peak flame temperatures and NOx in the diffusion flame combustor.

Recent results obtained at NETL's Fundamental Combustion Lab (FCL) show that reducing NOx emissions in a high-hydrogen diffusion flame gas turbine combustor is almost always better achieved by diluting the fuel stream than the air stream, which is currently common practice in syngas

combustors. NETL researchers' results show that for all lean diffusion flame combustor types, including swirl-stabilized combustors, flame temperatures are always minimized with dilution of the fuel stream, leading to lower NOx emissions. In addition, NETL's experimental results show that for non-swirl combustor types, such as dilute diffusion flame combustors, flame stability margins are improved and NOx formation times are reduced for fuel-side dilution vs. air-side dilution, which has important ramifications on how future high-hydrogen combustors are designed for low-NOx performance.

Additional testing at NETL has demonstrated the ability to reduce NOx emissions by incorporating a high-velocity coaxial air flow around the fuel tube to increase fuel/air mixing and suppress NOx formation. Analysis of these results has led to a new scaling law that relates the flame's NOx emissions to its initial velocity, composition, and geometric conditions. This NOx scaling accounts for the non-equilibrium flame strain effects resulting from rapid fuel/air mixing, and can be used to help design low-NOx array-style coaxial air dilute diffusion flame combustors.

In addition, hydrogen dilute diffusion flames have also been studied in NETL's SimVal Facility, which is capable of conducting experiments at pressures up to 20 atmospheres and at a size scale more typical of industrial gas turbine combustors. These studies have revealed that while NOx emission increases with combustion pressure and air preheat temperature, as expected, these changes also result in improved combustion efficiency and flame stability. This effectively extends the operating envelope to higher velocities, where NOx emissions can in some cases be lower than those at lower pressures or without air preheating.

Ongoing work at the FCL is investigating geometry and scalability issues involved in the design of a multi-point, array-style injector for achieving the DOE's NOx emissions goals. To provide insight into the complex fluid mechanics and chemistry occurring in these flames, a parallel effort is also being conducted using computational fluid dynamics (CFD) to model the flames. The CFD results, which are validated using the experimental data, are also being used to improve upon current injector designs in an effort to design a "next generation" combustor which will be tested in the SimVal facility at representative gas turbine conditions. Such a combustor, if successful, will provide a significant improvement in low-NOx combustion technology for the high-hydrogen gas turbines that would be used in a carbon-constrained power industry of the future. Note that similar to the LSI work, high pressure testing in the SimVal facility was pushed back to FY 2010 due to facility upgrades and availability.

Aerothermal Test Facility

Increasing the power efficiency of stationary land-based industrial gas turbines to meet Fossil Energy's (FE's) contribution to the U.S. Department of Energy's Advanced Power Systems 2010-2020 goals will require future turbine inlet temperatures to increase to greater than 1,400°C. Cooling air will simultaneously need to be controlled to avoid an increase in NOx emissions [7,8]. This effort focuses on advanced cooling approaches to achieve the FE Turbine efficiency goals, and represents work that is a part of an on-going collaboration with the University of Pittsburgh.

The ultimate goal of this work is to collect aerothermal heat-transfer data at elevated pressure and at simulated gas turbine conditions. These validation datasets will be used to improve aero-thermal cooling effectiveness, reduce NOx emissions, and increase turbine efficiencies. In order to achieve test conditions that are representative of fielded gas turbine systems, an aerothermal test section has been designed for use with NETL's pressurized combustion facility. The overall system layout is illustrated in Figure 2. In this illustration, the combustor is on the left (shown in red) and combustion products flow from left to right. Combustion products exit the combustor, flow through an instrumentation ring and then into the aerothermal test module.

In initial tests, flat test coupons (~5 cm x ~5 cm x ~0.64 cm) will be cooled by back-side impingement cooling while exposed to the hot combustion product stream. Gas compositions will be varied and will include the gas composition and temperature for a hydrogen turbine. Coupon temperatures will be measured using optical methods as well as thermocouples. Subsequent testing will also include an investigation of the effects of film cooling over the test coupon.

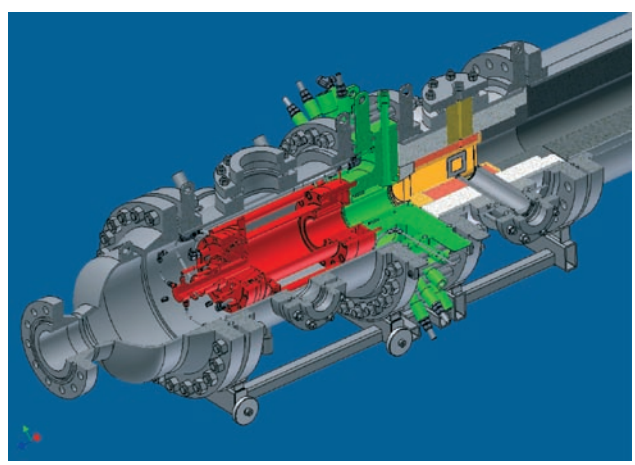

FIGURE 2. Schematic diagram of high pressure combustion rig with aerothermal test module. Combustor module (red), instrumentation ring (green), and aerothermal test section (orange) are illustrated.

The required high-pressure combustion facility upgrades as well as fabrication and installation of the new aerothermal test module have been completed. Initial hot-fire shakedown testing is expected to take place during the latter part of Q4/FY 2009 and initial experimental testing should commence thereafter. A Haynes 230 test coupon and coupon holder were installed in the test rig for shakedown testing. The plan is to monitor the coupon hot-side surface temperature contours using a band-pass charge-coupled device (CCD) camera. To monitor the cold-side surface temperatures, thermocouples were welded to the backside of the coupon (see Figure 3). Although this is not an optimal approach, it will provide some data about the local heat flux through coupon during shakedown testing.

Improved optical temperature diagnostic capabilities that were procured in FY 2008, were received in Q1/FY 2009. These capabilities include an emissivity-corrected pyrometer which will be used to collect real-time surface temperature contours on the hot-gas side of the coupon. Opportunities to work with a small company that has demonstrated the capability of producing high resolution imaging and measuring temperature contours on surfaces in harsh combustion environments are being explored for possible application to our system.

A CFD modeling effort was initiated in Q1/FY 2009 with the goal of simulating the internal and external flow fields through the test geometries. It is important to know the fluid flow properties across the heat transfer surface, and this information will play a key role in understanding the experimental results and aid in the data analysis. In conjunction with this, the team has identified the need for cold flow velocity measurements in order to anchor the CFD effort and quantify the turbulence levels in the aerothermal test section. Options for using either a hot-wire probe or a fiber-optic laser Doppler velocimeter system for these measurements are being explored.

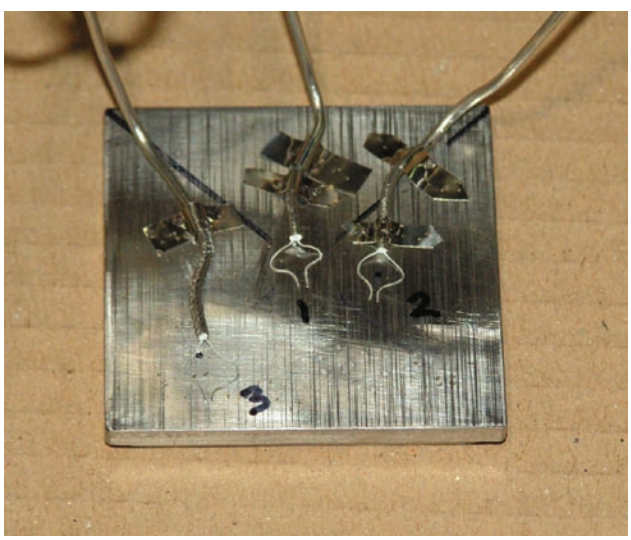

FIGURE 3. Instrumented Test Coupon for Aerothermal Cooling Tests

Conclusions and Future Directions

LSI

- High-pressure testing of an improved LSI developed at LBNL in the NETL SimVal facility is planned for early FY 2010.

Hydrogen Dilute Diffusion Experiments

- Ongoing work is under way to investigate geometry and scalability issues associated with the design of a multi-point, array-style dilute diffusion injector for H_2 applications.
- Based on these experimental results, a fixture will be designed, fabricated and tested in the SimVal high pressure combustion facility.

Aerothermal Test Facility

- An aerothermal test rig has been fabricated and installed in the refurbished high pressure combustion facility.
- In FY 2010, shakedown and Phase 1 testing will commence.

FY 2009 Publications/Presentations

1. R.K. Cheng, D. Littlejohn, P.A. Strakey and T. Sidwell, "Laboratory Investigations of a Low-Swirl Injector with H_2 and CH_4 at Gas Turbine Conditions," Proc. Comb. Inst. 32: 3001 (2009).

2. P.A. Strakey and G. Eggenspieler, "Development and Validation of a Thickened Flame Modeling Approach for Large Eddy Simulation of Premixed Combustion," Paper GT2009-60077, ASME Turbo Expo 2009, June 8–12, 2009, Orlando, Florida.

3. N.T. Weiland and P.A. Strakey, "Stability Characteristics of Turbulent Hydrogen Dilute Diffusion Flames," *Combustion Science and Technology.* 181: 756 (2009).

4. N.T. Weiland and P.A. Strakey, "NOx Reduction by Air-Side vs. Fuel-Side Dilution in Hydrogen Diffusion Flame Combustors," ASME Paper: GT2009-60128. Presented at ASME Turbo Expo, Orlando, Florida, June 8–12, 2009, and accepted for publication in *Journal of Engineering for Gas Turbines and Power.*

5. D.L. Straub and G.A. Richards, "Heat Transfer for Alternative Fuels and Engine Cycles," In: *Turbine Science and Technology, AIAA Progress Series*, ed. T. Shih, [in press].

6. G.A. Richards and K. Casleton, "Gasification Technology to Produce Synthesis Gas," In: *Syngas Combustion*, eds. T. Lieuwen, V. Yang, and R. Yetter, Taylor & Francis. [in press].

7. G.A. Richards, K.H. Casleton, and N.T. Weiland, "Syngas Utilization," In: *Syngas Combustion*, eds. T. Lieuwen, V. Yang, and R. Yetter, Taylor & Francis. [in press].

References

1. N. Weiland and P. Strakey, "Global NOx Measurements in Turbulent Nitrogen-Diluted Hydrogen Jet Flames," Paper B22, 5th U.S. Combustion Meeting, San Diego, California, March 25–28, 2007.

2. D. Ferguson, "Experimental Investigation of Oscillatory Heat Release Mechanisms and Stability Margin Analysis in Lean-Premixed Combustion," Ph.D. Dissertation, West Virginia University, https://eidr.wvu.edu/etd/documentdata.eTD?documentid=3854, 2005.

3. T. Sidwell, G. Richards, K. Casleton, D. Straub, D. Maloney, P. Strakey, D. Ferguson, S. Beer, and S. Woodruff, 2006, "Optically Accessible Pressurized Research Combustor for CFD Model Validation," AIAA Journal, 44(3), pp. 434-443.

4. M.R. Johnson, D. Littlejohn, W.A. Nazeer, K.O. Smith and R.K. Cheng, Proc. Comb. Inst., 30 (2005) 2867 - 2874.

5. D. Littlejohn and R.K. Cheng, Proc. Comb. Inst., 31 (2) (2007) 3155-3162.

6. C.K. Chan, K.S. Lau, W.K. Chin and R.K. Cheng, Proc. Comb. Inst., 24 (1992) 511-518.

7. http://www.netl.doe.gov/publications/factsheets/rd/R&D103.pdf (cited June 3, 2008).

8. M.A. Alvin, F. Pettit, G. Meier, M. Yanar, M. Chyu, S. Siw, W. Slaughter, V. Karaivanov, B. Kang, C. Feng, J.M. Tannebaum, R. Chen, B. Zhang, T. Fu, G. Richards, T. Sidwell, D. Straub, K. Casleton, and O. Dogan, "Materials and Component Development for Advanced Turbine Systems," Presented at the 22nd Annual Fossil Energy Materials Conference, Pittsburgh, Pennsylvania, July 8–10, 2008.

II.7 Micro-Mixing Lean-Premix System for Ultra-Low Emission Hydrogen/ Syngas Combustion

Dr. Adel Mansour (Primary Contact),
Dr. Erlendur Steinthorsson, Brian Hollon
Parker Hannifin Corporation
9200 Tyler Blvd.
Mentor, OH 44060
Phone: (440) 954-8100; Fax: (440) 954-8111
E-mail: amansour@parker.com

DOE Project Manager: Robin Ames
Phone: (304) 285-0978
E-mail: Robin.Ames@netl.doe.gov

Subcontractor:
University of California, Irvine (UCI), Irvine, CA

Contract Number: 42648

Start Date: October 1, 2008
End Date: September 30, 2009

FY 2009 Objectives

- Fabricate and test second generation micro-mixing cup fuel injectors for hydrogen and syngas fuels in both single-cup and four-cup injector modules, and demonstrate 5 ppm NOx on multi-cup modules when operating on hydrogen at an adiabatic flame temperature of 1,750 K (Phase II emissions target).
- Develop and fabricate a full-scale, 1 MW_{th} multi-cup micro-mixing cup injector for full-scale testing in Phase III.
- Demonstrate stable operation of the 1 MW_{th} injector over a range of operating conditions, achieving NOx emissions of 3 ppm or less.

Accomplishments

- Fabricated three variants of the second generation cups in single cup modules and four-cup modules.
- Demonstrated operability of second generation of micro-mixing cups operating without flashback at pressures up to 8 atm, adiabatic flame temperatures up to 2,000 K, and air pressure drops as low as 2.5%. Demonstrated NOx emissions below 5 ppm, when using second single cup modules, while operating on 100% hydrogen fuel with less than 20% nitrogen dilution.
- Demonstrated operability of the multi-cup modules at pressures up to 5 atm, achieving 8 ppm NOx emissions at 1,780 K flame temperature with 8% nitrogen dilution, closely replicating the performance of single cup injectors.
- Developed a full-scale 1 MW injector. Injector will be fabricated and tested in Phase III of the project.

Introduction

The focus of this project is to develop the next generation of fuel injection technologies for environmentally friendly, hydrogen syngas combustion in gas turbine engines that satisfy DOE's objectives of reducing NOx emissions to 3 ppm. Building on Parker Hannifin's proven macrolamination technology for liquid fuels, Parker is developing scalable high-performing multi-point injectors that utilize multiple, small mixing cups in place of a single conventional large-scale premixer. Due to the small size, fuel and air mix rapidly within the new mixing cups, providing a near-uniform mixture at the cup exit in a short time such that risks of auto-ignition are eliminated. Scalability is achieved by integrating multiple small mixing cups into a single larger injector.

Detailed studies and experimentation with these injectors are being conducted to elucidate the effects of various injector design attributes and operating conditions on combustion efficiency, lean stability and emissions. Through our university partner program, data on flame and stability characteristics, turbulent flame propagation, and impact of the anchoring mechanism, burning conditions and syngas composition are collected experimentally. Computational analyses, corroborated with diagnostics, are used to determine the role of chemistry, transport and fluid mechanics on combustion. Strategies are developed to mitigate the impact of flashback. In the initial phases of the project, the experimental studies focused on single-cup injectors and small multi-cup injectors, taking advantage of the modularity of the multi-cup approach to minimize cost of development and testing. In the final phase of the project, a full-scale 1 MW_{th} multi-cup injector will be tested.

Approach

Utilizing Parker Hannifin's macrolamination technology, the general approach is to adapt macrolaminated designs and concepts to hydrogen/ syngas combustion and hydrogen enriched combustion. With macrolamination technology, elegant and

sophisticated multipoint lean-premix nozzles and burners that incorporate complex geometry can be developed with exceptional affordability. We proposed to develop, build and test a large number of burners spanning a wide range of scales from small-scale single-cup premixers to 1 MW_{th} size premixers. The modularity of our approach affords us the flexibility to build multiple scales of these injectors from a basic building block (a single mixing-cup) affordably and expeditiously.

Lean conditions coupled with multiple point injection for fast and efficient mixing are our primary vehicle for achieving low NOx emissions. In order to further reduce NOx levels, consideration is given to operability at ultra-lean conditions, where flame stability can become a concern. Stability augmentation is achieved through optimization of swirl and other aerodynamic features. Zone staging is used to enhance lean operability for multi-cup, full-scale injectors.

Results

Building on last year's experience, a second generation of macrolaminated micro-mixing cup injectors were fabricated for testing at the UCI Combustion Laboratory. The new injectors, shown in Figure 1, use a mixed axial-radial air-flow mixing cup design with an eight-slot radial-inflow fuel injection scheme. Axial swirlers can be inserted into the axial-flow air circuit to change the overall swirl-number of the cup and affect fuel-air mixing. Computational fluid dynmaics analyses of the mixing cups showed the flow field within the cups to be free of recirculation zones where flame anchoring could occur. Each mixing cup has two fuel circuits to facilitate use of lower heating value syngas fuels and to enable injection of a diluent, such as nitrogen. Three variants of the injector design were fabricated, differing in swirl number.

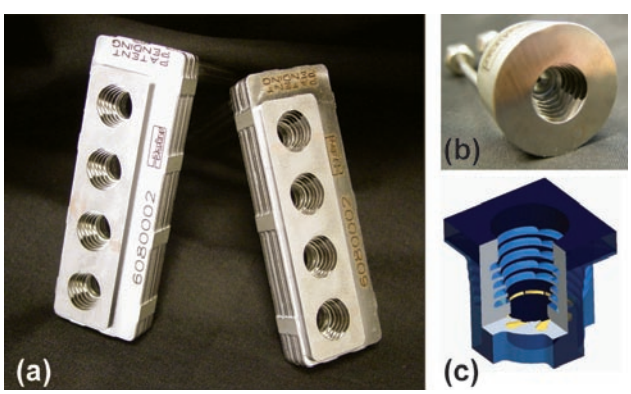

FIGURE 1. Injector modules utilizing second generation axial/radial micro-mixing cup design (a) four-cup injector modules, (b) a single cup injector module with an air swirler inserted into the axial air circuit, and (c) a schematic showing the air circuit design.

Based on OH-chemiluminescence images and emissions data, operation of the second generation single-cup injectors on 100% hydrogen fuel successfully demonstrated a very robust flashback resistance up to 8 atm pressure and flame temperatures up to 2,000 K. Operating without diluents at 3 atm pressure, emissions at the target flame temperature of 1,750 K were found to be 3 ppm. A typical exponential drop in emissions with decreasing flame temperature was obtained, as is characteristic of a well pre-mixed flame. Increasing the operating pressure to 5 atm and 8 atm pressure caused the emissions to rise to the 10 ppm to 20 ppm level and the exponential dependence on flame temperature was lost. However, moderate amounts of nitrogen diluent brought the emissions levels down to 7 ppm or less at the target 1,750 K flame temperature and the exponential dependence of emissions on flame temperature was regained. In aggregate, the single-cup combustion tests revealed a very robust injector with respect to flame stability and flashback. The robust operability is a significant improvement over the first generation of cups, while still meeting the emissions goals for the single-cup tests by a comfortable margin.

Flame imaging and emissions testing using selected multi-cup injectors, conducted using hydrogen fuel with and without nitrogen dilution, demonstrated a performance very similar to that obtained with single cup injectors. A sample flame image is shown in Figure 2. The figure shows that the flames are all lifted from the injector. The flames are also found to be compact with the main heat-release region extending less than 1 inch from the injector face. The flame imaging studies revealed overall flame characteristics that are similar to what was observed in the single cup tests.

Emissions results obtained using a four-cup injector module operating at 5 atm pressure, 3.5% pressure drop, with and without nitrogen dilution, are shown in Figure 3. For reference, the figure also shows emissions data obtained with a single-cup injector operating at 3 atm and 5% pressure drop on 100% hydrogen fuel, along with a line developed by Leonard and Stegmaier [1] representing emissions "entitlement" for natural gas combustion. When operated on 100% hydrogen the emissions at the 3.5% pressure drop are about 14 ppm NOx at the 1,750 K adiabatic flame temperature. With small amounts of nitrogen added to the fuel, the emissions were found to drop rapidly. With only 8% nitrogen dilution by volume, the NOx levels drop by nearly 50% from the level obtained at the same hydrogen flow without dilution, achieving 8 ppm NOx at about 1,780 K adiabatic flame temperature. This finding is consistent with results obtained in the single cup tests where similar drop in emissions was observed. Substantially greater NOx reduction can be achieved with additional dilution. Based on the results, Parker feels well positioned to achieve the project's emissions goals in the planned full-scale injector tests.

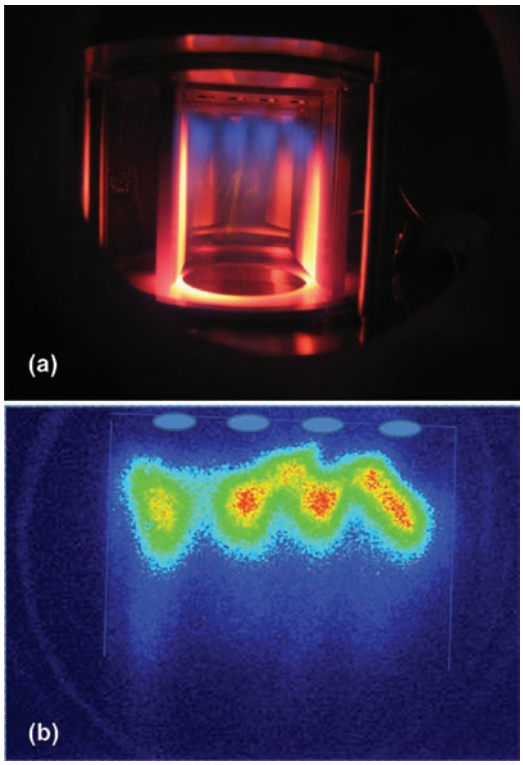

FIGURE 2. Flame images for 4x1 multi-cup injector operating at 3 atm, 3.5% ΔP/P, 300 K inlet temperature and 1,225 K adiabatic flame temperature: (a) visual flame image, (b) OH chemiluminescence image.

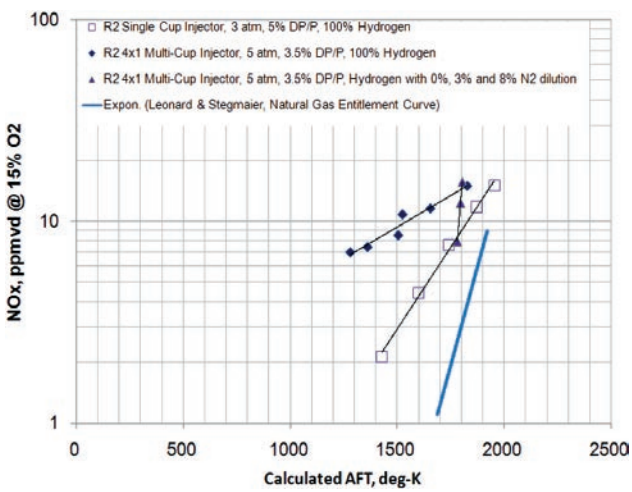

FIGURE 3. Emissions results for a 4x1 multi-cup injector operating on hydrogen with and without N_2 dilution (5 atm operating pressure, 3.5% pressure drop, and 300 K air inlet temperature; single-cup injector results at 3 atm, 5% ΔP/P shown for reference).

Building on the second-generation micro-mixing cup design, Parker has developed a 1 MW_{th} multi-cup injector to be used in the full-scale combustion tests in Phase III. The injector is shown in Figure 4 along with an exploded view of the multiple layers of metal

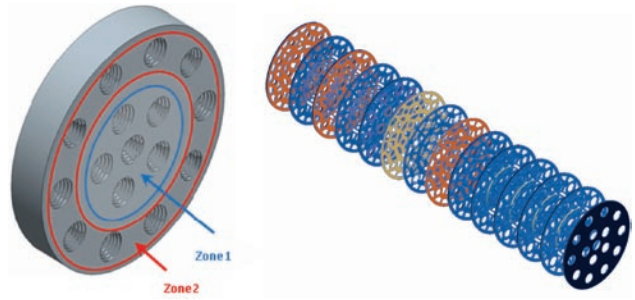

FIGURE 4. Full-scale, 16-cup injector with mixing cups arranged on two concentric circles surrounding an individually fueled pilot circuit in the center; separate fuel feeds supply fuel circuits in Zone 1 and Zone 2, respectively.

plates that make up the macrolaminated injector. After bonding, the multiple metal layers fuse into a single monolithic metal injector. Note that all manifolds that distribute fuel to the individual cups are incorporated into the micro-mixing cup. The injector will have four fuel feeds that supply fuel to the pilot and two mixing-cup zones to enable staging of the fuel flow during operation and independent control of the fuel-air ratio of the pilot-cup. This injector design will be carried forward to manufacturing and tested in Phase III at various operating conditions with fuel blends representative of syngas and high-hydrogen fuels.

Conclusions and Future Directions

Parker continues to make progress on developing scalable injectors for gas turbines. The second generation injectors tested during this fiscal year have demonstrated superior flashback resistance performance and NOx targets below 5 ppm were demonstrated with moderate (20%) nitrogen dilution when operated at adiabatic flame temperature of 1,750 K and pressures up to 8 atm.

Parker has developed a 1 MW injector for testing at an original equipment manufacturer's facility. The injector will use the second generation mixing cup building block replicated 16 times to reach the 1 MW heat release level. Phase III will focus on manufacturing of the injector and testing at operating conditions that are representative of medium-size gas turbine engines with operating pressures up to 13 atm.

Special Recognitions & Awards/Patents Issued

1. A patent application titled "Micro-Mixing Lean Pre-Mix for Ultra-Low Emission Hydrogen/Syngas Combustion" with U.S. Provisional Serial No. 61/082,329 was filed by Parker on July 21, 2008.

FY 2009 Publications/Presentations

1. Q. Wang, V.G. McDonell, E. Steinthorsson, A. Mansour, and B. Hollon, 2009, "Correlating Flashback Tendencies for Premixed Injection of Hydrogen and Methane Mixtures at Elevated Temperature and Pressure," GT2009-59500, TurboEXPO 2009, Orlando, Florida, June 2009.

2. H. Lee, S. Hernandez, V.G. McDonell, E. Steinthorsson, A. Mansour, B. Hollon, 2009, "Development of Flashback Resistant Low-Emission Micro-Mixing Fuel Injector for 100% Hydrogen and Syngas Fuels," GT2009-59502, TurboEXPO 2009, Orlando, Florida, June 2009.

3. H. Lee, Hernandez, Q. Wang, V.G. McDonell, A. Mansour, E. Steinthorsson, B. Hollon, "Evaluation of Micromixing Arrays for Low Emissions Combustion of Hydrogen and Syngas Fuels," Presentation at International Conference on Environmentally Preferred Advanced Generation, Newport Beach, California, February 11, 2009.

References

1. G. Leonard, and J. Stegmaier, "Development of an Aeroderivative Gas Turbine Dry Low Emissions Combustion System," *J. of Eng. for Gas Turbines and Power*, Vol. 116, No. 3, 1994, pp. 542-546.

II.8 Catalytic Combustion for Ultra-Low NOx Hydrogen Turbines

Shahrokh Etemad (Primary Contact), Benjamin Baird, Sandeep Alavandi, and William C. Pfefferle
Precision Combustion, Inc. (PCI)
410 Sackett Point Rd.
North Haven, CT 06473
Phone: (203) 287-3700; Fax: (203) 287-3710
E-mail: setemad@precision-combustion.com

DOE Project Manager: Robin Ames
Phone: (304) 285-0978
E-mail: Robin.Ames@netl.doe.gov

Subcontractors:
Solar Turbines, Inc., San Diego, CA
(Leonel O. Arellano, Ram Srinivasan)

Contract Number: 42647

Start Date: October 1, 2005
End Date: August 31, 2010

FY 2009 Objectives

- Demonstrate NOx <3 ppm, for megawatt-scale hydrogen gas turbine application.
- Same or lower pressure drop (4%) than existing gas turbine.
- Focus on hydrogen with fuel flexible capability: natural gas, syngas.
- New and retrofit machines (sized to fit existing combustor envelope).
- Meet 24,000-hour life requirement.
- Allowance for single injector fabrication and testing by utility original equipment manufacturers.

Accomplishments

- Atmospheric flow testing of performance parameters of the full-scale high pressure single injector module in progress at PCI.
- Test plan for high pressure H_2 testing at simulated engine conditions at Solar Turbines, Incorporated generated and milestones for full-scale module testing have been updated. Awaiting Solar Turbines, Incorporated high pressure hydrogen combustor rig availability.
- A full length technical paper documenting the results and progress of the hydrogen subscale testing was submitted and presented at the International Colloquium on Environmentally Preferred Advanced Power Generation 2009 conference.
- Solar Turbines, Incorporated has completed high-pressure rig upgrades for hydrogen combustion testing.
- A full-scale single injector assembly to be tested at Solar Turbines, Incorporated is complete.

Introduction

The project is progressing towards a full-scale, high pressure, single injector demonstration of an ultra-low NOx-rich catalytic system for fuel-flexible hydrogen combustors in megawatt-scale turbines. This is being achieved by developing PCI's rich catalytic combustion technology for fuel flexible hydrogen applications, in collaboration with Solar Turbines, Incorporated. This technology, in a previous DOE project, demonstrated subscale ultra-low NOx emissions with syngas and with fuel mixtures comprised of hydrogen diluted with nitrogen (subscale tests at PCI demonstrated low single-digit NOx - corrected to 15% O_2) with operation at integrated gasification combined cycle (IGCC) base-load combustor temperatures and 10-atm rig pressure. The successful achievement of the project objectives will lead to combustors capable of delivering near-zero NOx without costly post-combustion controls and without added requirements for sulfur control. This advances DOE's objectives for achievement of low single-digit NOx emissions, improvement in efficiency vs. post-combustion controls, fuel flexibility, a significant net reduction in IGCC system net capital and operating costs, and a route to commercialization across the power generation field.

The work plan is divided into three phases. Phase I (completed) involved the development of conceptual designs for catalytic combustion technology for hydrogen fuel and the production of a detailed research and development implementation plan. Phase II (ongoing), Detailed Design and Validation Test Program, concentrates on development of a full-scale module for validation (high-pressure rig) testing, and the resolution of key performance and durability issues. In Phase III, the full-scale design will be frozen, and a combustor comprised of multiple catalytic combustor modules will be fabricated for high pressure testing.

Approach

To achieve the project objectives, PCI, in close collaboration with Solar Turbines, Incorporated, is developing its catalytic combustion system for hydrogen fuel and for fuel-flexible operation in megawatt gas

turbines. Conceptually, work centers around three primary system functions: premixing, catalytic reaction, and gas-phase reaction (combustion). These primary systems need to be integrated with each other in a manner that resolves potential issues of flashback, autoignition, flame holding, and flame stabilization. Related scale-up issues must also be considered as the system is integrated into an engine. The overarching goal throughout the project is to achieve ultra-low NOx emissions below 3 ppm with good engine performance and operability using multiple fuels.

Results

For the combustion of natural gas, PCI has developed and demonstrated, in an engine (Saturn and Taurus 70), a Rich-Catalytic Lean-burn (RCL®) combustion system capable of delivering NOx emissions lower than 3.0 ppm. The RCL® system is based on the concept of stabilizing combustion with catalytically-reacted fuel and air having a temperature below the instantaneous autoignition temperature [1]. The combustion air stream is split into two parts upstream of the catalyst. One part is mixed with all or the majority of the fuel and contacted with the catalyst, while the second part of air is used to backside cool the catalyst. At the exit of the reactor, the catalyzed fuel/air stream and the cooling flow are combined to finalize combustion. Rich catalytic hydrogen combustion has been shown to offer the same low NOx advantage for hydrogen fuel in tests completed at PCI. Similarly, NOx emissions close to 2.5 ppm were demonstrated in a Taurus 70 engine using natural gas at full load with an RCL® system in the injector pilot stream.

In subscale experiments at 10 atm, a rich catalytic reactor design that closely approximates the selected engine hardware design showed good performance achieving low single-digit NOx levels at full load and good combustor stability and turndown. The reactor design has been optimized to produce greater catalytic conversion and has been down-selected and implemented in the full-scale reactor module.

Figure 1 shows the NOx emissions data obtained for two injector configurations in the Gen II design. Both Gen II Injectors (A & B) achieved <3 ppm NOx emissions for fuel mixtures of 42 and 52% hydrogen. Injector A achieved a wide turndown (~500°F) with NOx emissions <1 ppm for 42% H_2. A stable downstream flame could be achieved due to increased reaction in the catalyst bed.

Figure 2 shows the effect of decreasing flame temperatures on wall temperatures and the effect of increasing air split. At lower burner outlet temperatures the catalyst surface temperature increases since the fuel rich stoichiometry is reduced. With

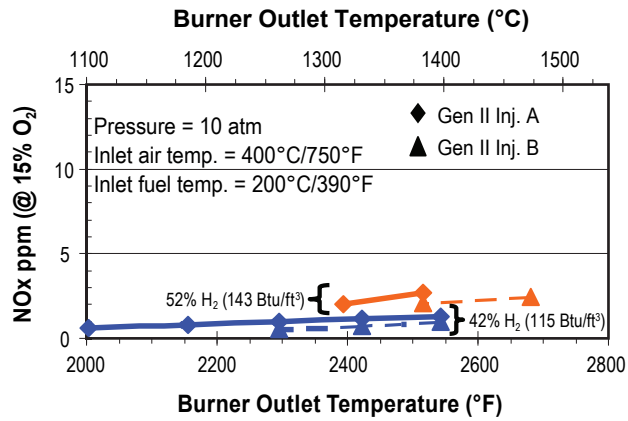

FIGURE 1. Results of Subscale Reactor Showing Low Single Digit NOx Emissions and Wide Turndown for Gen II Injectors (Tests completed at PCI)

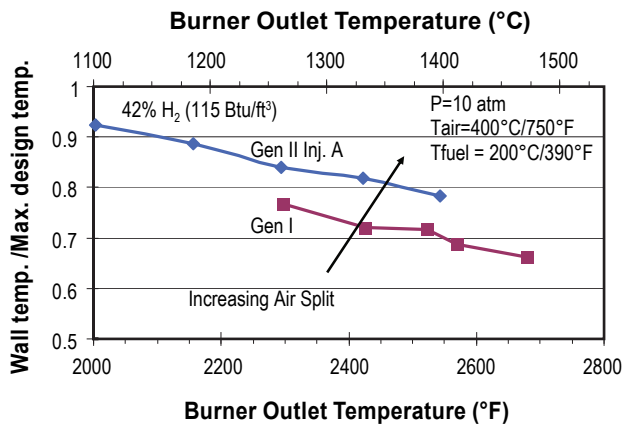

FIGURE 2. Catalytic Reactor Temperature for 42% H_2 with Increasing Air Split (Catalytic Conversion)

increased catalytic reaction there is more energy released within the catalyst bed thus producing higher surface temperatures (since cooling air flow is essentially constant for the ranges of air splits of interest and given hardware configuration). Improved flame stabilization at lower burner outlet temperatures due to increased catalytic reaction is achieved, an inherent advantage of the rich catalytic combustion.

PCI has completed fabrication of the catalytic injector hardware after design optimization. Figure 3 shows the hardware picture of the full-scale single injector module. Atmospheric flow testing (unmixedness, effective area etc.) at PCI's facility is currently in progress for injector validation. After full completion of this testing, the module will be shipped to Solar Turbines, Incorporated.

Solar Turbines, Incorporated has also upgraded a single-injector test facility to handle large flow rates of hydrogen and diluent necessary for simulated testing.

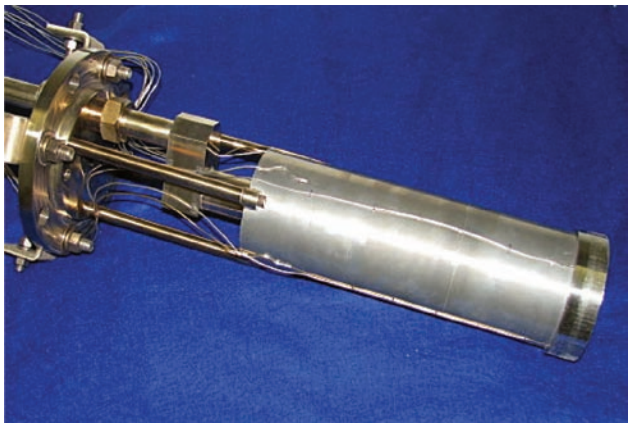

FIGURE 3. Full-Scale Injector Hardware for Hydrogen Combustion Fabricated by Solar Turbines, Inc. (Pilot) and PCI (Reactor)

In the near future, this reactor will be installed and tested at Solar Turbines, Incorporated atmospheric and high pressure test facilities. The injector will be started on 100% natural gas (introduced through the pilot) to assure safe, controlled ignition, and then transitioned to a hydrogen-nitrogen fuel mixture. This is in line with current starting procedures for IGCC plants. Injector tests will evaluate emissions, reactor operating temperatures, and flame stability at select simulated Taurus 70 operating conditions.

Milestones

The following technical milestones were discussed with the program manager and updated –

- Atmospheric flow testing in quartz rig at Solar Turbines, Incorporated is scheduled in September 2009.
- Full-scale high pressure single injector testing in January 2010.

Conclusions and Future Directions

- Successfully demonstrated <3 ppm NOx emissions with subscale testing.
- Full-scale high single injector reactor and pilot fabricated.
- Successful completion of atmospheric flow testing at PCI will lead to high pressure, single injector testing to demonstrate injector performance at Solar Turbines, Incorporated's high-pressure testing facility.
- This full-scale injector will be installed at Solar Turbines, Incorporated atmospheric rig and performance tested, including transition from methane startup to full hydrogen-mix fuel operation.
- High pressure single injector testing will be conducted at Solar Turbines upgraded test facility, once the rig is available.

FY 2009 Publications/Presentations

1. S. Alavandi, B. Baird, S. Etemad, H. Karim, and W. Pfefferle, "Ultra Low NOx MW-Scale Catalytic Hydrogen Combustor for Advanced Coal Power Systems," February 10–12, 2009, Newport Beach, California, ICEPAG2009-1035, submitted.

2. Presented the paper "Ultra Low NOx MW-Scale Catalytic Hydrogen Combustor for Advanced Coal Power Systems," at the ICEPAG 2009 conference.

References

1. L.L. Smith, H. Karim, M.J. Castaldi, S. Etemad, W.C. Pfefferle, V. Khanna, K.O. Smith (2005), "Rich-Catalytic Lean-Burn Combustion for Low-Single-Digit NOx Gas Turbines," Journal of Engineering for Gas Turbines and Power, Vol. 127, pp. 27-35.

III. ADVANCED OXY-FUEL TURBINES

III.1 Zero Emissions Coal Syngas-Oxygen Turbo Machinery

Mohan Hebbar
Siemens Energy, Inc.
4400 Alafaya Trail
Orlando, FL 32826
Phone: (407) 736-7379; Fax: (407) 736-4961
E-mail: mohan.hebbar@siemens.com

DOE Project Manager: Robin Ames
Phone: (304) 285-0978
E-mail: Robin.Ames@netl.doe.gov

Contract Number: 42646

Start Date: October 1, 2005
End Date: September 30, 2011

FY 2009 Objectives

- Establish atmospheric bond coat temperature limits for two SGT-900 turbine alloys (X-45 and Inconel 738) with current bond coat and thermal barrier coating (TBC) systems.
- Determine basic oxidation/corrosion behavior and characterize it under defined steam/CO_2 conditions for the alloys in SGT-900 hot gas path.
- Quantify the low cycle fatigue (LCF) life of select SGT-900 turbine alloys after exposure to steam/CO_2 environment for comparison with baseline (atmospheric) data.
- Conduct modeling of plant cycles with the SGT-900 turbine as the intermediate pressure turbine under two different fuels scenario – natural gas and syngas produced by the Siemens fuel gasifier.

Accomplishments

- The atmospheric bond coat temperature limit has been established for X-45 alloy under standard test conditions and is ~20% higher than the expected design temperature of row 3 vane where the alloy is used.
- Exposure of coated and uncoated buttons of two alloys has been completed under steam/CO_2 atmosphere up to 500 hours. Beta-phase depletion measurements to assess the oxidation resistance are 50% complete. On completion of the studies a comparison of the depletion curves can be made between the two environments – products of natural gas combustion and steam/CO_2.
- LCF was determined to be the most important mechanical property to quantify the effects of environmental exposure in steam/CO_2. Exposures of LCF specimens were completed at two temperatures and tests are 75% complete. The results will be compared to pre-existing data to determine environmental effects on LCF life, if any.
- Modeling of the selected near-term oxy-fuel cycle with CO_2 capture has been completed with two fuels – natural gas and coal syngas. The cycle utilizes a high pressure (HP) turbine with a combustor and SGT-900 Siemens gas turbine with a reheater as an intermediate pressure (IP) turbine.

Introduction

Advanced power systems that utilize nearly pure oxygen as the oxidant and coal-derived gaseous fuels are an attractive approach to highly efficient zero emissions systems that capture and sequester carbon dioxide. In these systems, the oxidant and fuel are combusted to create a working fluid composed mostly of steam and CO_2. This working fluid can be utilized in a Rankine cycle turbine to generate power while CO_2 can be captured after condensation of the drive gas mixture. In order to achieve high cycle efficiency, it is necessary to use the drive gas at temperatures comparable to or higher than those of today's gas turbines. Turbines using such a drive gas at high temperatures (1,750°C or higher) have not been developed. Power generation using the oxy-fuel combustion process has been demonstrated by Clean Energy Systems (CES), Inc. of Rancho Cordova, California, albeit on a small scale. The advantages of developing turbines which are large enough for commercial power generation are as follows:

- Use of coal – the least expensive and most abundant domestic fuel.
- Mitigation of NOx emissions since the oxidizer is pure oxygen instead of air.
- Greater than 99.5% of CO_2 captured.
- Materials and coatings development will benefit gas turbines used in combined cycle or peaking power generation applications.
- Steam cooling and other design technologies such as rim cavity sealing will also benefit gas turbine products.
- Technology will also apply to oxy-fuel turbines using natural gas (since the drive gas is the same) for near-term applications such as peaking power generation with enhanced oil recovery.

Approach

The project approaches the development of turbo machinery to use the working fluid produced by syngas-oxygen combustion products in a pragmatic way by evaluating the technology promise in the short-term as well as in the long-term. Siemens Energy, Inc. and CES have jointly arrived at an arrangement of combustors, re-heaters and turbines that provides competitive plant cycle efficiency. In order to achieve high efficiency, it is necessary to use the drive gas at a very high temperature. For the long-term, the target value of the drive gas (steam, CO_2 mixture) in this project is 1,760°C (3,200°F) for the IP turbine and 760°C (1,400°F) for the HP turbine. These temperatures are significantly higher than those utilized in current day industrial gas turbines or steam turbines.

Just as in Fiscal Year 2008, during FY 2009 the project approach was re-focused on near-term application of existing turbines (rather than developing a very high temperature turbine) to an oxy-fuel power generation demonstration project. Such an approach was seen to be necessary to understand the material behavior in steam/CO_2 environment and also to validate turbine performance assumptions since a turbine typically used as a 'gas' turbine is to be employed for expanding steam/CO_2 drive gas mixture.

Results

1. Atmospheric bond coat temperature limits: Nickel-based alloy IN738 and cobalt-based alloy X-45 are used in the SGT-900 turbine for row 1 blade and row 3 vane, respectively. Since the atmospheric bond coat temperature limits for these alloys are not available in Siemens' database, it was decided to obtain the data by testing pins and discs under standard cyclic test conditions of time and temperature. The test data yields a spallation curve indicating a relationship between time to failure (hours) and test temperatures. Figure 1 shows the curve arrived at for X-45 material. It was determined that the atmospheric bond coat temperature limit was higher than the design temperature of the vane 3 in the retrofitted SGT-900 thereby meeting basic design criteria. In order to generate such a curve, it is necessary to obtain the number of hours it takes to detach the TBC at three different temperatures. In the case of IN738 one of the three test temperatures has not yet yielded a failure (detachment) of the TBC. The spallation curve for IN738 can only be generated after this test point is obtained.

2. Beta-phase depletion studies under steam/CO_2 atmosphere: These studies are important because they provide additional safety margin if the protection from the TBC is lost due to thermal spallation or foreign

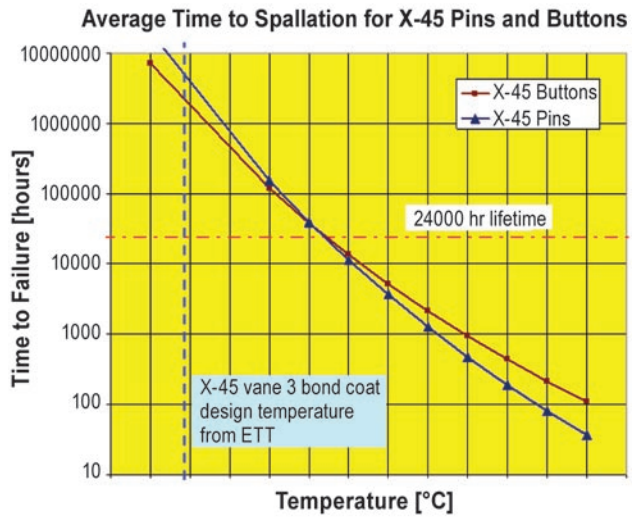

FIGURE 1. Average time to TBC spallation as a function of temperature for X-45 with bond coat and TBC.

object damage. In such an event the ability of the bond coat to resist oxidation becomes critical to avoid a component failure. Tests were run in order to assess the oxidation resistance of the bond coat when exposed to the actual turbine atmosphere (approximately 90% steam, 10% CO_2). The materials selected were the cobalt-based alloy ECY768 used in row 1 vane and the nickel-based alloy IN738 used in row 1 blade. (These rows experience the highest fluid temperatures in the turbine.)

The specimens were exposed at temperatures relevant to the SGT-900 oxyfuel calculated hot gas path. Every 100 hours a specimen was pulled for microstructural assessment and measurement of the depleted beta phase zone. (Atmospheres included products of natural gas combustion as well as steam/CO_2 for comparison.) Figure 2 shows the microstructure of one of the alloys, IN738, with bond coat and TBC from which beta phase depletion measurements were made. Depletion vs. time curves (as shown in Figure 3) have been generated for ECY-768 and IN738. Figure 4 shows a comparison of the depletion after 500 hours in steam/CO_2 and natural gas for all SGT-900 alloys with bond coat. In all cases, it was found that the steam/CO_2 atmosphere was more aggressive in depleting the bond coat beta phase when compared to a natural gas environment. In addition, modification of the protective oxides formed was observed in the steam/CO_2 atmosphere on bare alloys.

3. Low cycle fatigue testing on steam/CO_2 exposed specimens: In addition to the outside surfaces of the turbine airfoils getting exposed to the steam/CO_2 fluid, the airfoils that are cooled internally (vanes and blades in the first two stages) can also be degraded by the oxidizing nature of the coolant. The coolant

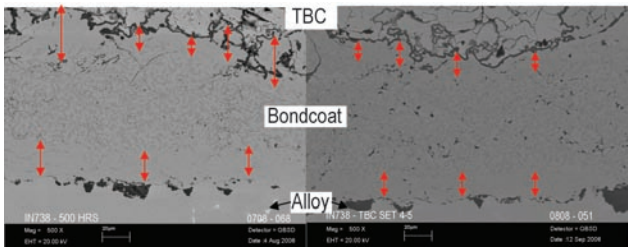

FIGURE 2. Example of microstructure of IN738 with bond coat and TBC after exposure in steam/CO_2 (left) and natural gas (right). Red arrows indicate the beta phase depletion regions.

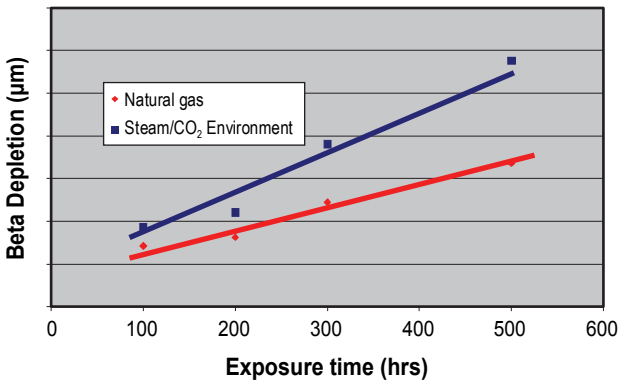

FIGURE 3. Depletion vs. time curve for ECY-768 with bond coat and TBC in steam/CO_2 and natural gas. (IN738 shows a similar trend.)

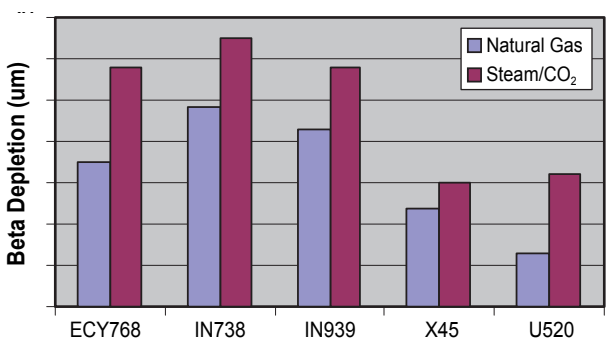

FIGURE 4. Comparison of depletion of system after 500 hours in steam/CO_2 and natural gas environments for hot gas path alloys.

temperature is lower than that of the working fluid; therefore steam/CO_2 exposure tests on LCF specimens were performed at different temperatures on non-coated and coated specimens. The lower temperature exposure was performed by Cranfield University (United Kingdom) and the higher temperature exposure was performed by the National Energy Technology Laboratory-Albany (OR). Subsequent LCF tests are being performed at expected bond coat operational temperatures. The LCF testing was started in May 2009 with an estimated completion date of October 2009.

4. Zero CO_2 emission plant cycle modeling: This work was subcontracted to The Advanced Power & Energy Programs group of the University of California, Irvine. The objective was to model the ZEPP (Zero Emission Power Plant) cycle suitable for the SGT-900 IP turbine. Both natural gas and coal syngas were considered for fuel since as a starter plant it is expected that natural gas will be used as fuel, with syngas being used in the later years with more operating experience. The cycle utilizes an HP combustor, an HP turbine, a reheater and modified SGT-900 turbine as the IP turbine. Both turbines work on steam/CO_2 mixture and heat recovery and a low pressure turbine are utilized downstream. (The IP turbine is assumed to run with an inlet temperature of only 1,080°C in the near-term case.) For the natural gas case, the model includes an air separation unit (ASU) to supply pure oxygen. The cycle efficiency, considering all parasitic loads was calculated as 33.9% (lower heating value [LHV] basis). The coal syngas case, in addition to utilizing the ASU, employs a Siemens engineered coal gasifier. The resulting efficiency (LHV basis) is 25.8%, again considering all of the parasitic loads.

Conclusions and Future Directions

The work performed during FY 2009 has focused on a near-term application of an existing Siemens turbine while keeping the development effort linked to the needs of the far-term syngas oxy-fuel cycle. The materials testing and analytical work undertaken is the first step towards adapting the Siemens SGT-900 IP turbine to perform under steam/CO_2 fluid. The principles applied here will work equally well whether the fuel is natural gas or coal-derived syngas since the resulting fluid in both cases is a mixture of steam and CO_2. While they still need to be consolidated, some preliminary conclusions about the material behavior can be stated as follows:

- Atmospheric bond coat limits for IN738 and X-45 exceeded the design temperatures of blade 1 and vane 3 in the redesigned SGT-900.
- Initial assessment showed that beta phase retention was adversely affected by steam/CO_2 atmosphere when compared to a natural gas baseline. (This could affect the oxidation resistance once the TBC is lost.) Work is continuing to attempt to quantify this into an effect on lifetime.
- The oxidation products observed after steam/CO_2 exposure indicated a more aggressive and unstable scale formation when compared to natural gas which will negatively impact life. Increased spinel formation was observed in the steam/CO_2 environment that has been shown to disrupt the formation of protective oxides.

- The generation of low cycle fatigue data after exposure in steam/CO_2 will provide a preliminary assessment of any debit for both hot gas path and cooling flow design.
- Modeling of the plant cycle has been completed with both natural gas and coal syngas as the fuels. Expected efficiencies for the plant are 33.9% and 25.8%, respectively (LHV) with only a moderate temperature (1,080°C) utilized for the IP turbine inlet.

In the future, this project will focus on the near-term natural gas application that requires an inlet temperature in the range of 1,080°C to 1,180°C (1,976°F to 2,156°F) for the SGT-900 IP turbine. The project will continue materials evaluation work to adapt the turbine to a plant cycle that uses the IP turbine by itself in a simple cycle or in conjunction with a HP steam/CO_2 turbine and a LP steam turbine as in a "combined" cycle. Further, it will seek opportunities to refurbish and deliver the IP turbine to a zero CO_2 emission power plant for demonstration and testing.

FY 2009 Publications/Presentations

1. R. Anderson, V. Viteri, R. Hollis, M. Hebbar, J. Downs, D. Davies, and M. Harris, "Application of Existing Turbomachinery for Zero Emissions Oxy-fuel Power Systems," ASME Turbo Expo 2009, paper GT2009-59995.

III.2 Coal-Based Oxy-Fuel System Evaluation and Combustor Development

Ronald Bischoff
Clean Energy Systems, Inc. (CES)
3035 Prospect Park Drive, Suite 150
Rancho Cordova, CA 95670-6071
Phone: (916) 638-7967; Fax: (916) 638-0167
E-mail: rwbischoff@cleanenergysystems.com

DOE Project Manager: Robin Ames
Phone: (304) 285-0978
E-mail: Robin.Ames@netl.doe.gov

Subcontractor:
Florida Turbine Technologies, Inc. (FTT), Jupiter, FL

Contract Number: 42645

Start Date: October 1, 2005
End Date: September 30, 2010

FY 2009 Objectives

- Complete detailed engineering design drawing package for CES oxy-fuel combustor enclosure.
- Evaluate and test the concept of using a modified gas turbine to serve as an oxy-fuel reheat combustor. Perform cold flow testing on a J79 combustor, modify the combustor and perform hot-fire tests at CES's Kimberlina Power Plant (KPP).
- Prepare validation test plan to support testing of the 100 MW_{th} oxy-syngas combustor (Phase III).

Accomplishments

- Completed piping layout overview and 14 engineering drawing packages for oxy-fuel combustor enclosure's system piping and valve layouts (Fiscal Year 2008). Remaining drawings (syngas and oxygen piping headers) in work and scheduled for completion in August 2009.
- Built prototype J79 oxy-fuel reheat combustors (FTT), instrumented combustors (FTT), and fabricated J79 Reheat Combustor Test Rig (CES). The test rig includes support structure, piping, attemperator, instrumentation, and wiring termination panel. The J79 reheater test rig was shipped to the test site in June 2009.
- Began test site structural, mechanical, and electrical modifications necessary to conduct hot-fire testing of J79 Reheat Combustor. Site modifications scheduled for completion in August 2009.
- Initial draft of validation test plan under review. Completion scheduled for September 2009.

Introduction

CES developed a novel oxy-fuel power generation concept that uses proven aerospace technology to enable near zero-emission power generation from fossil fuels. The core of the technology is a high-pressure oxy-combustor that burns gaseous fuels with oxygen in the presence of water to produce a steam/CO_2 working fluid for steam turbines or modified gas turbines. The CES oxy-combustor has been demonstrated with both natural gas and (simulated) synthetic fuel at CES's 20 MW_{th} KPP outside Bakersfield, CA, where it was used to produce electricity for export to the grid.

CES is also developing a second oxy-fuel combustor, termed a reheat combustor or "reheater", which burns fuel with oxygen to heat steam/CO_2 before it enters a high-temperature intermediate pressure turbine (IPT). This reheater can increase power cycle efficiency and overall plant performance by taking advantage of the higher inlet temperature capabilities inherent in aero-derivative IPTs. The key difference between the reheater and the oxy-combustor is that the reheater requires no water injection. It utilizes combustion techniques commonly deployed in gas turbine combustors, and is closely integrated with the gas turbine expander.

Under DOE award DE-FC26-05NT42645, CES is developing its oxy-combustion technology for coal-based power plants that utilize synthesis gas as the fuel. It is closely associated with DOE award DE-FC26-05NT42646 to Siemens Energy to develop high-temperature turbines powered by steam/CO_2 from the CES oxy-combustor [1]. Combining these two technologies represents an attractive approach to highly efficient, zero-emissions coal-based systems that capture and sequester carbon dioxide and that will meet the DOE goal of enabling high efficiency coal-based power generation with >99% CO_2 capture by 2015.

Approach

In Phase I of the project (FY 2006), CES conducted systems studies of long-term oxy-syngas power plants deployable by 2015. CES then confirmed the operability of its existing oxy-combustor on syngas by fabricating a pilot-scale oxy-syngas injector, installing it in CES's KPP, and successfully operating it with both simulated syngas and H_2-depleted syngas.

During the first portion of Phase II (FY 2007-2008), CES completed a detailed design for a near-zero emission 100 MW_{th} oxy-syngas combustor, its control system, and most associated piping and instrumentation. In FY 2009, CES advanced future oxy-fuel plant efficiency by exploring its concept of modifying an existing gas turbine combustor to serve as an oxy-fuel reheat combustor in the CES oxy-fuel cycle. A "first generation" reheater (a modified GE J79 combustor) will be hot-fire tested to confirm reheater modeling assumptions. Subsequently, a more powerful reheater will be designed and incorporated into a redesigned turbine expander (Siemens SGT-900) able to serve as an advanced "second generation" IPT. The latter provides the most productive approach in a budget-constrained environment to improve near-term cycle efficiency of oxy-coal-syngas power systems.

Results

Enclosure Design (100 MW_{th} Oxy-Syngas Combustor). Ninety-eight percent of engineering design work for the piping, instrumentation, and control system within the enclosure mounting the 100 MW_{th} oxy-syngas combustor was completed in FY 2008. Rapid design completion was feasible because similar process mechanics were used on a CES 170 MW_{th} natural gas-fired combustor in parallel development. As a result, a good deal of engineering could be "cross decked" for the oxy-syngas combustor enclosure. Remaining items for the enclosure design include piping headers (oxygen and syngas feed systems) and update of the overall piping layout. Engineering design is scheduled to be completed in August 2009.

J79 Reheat Combustor Test Rig. Following the completion of detailed component design in FY 2008, FTT fabricated two instrumented oxy-fuel reheat combustors (Figures 1 and 2) developed from J79 combustor "cans." A key modification was installation of oxygen tubes to inject oxygen into a portion of the incoming steam/CO_2 stream to permit further combustion with fuel. The balance of the steam/CO_2 stream is used to lower exhaust gas temperatures to the "normal" firing temperature of 1,700°F (926°C). The completed reheater "cans" were shipped to CES, where one was installed in a dedicated J79 Reheat Combustor Test Rig. The test rig (Figure 3) incorporates (1) a structural frame; (2) housings for the steam inlet, reheater, reheater test section, attemperator, and exhaust; (3) pressure and temperature instrumentation and transmitters; and (4) a wiring termination cabinet. Following completion of loop and pressure checks, the test rig was shipped to its KPP test location (Figure 4). Cold-flow testing of the J79 reheater begins in August 2009 followed by hot-fire testing.

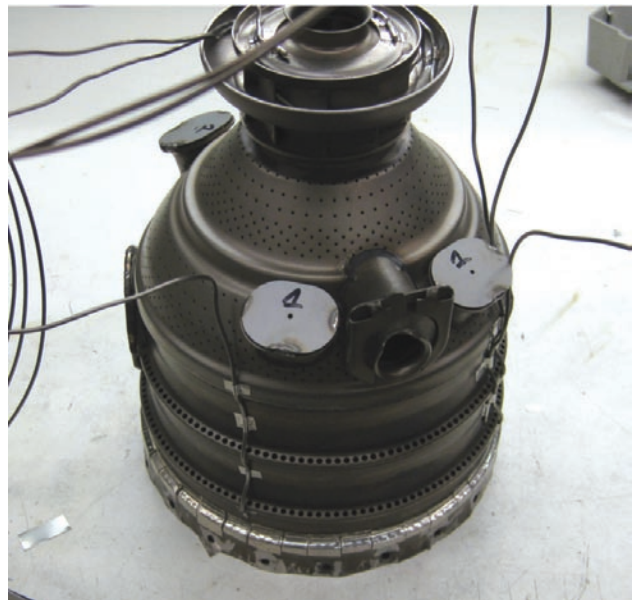

FIGURE 1. J79 Reheat Combustor Prior to Assembly

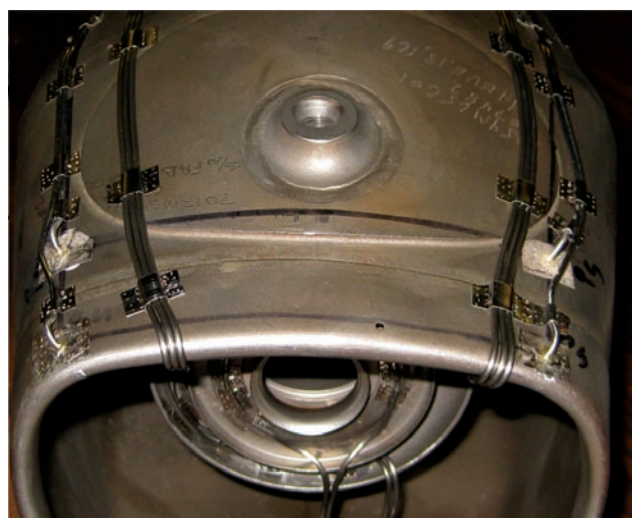

FIGURE 2. Instrumented J79 Reheat Combustor

Test Site Upgrade (KPP). Hot-fire testing of the J79 Reheat Combustor will require structural modifications to the KPP infrastructure. Plant modifications are underway to provide (1) concurrent fuel and oxygen streams to both the steam source (an existing 20 MW_{th} CES oxy-fuel combustor) and the J79 Reheater Test Rig, (2) a larger exhaust line to the existing stack, (3) demineralized water to cool the exhaust stream, (4) instrument air, and (5) wiring for power, control, and instrumentation systems. Plant modifications are scheduled for an August 2009 completion.

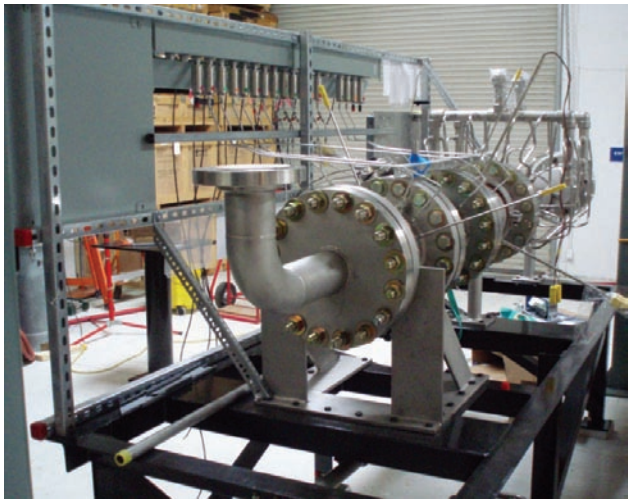

FIGURE 3. J79 Reheat Combustor Test Rig in Fabrication

FIGURE 4. J79 Reheat Combustor Test Rig at KPP

Validation Test Plan. Test plan completion has been deferred several times by funding uncertainties for Phase III, especially in regards to fabrication and testing of the 100 MW_{th} oxy-fuel combustor. A generic test plan is now in work and is scheduled for completion in September 2009.

Conclusions and Future Directions

CES has developed a detailed design for a functional, 100 MW_{th} oxy-syngas combustor which is ready for fabrication and testing. In collaboration with FTT, CES has also developed a prototype GE J79 oxy-fuel reheat combustor, and is currently upgrading the KPP test site to begin reheater validation testing in August 2009. Results from the reheater hot-fire tests will validate/update reheater modeling and then be used to prepare a detailed design of a "second generation" reheat combustor based on a combustor from a Siemens SGT-900 gas turbine. The CES oxy-syngas combustor coupled with a redesigned aero-derivative turbine (Siemens SGT-900) as an oxy-fuel IPT provide the technical steps towards providing a zero-emission power train deployable in the 2012-2013 timeframe.

Patent Applications

1. Utility application No. 12/381,278 for "Method and System for Enhancing Power Output of Renewable Thermal Cycle Power Plants."

2. Provisional application No. 61/209,324 for "Method of Oxy-combustion Power Generation Using Low-heating-value Fuel."

3. Provisional application No. 61/209,322 for "Method of Direct Steam Generation Using an Oxy-fuel Combustor."

FY 2009 Publications/Presentations

1. R.E. Anderson, R. Hollis, F. Viteri (Clean Energy Systems, Inc.); D.O. Davies, J.P. Downs, M. Harris (Florida Turbine Technologies, Inc.); and M. Hebbar (Siemens Energy, Inc.), "Application of Existing Turbomachinery for Zero-Emissions Oxy-Fuel Power Systems," Paper GT200959995, ASME Turbo Expo 2009, Orlando, Florida (June 8–12, 2009).

2. K.L. Pronske, "Carbon Capture and Storage Using Rocket Technology," Solar & Wind Energy Project, Stanford University Speaker Series, Palo Alto, California (April 7, 2009).

3. S. Griffiths (Jacobs Engineering) and K.L. Pronske (Clean Energy Systems–collaboration), "Lose the Carbon, not Your Capacity," *The Chemical Engineer Today* (December 2008/January 2009).

4. R.W. Bischoff, "Turbomachinery Development for Oxy-Combustion, Coal-Based Power Systems (100 MW to 1,000 MW)," International Colloquium on Environmentally-Preferred Advanced Power Generation (ICEPAG 2009), Newport Beach, California (February 10–12, 2009).

5. R. Kent, D. Berokoff (Southern California Gas Company); R. Ferguson, B. Hedman, R. Hite (ICF International); R. Anderson, C. Biebuyck, and S. MacAdam (Clean Energy Systems, Inc.), "CES Gas Generators in Regulation and Peaking Applications," International Gas Union Research Conference, Paris, France (October 8, 2008).

References

1. R.E. Anderson, S. MacAdam, F. Viteri, D.O. Davies, J.P. Downs, and A. Paliszewski, "Adapting Gas Turbines to Zero Emission Oxy-Fuel Power Plants," Proceedings of ASME Turbo Expo 2008: Power for Land, Sea, and Air. Berlin, Germany. June 9–13, 2008.

IV. ADVANCED RESEARCH

IV.1 Analysis of Gas Turbine Thermal Performance

Tom I-P. Shih (Primary Contact),
Kyle Chi, Kenny Hu, Brandon Williams,
K. Mark Bryden, and Minking Chyu
Ames Laboratory
U.S. Department of Energy
2271 Howe Hall, Room 1200A
Ames, IA 50011-2271
Phone: (765) 494-5118
E-mail: tomshih@purdue.edu

DOE Project Manager: Robin Ames
Phone: (304) 285-0978
E-mail: Robin.Ames@netl.doe.gov

Contract Number: AL05205018

Start Date: October 1, 2008
End Date: September 30, 2011

FY 2009 Objectives

- Develop and evaluate computational fluid dynamics (CFD) analysis tools that can be used to study heat-transfer issues in the design of turbine components to support the development of turbine technologies for advanced near-zero emission, coal-based power systems.
- Apply CFD analysis tools to explore and study heat transfer issues in turbine components to support the development of turbine technologies for advanced near-zero emission, coal-based power systems.

Accomplishments

- Studied the coupling between internal and external heat transfer across a flat plate in which the internal cooling passage is lined with rounded inclined ribs as a function of Biot number with and without thermal barrier coating (TBC). Results obtained show that the temperature variations in the turbine material could vary substantially along the lateral direction in the cooling passage, which needs to be accounted for but is not by "first-order" analysis tools used to design cooling strategies because only laterally averaged temperatures are used. Also, it was found that this temperature variation in the lateral direction increases with decreasing Biot number when inclined ribs are used to enhance surface heat transfer.
- Performed preliminary studies on heat transfer in the tip-turn region in a U-duct with and without pin fins.
- Developed and evaluated models for the "residual" in the discrete error transport equation (DETE) to estimate grid-induced errors in solutions generated by CFD.

Introduction

Developing turbine technologies to operate on coal-derived synthesis gas (syngas), hydrogen fuels, and oxyfuels is critical to the development of advanced power generation technologies such as integrated gasification combined cycle and the deployment of near-zero emission-type power plants that can lead to the capture and separation of carbon dioxide (CO_2). Whether the fuel burned is natural gas, syngas, or a hydrogen mixture, the efficiency and service life of a gas turbine are strongly affected by the turbine component, where the thermal energy in the high-pressure and high-temperature gas from the combustor is converted to mechanical energy to drive the compressor and the electric generator to create electricity. The most effective way to increase the efficiency of gas turbines is to raise the temperature of the gas entering the turbine component, which can be as high as the adiabatic flame temperature from the combustion of fuel and oxidizer. The challenge lies in the fact that the inlet temperatures sought today, though still considerably lower than the adiabatic flame temperature, already far exceed the maximum temperatures at which even the best materials can maintain structural integrity with reasonable service life.

This project has two objectives. The first is to develop and evaluate CFD-based analysis tools that can be used to study heat transfer issues in the design of the turbine component and to develop guidelines and best practices on their usage. The second is to apply those analysis tools to support the development of turbine technologies for advanced near-zero emission-type coal-based power systems. The analysis tools of interest are those that can properly account for the steady and unsteady three-dimensional heat transfer from the hot gas in the turbine blade/vane passages through the turbine material – the TBC system and the super alloy – to the internal cooling passages as a function of the cooling strategy as well as a function of the hot gas and coolant compositions, the mass flow rates, and the temperature of the hot gas and the coolant.

Approach

Analysis tools used to design gas-turbine cooling strategies are typically based on quasi-dimensional methods. These analysis tools require inputs on the details of the fluid-flow and heat-transfer processes such as pressure loss coefficients as well as regional or laterally-averaged heat-transfer coefficients. There are two ways to generate the information needed, and they are experimental measurements and CFD simulations. Here, CFD is used, and it is based on the conservation/balance equations of species, continuity, momentum, and energy that govern the three-dimensional flow and heat transfer processes. Depending on the nature of the problem, the effects of turbulence may be modeled by steady Reynolds-Averaged Navier-Stokes (RANS), unsteady RANS, detached eddy simulation, or large-eddy simulation.

Results

Advanced gas turbines are designed to operate at near the material's maximum allowable temperature. Thus, there is very little room for mistakes in the design of cooling strategies. Since the heat transfer coefficient varies significantly about ribs and pin fins in internal cooling passages, different parts of the turbine material exposed to the hot gas are cooled at different rates by internal cooling. Accordingly, there could be substantial temperature variations within the material, including hot spots (i.e., locations where the material temperature exceeds the maximum allowable). For a given hot gas temperature and a given coolant temperature, the amount of temperature variation within the material depends on the Biot number (Bi). Conjugate heat transfer analysis performed show that for two geometrically similar TBC-coated flat plates exposed to the same hot gas and coolant temperatures, if the Bi is nearly the same, then the magnitude of the temperature will be nearly the same and the contours of the temperatures will be nearly geometrically similar. The contours of heat flux, however, will be geometrically similar but have very different magnitudes because the gradients are different. These results show that Bi could be used in the design of experiments just like the Reynolds number. On the effects of Bi, it was found that though the variations in temperature from the hot gas to the coolant side of the TBC-coated plate decrease with decreasing Bi, which is what one would expect, the variation in temperature in the lateral direction could increase with decreasing Bi. When the Bi based on plate thickness is between 0.4 to 1, that temperature variation in the super alloy next to the TBC can differ by as much as 25 K along the lateral direction because of the large variations in the local heat transfer coefficients induced by the ribs in the lateral direction.

To improve turbine efficiency, in addition to the aggressive goals on the turbine inlet temperature, industry wants to reduce the cooling flow rate by 50%. One region, where cooling is an issue is the tip region of blades and vanes, especially with the markedly reduced coolant flow rate. The issue in the cooling design is how to place heat transfer enhancement devices inside internal cooling passages so that cooling in turn regions of U-shaped ducts (referred to as the tip-turn region) is nearly uniform with minimal pressure loss. Figure 1 shows results from a CFD simulation of a tip-turn region, where the heat-transfer enhancement device is the pin fin.

In order for CFD to truly impact design, it is important to be able to quantify errors in CFD solutions, similar to error bounds on experimental data. In this study, efforts were made to continue the development of the DETE approach to estimate errors in CFD solutions that are induced by poor quality grid or by an insufficient number of grid points to resolve the flow. Several models of the residual in the DETE equations were developed and evaluated. Results obtained show that the DETE approach developed is quite promising.

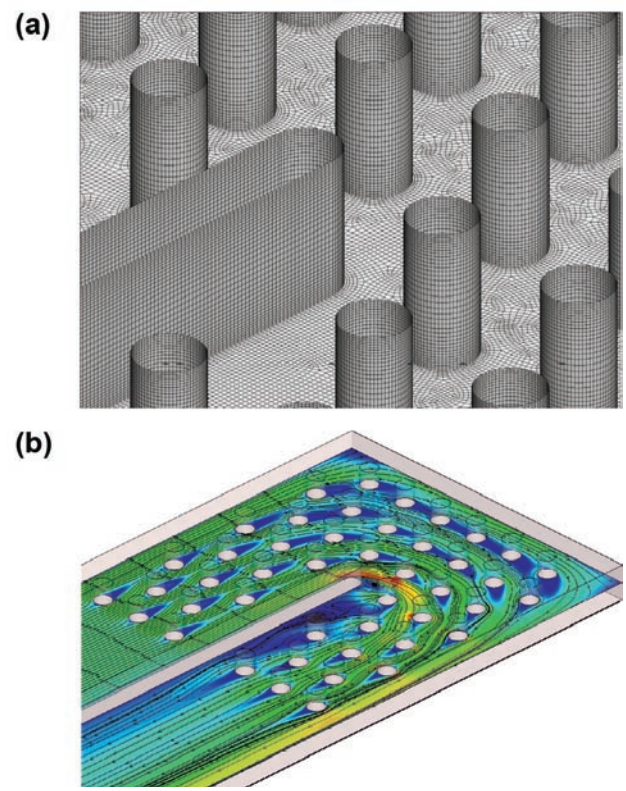

FIGURE 1. CFD simulation of flow and heat transfer in a U-duct lined with pin fins. (a) Grid near the tip-turn region of the U-duct. (b) Predicted streamlines colored by velocity magnitude in the mid plane.

Conclusions and Future Directions

Analysis tools used to design gas-turbine-cooling strategies must recognize that large local variations in heat transfer coefficient in the internal cooling passages induced by heat transfer enhancement devices such as inclined ribs could induce considerable temperature differences within the turbine material in directions perpendicular to the main flow direction. In this study, it was found that these variations in temperature are higher as the Biot number decreases. More study is needed to understand how to quantify and utilize the Biot number in the design and analysis of cooling strategies.

Preliminary studies of flows in the tip-turn region of internal cooling passages show a need to develop efficient and possibly automatic grid generation tools that can be used to explore design concepts on where to place heat transfer enhancement techniques to ensure nearly uniform cooling of that region with minimal pressure loss under rotating and non-rotating conditions.

The DETE method was found to be a promising method for estimating errors induced by the grid and in providing an error bound on computed CFD solutions. Also, the DETE method can be used as a method to refine grids to generate more accurate CFD solutions. Future work in DETE includes continuing the development of better models for the residual in the DETE equation and the development of a DETE approach for time-accurate CFD solutions.

FY 2009 Publications/Presentations

1. B. Williams and T.I-P. Shih, "Estimating Grid-Induced Errors in Navier-Stokes Solutions via a Discrete Error Transport Equation," AIAA Paper 2009-1499, January 2009.

2. T.I-P. Shih, X. Chi, K.M. Bryden, C. Alsup, and R.A. Dennis, "Effects of Biot Number on Temperature Distribution in a Flat Plate Cooled by Rib-Enhanced Internal Cooling," ASME Paper GT2009-59726, IGTI Conference, Orlando, Florida, June 2009.

3. S. Na, R.A. Dennis, C. Alsup, K.M. Bryden, T.I-P. Shih, "Effects of Hot-Gas Composition on Temperature Distribution in a Flat Plate Cooled by Internal and Film Cooling," ASME Paper GT2009-59727, IGTI Conference, Orlando, Florida, June 2009.

IV.2 Development of Comprehensive Detailed and Reduced Reaction Mechanisms for Syngas and Hydrogen Combustion

Dr. Chih-Jen Sung
Case Western Reserve University
10900 Euclid Ave.
Cleveland, OH 44106
Phone: (216) 368-2942; Fax: (216) 368-6445
E-mail: cjs15@case.edu

DOE Project Manager: Mark Freeman
Phone: (412) 386-6094
E-mail: Mark.Freeman@netl.doe.gov

Subcontractors:
- Hai Wang, University of Southern California, Los Angeles, CA
- Angela Violi, University of Michigan, Ann Arbor, MI

Contract Number: 42717

Start Date: March 1, 2006
End Date: February 28, 2009

FY 2009 Objectives

- Generate a detailed experimental database of syngas and hydrogen combustion at integrated gasification combined cycle (IGCC)-like conditions.
- Investigate the fundamental chemical kinetics of $H_2/CO/O_2/N_2/H_2O/CO_2$ at pressures, temperatures and concentrations typical of syngas and hydrogen combustion in gas turbines.
- Develop detailed and reduced chemical mechanisms based on this database, capable of predicting syngas and hydrogen combustion.

Accomplishments

- Obtained extensive experimental data of ignition delays for moist syngas mixtures at a compressed pressure of 30 bar and a temperature range of 930–1,080 K. The stoichiometric reactant mixtures are studied with water additions of 0–10% in the total mixture and H_2/CO molar ratios of 5/95–100/0.
- Experimental results are simulated using various literature reaction mechanisms to compare the trend in predicting autoignition response.

Introduction

This project aims to provide comprehensive and computationally efficient chemical kinetic mechanisms for facilitating the design of future coal-derived synthesis-gas (syngas) and hydrogen-fueled combustion turbines through computational fluid dynamics simulations. Benchmark experimental data are obtained for combustion characteristics, such as laminar flame speeds and autoignition delays, of syngas mixtures, over a wide range of conditions. This critical database is needed for validation of chemical kinetics of syngas combustion and is used in conjunction with computation methods, such as global uncertainty analysis, to assess the performance of the literature reaction mechanisms.

This report presents the experimental autoignition delay data of moist $H_2/CO/O_2/N_2/Ar/H_2O$ mixtures, with special emphasis on the effect of water addition on autoignition delay. The present experimental results provide an extensive database for the understanding of combustion characteristics at varying syngas compositions. In addition, the resulting experimental database will be of practical use in determining the desired syngas compositions for optimal IGCC operation, as well as improving the design and operation of advanced combustors fueled by syngas and hydrogen.

Approach

In order to obtain extensive experimental data for validation of chemical kinetic mechanisms over a wide range of physical conditions, experiments are carried out in a rapid compression machine (RCM) and a counterflow burner apparatus. A RCM allows access to the low-to-intermediate temperature autoignition chemistry at elevated pressures, whereas a counterflow burner allows experimentation with flames under conditions related to high-temperature kinetics. In conjunction with experimental data, quantum chemical calculations are conducted to determine the rate constants of critical reactions.

The experimental setup consists of a RCM, a flow control/supply system, and a mixing chamber. Both the RCM and the mixing chamber along with the manifolds have a provision for heating up to a maximum temperature of 400 K. For the current study, in order to cover the entire range of water addition, the

whole experimental setup is heated to a temperature of 350 K. This RCM consists of a reaction chamber in which the reactant gases are compressed by a creviced piston arrangement. The creviced piston is driven by an arrangement of the pneumatic piston and high-pressure air tank. It is held in place by an arrangement of the hydraulic cylinder. A trigger of a solenoid valve releases the pressure of the hydraulic chamber, and thus the piston arrangement moves forward by the pneumatic system. Towards the end of the compression stroke, the piston is decelerated and finally stopped by the piston stopping groove. The compression stroke of the RCM takes an average time of 30 ms. The end reaction chamber is equipped with a pressure transducer and a thermocouple. It is also provided with quartz windows for any required optical access. Figure 1 shows the schematic of the RCM with general details of the end reaction chamber and the creviced piston. The compression ratio of the machine can be changed by changing the clearance and/or the stroke length. Split shims are used to vary the clearance between hydraulic cylinder and the reaction chamber and the stroke can be adjusted by using spacers.

The mixing chamber consists of an airtight stainless steel tank, with an arrangement of magnetic stirrer for proper mixing of the constituents. The tank is provided with a rupture disc as a safety measure against accidental overpressure within the mixing tank. The gas mixtures are prepared at room temperature, gases are filled into the mixing chamber by the method of partial pressures, while water is gravimetrically measured and injected into the chamber. High-purity gases are used for this study: CO (99.998%), H_2 (99.999%), N_2 (99.999%), O_2 (99.993%), and Ar (99.999%). Moreover, deionized water (total dissolved solids <0.03571 ppm and ρ >14 MΩ-cm) is used.

Results

Experiments to be presented here are conducted at stoichiometric condition (ϕ=1.0) for three different CO/H_2 ratios of R_{CO}= 0, 0.5, and 0.95 with molar percentage of water in the mixture of 0%, 2.5%, 5%, and 10%, where R_{CO} is defined as the molar fraction of CO in the combined H_2+CO fuel mixture. Nitrogen and argon are used to adjust the specific heats of the gas mixtures to approximately the same value over the temperature range of 350–1,000 K. For a given mixture composition, the compressed gas temperature at the end of compression, T_C, is varied by altering the compression ratio, whereas the desired pressure at the end of compression, P_C, is obtained by varying the initial pressure of the reactive mixture. The compressed gas temperature is determined by the adiabatic core hypothesis.

Figure 2 shows the effect of water addition on ignition delay over a range of compressed temperatures for the pure hydrogen case (R_{CO}=0). The initial mixture temperature is T_0=350 K. It is seen that ignition delay increases with 2.5% water addition, as compared to the dry condition. However, the ignition delay decreases as water addition is increased to 5%, indicating higher reactivity of the moist mixture. The ignition delay further decreases with 10% water addition, as demonstrated in Figure 2.

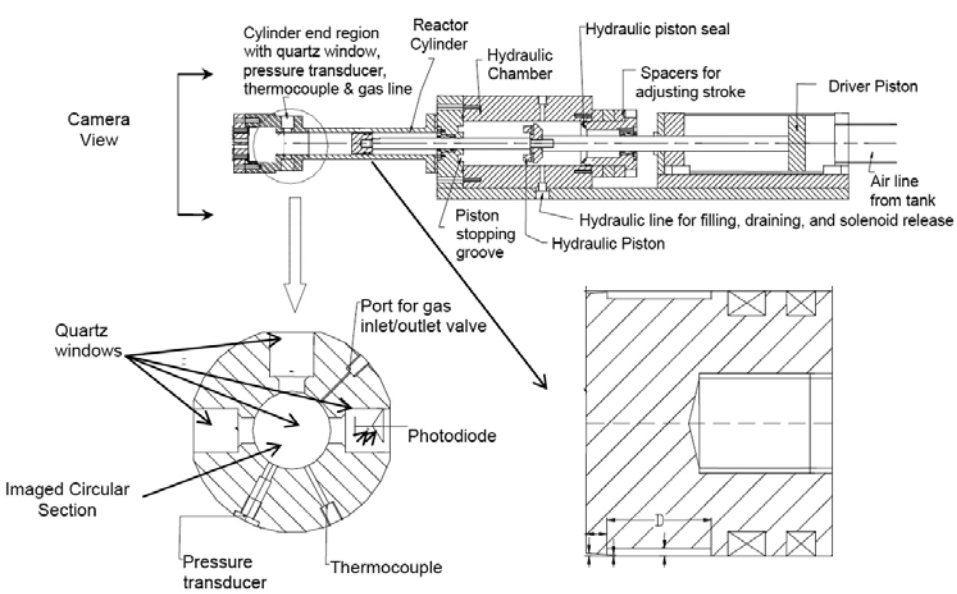

FIGURE 1. Schematic of the Rapid Compression Machine, the End Reaction Chamber, and the Creviced Piston Head

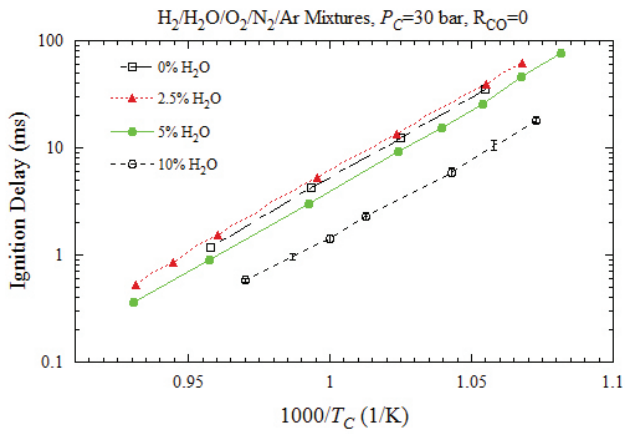

FIGURE 2. Ignition Delays at 30 Bar for ϕ=1, T_0=350 K, and R_{CO}=0 with Water Addition (0–10%)

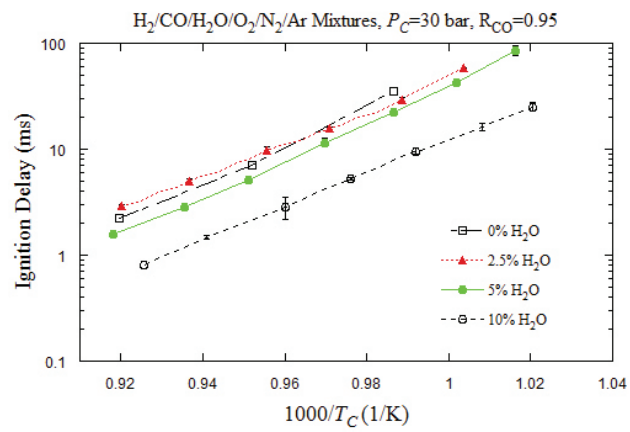

FIGURE 3. Ignition Delays at 30 Bar for ϕ=1, T_0=350 K, and R_{CO}=0.95 with Water Addition (0–10%)

Figures 3 and 4 show the ignition delay results for R_{CO}=0.95 and 0.5, respectively. It is also seen that with 5% and 10% water addition, ignition delay is reduced as compared to the corresponding dry case. At 2.5% water addition, however, the ignition response depends on the compressed charge temperature. In the case of R_{CO}=0.95, while at higher compressed temperatures (T_C>1,030 K) the ignition delay is higher when compared to 0% water addition, the ignition delay becomes shorter when T_C<1,030 K. For R_{CO}=0.5, with 2.5% water addition, the ignition delay is slightly more than the case without water addition for higher compressed temperatures, but at T_C<1,010 K, the ignition delay is shorter when compared to the dry case.

The ignition delay data at P_C=30 bar and T_C~1,010 K are further compared as a function of R_{CO}. It is found that at lower values of R_{CO}, the ignition delay is slower at 2.5% water addition, with comparison to the dry case. At R_{CO}=0.5 the difference is minimum, and at R_{CO}=0.95, the ignition delay becomes faster. It is also noted that with 5% and 10% water addition, the ignition delays are lower for all values of R_{CO}. However, the extent of reduction is minimum for R_{CO}=0, increases at R_{CO}=0.5, and is largest at R_{CO}=0.95.

The above experimental results indicate a complex behavior of ignition delay with water addition, which needs further study to understand fully. Constant volume, adiabatic calculations are conducted using SENKIN for pure hydrogen mixtures (R_{CO}=0) at initial conditions of 30 atm and 1,000 K to examine and compare the trends predicted by different reaction mechanisms reported in the literature. Because of different ignition delay values predicted by different mechanisms, for a fair comparison regarding the ignition delay response with respect to water addition, the predicted ignition delays in the water addition range of 0–10% are normalized by the ignition delay

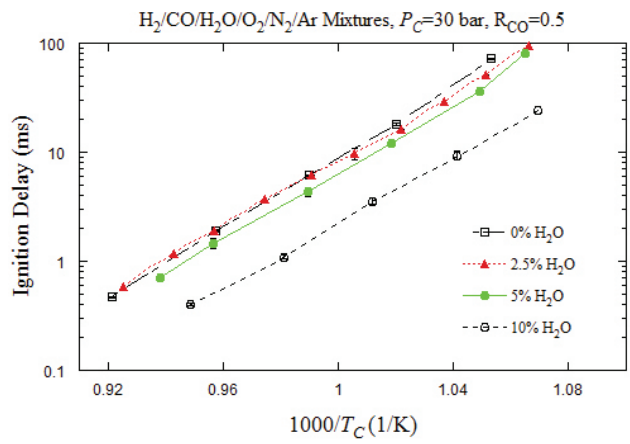

FIGURE 4. Ignition Delays at 30 Bar for ϕ=1, T_0=350 K, and R_{CO}=0.5 with Water Addition (0–10%)

with 0% H_2O addition. The normalized ignition delays, [$\tau(x\%\ H_2O)/\tau(0\%\ H_2O)$], obtained by using various mechanisms, are compared as a function of percentage water addition. It is found that the effect of water addition on ignition delay observed in our RCM experiments is only captured by the Lawrence Livermore mechanism for pure hydrogen. The other reported H_2/CO mechanisms tested fail to capture the experimental trend.

Conclusions and Future Directions

- Ignition delay experiments over a wide range of H_2/CO ratios (or R_{CO} values) are conducted using a RCM, with special emphasis on the effect of water addition on autoignition.
- The study so far reveals a complex dependence of ignition delay with water addition for various values of R_{CO}.

- For the pure hydrogen case (R_{CO}=0), it is seen that with 2.5% water addition, the ignition delay increases, and further water addition leads to a decrease in the ignition delay time.
- For the CO rich case (R_{CO}=0.95), the temperature dependence of ignition delay at 2.5% water addition is observed. While at higher temperatures the ignition delay with 2.5% water addition is higher than the dry case, at lower temperatures the ignition delay with 2.5% water addition becomes lower.
- For R_{CO}=0.95, with further water addition at 5% and 10%, the ignition delays consistently decrease as compared to the dry case, for the conditions tested.
- Further experiments at other pressures are required to fully understand the ignition response with water addition.
- Flux flow analysis using the Lawrence Livermore mechanism for pure hydrogen can also be helpful to understand the chemical kinetic aspect for the effect of water addition on ignition delay.

FY 2009 Publications/Presentations

1. A.K. Das, K. Kumar, and C.J. Sung, "Laminar Flame Speeds of Moist Syngas Mixtures," 6th U.S. National Combustion Meeting, Ann Arbor, May 2009.

2. A.K. Das, C.J. Sung, and G. Mittal, "Ignition Delay Study of Moist Syngas Mixtures Using a Rapid Compression Machine," 6th U.S. National Combustion Meeting, Ann Arbor, May 2009.

IV.3 Practical Multi-Step Turbulent-Combustion Model for Fuel-Flexible Gas Turbine Combustor Analysis

S.F. Owens, R.S. Mehta (Primary Contact)
CFD Research Corporation
215 Wynn Drive, Suite 501
Huntsville, AL 35805
Phone: (256) 726-4800; Fax: (256) 726-4806
E-mail: sfo@cfdrc.com, rsm@cfdrc.com

DOE Project Manager: Mark Freeman
Phone: (412) 386-6094
E-mail: Mark.Freeman@netl.doe.gov

Contract Number: 85007

Start Date: June 30, 2008
End Date: March 29, 2009

FY 2009 Objectives

The principal objective of this project was to develop a computationally efficient, turbulent combustion model that has the following features.

1. Model the subgrid-scale turbulence-chemistry interactions in a computationally feasible manner,
2. Incorporate the differential diffusion of the various species,
3. Generate computationally tractable reduced global reaction mechanisms that reproduce important flame characteristics such as the flame speed, ignition delay, and flammability limits for a given set of operating conditions, and
4. Incorporate the effects of local grid size (or filter width) on turbulence-chemistry interactions and, in particular, the species diffusivities.

Accomplishments

A new computationally efficient turbulent combustion model has been developed and validated. The Modified Global Mechanism (MGM) model has been implemented in a highly modular form consisting of user-defined functions. The MGM model is unique in that the effects of turbulent and differential diffusion can be included at the stage of global mechanism development itself. A substantial amount of validation effort has been undertaken for the MGM model using both Reynolds averaged Navier-Stokes (RANS) and large eddy simulation (LES). It is seen that LES coupled with the MGM model shows better agreement with experimental data than does RANS.

Introduction

Turbulent combustion modeling has been an actively researched topic for past several decades. Most recent combustion models include finer details and flame physics into the models [1,2]. These models are computationally prohibitive when used in conjunction with LES. LES of practical combustion configurations, such as gas turbine combustors, typically require tens of millions of grid cells. Simplistic models such as models using a single-scalar approach, cannot account for important physics such as preferential diffusion of lighter species compared to heavier ones in turbulent transport. In addition, accurate modeling of combustion processes may potentially require consideration of reaction mechanisms involving hundreds of species and thousands of reactions. Such a large number of species cannot be incorporated into any realistic combustion simulation. Current computing resources allow the inclusion of only up to ~20 species and a few hundred reactions in high-fidelity simulations of reacting flows in complex engineering configurations (e.g. gas turbine combustors, internal combustion engines, rocket engines).

In this project, a more practical turbulent combustion model named the MGM is being developed for modeling the subgrid scale turbulence-chemistry interactions. In Phase I, the initial MGM model has been developed and the feasibility of the proposed approach successfully demonstrated. Global multi-step reaction mechanisms are generated at the relevant flow conditions (e.g. pressure, inlet temperature, and range of equivalence ratios etc.) using Firefly technology developed by CFD Research Corporation [3,4]. The global reaction mechanisms generated by Firefly are modified, in the context of LES to account for the local subgrid diffusion and subgrid turbulence-chemistry interactions. The turbulent reaction rates also include effects of preferential molecular diffusion.

Approach

The overall objective of this Small Business Innovation Research project (Phase I and Phase II) is to develop and validate a practical turbulent combustion model called the MGM model for LES of gas turbine combustor applications. Three key features are addressed in the turbulent combustion model:

1. Effects of turbulent fluctuations in species concentrations and temperature,
2. Effects of molecular preferential diffusion, and
3. Effects of numerical diffusion (depending on the differencing schemes and grid size) on reaction kinetics.

The MGM model development starts with creation of an appropriate global mechanism that reproduces behavior of a validated detailed mechanism over a range of operating conditions such as equivalence ratios, temperature and pressure relevant to the problem at hand. The global mechanism is then modified to include effects of concentration fluctuations and turbulent diffusion of the species. The modified global mechanism is then used in an LES simulation. The basic approach for generating MGM model is shown in Figure 1.

To establish feasibility, the work done in Phase I focused on accounting for the effects of subgrid-scale turbulence-chemistry interactions in a computationally efficient manner. The Phase II efforts will focus on improving the model by adding capabilities such as accounting for effects of (insufficient) grid resolution on reaction kinetics, providing easy to use user-interface and efficient techniques to deliver a complete and practical turbulent combustion model.

Results

To validate the MGM model, the bluffbody-stabilized flame experimental data obtained by Nandula et al. [5] are used. The temperature contours obtained from the LES with and without the MGM model are shown in Figure 1. The flame blowout in the absence of the MGM model shows that turbulence-chemistry interactions are critical when predicting the flame-structure in turbulent combustion and they can be captured by the MGM model. The inclusion of the MGM model in the simulations results in only a nominal increase in computational expense. This encouraging result is a successful demonstration of the feasibility of the MGM modeling approach.

LES predictions with the MGM model included are compared with the corresponding experimental data in Figure 2. The LES predictions agree better with the experimental data than do the RANS predictions. We believe that further improvements in LES (and RANS) predictions can be attained by including radiation heat losses in the simulation. Numerical prediction of concentration profiles of minor species, e.g., CO, NO and OH, is particularly challenging because: (1) the minor species are much more sensitive to reaction kinetics than the major species; and (2) experimental measurement of minor species concentrations entails significant errors. The comparison of minor species can sometimes point to the specific strengths or deficiencies of the reaction mechanisms being used.

Figure 3 shows a comparison of the predicted CO mole fraction profiles with experimental data. The RANS simulations tend to over-predict the CO mole fractions at all the axial locations. The LES tend to under-predict CO mole fractions within a factor of ~2 for most of the domain, which is considered very reasonable for minor species.

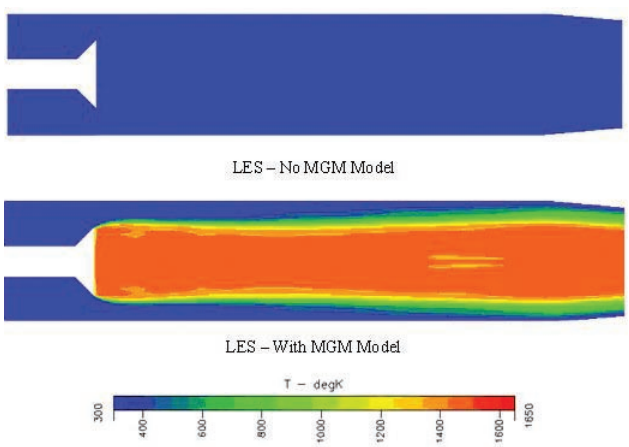

FIGURE 1. Temperature Contours for the Vanderbilt Combustor Using LES with and without MGM

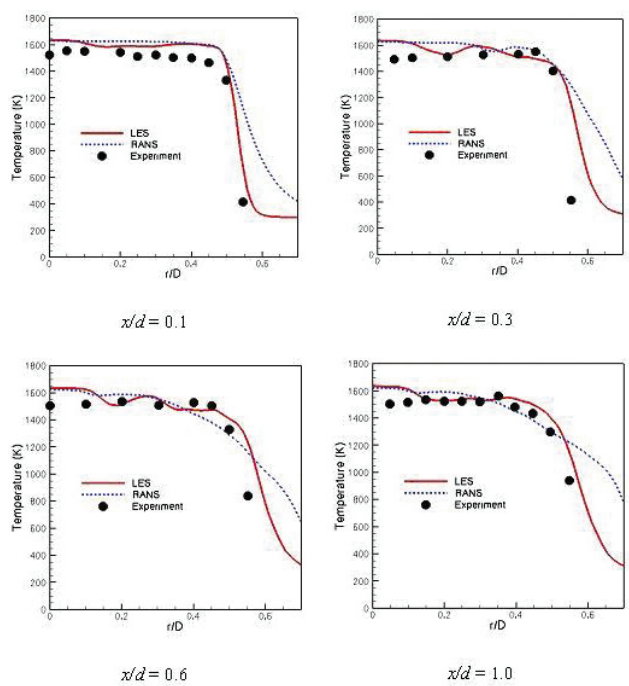

FIGURE 2. Computed and Measured Radial Temperature Profiles with Experiments at Various Axial Stations

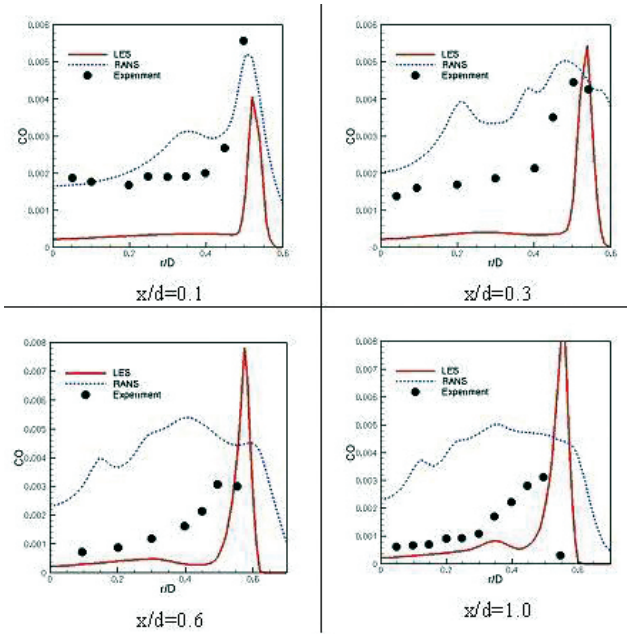

FIGURE 3. Computed and Measured Radial CO Mole Fraction Profiles with Experiments at Various Axial Stations

Conclusions and Future Directions

In Phase I, the aim was to demonstrate the feasibility of a turbulent combustion model, including effects of differential diffusion and subgrid-scale turbulence-chemistry interactions in a computationally efficient manner. All the objectives proposed in the Phase I study have been achieved and feasibility of a practical multi-step turbulent combustion model was demonstrated as well as validated. Specific accomplishments and conclusion of the Phase I study along with recommendations for future work are discussed below.

Some specific achievements and findings from the Phase I efforts are summarized below.

- A new computationally efficient model, namely the MGM model for turbulence-chemistry interactions has been developed and validated.
- The MGM model is implemented in a highly modular form consisting of user-defined functions and designed to be completely flexible in terms of its usability with different computational fluid dynamics codes.
- The model's ability to use a species-based approach, rather than a mixture fraction-based one, greatly enhances the amount of physics that can be included during the development of modified mechanisms, while still being computationally very inexpensive. For example, the MGM model can include a full multi-component diffusion treatment for various species, instead of using the Lewis number (Le=1) criterion common in single-scalar approaches for premixed combustors.
- Validation case results demonstrate feasibility of the proposed MGM modeling methodology. As such, there is great promise for further development of the MGM model during a prospective Phase II.

The primary Phase II objective is to further refine and advance the MGM model through the following proposed efforts.

- The effects of insufficient grid resolution and numerical diffusion will be incorporated into the MGM model. Such an inclusion will allow use of relatively coarser grids without loss of accuracy during simulations, thereby reducing the simulation times significantly.
- A new interface will be created for easier generation of the Modified Global Mechanisms for a range of parametric values. This software would greatly enhance the MGM model and hence, the commercialization potential.
- Use of experimental data directly for generation of global mechanisms will be undertaken as a part of the Phase II effort. This capability will allow for generation of global mechanisms for complex fuels and fuels with uncertain compositions, such as bio-fuels, bio-diesels and waste matter. This effort would be highly significant toward accurate modeling of fuel-flexible combustors.

References

1. N. Peters, Turbulent Combustion, Cambridge University Press, 2000.

2. D. Veynante and L. Vervisch, "Turbulent Combustion Modeling," Prog. Energy Combust. Sci. 28, 2002, 193-266.

3. D.L. Black and K.V. Meredith, "Automated Global Mechanism Generation for Use in CFD Simulations," AIAA 44th Aerospace Sciences Meeting and Exhibit, Reno, Nevada, AIAA-2006-1168, 2006.

4. M.E. Lee and K. Meredith, "Automated Generation of Accurate Multi-Step Global Mechanisms via Detailed Kinetic Calculations," JANAFF Paper, 2006.

5. S.P. Nandula, R.W. Pitz, R.S. Barlow, and G.J. Fiechtner, "Rayleigh/Raman/LIF Measurements in a Turbulent Lean Premixed Combustor," AIAA 34th Aerospace Sciences Meeting, Reno, Nevada, AIAA#96-0937, 1996.

IV.4 Faradayic ElectroPhoretic Deposition of YSZ for Use in Thermal Barrier Coatings

Ms. Heather McCrabb (Primary Contact), Joseph Kell
Faraday Technology, Inc.
315 Huls Drive
Clayton, OH 45315
Phone: (937) 836-7749; Fax: (937) 836-9498
E-mail: heathermccrabb@faradaytechnology.com

DOE Project Manager: Mark Freeman
Phone: (412) 386-6094
E-mail: Mark.Freeman@netl.doe.gov

Subcontractor:
University of Dayton Research Institute, Dayton, OH

Contract Number: 84202

Start Date: June 27, 2005
End Date: August 6, 2009

FY 2009 Objectives

- Optimization and validation of the Faradayic electrophoretic deposition (EPD) process for deposition of thermal barrier coatings (TBCs) with the appropriate microstructures to prevent coating failure during standard and accelerated turbine engine operation in natural and syngas environments.
- Development and validation of a post deposition thermal treatment for the EPD coatings to preserve the necessary microstructure to maintain coating durability and reliability during operation.
- Qualification of coating durability and reliability through appropriate tests of merit, e.g. thermal stability, thermal cycling, thermal conductivity, etc.

Accomplishments

- Demonstrated that the Faradayic EPD process can reduce surface roughness and hydrolysis related coating defects observed during conventional EPD.
- Confirmed through X-ray diffraction that yttria stabilized zirconia (YSZ) TBC does not undergo a detrimental phase change from tetragonal to monoclinic during post deposition thermal treatment.
- Confirmed through scanning electron microscopy analysis a porous, laminar coating microstructure.
- Preliminary thermal cycling data has shown that the Faradayic EPD process can produce films that survive in excess of 100 cycles on bond-coated IN939 substrate at both 1,000°C and 1,092°C.
- A method for fabricating freestanding films for thermal conductivity tests was developed.
- Initiated negotiations with an interested party to conduct component testing in a simulated turbine environment.
- Agreement with commercial partner to conduct coating qualification tests for comparison with commercially available TBC manufacturing processes.

Introduction

The design and manufacturing of gas turbine engines is challenging from both an engineering and material science standpoint due to the engine's high rotational speeds and high operating temperatures. Component failure stems from several sources including corrosion due to hot gases contaminated with chloride and sulfate, oxidation in an enriched oxygen environment, mechanical wear and erosion. Additionally, the components experience extreme temperatures, constant thermal cycling and thermal shock. Turbine blades are especially susceptible to damage, requiring routine maintenance for repairs, refurbishing or replacement. TBCs are employed to protect the turbine engine components. These coating systems provide thermal, oxidation and mechanical protection, reduce thermal gradients and lower the metal substrate surface temperature, extending the life of the engine components.

Faraday is developing a new manufacturing process, the Faradayic EPD process, for TBC deposition of YSZ onto gas turbine components. It should be noted that EPD can deposit any material that can be manufactured in submicron powder form, thus it is not restricted to YSZ and would be suitable for new TBC material sets that have lower thermal conductivity necessary for increased turbine operating temperatures. The Faradayic EPD process combines conventional EPD with pulsed electric fields to induce migration of charged particles in a suspension to uniformly deposit the TBCs onto the gas turbine components. It is a non-line-of-sight process, making it suitable for coating complex shaped components with a TBC of controllable thickness and a microstructure

that is sufficiently strain tolerant to survive in the turbine environment.

Approach

Conventional EPD is similar to electrolytic deposition except that the deposited particles do not undergo a valence change during deposition. Conventional EPD involves charging the particles in suspension, applying a direct current electric field induced migration of the particles toward the oppositely charged component to be coated and deposition and adherence of the particles onto the component. Conventional EPD has the benefits of fast deposition rates, non-line-of-sight deposition, simple deposition equipment, low levels of contamination and reduction of waste relative to dipping or spraying processes.

The Faradayic EPD process combines conventional EPD with pulsed electric fields to induce migration of charged particles in a suspension to uniformly deposit the TBCs onto the gas turbine components. Figure 1 shows a schematic drawing of a Faradayic pulse reverse electric field used to electrically mediate the applied electric field during the Faradayic EPD process.

The application of a coating using conventional or Faradayic EPD results in a loosely bonded layer of coating particles defined as a green coating. A post-processing thermal treatment is required to transform the green coating into its final form. Since the green coating has limited strength, the post-processing methods must be controlled from several aspects, including care in handling, exposure to contaminants, and elapsed time between operations. The approach for the post-processing of EPD coatings is to establish the requirements for a coating system in terms of

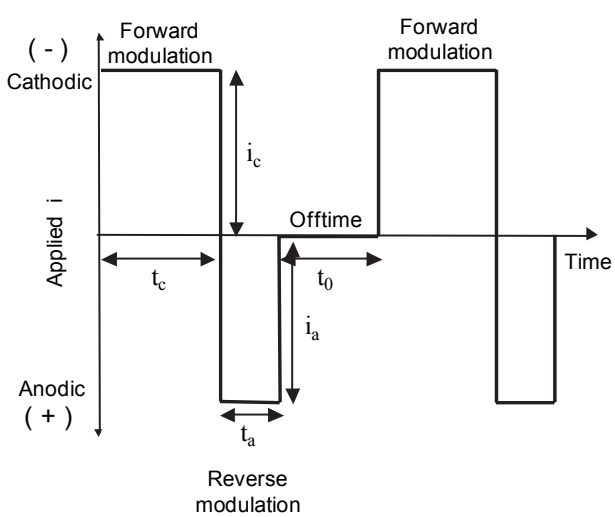

FIGURE 1. Faradayic Electric Field

thickness, grain morphology, thermal properties and bond strength to the substrate. There are a variety of post-processing methods that are applicable to EPD methods; for TBCs, Faraday is investigating thermal sintering as well as alternative techniques such as directional heating, microwave and infrared sintering. The priorities for a post-deposition process are as follows:

- Establishment of a quality bond between the coating layer and the bond coated substrate material.
- Diffusion, densification, and consolidation to the required percentage theoretical density.
- Preservation of the coating and substrate microstructures.
- Control of the dimensional thickness.

Results

Faraday is performing deposition experiments with bond-coated IN939 and Haynes 230 button samples supplied by Siemens Power Generation, Inc. in Orlando, Florida. The substrate alloys are formulations currently used in the turbine engines and the bond coat is sufficiently rough enough to enable the adhesion of the YSZ particle applied using EPD. A benchtop EPD system that includes an EPD deposition cell, a TEGAM arbitrary waveform generator, a Kepco bipolar power supply/amplifier, a Sears multimeter, and a Fluke oscilloscope was assembled for the deposition experiments.

Coatings were deposited from a suspension of YSZ particles suspended in ethanol. Organic dispersants and binders were used to charge the particles and enhance the green coating adhesion. Scanning electron microscopy (SEM) analysis of a cross section of the green coating suggests that the microstructure is porous and laminar with intermittent microcracks that should provide a low thermal conductivity (Figure 2). Our currently optimized EPD coatings are ~110 µm thick and the coating porosity is estimated at ~40% (yielding an approximate density of 60% of the theoretical density).

Faraday has also continued to develop the post-deposition thermal treatment process to consolidate the EPD green coatings and increase the mechanical integrity of the coating. The thermal post-deposition treatment includes an integrated binder burnout step and sintering step. Differential scanning calorimetry and gravimetric analysis were used to determine the temperature at which the binders can be successfully removed from the coating before sintering. Energy dispersive X-ray spectroscopy (EDS) was used to confirm the organics were removed (binders and dispersants) from the coating prior to sintering. Faraday has made the following conclusions about

the post-deposition thermal treatment based on the experiments that have been conducted:

- Mud cracks, which are known to be related to the drying step, seem to be associated with relative maximum peaks in the underlying bond coat, likely meaning that smoother bond coats may help with the mud cracks (see Figure 2).
- Hardness testing of sintered samples has shown that the samples are still continuing to sinter at 1,092°C, showing that the post-processing plays a significant role in the mechanical properties of the sample.
- X-ray diffraction studies showed that no detrimental monoclinic phase changes have occurred due to the process or sintering.
- Thermal cycling tests have demonstrated the samples are at least moderately resistant to thermal cycling induced stresses and have, in preliminary testing, survived over 100 one hour cycles at 1,000°C and 1,100°C (see Figure 3).

SEM/EDS were performed to examine the bond coat and substrate interfacial region subsequent to the post-deposition thermal treatment. EDS was performed on a sample deposited using a waveform that consisted of a medium γ and low frequency to analyze the bond coat/TBC interface region. Figure 4 shows the region of the sample that was investigated.

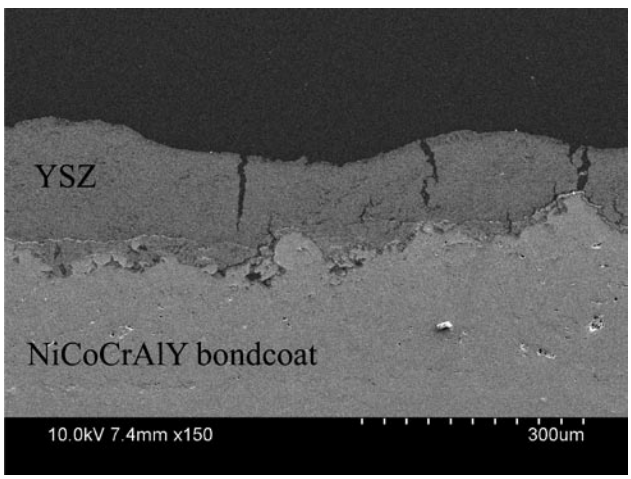

FIGURE 2. Cross-sectional image from a low duty cycle sample. Vertical cracks are mud-cracking effects due to drying.

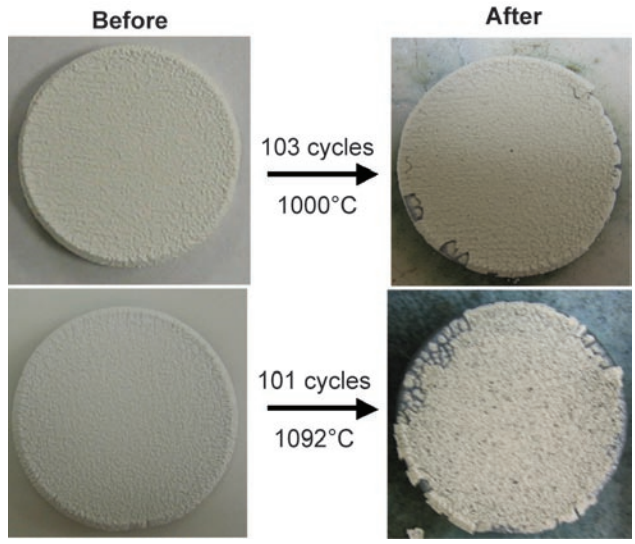

FIGURE 3. Photographs of samples before and after undergoing thermal cycling. Several black flakes are on 1,092°C sample and are believed to be oxide from the exposed metal of the sample. Spallation always started from the edges and proceeded inwards.

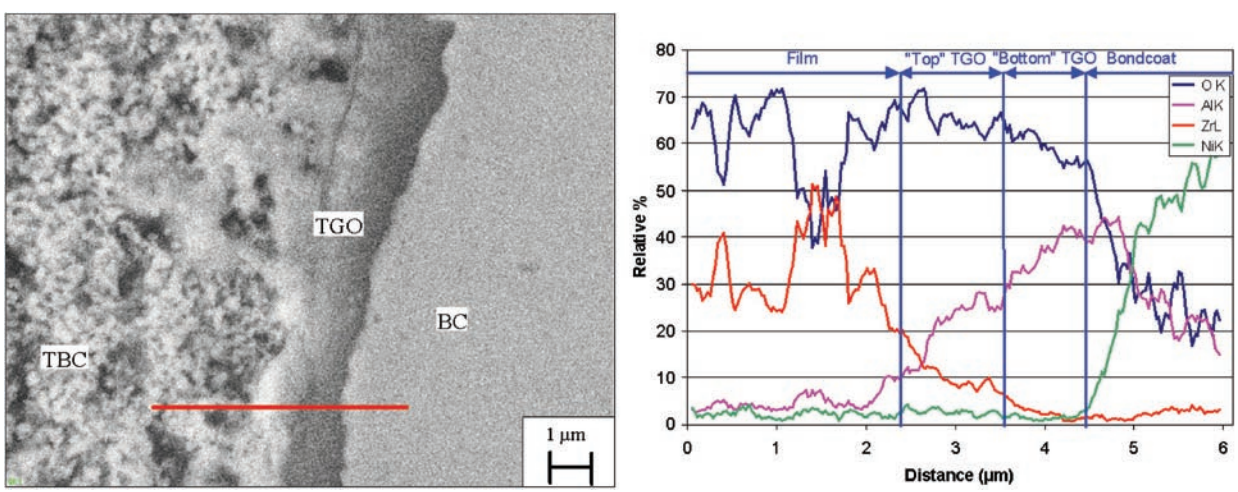

FIGURE 4. Left - region investigated in the SEM/EDS investigation. Horizontal line depicts region scanned to determine compositions of layers and the diffusion of species throughout the TBC, TGO, and bond coat. Right - linear scan showing major constituents of the various layers. The TGO contains two distinct regions (also evident in the picture).

It appears from both the picture and the trace that the thermally grown oxide (TGO) that forms between the bond coat and TBC consists of two distinct phases, an aluminum/zirconium rich oxide phase and an aluminum rich oxide phase. This may be due to TGO growth into the TBC due to the high porosity of the TBC and may be potentially advantageous for increasing coating adhesion, although further tests will need to be done to confirm this theory. The TGO is approximately 2 microns thick, with each phase being approximately 1 micron thick. As expected, nickel does not have a significant presence within the TGO and the oxide content drops off rapidly within the bond coat.

Conclusions and Future Directions

In addition to the completed activities described previously, several activities are ongoing:

- Continued optimization of the Faradayic EPD processing parameters, including peak voltage, total deposition time, and pulsed-reverse parameters.
- Further exploration of post deposition thermal processing parameters, more specifically processes that preferentially heat the TBC so as not to damage the substrate.
- Further analysis of coating properties as they relate to the various processing parameters, most notably the pulse reverse parameters, including thickness, roughness, uniformity, and hardness.
- Determination of the coating thermal conductivity.
- Further analysis of the coating properties as they relate to thermal stability and thermal cycling tests.

FY 2009 Publications/Presentations

1. J.W. Kell, H.A. McCrabb, B. Kumar, "Thermal Barrier Coatings Deposited by the Faradayic EPD Process," Proceedings of the 33rd International Conference on Advanced Ceramics and Composites (ICACC 2009), Ceramic Transactions, Accepted April 2009.

2. J.W. Kell, H.A. McCrabb, B. Kumar, "Faradayic Process for Electrophoretic Deposition of Thermal Barrier Coatings for Use in Gas Turbine Engines," Oral presentation at the 33rd International Conference on Advanced Ceramics and Composites (ICACC 2009), January 2009.

3. J.W. Kell, H.A. McCrabb, B. Kumar, "Thermal Barrier Coatings Deposited by the Faradayic EPD Process," Poster to be presented at the 33rd International Conference & Exposition on Advanced Ceramics and Composites (ICACC 2008), Dayton Beach, Florida, The American Ceramics Society, January 2009.

4. J.W. Kell, H.A. McCrabb, "Faradayic Process for Electrophoretic Deposition of Thermal Barrier Coatings for Use in Gas Turbine Engines," Proceedings of the American Ceramic Societies Fall Meeting at the Materials Science and Technology 2008 Conference, Ceramic Transactions, Accepted 4 May 2009.

IV.5 High Temperature Capability and Innovative Cooling with a Spar and Shell Turbine Blade

James P. Downs
Florida Turbine Technologies, Inc.
1701 Military Trail, Suite 110
Jupiter, FL 33458-7101
Phone: (561) 427-6250; Fax: (561) 427-6190
E-mail: jdowns@fttinc.com

DOE Project Manager: Robin Ames
Phone: (304) 285-0978
E-mail: Robin.Ames@netl.doe.gov

Contract Number: 84668

Start Date: June 20, 2007
End Date: August 14, 2010

FY 2009 Objectives

- Develop detailed mechanical design concept that can be manufactured for test within a follow-on project.
- Identify materials best optimized to the spar and shell turbine blade for use in specific environments.
- Define cooling system features required to produce high thermal efficiency.
- Identify manufacturing and fabrication requirements.
- Evaluate benefits and costs of this system.

Accomplishments

- Florida Turbine Technologies (FTT) has demonstrated the feasibility of the spar-shell technology mechanical design, cooling and structural aspects.
- Assembly of the spar and shell has been verified with the construction of a prototype model.
- Additional concept variants and design approaches have been identified as a result of the conceptual design development.

Introduction

The use of cooling in the turbine, although permitting turbine components to operate within an environment of high temperature and pressure, causes an efficiency debit to the turbine subsystem and overall power plant. Current gas turbine systems already operate at temperature and pressure levels that are sufficiently high to require the use of advanced materials systems and cooling of the turbine components. Technology advances within the turbine systems therefore represent an excelled avenue for improving the overall power plant efficiency. In particular, technologies that permit turbines to operate at increased temperatures and pressures are desired to achieve the specific performance goals. Advances of both the materials and cooling systems are clearly required to extend the envelope for improved performance and efficiency in the future systems.

To meet future power generation needs, FTT is developing an innovative design approach to provide highly durable turbine components that increase efficiency by requiring the lowest cooling flow possible. The proposed gas turbine blade design is constructed of an internal structurally supporting member (spar) and a separate external shell to provide the aerodynamic envelope. The so-called spar-shell system enables the use of advanced, high temperature materials that are not available based on current design philosophies and manufacturing approaches. In addition to providing higher temperature capabilities, features of this system resolve the well-known technical barrier, thermal-mechanical-fatigue (TMF). This barrier limits heat flux levels and cyclic life of today's turbine components, particularly at the interface between the main airfoil body and the platform/attachment structure. Further, this architecture facilitates the cooling system to be optimized to the smallest possible cooling flow required by enabling the use of practical and robust near wall cooling features while minimizing the plugging risk of systems such as those associated with effusion and other porous hole schemes. With this project, FTT has laid out a comprehensive plan for the design and development of this concept. Further, FTT has the full support and backing of a primary original equipment manufacturer, namely Siemens Energy, Inc. with the expressed commitment to evaluate the design within the Siemens design review process. Further, upon successful completion of these reviews, Siemens has agreed to install development hardware in an engine to permit validation test data to be acquired.

Approach

FTT has proposed the development of a spar and shell turbine component system to realize the future turbine system goals of reduced cooling flow consumption and increased efficiency. Development

of the proposed spar-shell turbine component system offers several advantages relative to the current state-of-the-art. To realize these goals, several objectives, as delineated in the following paragraphs, must be pursued.

The concept of a spar-shell turbine component is not new. FTT recognizes the limitations of current material and cooling systems and has been actively investigating alternatives to resolve the major issues. As a result, development of the spar-shell system has proceeded to the point where detailed analytical and empirical verification is required as a prerequisite to ultimate verification of the design concept in a test engine. One example of such a component is described in U.S. patent #7080971, "Cooled Turbine Spar Shell Blade Construction" by Wilson and Brown. Although development of the spar-shell system has proceeded beyond this patent, namely with respect to attachment features and shell loading, the art reproduced in Figure 1 illustrates the basic concepts of this design approach. As shown, this design approach utilizes an internal spar which is surrounded by an external shell. This fabrication approach has several advantages relative to the current state-of-the-art monolithic cast structures. First, the internal spar represents the primary framework of this concept. Since this member is thermally protected by the shell from the hot working fluid passing around the airfoil, it can be maintained at a relatively low temperature very near that of the coolant. The spar material can therefore be optimized for very high strength at a moderate temperature level. Second, since the shell is structurally isolated from the spar, its material can be selected on the basis of high temperature capability. Thermally induced stresses are a primary driver and limiter of existing cooled turbine components. This design approach serves to mitigate the associated effects on low cycle fatigue and TMF distress through both thermal and mechanical isolation of the spar and shell. Further, other desirable thermal attributes, such as the ability to support high temperature and heat flux, can be considered as primary drivers in the shell material selection.

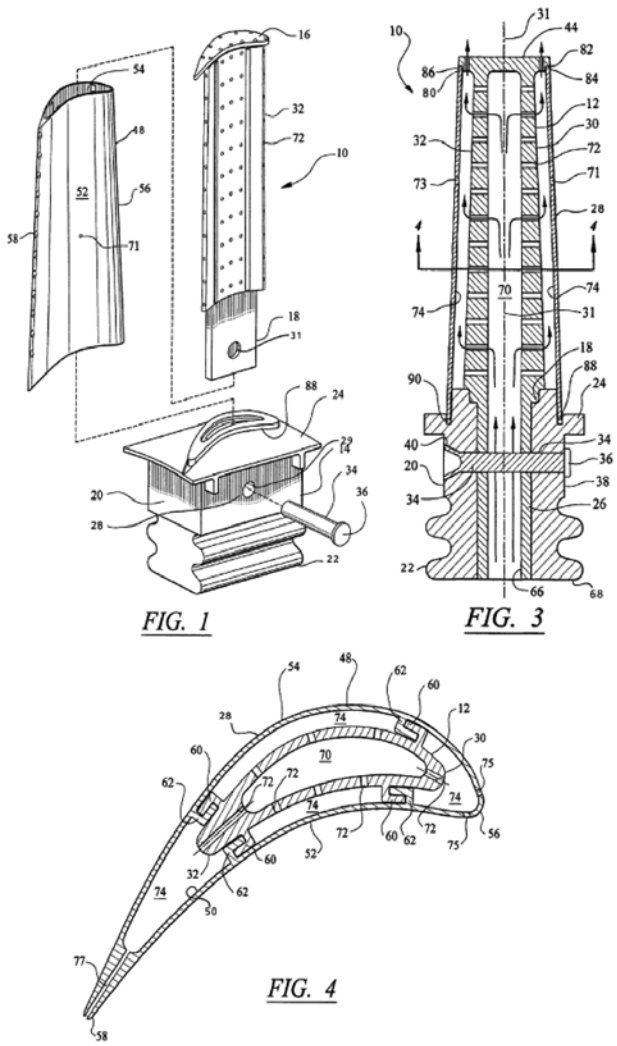

FIGURE 1. U.S. Patent #7080971, "Cooled Turbine Spar Shell Blade Construction"

Results

Design and analysis of the spar-shell technology have been performed to support the feasibility of the concept. From a cooling perspective, the spar-shell blade may take many possible forms. However, to improve the performance of the cooling system while reducing the amount of cooling flow requires that the efficiency of the internal convection cooling system be increased while film cooling benefits are reduced with the reduction of overall cooling flow. To this end, a conceptual cooling circuitry has been defined to provide the required heat transfer characteristics. In addition, structural analyses have been performed in a finite element model (Figure 2) to verify the basic

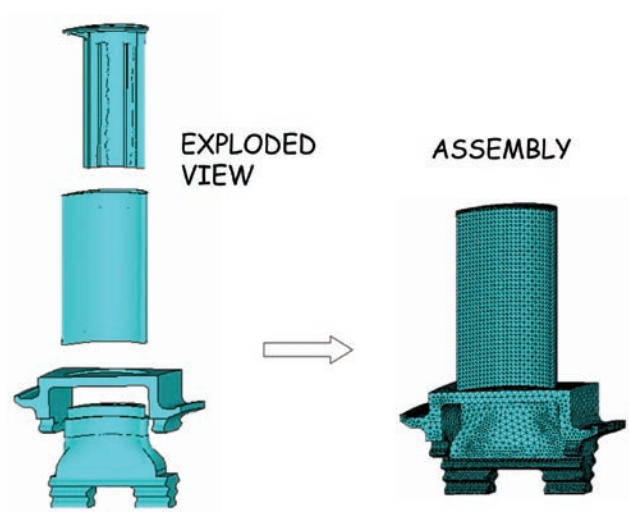

FIGURE 2. Analytical Model/Finite Element Mesh

structural and vibration characteristics. Results from these analyses support the feasibility of the design and indicate the need for continued research to refine and optimize the design.

During the course of this project, a prototype model of one possible representation of the spar-shell system was developed and constructed using a three-dimensional printing process. The geometry selected for this demonstration was based on a spar which supports the shell from the tip of the airfoil. In this construction, the spar must be inserted through the shell from the tip of the airfoil with a mechanical joint used to fix the spar to an attachment and platform structure. For the purposes of this initial development, an airfoil having constant cross-sectional area was assumed and wall thickness was assumed to be constant from the root of the airfoil to the tip. The shell includes separate leading edge and trailing edge cooling cavities as might be employed with impingement-style cooling systems and four L-shaped hooks were modelled to provide support of the shell from the spar. The entire system was modelled in the ProEngineer computer-aided design system, and a model was constructed from this geometry definition (Figure 3).

FIGURE 3. Spar-Shell Prototype Model

Conclusions and Future Directions

Results from conceptual design work performed during the initial Phase I Small Business Innovation Research (SBIR) supported continued development of the technology and FTT was selected for a Phase II SBIR award to define a detailed design of a spar-shell turbine component. Work on the Phase II project has produced two viable design concepts from which one will be selected to complete the detailed design phase.

Beyond the Phase II SBIR, development would consist of fabrication of test articles based on a Phase III SBIR or other funding source. The development project plan culminates in a prototype demonstration of the technology. To facilitate this demonstration, a test in an actual industrial gas turbine engine is proposed to:

- verify the feasibility of the spar-shell concept,
- demonstrate thermally free platforms,
- demonstrate thin-wall structures,
- demonstrate increased manufacturing yields and lower cost with single crystal,
- evaluate advanced airfoil cooling,
- evaluate advanced platform cooling,
- test advanced materials,
- evaluate advanced thermal barrier coatings, and
- evaluate fabricated blade and high speed machining capabilities.

To perform this demonstration, FTT has the expressed commitment of Siemens to test approved engine hardware in their full engine test bed. To be approved for demonstration, the prototype hardware must pass all engineering and design review requirements. This type of test permits the construction of a so-called rainbow wheel where a mix of turbine blade configurations, materials and technologies may be installed in a single turbine rotor and be evaluated in a single engine test.

FY 2009 Publications/Presentations

1. James P. Downs, "Turbine Cooling Challenges for Clean Power Applications," International Colloquium on Environmentally Preferred Power Generation, ICEPAG2009-1043, February 10–12, 2009.

2. S. Coates-Brostmeyer, "Turbine Efficiency Improvements for Existing Power Plants – How Technology Can Revolutionize Efficiency," Testimony before the Select Committee on Energy Independence and Global Warming – U.S. House of Representatives, February 25, 2009. http://globalwarming.house.gov/tools/3q08materials/files/0104.pdf.

IV.6 Prediction of Combustion Stability and Flashback in Turbines with High-Hydrogen Fuel

Tim Lieuwen (Primary Contact),
Dom Santavicca, and Vigor Yang
School of Aerospace Engineering
Georgia Institute of Technology
Atlanta, GA 30332
Phone: (404) 894-3041
E-mail: tim.lieuwen@ae.gatech.edu

DOE Project Manager: Mark Freeman
Phone: (412) 386-6094
E-mail: Mark.Freeman@netl.doe.gov

Contract Number: 43069

Start Date: April 1, 2007
End Date: March 31, 2010

FY 2009 Objectives

- Remove critical barriers to usage of high-hydrogen fuels in low emissions turbines by developing predictive capabilities for combustion instability.
- Develop computational simulation capabilities to predict the conditions under which combustion instabilities occur.
- Perform validating experiments of conditions under which instabilities occur.
- Distill knowledge gained from simulations and experiments into reduced order model which can be used as a design tool.

Accomplishments

- Developed predictive model quantifying how a turbulent flame responds to velocity and fuel/air ratio forcing.
- Measured the forced response of hydrogen-enriched natural gas/air premixed and partially premixed flames.
- Measured the dynamics of premixed and partially premixed flames subjected to acoustic velocity and/or equivalence ratio modulations.
- Worked closely with industrial partners to facilitate transition of models and understanding into design process for next generation gas turbines.

Introduction

This project is motivated by the fact that the inherent variability in composition and heating value of coal-derived, high-hydrogen fuels provides one of the largest barriers towards their usage. This fuel composition variability is of concern because low emissions combustion systems are generally optimized to operate with fuels that meet tight specifications. The objective of this proposed project is to improve the state-of-the-art in understanding and modeling combustion instabilities, associated with some of the most critical problems derived from burning high-hydrogen fuels in low emissions turbines. "Combustion instabilities" refer to damaging pressure oscillations excited by the combustion process. The damage due to these oscillations causes significant damage in low emissions turbines every year, through forced outages and broken parts.

Approach

This project is investigating this problem with a three pronged approach: experiments, computational kinetic calculations, and analytic modeling. It consists of a collaborative effort involving two universities, both with strong expertise in dynamical combustion phenomenon, and gas turbine manufacturers. In addition, the proposed research is structured to provide significant student involvement (including high school teachers, undergraduate students, and graduate students) and therefore will make an important contribution to the future science and technology base of our nation. Its focus upon high fidelity simulations, coupled with validating measurements, and development of reduced order models will significantly improve understanding of these phenomenon and capabilities for predicting their occurrence.

Results

Analysis: Analytical work has continued on the development of engineering prediction models that can be used to predict flame characteristics. The basic modeling framework developed by the authors utilizes a level-set approach to quantitatively describe the flame dynamics. This approach essentially eliminates phenomenological or heuristic descriptions of the flame dynamics. The investigated geometry is illustrated schematically in Figure 1. The instantaneous location

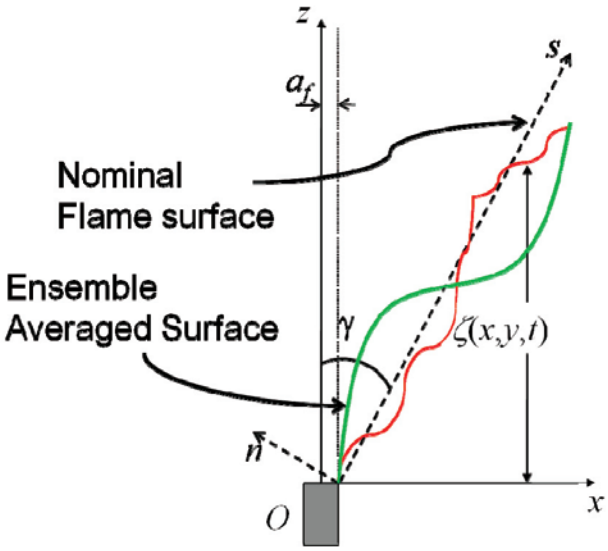

FIGURE 1. Schematic of investigated geometry showing one half of the instantaneous flame surface (solid red curve), the instantaneous coherent flame surface (solid green curve) and the nominal flame surface (broken black line). The flow is from bottom to top.

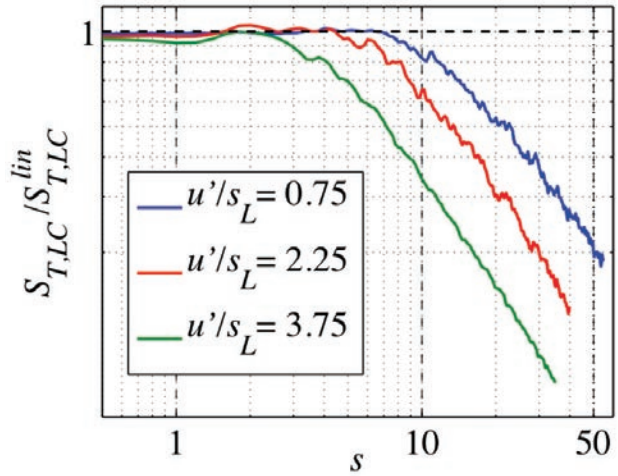

FIGURE 2. Spatial variation of local consumption speed normalized by the linearized value at three different turbulence intensities (solid curves) given by the value of u'/s_L. Flame angle, $\gamma \sim 4°$.

of the flame surface $\zeta(x,y,t)$ is given by the flame-front tracking equation,

$$\frac{\partial z}{\partial t} + u\frac{\partial z}{\partial x} + v\frac{\partial z}{\partial y} - w = -s_L\sqrt{1+\left(\frac{\partial z}{\partial x}\right)^2+\left(\frac{\partial z}{\partial y}\right)^2}$$

During the past year, we have spent a significant amount of time understanding the quantitative and qualitative characteristics of solutions of this nonlinear, partial differential equation. These solutions are first of their kind. For example, we have been performing two parameter asymptotic expansions of this equation, where the harmonic and random turbulent excitation amplitudes can be varied. In addition, detailed numeric solutions using level set solvers have been used for analytically intractable cases. These solutions have been worked out for flame responses to vortices excited by the oscillating flow and fuel/air ratio oscillations. A typical result showing asymptotic model results for flame response to broadband turbulence is illustrated in Figure 2.

In addition, we have used these models to understand the relationships between unsteady flame heat release and chemiluminescence from the flame. Currently, there is no direct measurement approach for determining the flame's instantaneous heat release, an absolutely critical parameter for understanding combustion instabilities. As such, chemiluminescence emissions from the flame are used as an indicator. While it is known that such an approach works reasonably well for quantifying the flame's response to velocity oscillations, there have

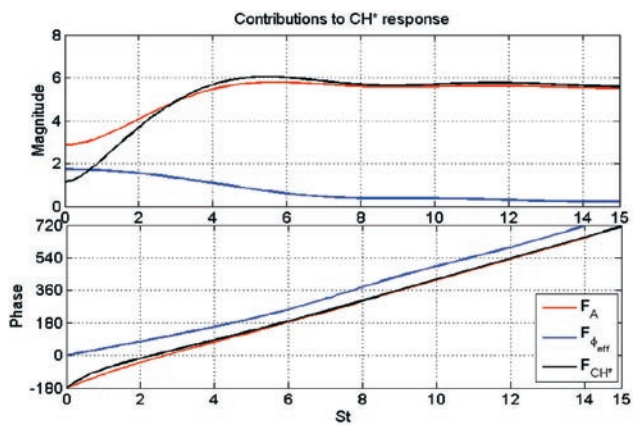

FIGURE 3. Chemiluminescence intensity response characteristics for $f_o = 0.7$, $b = 4$.

been a number of questions for flames with varying fuel-air ratio. Our analysis of this problem shows that there are differences in the flames heat release and chemiluminescence emissions for both OH*, CH*, and CO_2* bands, but that they all give qualitatively correct results. Quantitative differences can be as large as 50%, however. Typical results are shown in Figure 3.

Experiments: The flame's response to velocity fluctuations as large as 60% has been measured over a range of frequencies from 100 Hz to 450 Hz. The velocity fluctuation is measured using a two-microphone technique near the exit of the nozzle and the flame's response is defined by the fluctuation in the flame's rate of heat release, which is determined from CH* chemiluminescence measurements. H_2-blended natural gas fuels with $X_{H2} = 0.00 \sim 0.60$ were utilized.

Figure 4 presents the flame transfer function (FTF) for a constant forcing amplitude. The amplitude of the velocity perturbation imposed on the airflow is limited to 10% of the mean velocity, to ensure a linear response of the flame to the acoustic forcing. Other operating conditions are the same, except for the H_2 mole fraction: $X_{H2} = 0\%$ and 15%. The global flame response can be described as a low-pass filter, in that the gain decreases as the frequency increases. These results also show that with increasing X_{H2}, the maximum gain of FTF decreases by 43% and the phase decreases at a given forcing frequency, indicating that the gain depends strongly on flame length. The phase can be approximated by $\Delta\phi = \tau(2\varpi f)$, since the phase linearly evolves with increasing modulation frequency.

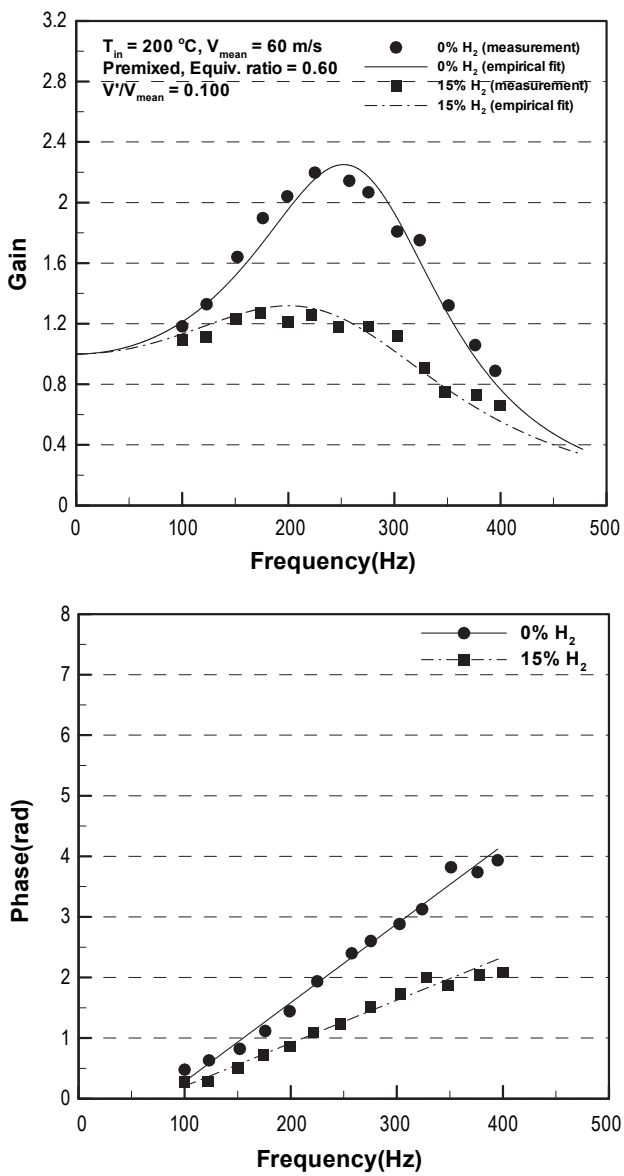

FIGURE 4. Gain and phase of the flame transfer function vs. forcing frequency at $V'/V_{mean} = 0.100$. Inlet conditions: $T_{in} = 200°C$, $V_{mean} = 60$ m/s, $\Phi = 0.60$, premixed, and $X_{H2} = 0.00$, 0.15. Note that the gain of FTF is well fitted by a second-order oscillator model (lines).

The nonlinear dynamics of swirled flames were characterized by phase-resolved flame image measurements. Deconvoluted and line-of-sight integrated phase-averaged CH* chemiluminescence images at a modulation frequency of 200 Hz and amplitude of $V'/V_{mean} = 25\%$ are shown in Figure 5. As forcing amplitude increases, the flame front bends toward the inner recirculation zone at $\phi = 270°$. The interaction between a vortex-ring structure and the flame is significant at $\phi = 180°$~$300°$. In particular, line-of-sight integrated images at $\phi = 150$ and 240° clearly show rollup of the shear layer and convection in the flow direction, respectively. It has been reported that the nonlinear flame response is related to the shear layer rollup. The shear layer rollup shortens the flame length, which in turn decreases the flame area in a nonlinear manner.

The dynamics of H_2-enriched natural gas/air premixed flames are shown in Figure 6. It is evident that the flame angle changes over the course of modulation cycle is substantial. In the case of natural gas flames on the other hand, the flame oscillates in

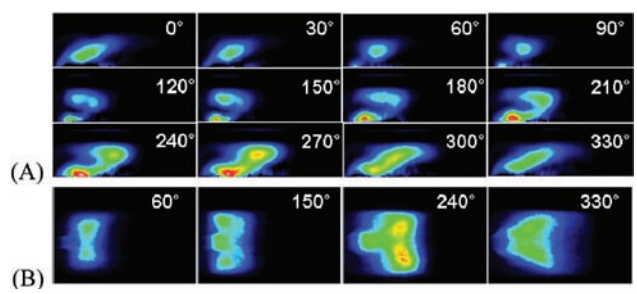

FIGURE 5. (A) Phase-synchronized CH* chemiluminescence imaging at modulation frequency of 200 Hz and $V'/V_{mean} = 25\%$. (B) line-of-sight integrated, background-corrected CH* images at $\phi = 60$, 150, 240, 330°. Inlet conditions: $T_{in} = 200°C$, $V_{mean} = 60$ m/s, $\Phi = 0.60$, premixed, and $X_{H2} = 0.00$.

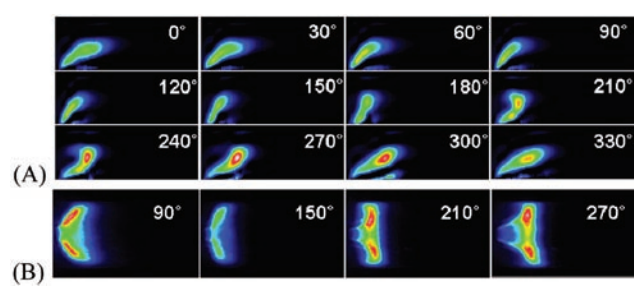

FIGURE 6. (A) Phase-synchronized CH* chemiluminescence imaging at $f = 200$ Hz and $V'/V_{mean} = 25\%$, (B) line-of-sight integrated CH* images at $\phi = 90°$, 150°, 210°, and 270°. Inlet conditions: $T_{in} = 200°C$, $V_{mean} = 60$ m/s, $\Phi = 0.60$, premixed, and $X_{H2} = 0.30$.

the flow direction, which means that the flame length changes over a period of perturbations, as shown in Figure 5. These oscillations in the flame position (angle) result from fluctuations in the outer shear layer. It has been reported that if the shear layers in the swirl-stabilized gas turbine combustor are acoustically excited to form a coherent vortex ring structure, the inner shear layer rolls up inward and the outer shear layer rolls up outward. This result suggests that the dynamics of H_2-enriched "M" flames is totally different from that of "V" flames. It was found that even though periodic formation and convection of vortex structures occur at $\phi = 210\sim270°$, the flame response remains in the linear regime.

Conclusions and Future Directions

Work to date has made important progress in modeling and measuring flame responses to flow perturbations. Such capabilities are absolutely essential in developing robust, ultra-clean engines capable of operation with a range of fuels. Future work will continue toward obtaining quantitative measurements and predictions of flame response to flow and fuel/air ratio perturbations. In addition, future work will focus on continuing transition of these results to conditions encountered in practical systems.

FY 2009 Publications

1. D.H. Shin, S. Shanbogue, and T. Lieuwen, "Premixed Flame Kinematics in an Axially Decaying, Harmonically Oscillating Vorticity Field," AIAA Paper #2008-5042, Presented at the 44th AIAA/ASME/SAE/ASEE Joint Propulsion Conference, 2008.

2. Sai K. Thumuluru, K. Periagaram, and T. Lieuwen, "Flame Brush Dynamics in a Harmonically Oscillating, Turbulent Jet Flame," Proceedings of the 2008 Technical Meeting of the Central States Section of the Combustion Institute, 2008.

3. S.A. Vishal, H. Santosh, and T.C. Lieuwen, "Influence of Flame Wrinkling on the Upstream Disturbance Field of an Acoustically Excited Premixed Flame," Proc. of the Twelfth International Conference on Numerical Combustion, SIAM, 2008.

4. Preetham, H. Santosh, and T. Lieuwen, "Forced Response of Premixed Flames: Effect of Flow Non-Uniformity," AIAA paper #2009-0978, Presented at the 46th AIAA Aerospace Sciences Meeting, 2008.

5. K.T. Kim, H.J. Lee, J.G. Lee, B.D. Quay, and D.A. Santavicca, "Flame Transfer Function Measurement and Instability Frequency Prediction Using a Thermoacoustic Model," Proceedings of ASME Turbo Expo 2009, #GT2009-60026, June 2009.

6. K.T. Kim, J.G. Lee, H.J. Lee, B. Quay, and D. Santavicca, "Characterization of Forced Flame Response of Swirl-Stabilized Turbulent Lean-Premixed Flames in a Gas Turbine Combustor," Proceedings of ASME Turbo Expo 2009, #GT2009-60031, June 2009.

7. S. Shanbogue, D.H. Shin, S. Hemchandra, D. Plaks, and T. Lieuwen, "Flame Sheet Dynamics of Bluff Body Stabilized Flames During Longitudinal Acoustic Forcing," *Proceedings of the Combustion Institute*, Vol. 32, pp. 1787-1794, 2009.

8. S.K. Thumuluru and T. Lieuwen, "Characterization of Acoustically Forced Swirl Flame Dynamics," *Proceedings of the Combustion Institute*, Vol. 32, pp. 2893-2900, 2009.

IV.7 Materials and Component Development for Advanced Turbine Systems

Mary Anne Alvin
U.S. Department of Energy (DOE)
National Energy Technology Laboratory (NETL)
626 Cochrans Mill Road
Pittsburgh, PA 15236-0940
Phone: (412) 386-5498; Fax: (412) 386-4806
E-mail: Maryanne.Alvin@netl.doe.gov

DOE Project Manager: Cynthia Powell
Phone: (541) 967-5803
E-mail: Cynthia.Powell@netl.doe.gov

Subcontractors:

- Coatings for Industry, Souderton, PA
- Westinghouse Plasma Corporation, Madison, PA
- University of Pittsburgh, Pittsburgh, PA
- West Virginia University, Morgantown, WV

Contract Number: 41817

Start Date: October 1, 2008
End Date: September 30, 2009

FY 2009 Objectives

- To develop high temperature thermal barrier coating (TBC) systems and substrate materials for advanced hydrogen-fired and oxy-fuel turbine applications.
- To computationally simulate and experimentally characterize aerothermal heat transfer in advanced hydrogen-fired and oxy-fuel turbine applications.
- To develop non-destructive evaluation (NDE) techniques and portable test equipment for assessment of TBC material properties and life.

Accomplishments

- In order to provide extended high temperature turbine operating life, high purity, low density TBC systems were developed which exhibited minimal sintering and phase transformation at temperatures ≥1,300°C.
- With respect to the production of low cost, nickel-based, oxide dispersion strengthened (ODS) alloys, efforts have recently shown that a nano-amorphous layer of Y_2O_3 can be homogenously deposited along the surface of Ni and Cr particles using a mechano-chemical bonding process.
- Improved heat transfer was demonstrated through three-dimensional finite element modeling and experimental testing for skin-cooled or double-wall airfoil architectures, with internal pin fin vortex generators.
- A computational methodology, based on three-dimensional finite element analysis and damage mechanics was developed for predicting the evolution of creep and fatigue in airfoils for the advanced turbine applications. The current model projects extended operating life (i.e., >16,000 hrs) with limited localized areas of non-through-wall creep damage for hydrogen-fired turbine airfoils.
- A high temperature NDE micro-indentation system was developed to address TBC stiffness at temperature up to ~1,200°C.
- Pulse-echo, acousto-ultrasonic, NDE techniques were shown to provide an early warning of high temperature TBC delamination prior to visually observing debonding.

Introduction

Hydrogen-fired and oxy-fueled land-based gas turbines currently target inlet operating temperatures of ~1,425-1,760°C (~2,600-3,200°F; Table 1). In view of natural gas or syngas-fired engines, advancements in both materials, as well as aerothermal cooling configurations are anticipated prior to commercial operation of these systems.

During Fiscal Year 2009, the *Materials and Component Development for Advanced Turbine Systems* project supported 10 subtasks that focused on materials development, aerothermal heat transfer, and non-destructive evaluation techniques. The project:

- Combined the expertise of NETL, University of Pittsburgh (Pitt), and West Virginia University (WVU) researchers, working in conjunction with commercial metal and coating suppliers as Howmet International, Coatings for Industry (CFI), and Praxair to develop potentially reduced cost bond coat systems, as well as high purity, low density plasma sprayed, yttria-stabilized zirconia (YSZ) TBC material systems for extended in-service turbine operating life. Efforts with Hosokawa were focused on the potential production of reduced cost ODS alloys for use in the manufacturing of high temperature turbine blades. As new initiatives in FY 2009, efforts were focused on the proof-of-concept (POC) testing for development/application of plasma sprayed diffusion barrier coatings (DBC) ultimately for provision of enhanced oxidation protection of

TABLE 1. Advanced Turbine Operating Conditions [1]

	Syngas Turbine 2010	Hydrogen Turbine 2015	Oxy-Fuel Turbine 2010	Oxy-Fuel Turbine 2015
Combustor Exhaust Temp, °C (°F)	~+1,480 (~+2,700)	~+1,480 (~+2,700)		
Turbine Inlet Temp, °C (°F)	~1,370 (~2,500)	~1,425 (~2,600)	~620 (~1,150)	~760 (~1,400) (HP) ~1,760 (~3,200) (IP)
Turbine Exhaust Temp, °C (°F)	~595 (~1,100)	~595 (~1,100)		
Turbine Inlet Pressure, psig	~265	~300	~450	~1,500 (HP) ~625 (IP)
Combustor Exhaust Composition	9.27% CO_2 8.5% H_2O 72.8% N_2 0.8% Ar 8.6% O_2	1.4% CO_2 17.3% H_2O 72.2% N_2 0.9% Ar 8.2% O_2	82% H_2O 17% CO_2 0.1% O_2 1.1% N_2 1% Ar	75-90% H_2O 25-10% CO_2 1.7% O_2, N_2, Ar

superalloys and single crystal matrices, and the generation of high temperature overlayer zirconate systems to facilitate possible use of the TBC architecture at temperatures exceeding 1,400°C.

- Combined the expertise of Pitt and NETL to develop advanced aerothermal cooling concepts and computational high temperature creep and fatigue life prediction models. Additionally, this project supported demonstration of the validity of advanced cooling concepts in bench-scale laboratory test facilities that were designed and constructed in FY 2009, and are currently operational on NETL's and Pitt's campuses.
- Combined the expertise of WVU and NETL to develop NDE micro-indentation and acousto-ultrasonic diagnostic techniques to address material properties as stiffness and Young's modulus to project potential impending failure of TBC architectures.

Approach

The materials development focus in this project addressed the viability of the TBC-metal architecture for use in the advanced high temperature hydrogen-fired and oxy-fuel turbine applications. Current commercial bond coat and YSZ TBC material systems will require additional thermal protection for long-term operation at temperatures >1,300°C. To achieve long-term durability, thicker TBCs and higher purity materials are being developed to increase the thermal insulating capability of the YSZ matrix, as well as to retain the low thermal conductivity of the YSZ during service operation. Due to their high melting point and low thermal conductivity, rare earth zirconates have recently been identified as potential TBC overlayer coatings to provide added thermal protection beyond temperatures of 1,400°C. An initial POC assessment of thermal sprayed $La_2Zr_2O_7$ coatings was undertaken during FY 2009 to demonstrate adherence and potential thermal performance when overlayers are deposited along the outer surface of commercially manufactured air plasma sprayed (APS) YSZ test coupons.

Even with the added thermal protection resulting from advanced YSZ and overlayer coatings, interdiffusion between the bond coating and underlying superalloy or single-crystal substrate will occur during extended exposure time at high temperature. As a result, oxidation protection provided by alumina-forming MCrAlY or platinum aluminide (PtAl) bond coat systems, and the overall life of TBCs are often reduced. To limit diffusion of aluminum, DBCs consisting of a Cr-Ni-Re-rich σ-layer(s) have been identified for application along the bond coat/substrate interface. During FY 2009, an initial POC assessment was also undertaken to demonstrate the potential feasibility of DBCs architectures at temperatures of 1,150-1,200°C.

With the potential for spallation of the overlayer and TBC coatings to occur during in-service turbine operation, exposure of current base metal substrates at temperatures >1,150-1,200°C would lead to rapid degradation and component failure. As a result, efforts during FY 2009 were focused on the potential development of reducing manufacturing costs for the production of high strength, high temperature creep and oxidation resistant, ODS alloys. Preliminary efforts in FY 2009 addressed establishing suitable processing conditions using the Hosokawa mechano-chemical bonding (MCB) process to achieve homogenous Cr-Al-Y_2O_3-Ni powder mixtures comparable to those produced via mechanical alloying. When coupled with cold spray techniques, adherent coatings were produced on metallic substrates.

As each of the TBC-metal technology areas are more fully developed, integration of these material systems into a composite architecture is planned. Once *overlayer/YSZ/bond coat/diffusion barrier coating/*

substrate test coupons are manufactured, extended bench-scale high temperature thermal flux (HTTF) testing will be conducted at the Westinghouse Plasma Corporation (WPC) in Madison, Pennsylvania.

Previous efforts in the aerothermal heat transfer area included development of a three-dimensional computational simulation that projected the external surface temperature and heat transfer distribution over a National Aeronautics and Space Administration (NASA) E^3 airfoil configuration for the hydrogen-fired and oxy-fuel turbines. During FY 2009, these efforts were extended to include a similar assessment of skin-cooled or double-wall airfoil architectures, as well as the impact of internal pin fin vortex generators and alternate cooling fluids on heat transfer.

To confirm the computational modeling efforts, three bench-scale test facilities were designed and constructed. These included the incorporation of an aerothermal test passage section into NETL's combustion test facility in Morgantown, WV, for exposure of base metal and TBC coated Haynes 230 coupons to high temperature, pressurized combustion gases, in order to assess the impact of film cooling hole geometries and orientation on cooling effectiveness of metal substrates under conditions that approach turbine firing conditions. Two bench-scale experimental test facilities at Pitt are currently operational which introduce warmed air or superheated steam into a test passage channel containing aluminum pin fin arrays to assess potential internal airfoil cooling enhancement.

In addition to the aerothermal modeling effort, the damage mechanics, high temperature creep, life prediction model was extended to address the interactions of creep and fatigue in the NASA E^3 and skin-cooled airfoil configurations. To validate the damage mechanics models, isothermal furnace testing is being conducted at temperatures up to 1,100°C where TBC-coated single crystal coupons are being subjected to an applied uniaxial compressive load for extended periods of time. Microstructural characterization and nano-indentation are being utilized to address changes within the various ceramic, thermally grown oxide (TGO), and substrate matrices.

Monitoring the stability or degradation of commercial TBCs or developmental material systems has traditionally been conducted via destructive analyses of numerous coupon samples. Frequently, however, destruction of coupons or full airfoils is not warranted since continued exposure or in-service use is required. Therefore development of NDE techniques was considered to be essential for assessment of extended component life. The objectives of the NDE effort in this project were to develop a micro-indentation methodology or technique, as well as prototype test equipment to assess the residual stiffness of TBCs on flat, as well as curved surfaces (i.e., leading edge of the airfoil; tubular samples) to project material/component performance longevity and/or impending spallation of the applied protective coatings. Currently room temperature TBC stiffness is being determined at WVU using table-top and portable hand-held micro-indentation equipment developed in this project, with high temperature capabilities for determining stiffness at temperatures ≥1,200°C in the near future. Non-linear acousto-ultrasonic diagnostics using pulse-echo and pitch/catch techniques continued to be developed at WVU for prediction of TBC spallation and ultimate life.

Subtask Description, Results and Future Directions

Materials

Bond Coat Development

Existing commercial bond coats utilized for production of TBCs consist of MCrAlY (M = Ni, Co) and Pt-aluminide matrices produced via low pressure plasma spray (LPPS), high velocity oxygen fuel (HVOF) thermal spray, air plasma spray, and/or packed cementation. In order to demonstrate the feasibility for development of a reduced-cost, high-temperature, oxidation-resistant bond coat, NETL has collaboratively worked with CFI to develop bond coat systems targeted for use in advanced hydrogen-fired and oxy-fuel land-based turbine applications.

Efforts in this subtask were initially focused on addressing the feasibility of producing a functional metallic-ceramic gradient TBC, that combined metallic particles (i.e., aluminum) contained within a chromium phosphate inorganic binder, with that of YSZ particles typically used in production of the high temperature TBC insulating top coat layer. Efforts were additionally directed to enhancement and production of a homogeneous metallic bond coat. The performance of these systems were monitored through mass change data as a function of time at temperatures of 900-1,100°C, as well as cross-sectional scanning electron microscopy (SEM) to determine the isothermal and cyclic oxidation performance response of the matrices relative to commercial state-of-the-art (SOTA) bond coat systems. Flat coupon substrates used in this subtask included the nickel-based, chromia-former, Haynes 230 superalloy, and the single crystal, nickel-based, alumina-former, René N5, with/without the application of commercial MCrAlY and Pt-aluminide bond coat systems.

To address fabrication and high temperature cyclic oxidation performance of an entire TBC architecture for land-based turbine operations, efforts were directed to defining the appropriate bond coat

surface roughness for application of the APS YSZ TBC. Similar to the bond coat development effort, mass change data as a function of time principally at temperatures of 1,100°C, as well as cross-sectional SEM analyses were utilized to demonstrate the cycle-to-failure life and performance of the NETL-bond coat/YSZ architectures in comparison to MCrAlY and Pt-aluminide bond coats, and bare base metals, with APS and electron beam physical vapor deposition (EBPVD) YSZ top coat architectures.

To demonstrate the feasibility of utilizing TBC architectures at temperatures greater than 1,100-1,150°C, internal cooling is required to maintain the integrity of the applied bond coat and underlying supporting base metal substrate. Tubular René N5 architectures were manufactured and coated with commercially applied MCrAlY and Pt-Al bond coats, and an EPBVD YSZ top coat prior to HTTF testing. Initial baseline testing included exposure of these systems to heat generated from an argon/ H_2 torch which continuously maintained the surface temperature of the YSZ at 1,100°C, while the interior of the René N5 tube was cooled with flowing dry air, with the tube rotating at 500 rpm. Optical pyrometer measurements monitored the stability of the TBC during HTTF testing. Future HTTF testing is currently planned to address the stability and long-term performance of advanced material architectures at temperatures representative of hydrogen-fired and oxy-fuel turbine conditions. These architectures include the NETL bond coat and APS YSZ system with additional high temperature zirconate overlayers, and if necessary, DBCs.

Significant Results:

- On René N5 substrates, mass change (oxidation) of the NETL-A1 bond coat system was shown to be comparable to Pt+Hf-mod $\gamma+\gamma'$ (G2P) bond coats during 1,100°C cyclic oxidation testing.
- The NETL-A1/EBPVD YSZ system:
  - Exceeded MCrAlY/EBPVD YSZ 1,100°C cycle life to failure (560 vs. 140 cycles).
  - Achieved ~61% of the 1,100°C cycle life to failure in comparison to Pt-Al/ EBPVD YSZ on René N5 (560 vs. 910 cycles).
- The NETL-A1/APS YSZ system:
  - Achieved comparable 1,100°C cycle life to failure (260 cycles) as MCrAlY/APS (200 cycles), PtAl/APS (220 cycles), and bare base metal (240 cycles).
- Completed three test campaigns at the WPC totaling 406 hrs of unattended operation at 1,100°C:
  - HTTF testing confirmed enhanced performance of Pt-Al/EBPVD systems.
  - HTTF testing confirmed early failure of MCrAlY/EBPVD systems (97 hrs).

Planned Future Directions:

- Further optimize the NETL bond coat system with respect to thickness, processing temperature and matrix composition.
- Address bond coat stability and response on alternate metal substrates as IN939 and PM2000.
- Generate full TBC-metal architecture. This will include the incorporation of high temperature overlayer coatings deposited along the surface of an APS YSZ, as well as a DBC layer as an interface between the bond coat and underlying single crystal or superalloy substrate. The performance of the TBC-metal architecture will be assessed in HTTF testing at the WPC test facility.

APS Development

This subtask effort was directed to the development of high-purity, low-density (85%) (HP-LD) APS YSZ TBCs with NiCoCrAlY bond coats deposited by argon-shrouded plasma spraying. The microstructure of the APS top coats was controlled to maximize the coating thicknesses that can be applied without spallation and to minimize the thermal conductivity of the TBC. Test coupons were evaluated using cyclic oxidation and thermal shock tests in bottom loading furnaces at temperatures up to 1,100°C and in the Praxair JETS test facility. Important properties of the TBCs, such as resistance to sintering and phase transformation, thermal conductivity, and fracture toughness were determined.

Significant Results:

- Primary variables influencing cyclic oxidation life were found to be top coat thickness and coefficient of thermal expansion (CTE) mismatch between the top coat and superalloy substrate.
- Top coat thickness strongly influences lifetime behavior of TBCs, where thinner coatings last longer than thicker coatings when other variables such as substrate selection are held constant.
- The fracture paths in the APS coatings were found to depend on top coat thickness and the nature of the thermal exposure (e. g. cycle frequency). Two failure mechanisms were identified:
  - Thick TBCs (>1 mm) develop cracks well within the YSZ top coat.
  - Thinner TBCs (<1 mm) have longer lives and fail by cracking associated with bond coat oxidation.

- High purity coatings showed minimal sintering and phase transformation from the metastable tetragonal phase to the equilibrium mixture of monoclinic and cubic phases.
- Alloy selection and subsequently alloy CTE were shown to have a substantial effect on the lifetime and failure modes of the APS YSZ coating.
- A 750 µm thick APS coating was projected to have a cyclic life that was at least as long as that of a standard 100 µm thick EBPVD coating, as measured in a furnace cycle test.

Planned Future Directions:

- Compare performance of HP-LD APS TBCs with dense vertically cracked TBCs.
- Optimize TBC processing.
- Optimize bond coat surface topography by micro-machining.
- Address TBC degradation in high H_2O/CO_2 environments.

Diffusion Barrier Coating Development

As a newly initiated effort in FY 2009, this subtask was focused on a substrate-surface modification that will enable long-term service of nickel-based superalloys and refractory-based alloys in steam-bearing oxidizing atmospheres at very high temperatures (i.e., above ~1,200°C). Important criteria in this area include sufficient stability in the surrounding environment, low vapor pressure of the surface materials and/or the reaction product(s) formed, and compatibility with the substrate material. With regard to this last criterion, it is important to maintain substrate surface modification for the duration of extended in-service (i.e., 8,000-30,000 hrs) operation. This means that there must be minimal interdiffusion between the substrate and the surface-modified region. The constraints of long-term resistance and steam-bearing conditions at very high temperatures remove surface modifications that are or react to form silica- or chromia-based products. Accordingly, in this effort the viability of metallic alumina-forming surface coatings with an intermediate diffusion barrier (i.e., an Ni-Re-Cr intermetallic phase) is being investigated.

Significant Results:

- Powders of Re, Ni and Cr were purchased, mechanically milled, and heated at 1,200°C for 6 hrs.
- A coating [40Re-40Cr-20Ni (at%)] was deposited by air plasma spray on Haynes 214 coupons, and an assessment of thermal stability of APS-DBC at 1,150-1,200°C over a period of ~60 hrs demonstrated minimal diffusion of aluminum into the σ-diffusion barrier layer.

Planned Future Directions:

- Assess and optimize the oxidation resistance of Re-Cr-based DBC compositions.
- Modify DBCs to contain a reactive element reservoir (Hf, Y and/or Si).
- Assess Al_2O_3-scale forming coatings for DBC systems:
  - Reduce oxidation kinetics (k_p) by the supply of reactive elements.
  - Verify thermal stabilities.

Overlayer Coating Development

In TBC systems for advanced gas turbine engines, the actual thermal barrier is a ceramic top layer with the prime function to reduce heat transfer to the metallic substrate. For many years YSZ has been the prime choice, because it provides a thermal conductivity which is more than an order of magnitude below that of the Ni-base superalloy. However, as advanced engine temperatures are expected to continue to increase as higher efficiency engines with higher power-to-weight ratios are being designed, alternatives to YSZ for TBCs are being sought. In part, this is because the YSZ currently used consists of t-prime (t') zirconia which, being metastable, becomes increasingly unstable at higher temperatures, decomposing to a mixture of tetragonal and cubic zirconia. On cooling, the tetragonal phase transforms to monoclinic zirconia, which is a disruptive transformation.

Recent research efforts have demonstrated that the rare earth zirconates of the type $Ln_2Zr_2O_7$ (Ln represents rare earth element; such as $Sm_2Zr_2O_7$, $Gd_2Zr_2O_7$, $Nd_2Zr_2O_7$ and $La_2Zr_2O_7$), have lower thermal conductivity than 8YSZ, with thermal expansion coefficients that almost correspond to that of 8YSZ. These materials are currently being considered as ceramic overlayers for future TBCs.

The focus of this subtask is to design an APS YSZ TBC overlayer for use at temperatures >1,300°C for advanced land-based gas turbine applications. As a newly initiated effort in FY 2009, initial POC development included selection of the type of rare earth zirconates to be used to manufacture the overlayer, determination of the overlayer thickness and processing technique/parameters, and demonstration of overlayer fabrication on commercially supplied René N5/MCrAlY/APS YSZ test coupons. Future efforts

are planned to refine further processing of alternate overlayer architectures, measurement of their heat insulating capabilities, and high temperature stability and performance.

Significant Results:

- $La_2Zr_2O_7$ was selected as the initial overlayer coating composition. Initial processing parameters and overlayer thicknesses were identified.
- Computational analysis was completed which addressed the overlayer thickness requirements relative to through-wall overlayer/YSZ/bond coat/metal substrate temperature gradients for the oxy-fuel turbine.
- 50-350 μm $La_2Zr_2O_7$ overlayers were successfully deposited at Stony Brook University on commercially supplied APS YSZ/MCrAlY/René N5 test coupons.

Planned Future Directions:

- Address the adherence of the $La_2Zr_2O_7$ overlayer system to the underlying APS YSZ surface.
- Determine the Young's modulus of the applied $La_2Zr_2O_7$ overlayer using nano-indentation characterization.
- Demonstrate the high temperature thermal stability of the $La_2Zr_2O_7$ overlayer/APS YSZ architecture.

ODS Alloy Development

ODS alloys have been under intensive development over the past four decades due to their excellent high temperature creep strength and good oxidation resistance. Nickel-based ODS alloys are the combination of gamma prime (γ') strengthened superalloy with yttrium oxide evenly distributed throughout the matrix which permits strength to be maintained to much higher temperatures than conventional superalloys.

Mechanical alloying (MA) is a powder metallurgy processing technique to produce alloys by mixing elemental alloy powders in a high-energy ball mill, and has now become an established commercial technique to produce nickel- and iron-based ODS alloys. However, a key factor that limits their wide usage is the high manufacturing cost. The traditional MA-based process is not only expensive, but also not robust. In this effort, an innovative powder mixing technique, Hosokawa MCB technology, is being used to produce ODS powder mixtures with much less manufacturing cost. The resulting alloys, after proper hot isostatic pressing and extrusion, are also expected to have more uniform dispersions of nano-size stable yttrium oxides or even oxide nano-clusters. Assessment of mechanical behavior of the ODS alloys, in particular high temperature creep strength measurements, will be evaluated using the micro-indentation technique recently developed at WVU.

Significant Results:

- Demonstrated that a Y_2O_3 nano-amorphous layer can be formed along the outer surface of larger Ni and Cr particles using the Hosokawa mechano-chemical bonding process.
- An initial adherent Ni-Cr-Y_2O_3 coating was successfully deposited on IN625 coupons using cold spray techniques.

Planned Future Directions:

- Optimization of the powder processing, cold spray, and techniques for solution annealing and hardening will be undertaken.
- The resulting powder morphology and composition will be further characterized via scanning transmission electron microscopy, field transmission electron microscopy and energy dispersive X-ray (EDX) analysis.
- Young's modulus of the deposited ODS coating will be determined using micro-indentation techniques.
- High temperature creep strength of the deposited ODS coatings will be determined.

Aerothermal

Airfoil Heat Transfer Modeling and Experimental Testing

Future advanced turbine systems for electric power generation, based on coal-gasified fuels with CO_2 capture and sequestration, are being developed to achieve higher cycle efficiency and near-zero emissions. The most promising operating cycles that are being developed are the hydrogen-fired cycle and the oxy-fuel cycle. Both cycles will likely have turbine working fluids significantly different from that of conventional air-based gas turbines. In addition, the oxy-fuel cycle is targeted to have turbine inlet temperatures (TITs) reaching ~1,760°C, significantly higher than current operating engines.

To predict the gas side thermal loading and the heat transfer imposed on the external surface of an airfoil, a numerical simulation based on three-dimensional computational fluid dynamics modeling has been pursued. Results obtained from this modeling effort suggest that the level of heat transfer over the external surface of an airfoil is comparable between the hydrogen-fired cycle and the existing integrated gasification combined cycle (IGCC). However, the heat transfer coefficient for the oxy-

fuel cycle is found to be substantially higher, by about 50-60%, than that of the IGCC and hydrogen-fired turbines. This is caused primarily by the high steam concentration in the turbine flow. These findings further affirm that advances in cooling technology and thermal barrier coatings are critical for the developments of future coal-based turbines.

To reach the efficiency goals targeted for the future turbines, the amount of coolant must be substantially reduced from the current level used in today's turbine power generation systems. With the continuing advancement in airfoil manufacturing technology, future internal cooling passages will likely be positioned much closer to the external surface (i.e., double-wall cooling or skin-cooling designs), and equipped with three-dimensional vortex generators, such as pin-fin arrays. Using a combined computation and experiment approach, several novel concepts for further enhancing the internal heat transfer performance have been explored and analyzed. The experimental subtasks utilize both an air-flow rig and a steam/CO_2 testing loop to characterize the local heat transfer distributions in pin-fin channels and the effects of working fluid properties. Another significant aspect of the experimental subtask is the development of a high-pressure, high-temperature turbine aerothermal research facility at NETL-Morgantown. This facility, built downstream of NETL's combustor, is capable of providing realistic turbine gas-side flow and thermal conditions.

Additional Significant Results:

- The pressure and temperature distribution for hydrogen-fired and oxy-fuel airfoil exhibit similar trends to those under convection dominated flow.
- The internal cooling heat transfer coefficient significantly affects the substrate metal temperature. For the hydrogen-fired turbine, 3X increase in internal heat transfer coefficient decreases the metal surface temperature about 150-250°C. The temperature gradient inside the metal, however, is higher.
- The near surface skin-cooled internal airfoil arrangement leads to a significant reduction of metal surface temperature by ~50-100°C as compared to conventional serpentine cooling designs. This suggests double-wall cooling, or alternate configurations, could be a viable cooling design for future turbines.
- In the event of complete TBC spallation, the local surface temperature is projected to increase by ~200-250°C in either the hydrogen-fired or oxy-fuel turbine.
- Increasing the thickness of the TBC to 550 µm on the skin-cooled airfoil could reduce the temperature by ~50-70°C.
- Jet impingement from 90° inlet passages has demonstrated an increase in the overall average heat transfer coefficient throughout the entire double-wall cooling passage.
- Pin fins at serpentine tip turn regions alter the fluid flow field and enhance heat transfer in these regions.

Planned Future Directions:

- Computationally address external cooling via shaped-hole film cooling and pulse (unsteady) film cooling.
- Conduct conjugate heat transfer analysis combining internal and external thermal modeling.
- Measure film cooling effectiveness, η, under realistic turbine operating conditions in the NETL aerothermal test facility in Morgantown, WV. Explore innovative cooling concepts and hole shapes/arrangements. Develop cooling design data and correlations.
- Continue conduct of heat transfer testing utilizing superheated steam as the internal cooling fluid. Develop flow and heat transfer correlations for steam cooling. Assess heat transfer for various pin fin high aspect ratios and narrow flow passage designs.

Airfoil Life Prediction Modeling

Future oxy-fuel and hydrogen-fired turbines promise increased efficiency and low emissions for coal-based power generation. However, these turbine cycles require substantially higher TITs and have significantly different working fluid compositions than are used in current SOTA turbine cycles. Thus, the development of new airfoil designs and materials that can withstand these conditions is critical to the realization of these near-zero emission power generation technologies. A computational methodology, based on three-dimensional finite element analysis and damage mechanics was developed in this subtask for predicting the evolution of creep and fatigue in airfoils in these advanced turbine systems. Visualization of the creep and fatigue damage evolution over the airfoil shows the regions that are most susceptible to failure by these mechanisms. TBC systems reduce the thermal load on the airfoil and the rate of oxidation and corrosion into the airfoil substrate. Typical TBCs consist of a top layer of YSZ and an intermetallic plasma sprayed bond coat, with a TGO layer that forms during high temperature exposure. The reduction in the thermal load provided by the TBC is included in the damage mechanics model.

In conjunction with the model development, laboratory-scale experimental validation has been

undertaken to better understand the underlying damage mechanics concepts for the evolution of TBC damage. Test coupon samples with a TBC have been isothermally exposed to temperatures as high as 1,100ºC for times as long as 3,000 hrs and examined using SEM and EDX analyses to study the resulting microstructure and elemental distribution in the TBC architecture after exposure. Nano-indentation is being used to study the mechanical properties of the TBC, TGO and underlying substrate, and their evolution with temperature and time.

Significant Results:

- Damage mechanics-based life prediction models were developed to address high temperature creep and fatigue damage in airfoils during use in hydrogen-fired and oxy-fuel turbine applications.
- Incorporated compact TGO growth, inward growth and phase depletion into the damage mechanics model at the outer boundary of the airfoil.
- Utilizing the current damage mechanics model for the NASA E^3 airfoil:
  - Hydrogen-Fired Turbine – After 8,000-16,000 hrs with h_c=3,000 W/m^{2}K, the greatest creep damage was projected along the suction side towards the base of the airfoil at the highest temperature and stress locations. Damage was not through-wall, but was confined to the outer airfoil surface. Damage was also projected towards the base of the leading edge.
  - Oxy-Fuel Turbine – After 50-100 hrs, significant creep damage was projected along the first half of the airfoil's suction surface and along the leading edge.

Planned Future Directions:

- Apply models to assess the viability of alternate cooling configurations (i.e., double-wall or skin-cooled architectures).
- Address combinations of TBC thermal conductivity and internal convective cooling strategies that are most effective at mitigating damage for advanced turbine applications.
- Incorporate models for additional coating layer damage mechanisms.
- Experimentally assess the viability of the interface damage models that are being developed.
- Assess the material performance and material property data that are being generated for the coupons that are currently undergoing long-term uniaxially applied compressive stress at elevated temperatures.

Non-Destructive Evaluation

Micro-Indentation Testing

Under elevated temperatures or thermal cyclic conditions, the presence of high stresses within TBCs can lead to the development of micro-cavities which can ultimately form microcracks and result in interfacial debonding in the TBC/bond coat region. Several NDE methods have been applied for TBC damage assessment and debonding/spallation detection at the TGO/bond coat region. However, the difficulty of determining interfacial debonding and degradation assessment of the TBC remains a significant hurdle to overcome due to the TBC's complex multilayer structure, and frequently rough surface morphology. The TBC has high attenuation, high porosity, and several material interfaces, which are the challenges that need to be overcome by the NDE techniques.

In this subtask, a load-based micro-indentation methodology has been developed for evaluating material mechanical properties, and is being used to evaluate degradation and detection of TBC debonding/spallation. Coupled with a multiple-partial unloading procedure during the indentation process, this technique results in a load-depth sensing indentation system capable of determining Young's modulus of metals, superalloys, and single crystal matrices, and stiffness of coated material systems with flat, tubular, or curved architectures. This micro-indentation technique is viewed as a viable NDE technique for determining as-manufactured and process-exposed metal, superalloy, single crystal, and TBC-coated material properties. When incorporated into a portable hand-held unit, mechanical property measurements of structural components, including industrial turbine components, can be made.

In bench-scale studies, stiffness of several bond-coated substrates and TBC systems (EBPVD or APS) was determined at various stages of high temperature cyclic oxidation exposure. The time-series evaluation of test material surface stiffness responses revealed the status of coating strength degradation and the susceptible spallation initiation site. Currently TBC coupons (René N5/MCrAlY/APS YSZ) are under evaluation during extended 1,100°C thermal cyclic testing. The test data are planned to be correlated with a time-series cross-sectional microstructural analysis at specified thermal cycle intervals. The aim of this effort is to study the cross-sectional interfacial microstructural evolution, which eventually leads to

debonding/spallation failure, with correlation to the measured time-series surface stiffness responses.

The load-based micro-indentation methodology has also led to the development of a high temperature micro-indentation test apparatus with the capability of conducting micro-indentation testing and stiffness analysis up to temperatures of 1,200°C in either ambient or an inert gas environment.

Significant Results:

- Portable and hand-held micro-indentation test units were developed for surface stiffness characterization of TBCs on flat coupon and tubular architectures.
- SEM analysis of test coupons showed no additional YSZ cracking or degradation near or around the indented region, implying that the micro-indentation technique is non-destructive.
- Using the portable and hand-held units, a Young's modulus of ~200-210 GPa for Haynes 230 was determined, comparable to literature reported modulus values. A Young's modulus of ~130-150 GPa was determined for René N5.
- Loss of surface stiffness was demonstrated for the initial NETL-1 bond coat system. After 400 thermal cycles at 1,100°C, surface stiffness was reduced by ~41.7% on René N5, and ~62.5% on Haynes 230. The surface stiffness data strongly correlate with observed mass and microstructural changes.
- Surface stiffness contour profiles were developed for commercially applied TBC systems on René N5 and Haynes 230 test coupons. Within the initial 20 thermal cycles of exposure at 1,100°C, surface stiffness was reduced by ~2.8% for APS/MCrAlY, and ~15.1% for EBPVD/MCrAlY systems.
- Utilizing the micro-indentation technique, an initial increase in the surface stiffness for the APS YSZ TBC was identified during isothermal exposure at 1,100°C. After the apparent initial conditioning of the matrix and/or interfacial micro-debonding at high temperature, surface stiffness was reduced.
- A high temperature micro-indentation system was developed to address TBC stiffness at temperatures up to ~1,200°C. To date, POC testing has confirmed literature reported modulus values for tool steel at 600°C.

Planned Future Directions:

- Identify room temperature and high temperature surface mechanical stiffness response of a second production lot of René N5/MCrAlY/APS YSZ coupons during exposure to 1,100°C isothermal and cyclic oxidation conditions, validating the micro-indentation stiffness data, as well as demonstrating potential surface stiffness variability between and within commercial production lots. Correlate stiffness response with microstructural changes within the TBC architecture. Refine life prediction capabilities.
- Refine the micro-indentation testing capabilities for full blade architectures. Develop an automated characterization process for rapid assessment of turbine blades and vanes.

Non-Linear Acousto-Ultrasonic Diagnostics

In this subtask, nondestructive testing using an acousto-ultrasonic technique has been developed to detect the change of material properties and provide early warning of delamination of TBC systems. Testing was performed on René N5 and Haynes 230 coupons with an applied NETL-bond coat, as well as on coupons containing a commercially applied MCrAlY bond coat and YSZ top coat. The coupons were subjected to either cyclic or isothermal exposure at 1,100ºC. Ultrasonic testing was performed before and after thermal testing. POC test results indicated that changes in the properties of TBCs can be detected using the proposed technique. Ultrasonic Pitch/Catch results indicated that minor changes resulted within the bond coat applied to René N5 coupons after 400~500 hrs of cyclic oxidation. In contrast, marked differences in waveforms and travel time reflected significant crack formation and spallation of the bond coat from the Haynes 230 substrate.

The Pulse-Echo traveling time and amplitude measurement, performed on isothermally oxidized René N5 coupons coated with MCrAlY/YSZ, provided an early warning of delamination between top coat/bond coat interface at 350 hrs before debonding was visually observed after 400 hrs of isothermal exposure. The Young's modulus values of the YSZ top coat at different exposure hours were calculated using the Pulse-Echo traveling time for stressed and non-stressed coupons. Surface wave measurements were generated for estimating top coat thickness and material degradation after thermal exposure.

The mass density of the free standing APS and EBPVD YSZ top coats was measured using Archimedes' principle. Finite element analysis (FEA) simulation of the wave propagation on a simplified TBC system with nonlinear effects was conducted. The FEA results correlate well with the experimental observations and can clearly show detection of a small embedded void simulating delamination. The FEA was also used to estimate the material properties of different locations within the TBC system.

Significant Results:

- Results from this study show that the acousto-ultrasonic technique can nondestructively detect internal delamination and degradation of the YSZ top coat as a function time during high temperature exposure. Early warning of delamination was identified before debonding was visually observed.
- The ultrasonic signals were found to be very sensitive to the growth of the spallation area, and the Young's modulus of APS YSZ top coat can be predicted using the measured signals.

Planned Future Directions:

- Validate NDE analyses using a second production lot of René N5/MCrAlY/APS YSZ coupons during exposure to 1,100°C isothermal and cyclic oxidation conditions.
- Modify surface wave measurement equipment to reduce sensor contact area to improve accuracy of the top coat thickness measurements and material property predications.
- Address the use of non-contact (laser) acousto-ultrasonic diagnostics.

FY 2009 Publications/Presentations

Materials

1. M.A. Alvin, "Materials and Component Development for Advanced Turbine Systems," 25th Annual International Pittsburgh Coal Conference, Pittsburgh, Pennsylvania, September 29 – October 2, 2008.

2. M.A. Alvin, "Materials and Component Development for Advanced Turbine Systems," TMS 2009 – 138th Annual Meeting & Exhibition, Moscone West Convention Center, San Francisco, California, February 16, 2009.

3. M. Helminiak, N.M. Yanar, F.S. Pettit, G.H. Meier, and T.A. Taylor, "The Behavior of High-Purity, Low-Density Air Plasma Sprayed Thermal Barrier Coatings," Thermal Barrier Coating Symposium at ICMCTF, April 30, 2009.

4. B. Kang, L. Ma, K. Ogawa, M.A. Alvin, N. Wu, and G. Smith, "Materials and Component Development for Advanced Turbine Systems – ODS Alloy Development," Paper presented at the 23rd Annual Conference on Fossil Energy Materials, Pittsburgh Airport Marriott Hotel, Pittsburgh, Pennsylvania, May 12, 2009.

5. M.A. Alvin, "Materials and Component Development for Advanced Turbine Systems," Poster presented at the 23rd Annual Conference on Fossil Energy Materials, Pittsburgh Airport Marriott Hotel, Pittsburgh, Pennsylvania, May 13, 2009.

6. M. Helminiak, N.M. Yanar, F.S. Pettit, G.H. Meier, and T.A. Taylor, "Advanced APS Thermal Barrier Coatings," Poster presented at the 23rd Annual Conference on Fossil Energy Materials, Pittsburgh Airport Marriott Hotel, Pittsburgh, Pennsylvania, May 13, 2009.

7. M.A. Alvin, "Materials and Component Development for Advanced Turbine Systems," ASME Turbo Expo 2009, Orlando, Florida, June 8–12, 2009 (GT2009-59106).

Aerothermal

1. S. Siw, M.K. Chyu, V. Karaivanov, W. Slaughter, and M.A. Alvin, "Influence of Internal Cooling Configuration on Metal Temperature Distributions of Future Coal Fuel-Based Turbine Airfoils," ASME Turbo Expo 2009, Orlando, Florida, June 8–12, 2009.

2. V. Karaivanov, S. Siw, M.K. Chyu, W. Slaughter, and M.A. Alvin, "Substrate Damage Modeling for Advanced Turbine System Airfoils," ASME Turbo Expo 2009, Orlando, Florida, June 8–12, 2009.

3. M.K. Chyu, D.W. Mazzotta, S.C. Siw, V.G. Karaivanov, W.S. Slaughter, and M.A. Alvin, "Aerothermal Challenges in Syngas, Hydrogen-Fired, and Oxyfuel Turbines–Part I: Gas-Side Heat Transfer," Journal of Thermal Science and Engineering Applications **1**, 011002, March 2009.

4. M.K. Chyu, S.C. Siw, V.G. Karaivanov, W.S. Slaughter, and M.A. Alvin, "Aerothermal Challenges in Syngas, Hydrogen-Fired, and Oxyfuel Turbines–Part II: Effects of Internal Heat Transfer," Journal of Thermal Science and Engineering Applications **1**, 011003, March 2009.

5. V.G. Karaivanov, S.C. Siw, M.K. Chyu, M.A. Alvin, and W.S. Slaughter, "A Lifing Methodology for Airfoils in Hydrogen-fired and Oxy-fuel Turbines: Creep Damage," ASME Journal of Engineering Materials and Technology (Paper submitted March 30, 2009).

6. M. Chyu, P. Ganmol, S. Siw, W. Slaughter, V. Karaivanov, and M.A. Alvin, "Aerothermal Modeling and Experiments of Turbine Airfoils," Poster presented at the 23rd Annual Conference on Fossil Energy Materials, Pittsburgh Airport Marriott Hotel, Pittsburgh, Pennsylvania, May 13, 2009.

7. V. Karaivanov, S. Siw, M. Chyu, W. Slaughter, and M.A. Alvin, "Airfoil Life Prediction Modeling," Poster presented at the 23rd Annual Conference on Fossil Energy Materials, Pittsburgh Airport Marriott Hotel, Pittsburgh, Pennsylvania, May 13, 2009.

Non-Destructive Evaluation

1. C. Feng, J.M. Tannenbaum, B. Kang, and M.A. Alvin, "A Load-Based Indentation Technique for Mechanical Property Evaluation," Society of Experimental Mechanics, Submitted December 8, 2008 (Accepted).

2. B. Kang, C. Feng, J.M. Tannenbaum, and M.A. Alvin, "A Load-Based Depth-Sensing Indentation Technique for NDE and Life Assessment of Thermal Barrier Coatings," ASME Turbo Expo 2009, Orlando, Florida, June 8–12, 2009.

3. R. Chen, B. Zhang, and M.A. Alvin, "Nondestructive Detection of Delamination in Thermal Barrier Coatings Using Ultrasonic Techniques," ASME Turbo Expo 2009, Orlando, Florida, June 8–12, 2009.

4. B. Kang, C. Feng, J. Tannebaum, and M.A. Alvin, "A Load-Based Micro-Indentation Technique for Materials Young's Modulus Measurement and TBC Bond Coat Degradation Evaluation," Materials Science and Engineering: A, Submitted December 8, 2008.

5. J. Tannebaum, B. Kang, and M.A. Alvin, "A Load-Based Depth-Sensing Indentation Technique for NDE and Damage Assessment of TBCs," Poster presented at the 23rd Annual Conference on Fossil Energy Materials, Pittsburgh Airport Marriott Hotel, Pittsburgh, Pennsylvania, May 13, 2009.

6. R. Chen, B. Zhang, and M.A. Alvin, "Nondestructive Evaluation of Thermal Barrier Coatings Using Acousto-Ultrasonic Techniques," Poster presented at the 23rd Annual Conference on Fossil Energy Materials, Pittsburgh Airport Marriott Hotel, Pittsburgh, Pennsylvania, May 13, 2009.

7. B. Kang, C. Feng, J.M. Tannenbaum, and M.A. Alvin, "A Load-Based Micro-Indentation Technique for Mechanical Property and NDE Evaluation," SEM Annual Conference and Exposition on Experimental and Applied Mechanics, Albuquerque, New Mexico, June 1–4, 2009.

References

1. R.A. Dennis, "FE Research Direction – Thermal Barrier Coatings and Health Monitoring Techniques," Workshop on Advanced Coating Materials and Technology for Extreme Environments, Pennsylvania State University, State College, Pennsylvania, September 12–13, 2006.

Project Team

M.A. Alvin, *NETL-Pittsburgh*
D. Straub, T. Sidwell, K. Casleton, *NETL-Morgantown*

F. Pettit, G. Meier, M. Yanar, M. Helminiak
M. Chyu, S. Siw, P. Ganmol, W. Slaughter, V. Karaivanov
S. Mao, B. Gleeson, N. Mu,
University of Pittsburgh

B. Kang, C. Feng, J.M. Tannebaum, N. Ma
R. Chen, B. Zhang, T. Fu,
West Virginia University

K. Klotz, *Coatings for Industry*
K. Murphy, R. Honick, J. Colston, T. Hansen,
R. Grunstra, *Howmet International*

S. Dighe, I. Martorell, *Westinghouse Plasma Corporation*
T. Taylor, *Praxair*
B. Nagaraj, *GE*

IV.8 Materials Performance in Oxy-Fuel Turbine Environments

Gordon R. Holcomb
National Energy Technology Laboratory
1450 Queen Ave. SW
Albany, OR 97321
Phone: (541) 967-5874; Fax: (541) 967-5914
E-mail: Gordon.Holcomb@netl.doe.gov

Contract Number: 220682-2/a

Start Date: October 1, 2008
End Date: September 30, 2009

FY 2009 Objectives

- Obtain uncoated and coated low-cycle fatigue (LCF) test specimens and oxidation coupons from Siemens, and reach agreement with Siemens as to specific exposure test details.
- Complete all of the 1,000-hour exposure tests in steam with 10% CO_2 and 0.2% O_2, and deliver all of the LCF test specimens to Siemens.
- Complete thermodynamic analysis of environment-alloy interactions. Included is an examination of the potential for significant chromia evaporation to occur.
- Complete analysis of oxidation specimens. Analysis includes light microscopy of as-oxidized and cross-sectioned surfaces, and scanning electron microscopy (including elemental mapping of selected samples) of selected as-oxidized and cross-sectioned surfaces.
- Demonstrate, based on completing the above objectives, the ability of the tested alloys to function properly in the oxy-fuel turbine environment.

Accomplishments

- Reached agreement with representatives from Siemens as to optimal experimental details and procedures. This included the determination, through a 250-hour test, that two coats of Zircar-CEM, an alumina-based coating system, would provide adequate protection to protect the threads on the LCF specimens for subsequent LCF tests.
- Completed four 250-hour test segments at 630°C and 748°C, and 31 LCF test specimens were delivered to Siemens. The first of four 250-hour test segments at 691°C and 821°C were completed, and the second test segment is underway.
- Showed from mass change measurements that the cobalt-base alloys exhibited significantly less mass gain at 748°C than the nickel-base alloys. Mass gains for all the alloys were low and very similar to each other at 630°C.
- The thermodynamic evaluation of the alloys in this environment is partially complete. This includes an evaluation of uncoated or bond coated alloys as to their predicted chromia evaporation tendency during operations within the high velocity environment.
- Metallographic examinations of bare, bond coat (BC), and thermal barrier coated (TBC) oxidation coupons are underway, which includes optical and scanning electron microscopy of the oxide surface and metal-scale cross section, and X-ray diffraction of the oxide surface.

Introduction

An Advanced Turbine Program research goal is to develop, by 2012, oxy-fuel turbine and combustor technologies for highly efficient (50-60 percent), near zero emissions, coal-based power systems. Oxy-fuel combustion, which burns fuel in oxygen rather than in air, has a distinct advantage of generating combustion gas with a much higher percentage of CO_2 than conventional systems. This higher percentage of CO_2 allows for easier and more efficient carbon capture. Gas turbines, such as the Siemens SGT-900 (formerly Westinghouse W251), are prime candidates for use in oxy-fuel turbine systems as the intermediate pressure turbine (IPT), operating at approximately 1,180°C, Figures 1-2 [1]. Conventional steam turbines are proposed for use as the high pressure turbine and low pressure turbine.

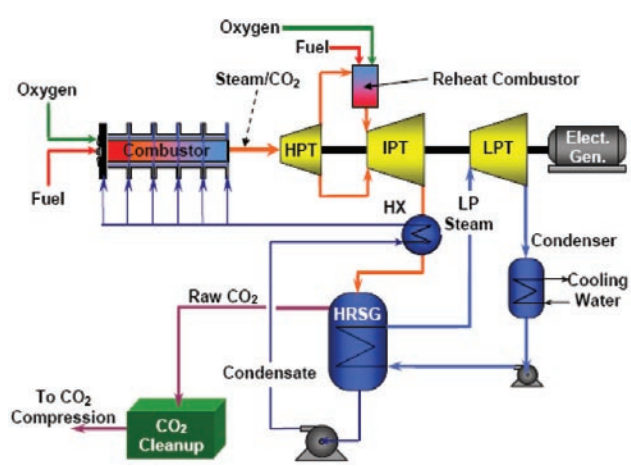

FIGURE 1. Conceptual Layout of Oxy-Fuel System [1]

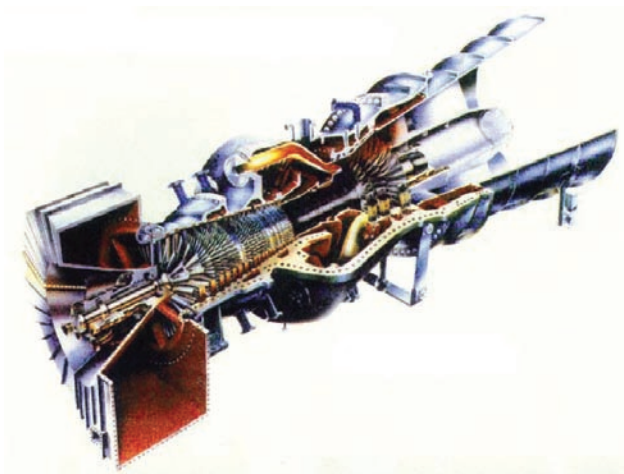

FIGURE 2. Cross-Section of a SGT-900 Gas Turbine Proposed for Use as the IPT in Figure 1 [1]

Approach

The goals of this project are to 1) understand the behavior of candidate alloys and alloy/coating systems in oxy-fuel combustion and turbine environments, and 2) to preoxidize LCF test specimens at four temperatures for subsequent fatigue tests by Siemens. The alloy systems and coating systems that are to be studied, both as oxidation coupons (Ox) and LCF test specimens are listed in Table 1 and are alloys and alloy/coating systems that are in the SGT-900 gas turbine proposed for use in the IPT. The Ox and LCF test specimens will be exposed at four temperatures for up to 1,000 hours in steam-10% CO_2-0.2% O_2. Oxidation coupon mass changes will be measured every 250 hours. Upon completion of the exposures, the LCF samples will be delivered to Siemens for LCF testing and the Ox samples will undergo metallographic examination.

TABLE 1. Alloy and Coating Systems

Alloy	Base	Uncoated		BC		BC & TBC	
		Ox	LCF	Ox	LCF	Ox	LCF
ECY768	Co	X				X	X
X-45	Co	X		X	X		
Inconel 738	Ni	X		X	X	X	X
Inconel 939	Ni	X				X	X
Udimet 520	Ni	X	X	X			

Results

A 250-hour test of various coatings to protect the LCF test specimen threads during exposures in steam-CO_2-O_2 was completed. It was determined that two coats of Zircar-CEM, an alumina-based coating system, would provide adequate protection. Experimental details, including the thread-protection procedure, were agreed upon with representatives from Siemens.

Four 250-hour test segments at 630°C and 748°C were completed, and 31 LCF test specimens were delivered to Siemens. The first of four 250-hour test segments at 691°C and 821°C were completed, and the second test segment is underway. The samples included in these tests are shown in the test matrix, Table 2.

Overall mass change results showed that the cobalt-base alloys exhibited less mass gain at 748°C than the nickel-base alloys. However, the downward

TABLE 2. Test Matrix for 1,000 Hour Exposures in H_2O-10% CO_2-0.2% O_2

T °C	Type	ECY-768		X-45		IN-738			IN-939		U-520		Total
		Un	TBC	Un	BC	Un	BC	TBC	Un	TB	Un	BC	
630	LCF										8		8
	Ox	2		2		2			2	1	2	1	12
693	LCF									8			8
	Ox	2	1	2	1	2	1	1	2	1	2	1	16
748	LCF		8		8		7						23
	Ox	2	1	2	1	2	1	1	2	1	2	1	16
821	LCF							8					8
	Ox	2	1	2	1	2	1	1	2		2		14
Spare	Ox	2	1	2	1	2	1	1	2	1	2	1	16
Total	LCF		8		8		7	8		8	8		47
	Ox	10	4	10	4	10	4	4	10	4	10	4	74

"Un" are uncoated samples, "BC" are samples with a bond coat, "TBC" are samples with a bond coat and thermal barrier coating, "LCF" are low cycle fatigue specimens, and "Ox" are oxidation coupons.

trend for some of the cobalt-base alloys after the first 250 hours of exposure could show tendencies towards scale spallation or chromia evaporation. Mass gains for all the alloys were low and very similar to each other at 630°C. Figures 3-4 show the mass change results for alloys X-45 and Udimet 520.

The thermodynamic evaluation of the alloys in this environment is partially complete. This includes an evaluation [2] of uncoated or bond coated alloys as to their predicted chromia evaporation tendency during operations within the high velocity environment.

Metallographic examinations of bare, BC, and TBC oxidation coupons are underway after 500 and 1,000 hours of exposure, which includes optical and scanning electron microscopy of the oxide surface and metal-scale cross section, and X-ray diffraction of the oxide surface.

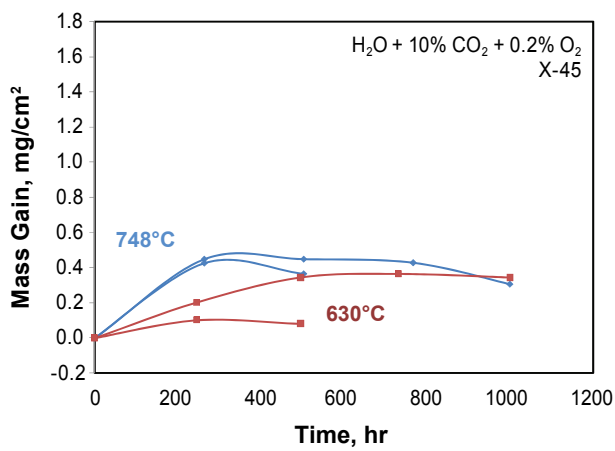

FIGURE 3. Mass Change Results for the Uncoated Cobalt-Base Superalloy X-45

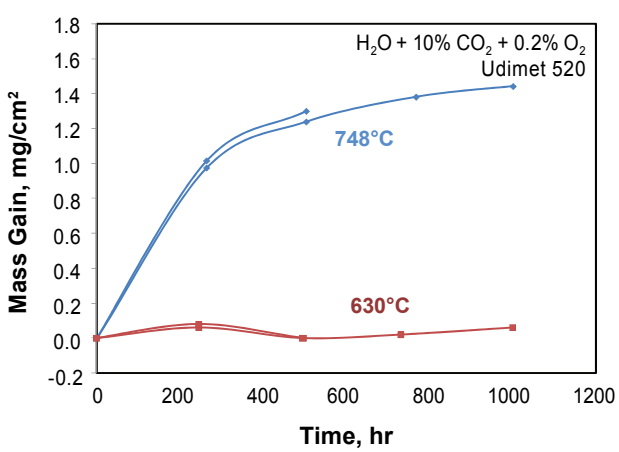

FIGURE 4. Mass Change Results for the Uncoated Nickel-Base Superalloy Udimet 520

Conclusions and Future Directions

At this point in the project, oxidation behavior is only based on mass change measurements and not metallographic examination. Overall mass change results showed that the cobalt-base alloys exhibited less mass gain at 748°C than the nickel-base alloys. However, the downward trend for some of the cobalt-base alloys after the first 250 hours of exposure could show tendencies towards scale spallation or chromia evaporation. Mass gains for all the alloys were low and very similar to each other at 630°C. Further metallographic examination and thermodynamic evaluation of chromia evaporation is required (and planned) to better understand these results.

Beyond this year's work, several issues remain to be examined:

- Some alloys, such as T91 and T92 [3] show much greater oxidation rates in steam-CO_2-O_2 than they do in steam, steam-CO_2, moist air, or Ar-CO_2 environments. Understanding the agressive nature of the steam-CO_2-O_2 environement could allow better alloy selection (in terms of effectiveness and cost) in oxy-fuel turbine and combustion systems.
- The use of the SGT-900 gas turbine as the IPT in the proposed system is only possible at the temperatures in this stage of oxy-fired turbine developement. The eventual plan [1] is to significantly increase the temperature of the IPT. Additional materials development and materials performance efforts will be required to realize these temperature increases.

FY 2009 Publications/Presentations

1. G.R. Holcomb, "Oxidation in Environments with Elevated CO_2 Levels," 23rd Annual Conference on Fossil Energy Materials, Pittsburgh, Pennsylvania, May 12–14, 2009.

References

1. R.E. Anderson, S. MacAdam, F. Viteri, D.O. Davies, J.P. Downs, A. Paliszewski, "Adapting Gas Turbines to Zero Emission Oxy-fuel Power Plants," Proceedings of ASME Turbo Expo 2008: Power for Land, Sea and Air, GT 2008, June 9–13, Berlin, Germany GT2008-51377.

2. G.R. Holcomb, "Steam Oxidation and Chromia Evaporation in Ultra-Supercritical Steam Boilers and Turbines," presented at PRIME 2008, Honolulu, Hawaii, October 12–17, 2008, accepted for publication in the Journal of the Electrochemical Society.

3. G.R. Holcomb, "Oxidation in Environments with Elevated CO_2 Levels," 23rd Annual Conference on Fossil Energy Materials, Pittsburgh, Pennsylvania, May 12–14, 2009.

IV.9 Data for Thermophysical Properties of Humid Gases in Power Cycles

Dr. Allan H. Harvey
Thermophysical Properties Division
National Institute of Standards and Technology (NIST)
325 Broadway, MS 838.08
Boulder, CO 80305
Phone: (303) 497-3555; Fax: (303) 497-5224
E-mail: aharvey@boulder.nist.gov

DOE Project Manager: Travis Shultz
Phone: (304) 285-1370
E-mail: Travis.Shultz@netl.doe.gov

Contract Number: 42957

Start Date: August 1, 2006
End Date: December 31, 2009

FY 2009 Objectives

- Use results of first-principles quantum mechanics to develop description of thermodynamics of humid gases in power cycles.
- Validate thermodynamic description by high-accuracy density measurements at high temperatures.
- Measure thermal conductivity of key water/gas mixtures at conditions relevant to power cycles.

Accomplishments

- Fabrication of high-temperature densimetry system has been completed and performance testing has begun.
- Completed thermal conductivity measurements of pure N_2, CO_2, H_2O, and mixtures of N_2 with H_2O at temperatures from 500 K to 740 K.

Introduction

Innovative power cycles (such as integrated gasification combined cycle and oxyfuel) are being developed for production of electric power with higher efficiency and reduced environmental impact, including the possibility of CO_2 sequestration. For optimizing the design of these systems, it is important to have accurate values of the thermophysical properties (density, heat capacity, thermal conductivity, etc.) of the fluid mixtures in the turbines and other parts of these cycles. These mixtures have a large water content, along with other gases such as nitrogen and carbon dioxide; they are at high temperatures where thermodynamic data are scarce, but the pressures are only moderately high. Typical approaches such as ideal-gas thermodynamics or common engineering equations of state are inaccurate for such systems, primarily due to the presence of water. Therefore, it is necessary to develop alternative modeling approaches, supplemented by selected high-temperature experimental measurements.

Approach

The description of the thermodynamic properties is developed at the level of the second virial coefficient, which is the first-order correction to the ideal-gas law. The key parameters are the "cross" second virial coefficients representing interactions between one water molecule and one gas molecule. Our approach is to use computational quantum mechanics to develop accurate surfaces describing the potential energy between the molecules, from which the virial coefficients can be calculated with high accuracy.

In order to validate our theoretical results, we will perform high-accuracy density measurements on the key water-nitrogen and water-CO_2 systems at high temperatures. The high temperatures are necessary because adsorption renders the measurements nearly impossible below about 500 K, but few laboratories have the capability for precision densimetry at high temperatures. We are developing such capability in conjunction with this work. The instrument is known as a "single-sinker magnetic-suspension densimeter." It operates on the Archimedes or buoyancy principle. By knowing the sinker volume and comparing the apparent weight while it is immersed in the gas mixture to the known mass of the sinker, the density is determined. This is an absolute method, meaning that no calibration fluids are required. The key elements of the instrument are the sinker (which is the actual sensing element), a magnetic suspension coupling which transmits the weight of the sinker to the balance and isolates the balance from the extreme conditions of the fluid, and the balance (which provides the quantitative measurement).

We have developed parallel capability for measuring the thermal conductivities of these mixtures at high temperatures; in this case the measurements are essential because no good theoretical approach is available for this property. The measurements will use the transient hot-wire method, which has become the method of choice for high-accuracy thermal conductivity measurements. Because water's electrical conductivity is problematic for the traditional direct current implementation of this technique, an

alternating current (AC) version of the apparatus has been developed.

Results

As a preliminary to this work (not funded by this project), we have produced potential-energy surfaces for the water-nitrogen and water-oxygen molecular pairs and used them to calculate second virial coefficients in a large temperature range with uncertainties better than all but the most precise experimental data. The water-carbon dioxide pair, which is the central theoretical work in this project, is almost finished but results are not yet available. Second virial coefficients for pairs not involving water have also been correlated based on available data.

Accurate measurements of the density and thermal conductivity of the water-nitrogen and water-carbon dioxide mixtures require samples with well-known compositions. Because of the very large volatility difference of water compared to nitrogen or carbon dioxide, it is not possible to prepare mixtures outside the measurement system at room temperature. Thus, the mixture samples for this work are prepared in situ in each measurement apparatus, with compositions determined from difference weighings of separate gas-charge (nitrogen or CO_2) and smaller water cylinders. The two are connected in series for charging the sample into the apparatus, with the high-pressure gas sample pushing the water sample into the measuring cell. The gas-charge cylinders are shown in Figure 1; they are initially filled with 100 cm^3 of high-purity nitrogen or carbon dioxide at pressures up to 70 MPa, with the mass of gas determined with a 10 kg mass comparator that has a resolution of 0.1 mg. Each gas-charge cylinder is also equipped with a pressure transducer to monitor the charging process. The water-injector cylinders vary from 5 cm^3 to 15 cm^3 volume depending on the apparatus volume and the desired composition (gas chromatography sample loops with 0.08 cm^3 to 1 cm^3 volume are used when small amounts of water are required). The water-injector cylinders or sample loops are initially evacuated and then filled with the desired quantity of water that has been deionized and degassed. The water mass in the injector cylinder is also determined with the 10 kg mass comparator. Each cylinder weighing is made relative to a matching reference cylinder to eliminate errors due to atmospheric buoyancy. Differences in the mass of each cylinder, before and after charging each apparatus, give the quantity of sample charged and allow the mixture composition in the apparatus to be determined with high accuracy.

Fabrication of the high-temperature densimetry apparatus that is being constructed by NIST for use in this project has been completed. The key parts include the measuring cell/pressure vessel; the density measuring system; a multi-layer thermostat for temperature control up to 773 K with stability and uncertainty in temperature of a few mK; a vacuum chamber (for thermal isolation) and vacuum pumping system; a sample-handling system; and pressure instrumentation. Figure 2 is a photograph of the apparatus.

The densimeter "kernel," which was contracted to Rubotherm, GmbH, Bochum, Germany, has been fabricated and delivered. The densimeter is positioned in the center of the thermostat. The system is built around a custom version of the Rubotherm high-temperature, high-pressure magnetic suspension coupling. The major custom items are a silicon sinker

FIGURE 1. Gas-charge cylinders (large cylinders with one valve and pressure transducer) and water-injector cylinders (small cylinders with two valves) shown with 10 kg mass comparator during the weighing process for gravimetric preparation of water mixtures.

FIGURE 2. Photo showing the high-temperature densimeter. From left to right the major components are: vacuum system; main part of densimeter with the mass-comparator balance at the top and the vacuum chamber containing the measuring cell at the bottom; instrument rack; and display for the control computer.

and a high-resolution mass-comparator balance. The density-sensing system comprises the silicon sinker together with the balance and magnetic suspension coupling. The thermal expansion of silicon is known to very high accuracy, and thus the volume of the sinker as a function of temperature can be computed accurately. The measuring cell is designed for pressures up to 50 MPa. The density system was installed by Rubotherm personnel in March 2009. These components were installed into the thermostat that was designed and fabricated at NIST. Performance testing is now underway.

The modifications to the electronics and software to enable transient hot-wire measurements with AC drive voltage and phase-sensitive determination of the wire temperature rise have been completed. Performance measurements with the AC technique have been successfully completed on argon at moderate temperatures. The high-temperature hot-wire cell for the water mixtures has been assembled, calibrated, and tested with pure H_2O, N_2, and CO_2 at temperatures from 500 K to 740 K with pressures up to 40 MPa.

The components for the new hot-wire cell are shown in Figure 3 during assembly. A reference platinum resistance thermometer is located in an axial hole in the isothermal cylinder. The pressure vessel has a volume of 5 cm^3 and is pressure rated to 117 MPa at 700 K. The tantalum lead wires enter the cell from the right through a ceramic sealant in a compression gland and are insulated with rigid ceramic spacers. The hot wire is supported with rigid ceramic parts that also provide electrical insulation. The hot wire is tensioned by spring arrangement at the bottom of the hot wire. The hot wires are located between the thin-ceramic support tubes, and near the central axis of the cylindrical cavity formed by the inner wall of the pressure vessel when the wire and its support system is inserted in the pressure vessel.

The new hot-wire cell is enclosed in an electrical furnace that provides temperature control from ambient to over 750 K. The temperature is measured with the reference platinum resistance thermometer with an uncertainty of 5 mK, while the pressure is measured with a pressure transducer (0 to 70 MPa) with an uncertainty of 0.007 MPa. The filling manifold and pressure transducer have small volumes and are water-filled to reduce uncertainty in the composition of the sample that would result from condensation of water from the mixture in these colder regions of the pressure system.

Thermal conductivity measurements of mixtures of N_2 with H_2O have been completed for two compositions each at temperatures of 500, 560, 620, 680 and 740 K. The dilute-gas thermal conductivity (low-density limiting value) of the mixtures is larger than that of either pure N_2 or H_2O at a given temperature. This behavior has been reported for a few limited measurements of thermal conductivity for mixtures of polar with nonpolar gases but is not understood at a fundamental level. The density dependence of the mixture thermal conductivity falls between those of the pure components at a fixed temperature. Figure 4 shows this behavior at temperatures near 500 K; this figure also shows the good agreement of the present data with the accepted values for pure nitrogen and water in the NIST REFPROP database.

Conclusions and Future Directions

All main objectives of this work are still "in progress," so no conclusions can be drawn yet. In the following, we describe the future directions of the work.

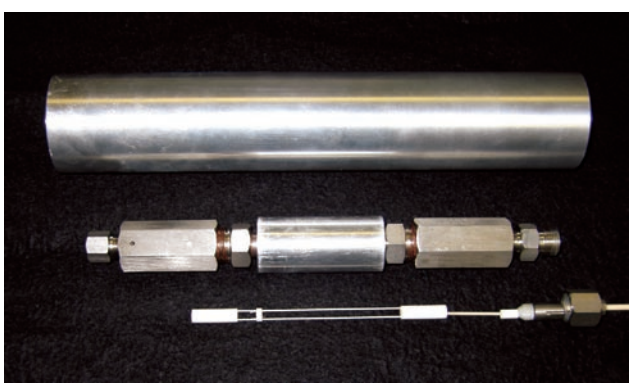

FIGURE 3. Hot-wire cell components during assembly of the high-temperature cell for the water mixtures. From top to bottom: 1) isothermal cylinder, 2) pressure vessel, 3) ceramic hot-wire supports and lead wire insulation/pressure sealant.

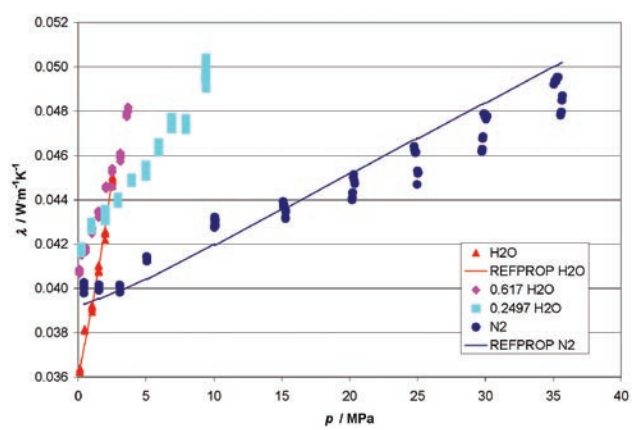

FIGURE 4. Thermal conductivity of mixtures of N_2 with H_2O at temperatures near 500 K. The upper pressure and density for the pure water and the mixtures is limited by condensation of liquid.

For the modeling part of the work, in Fiscal Year 2009 a potential-energy surface will be completed for the interaction between water and carbon dioxide. The thermodynamic quantities (second virial coefficients) derived from this surface will be combined with previous results to provide a complete description of the gas-phase thermodynamics of the main components of combustion gases. These results will be integrated into a mixture equation-of-state model.

On the experimental side, the mixture preparation equipment has been assembled and tested at pressures up to 70 MPa. Results for the density of the H_2O/N_2 and H_2O/CO_2 systems will be obtained in the second half of 2009. The modifications to the thermal conductivity instrumentation have been completed. Measurements of the thermal conductivity of pure H_2O, N_2 and CO_2 and the binary H_2O/N_2 mixture system have been completed at temperature of 500, 560, 620, 680, and 740 K with pressures up to 40 MPa. Results for the thermal conductivity of the CO_2/H_2O binary mixture system will be completed in the final quarter of FY 2009.

While this will complete the present project, there are related areas of need that could be considered as extensions to this work. These would include:

- Extension of the thermodynamic framework to allow prediction of condensation of water and of vapor-liquid equilibria more generally.
- Experimental measurements of the sound speed and/or the viscosity for gaseous H_2O/N_2 and H_2O/CO_2 mixtures.

IV.10 Reduced and Validated Kinetic Mechanisms for Hydrogen-CO-Air Combustion in Gas Turbines

Professor Yiguang Ju (Primary Contact),
Professor Frederick L. Dryer, Michael P. Burke
Princeton University
D115 Equad, Olden Street
Princeton, NJ 08544
Phone: (609) 258-5644; Fax: (609) 258-6233
E-mail: yju@princeton.edu

DOE Project Manager: Mark Freeman
Phone: (412) 386-6094
E-mail: Mark.Freeman@netl.doe.gov

Contract Number: 42716

Start Date: January 1, 2006
End Date: December 31, 2008

FY 2009 Objectives

- Measure flame speed and burning rate data of $H_2/CO/CO_2$ mixtures at high pressure and low flame temperature conditions characteristic of gas turbine engines.
- Develop and validate chemical models for $H_2/CO/CO_2$ combustion for use in the numerical design of low-emission syngas turbine combustion systems.
- Construct new methodologies to reduce computational time for combustion calculations to make detailed engine simulations feasible.

Accomplishments

- Gathered flame speed and burning rate data spanning a significant range of typical syngas turbine conditions, employing a parametric approach by individually varying:
  - Pressure: 1 to 25 atm
  - Flame temperature: 1,500 to 1,800 K
  - Equivalence ratio: 0.85 to 2.5
  - CO fuel fraction: 0 to 90%
  - CO_2 dilution fraction: 0 to 40%
- Mapped the pressure dependence of $H_2/CO/CO_2$ burning rates experimentally and numerically and identified the existence of *negative pressure dependence* in the measured burning rates at high pressure, low flame temperature conditions, which results in atypical engine stability behavior.
- Validated two state-of-the-art models against burning rate data up to 10 atm for low flame temperature conditions and identified that significant improvements to the models must be made to predict burning rates above 15 atm or with CO_2 dilution.
- Identified key kinetic pathways in high-pressure, low-flame temperature flames, potential for previously unconsidered pathways, and possible areas for improvement in kinetic modeling. Efforts to improve model performance are underway with our collaborators in the elementary reaction kinetics field.
- Formulated and tested strategies that reduce computational time in combustion calculations by over an order of magnitude.

Introduction

Although renewable energy sources will have a growing share in the energy market, we will still need to rely on fossils fuels as a major energy source for many years. With more stringent environmental standards and climate change concerns, coal-based integrated gasification combined cycle systems for generation of syngas, hydrogen, and electricity offer opportunities to control air pollutant emissions, achieve high energy conversion efficiencies, and sequester carbon. In gas turbine engines, low flame temperatures are utilized to reduce NOx emissions, which are formed more readily at higher temperatures.

A successful design of reliable and efficient gas turbine engines operating on high hydrogen content sygnas fuels strongly depends on the knowledge of the combustion properties of syngas at actual gas turbine conditions and on the availability of reliable chemical kinetic models for numerical modeling. Unfortunately, very limited experimental data of syngas and hydrogen burning properties such as flame speeds and burning rates at typical gas turbine pressures are currently available. Most available high pressure data do not focus on low flame temperature conditions. Consequently, no kinetic model for syngas and hydrogen combustion has been validated against flame speeds and burning rates for low flame temperatures over an extensive range of conditions. Therefore, there exists a great need for more experimental data and validated models for high pressure, low flame temperature conditions. Additionally, methods to

reduce computational time using these validated syngas models are necessary to facilitate utilization of engine simulations in the design process.

Approach

Experiments are conducted in a high-pressure, dual-chambered cylindrical bomb developed in our lab [1]. Mixtures of H_2, CO, CO_2, O_2, and other diluents are prepared using the partial pressure method. Outwardly propagating spherical flames are initiated by a spark across two electrodes at the center of the chamber. Evolution of the flames is filmed using high-speed Schlieren photography. The radius of the flame front as a function of time is measured from the images, such that the flame speed and mass burning rate can be extracted from the experiments using improved methodologies developed in the course of this study [2].

Experimental values for flame speed and burning rate are obtained from the experiment over a variety of conditions. Conclusions are drawn from the trends in the experimental data. The measured values are compared with the predicted values by available chemical models. If agreement is acceptable, the model is considered validated for use at those conditions. If agreement is poor, the model must be revised to yield acceptable agreement at those conditions.

In order to reduce computational time for combustion calculations, a dynamic multi-timescale (MTS) kinetic reduction method has been developed which splits and solves each species with a time step appropriate for its characteristic time scale. In such a way, "fast" species are calculated with smaller time steps and "slow" species are calculated with larger time steps. Consequently, the number of time steps for which all species is calculated is reduced.

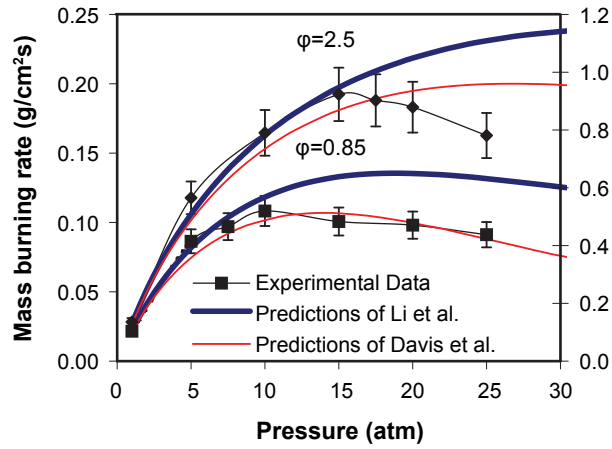

FIGURE 1. Mass Burning Rates for H_2 Mixtures at High Pressures and Low Flame Temperatures

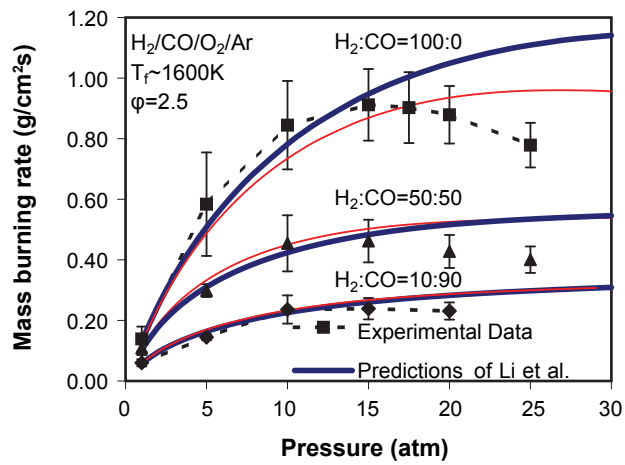

FIGURE 2. Mass Burning Rates for H_2/CO Mixtures at High Pressures and Low Flame Temperatures

Results

Flame speeds and burning rates were measured across a range of pressures from 1 to 25 atm, equivalence ratios from 0.85 to 2.5, CO fuel fractions from 0 to 0.9, CO_2 dilution ratios from 0 to 40% and flame temperatures from 1,500 to 1,800 K. Measured flame speeds for H_2/O_2/diluent mixtures of various equivalence ratios show a decreasing trend of flame speed with pressure across the entire range of equivalence ratio. Figure 1 presents the mass burning rates for the same conditions. The data indicate that *negative reaction orders* are present for the dependence with pressure. While the burning rate increases with pressure up to ~15 atm, the burning rate decreases with pressure thereafter. Non-monotonic pressure dependences for the mass burning rate are somewhat unusual. Flames with negative pressure dependence have opposite thermo-acoustic stability characteristics in engines compared to typical flames.

Measured mass burning rates are compared to predictions using two recently published, extensively validated kinetic models for H_2/CO combustion [3,4] in Figure 1. The two models demonstrate excellent agreement with the experimental data up to ~10 atm. For higher pressures, however, there exist large disparities between the measured and predicted burning rates. In fact, for the fuel-rich case (equivalence ratio of 2.5), both models fail to capture the observed pressure dependence – while the experimental data show a decreasing trend with pressure above 15 atm, the models predict an increasing trend.

As displayed in Figure 2, mass burning rates of H_2/CO flames with CO fuel fractions as high as 0.5

also exhibit *negative reaction orders*. Similar to pure H_2 flames of the same flame temperature (1,600 K), the burning rate increases with pressure up to ~15 atm, the burning rate decreases with pressure thereafter. Likewise, both models fail to capture the observed pressure dependence – while the experimental data show a decreasing trend with pressure above 15 atm, the models predict an increasing trend. Measurements of H_2/CO flames with a CO fuel fraction of 0.9 reveal a weaker pressure dependence and better agreement with model predictions.

When CO_2 is used to dilute the mixture, the pressure dependence becomes stronger due to the high third-body efficiency of CO_2 in the inhibitive $H+O_2+M=HO_2+M$ reaction. Negative pressure dependence was observed for CO_2-diluted flames with flame temperatures as high as 1,800 K, as shown in Figure 3. Due to the higher third-body efficiency of H_2O in the inhibitive $H+O_2+M=HO_2+M$ reaction, dilution with H_2O is expected to have an even stronger effect.

Results from our numerical analysis indicate that further investigation into the pressure fall-off for $H+O_2+M=HO_2+M$ and the temperature dependence of HO_2 reactions with key radical species is required to improve modeling performance. In addition, the present level of understanding of elementary processes allow for the possibility that one or more elementary reactions that could be important in high pressure H_2 flames but are not included in most of the current hydrogen combustion models. For example, the reaction $O+OH+M=HO_2+M$ is not included in almost all recent H_2 models and has largely been believed to be unimportant. Figure 4 compares burning rate predictions using the model of Li et al. modified to include $O+OH+M=HO_2+M$ for the range of values proposed for the rate available in the scientific literature. For higher rate values, the

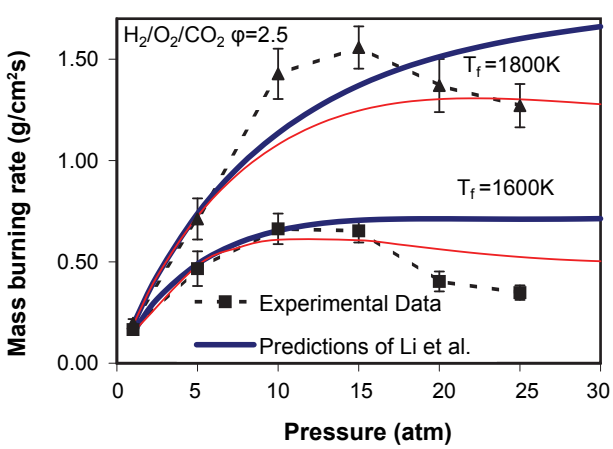

FIGURE 3. Mass Burning Rates for H_2/CO_2 Mixtures at High Pressures and Low Flame Temperatures

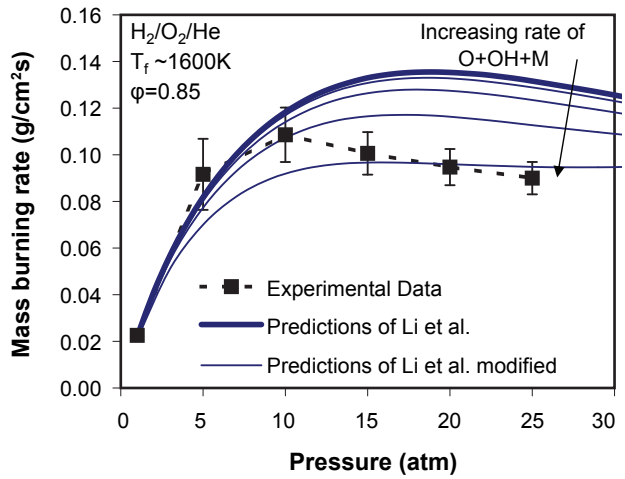

FIGURE 4. Comparison of Predicted Burning Rates Using a Range of Rate Values for $O+OH+M = HO_2+M$ Available in the Scientific Literature

reaction reduces the predicted mass burning rate at higher pressures by up to 35% at 25 atm. At present, it appears that $O+OH+M=HO_2+M$ may be in part be important to achieving more accurate syngas burning rate predictions at conditions relevant to gas turbine engines.

The MTS modeling technique was implemented and validated for hydrogen ignition computations. The technique reduces the computational time by an order of magnitude.

Conclusions and Future Directions

Flame speeds and burning rates were measured across a range of pressures from 1 to 25 atm, flame temperatures from 1,500 to 1,800 K, equivalence ratios from 0.85 to 2.5, CO fuel fractions from 0 to 0.9, CO_2 dilution ratios from 0 to 0.4. *Negative pressure dependence* was observed for burning rates in H_2 flames at high pressure, low flame temperature conditions. The pressure dependence of H_2/CO flames was observed to be similar to pure H_2 flames with CO fuel fractions as high as 0.5. Dilution with CO_2 was observed to strengthen the pressure dependence. For similar reasons (discussed above), dilution with H_2O is expected to strengthen the pressure dependence to an even larger extent than CO_2. Since flames with negative pressure dependence are somewhat unusual, flames of this sort have opposite thermo-acoustic stability characteristics in engines compared to typical flames. Predictions for the flame speed and burning rate exhibit good agreement with the measured data, except at high pressure, low flame temperature conditions. The models require significant improvements to predict burning rates above ~15 atm or with CO_2 dilution at the low flame temperatures

used in gas turbine engines. Key kinetic pathways in high-pressure, low-flame temperature flames, potential for previously unconsidered pathways, and possible areas for improvement in kinetic modeling were identified. Now efforts to increase model performance are underway with our collaborators in the elementary reaction kinetics field. A MTS modeling approach was developed, validated, and demonstrated to reduce computation time for hydrogen ignition calculations by an order of magnitude.

Selected FY 2009 Publications/Presentations

1. M.P. Burke, Z. Chen, Y. Ju, and F.L. Dryer, "Effect of Cylindrical Confinement on the Determination of Laminar Flame Speeds Using Outwardly Propagating Flames," *Combustion and Flame* 156 (2009) 771-779.

2. Z. Chen, M.P. Burke, and Y. Ju, "Effects of Lewis Number and Ignition Energy on the Determination of Laminar Flame Speed Using Propagating Spherical Flames," *Proceedings of the Combustion Institute* 32 (2009) 1253-1260.

3. Z. Chen, M.P. Burke, and Y. Ju, "Effects of Compression and Stretch on the Determination of Laminar Flame Speed Using Propagating Spherical Flames," *Combustion Theory and Modelling* 13 (2009) 343-364.

4. X. Gou, Z. Chen, W. Sun, and Y. Ju, "An Efficient Multi Time Scale Method for Solving Stiff ODEs with Detailed Kinetic Mechanisms and Multi Scale Physical Chemical Processes," 47th AIAA Aerospace Sciences Meeting and Exhibit, Orlando, Florida, January 2009, Paper No. 2008-1369.

5. M.P. Burke, M. Chaos, F.L. Dryer, and Y. Ju, "The Dependence of Mass Burning Rates of $H_2/CO/CO_2$ Flames on Pressure and Flame Temperature," 6th U.S. Combustion Meeting, Ann Arbor, Michigan, May 2009.

6. M. Chaos, M.P. Burke, Y. Ju, and F.L. Dryer, "Syngas Chemical Kinetics and Reaction Mechanisms," Synthesis Gas Combustion: Fundamentals and Applications. Ed. T.C. Lieuwen, V. Yang, R.A. Yetter. Taylor & Francis, in press.

References

1. X. Qin and Y. Ju, *Proceedings of the Combustion Institute* 30 (2005) 233-240.

2. M.P. Burke, Z. Chen, Y. Ju, and F.L. Dryer, *Combustion and Flame* 156 (2009) 771-779.

3. J. Li, A. Kazakov, Z. Zhao, M. Chaos, F.L. Dryer, and J.J. Scire, *International Journal of Chemical Kinetics* 39 (2007) 109-136.

4. S.G. Davis, A. Joshi, H. Wang, and F.N. Egolfopoulos, *Proceedings of the Combustion Institute* 30 (2005) 1283-1292.

IV.11 Compact and Streamlined Oxy-Syngas Reheat Combustor

Shahrokh Etemad (Primary Contact), Sandeep Alavandi, Benjamin Baird, and William C. Pfefferle
Precision Combustion, Inc.
410 Sackett Point Rd.
North Haven, CT 06473
Phone: (203) 287-3700 x217; Fax: (203) 287-3710
E-mail: setemad@precision-combustion.com

DOE Project Manager: Mark Freeman
Phone: (412) 386-6094
E-mail: Mark.Freeman@netl.doe.gov

Contract Number: 85015

Start Date: June 30, 2008
End Date: March 29, 2009 (Phase I)

FY 2009 Objectives

- Design and develop injector for intermediate pressure reheat combustor for oxygen, steam and syngas streams.
- Evaluation and analysis of advanced concepts for liner cooling.
- Generate combustor design for future fabrication and testing.
- Fabricate and test subscale performance at simulated engine conditions (Phase II).

Accomplishments

- All Phase I objectives were successfully met, and one objective was exceeded. The Phase I analytical results successfully demonstrated the robustness and uniqueness of the design and validated the proof-of-concept.
- Phase I results provide a strong technology base and momentum for Phase II development of a robust and stable injector with low level of unmixedness and high combustion efficiency.
- Fast CO burnout indicating the potential for integrating this technology for oxy-fuel applications.
- Potential path for high temperature liner cooling evaluated, analyzed and identified.

Introduction

Concerns about global climate change due to CO_2 emissions from power generation (in particular coal) have led to significant interest in innovative power plant cycles [1]. Three CO_2 capture cycles currently under study are pre-combustion, post-combustion and oxy-fuel. Pre-combustion CO_2 capture is done by an upstream water-gas shift catalyst and a CO_2 absorber. In this the carbon-based fuel is converted to hydrogen for combustion. This demands a chemical plant for CO_2 removal that needs to be regenerated. Also, after CO_2 capture, there are issues of downstream H_2 combustion. Post-combustion CO_2 capture is done downstream of the plant using a scrubber removing CO_2 from the flue gases. This needs multiple components to be integrated on the downstream end, leading to efficiency penalties [2]. The third cycle is oxy-fuel combustion that removes the nitrogen component from the air and combusts the fuel (natural gas or syngas) directly with oxygen using steam as the diluent producing steam and CO_2 as the working fluid. This cycle has significant advantages compared to the other two technologies for CO_2 capture. Firstly, use of oxygen, fuel, and steam for combustion produces an exhaust stream consisting of primarily CO_2 and H_2O that makes sequestration simple through condensing the water out. This eliminates the need to use expensive CO_2 separation units. This is in contrast to conventional combustors using air as the oxidant having product gases with a high nitrogen concentration and low CO_2 concentration leading to efficiency penalties due to N_2 separation. Secondly, using pure oxygen has the binary benefit of near zero NOx emissions. Thirdly, since no emissions are generated hence no expensive exhaust stack clean-up is required, leading to further cost savings [3-6]. In summary, oxy-fuel power plants have the potential to re-define the power production industry.

Oxy-fuel combustion technology offers both the benefits of zero-emission power generation coupled with economical carbon capture and storage effectively. However, in order to boost cycle efficiency levels equal to or greater than other fossil fuel power generating cycles, the reheat combustor is a critical component that needs to be integrated. A robust reheat combustor capable of driving the working fluid temperature up to 1,760°C/3,200°F necessitates innovative injector/combustor design and advanced liner cooling techniques and material. Currently

there is no existing re-heat combustor design that can operate in the harsh steam/CO_2 environment expected in the cycle. In addition, due to high combustion temperatures, advanced liner cooling mechanism using a minimal amount of steam as a coolant is required to be implemented. Precision Combustion, Inc.'s (PCI's) unique design approach addresses and resolves these key challenges.

Approach

PCI's novel injector for oxy-syngas reheat combustion provides fast and efficient steam/O_2/syngas mixing and complete CO burnout using its distinctive mixing and flame zone design. This system can effectively mix the fluid streams (the steam-rich high-pressure turbine exhaust, O_2 and syngas) in a unique design delivering ultra-low unmixedness and establishing a stable flame zone. This novel design enhances combustion, avoids excess O_2, reduces CO quenching, avoids high local primary zone temperatures, and reduces combustion acoustics. This technology offers the potential to be simple, robust and cost-effective as a reheat combustor for the high temperature working fluid of an intermediate pressure steam/CO_2 turbine thus enabling higher cycle efficiencies.

Results

The drivers are simplicity and achieving effective (steam, O_2, syngas) mixing integrated with compact combustion flame to enable a short residence time, low pressure drop reheat combustor with uniform heat release and minimized CO emissions. Phase I analytical results successfully demonstrated the proof-of-concept for the injector liner system. Computational fluid dynamics and kinetics modeling showed low unmixedness and complete CO burnout was achieved within a short length showing benefit of the novel PCI injector design. The Phase I analytical work demonstrated the proof-of-concept for the injector capable of providing:

(a) Rapid mixing with <5% unmixedness in 1-2 ms.

(b) Reacting flow analysis verifying well stabilized combustion with syngas and high level of steam.

(c) Achieving equilibrium CO levels within three inches from the exit plane of the injector.

With rapid mixing and compact flames, reduced combustor liner length and lower cooling flow are also required for gas turbine engines application.

Conclusions and Future Directions

In Phase II, PCI will expand on the success of Phase I work by demonstrating the performance of the novel injector liner system in subscale testing. A subscale module will be fabricated and tested to demonstrate stable combustion and low emission performance. At the conclusion of Phase II, an optimized single injector module will be fabricated for testing at a high pressure/temperature test facility at simulated engine conditions in a Phase III project. The work plan is designed to demonstrate high pressure full-scale simulated engine testing readiness by addressing the key technical challenges of aerodynamics, mechanical robustness, emissions, and reliability with stable system performance. Further effort will be directed towards:

- Finalize the design configuration for the injector and liner system.
- Fabricate subscale injector and liner system for testing.
- Testing and validating injector and liner system.
- Design and build prototype injector for DOE/engine manufacturer for high pressure testing and validation.

Special Recognitions & Awards/Patents Issued

1. One patent application has been applied.

References

1. K. Zanganeh, A. Shafeen, M. Gupta, E. Ogedengbe, and M. Mitrovic, "Gas Turbine Integrated High Efficiency Oxy-Fuel Combustion Process with CO_2 Capture," ASME GT2008-51456.

2. Jordan, Haywood, "Oxy-Fuel Combustion Cycle for CO_2 Capture," A&WMA Florida Section Annual Conference, October 2007, Deerfield Beach, Florida.

3. B. Buhre, L. Elliott, C. Sheng, R. Gupta, and T. Wall, "Oxy-Fuel Combustion Technology for Coal Fired Power Generation," Progress In Energy and Combustion Science, vol. 31, 2005, pp. 283-307.

4. R. Anderson, S. Doyle, and K. Pronske, "Demonstration and Commercialization of Zero Emission Power Plant," 29th International Technical Conference on Coal Utilization and Fuel Systems, Florida, USA.

5. R. Anderson, S. Macadam, F. Viteri, D. Dvies, J. Downs, and A. Paliszewski, "Adapting Gas Turbines for Zero Emission Oxy-Fuel Power Plants," ASME GT2008-51377.

6. J. Martinez-Frias, S. Aceves, J. Smith, and H. Brandt, "A Coal Fired Power Plant with Zero Atmospheric Emissions," 2003 ASME International Mechanical Engineering Congress and RD&D Expo, 2003, Washington, D.C.

V. UNIVERSITY TURBINE SYSTEMS RESEARCH

A. Aero-Heat Transfer

V.A.1 Deposition of Alternative (Syngas) Fuels on Turbine Blades with Film Cooling

Thomas H. Fletcher
Brigham Young University (BYU)
260 E 1060 N
Provo, UT 84602
Phone: (801) 422-6236; Fax: (801) 422-0151
E-mail: tom_fletcher@byu.edu

DOE Project Manager: Mark Freeman
Phone: (412) 386-6094
E-mail: Mark.Freeman@netl.doe.gov

UTSR Manager of Research: Richard Wenglarz
Phone: (864) 656-2267
E-mail: RWNGLRZ@exchange.clemson.edu

Subcontractor:
Jeffrey P. Bons, Ohio State University, Columbus, OH

Contract Number: 41431/UTSR 05-01-SR120

Start Date: August 1, 2005
End Date: May 15, 2009 (including a no-cost extension)

FY 2009 Objectives

- Characterize deposition on turbine hardware from the combustion of synfuels that are or could be used in the power generation industry, including effects of fuel type, temperature, particle size, and backside and film cooling.
- Evaluate the influence of these deposits on turbine blade cooling.
- Determine the effects of these deposits on spallation of thermal barrier coatings (TBCs).

Accomplishments

During the last fiscal year experimental deposition tests were conducted with finely ground subbituminous coal flyash on film-cooled turbine components, including:

- Spacing of cylindrical film cooling holes.
- Bare metal coupons verus coupons with TBCs.
- Blowing ratios from 0 to 4.0.
- Two different flyash particle sizes (mass mean diameters of 3 and 13 µm).
- A trench configuration.

Measurements included:

- Photos of deposition patterns.
- Maps of the surface temperature of the deposit.
- Time-dependent movies of surface buildup.
- Capture efficiencies.
- Surface roughness characteristics.

Several 20x scaled models of film cooling configurations with deposits were manufactured using stereolithography and tested in a transient wind-tunnel to determine the film effectiveness and heat transfer coefficient distributions. Computational fluid dynamics modeling of the heat transfer and deposition in these experiments was completed.

Introduction

Turbine inlet temperatures for large power generation gas turbines have been steadily increasing over the last several decades due to significant advances in materials and cooling technologies. By incorporating these critical advancements, the H-class combined cycle machines are expected to operate at up to 1,425°C. While this higher combustor exit temperature translates directly to higher cycle efficiency, it does not bode well for the severe operating environment of turbine materials. At the same time, political and economic pressures are pushing utilities to consider fuel flexibility. Intermediate goals of the DOE FutureGen and DOE Turbine Program focus on coal syngas as a turbine fuel in an effort to reduce dependency on foreign supplies of natural gas. Petroleum coke and biomass fuels are also being considered. Compared to “clean” burning natural gas, these alternative fuels have higher concentrations of trace elements and ash that present significant corrosion challenges to turbine operation.

Although filters are installed in gas turbine systems to remove flyash from synfuels, small concentrations of fine particles pass through the filters and reach the turbine surfaces, even if the filters are well maintained. Deposits build up over a year or two of operation and cause operational problems. This project is a study of synfuel flyash deposition on representative film cooled turbine blade surfaces that include thermal barrier coatings, with the goal of determining the magnitude of deposition, erosion, and corrosion for the application of alternative fuels in modern gas turbines.

Approach

A turbine accelerated deposition facility (TADF) was originally built in 2004 (Figure 1), consisting of a partially premixed natural gas fired combustor capable of operating at an exit Mach number of 0.3 and an exit temperature of 1,183°C, thus simulating the conditions at the entrance of a typical first stage nozzle guide vane for an F-class power generation turbine. Coupons are obtained from turbine blade manufacturers that include the TBC. These coupons are placed at the exit of the combustor, and flyash particles are fed through the combustor to cause deposition on the coupon. Tests at atmospheric pressure have shown that deposits formed in 4 hours in the TADF are similar to deposits generated in 8,000 hours of turbine operation [1].

Deposits formed in the TADF are photographed in situ, and then the coupon is removed for further analysis. Surface roughness characteristics are analyzed using a profilometer. An optical scanner is used to produce surface maps suitable for scaled model fabrication. Environmental scanning electron microscopy (ESEM) analysis is used to take photos of the surface and perform X-ray elemental analysis. Coupons are then encased in epoxy, sliced in half, and the cross section is analyzed by ESEM.

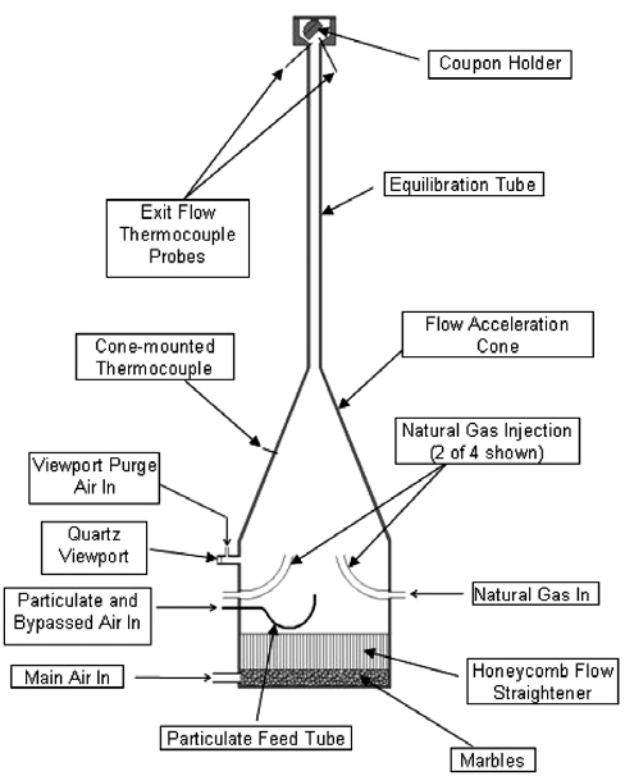

FIGURE 1. Schematic of the BYU Turbine Accelerated Deposition Facility (TADF)

Results

The results shown here are from subbituminous coal flyash particles with a mass mean diameter of 13 μm. Figure 2 shows post-test images of the bare metal test coupon at different blowing ratios with cylindrical holes for two different hole spacings. At low blowing ratios, the film cooling holes are completely covered at the conclusion of the tests. At blowing ratios of 1.0, the cooling holes are still visible, but significant deposits are formed downstream of the film cooling holes. At blowing ratios of 2.0, little deposition has occurred. There was little difference in the deposition characteristics between the hole spacing of 3.4d and 4.5d.

The reason for the non-linear dependence of deposition on blowing ratio seems to be surface temperature. Figure 3 shows surface temperature maps taken during the experiments corresponding to Figure 2. Temperatures were measured using a 2-color technique from the RGB ports of a standard camera. As the blowing ratio was increased in these tests, significantly more coolant flow rate was used. All of the coolant flowed through the holes, but provided significant backside impingement cooling before flowing through the cooling holes. As seen in Figure 3, the surface temperature downstream of the cooling holes (flow is up in these figures) is lower than upstream of the cooling holes. Also, it can be seen that the overall surface temperature decreases as blowing ratio increases.

The particle capture efficiency is defined as the percentage of particles in the flow stream that deposited on the surface. Figure 4 shows a comparison of the capture efficiencies for a bare metal coupon versus the capture efficiencies for a TBC coupon, measured at different blowing ratios. The surface temperatures were higher for experiments with TBC coupons than for the bare metal coupon, due to the insulating effect of the TBC. This increased the capture efficiency for the TBC coupon, depending on the blowing ratio.

Additional experiments in the TADF were completed to examine the effects of particle size on deposition with film cooling holes. At low blowing ratios, deposition was significantly lower when 4 μm particles were used instead of 13 μm particles. However, deposition was actually slightly higher with the smaller particles at higher blowing ratios, depending on the hole spacing. A series of deposition tests was also conducted with a trench configuration, with the intention of providing better cooling effectiveness. However, deposition occurred in the trench, mitigating the enhanced cooling effects.

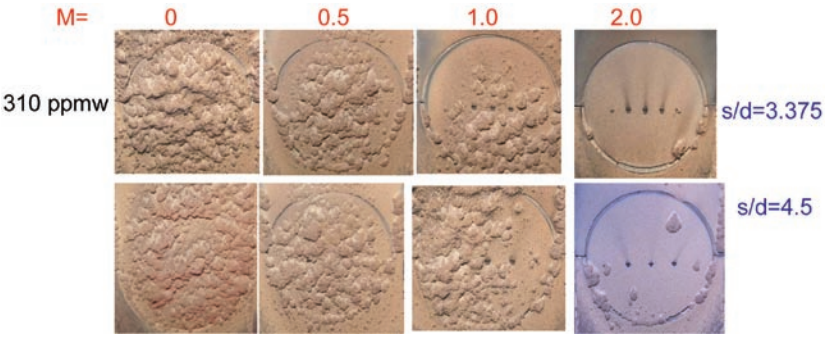

FIGURE 2. Deposits Formed on Bare Metal Coupons for Different Blowing Ratios

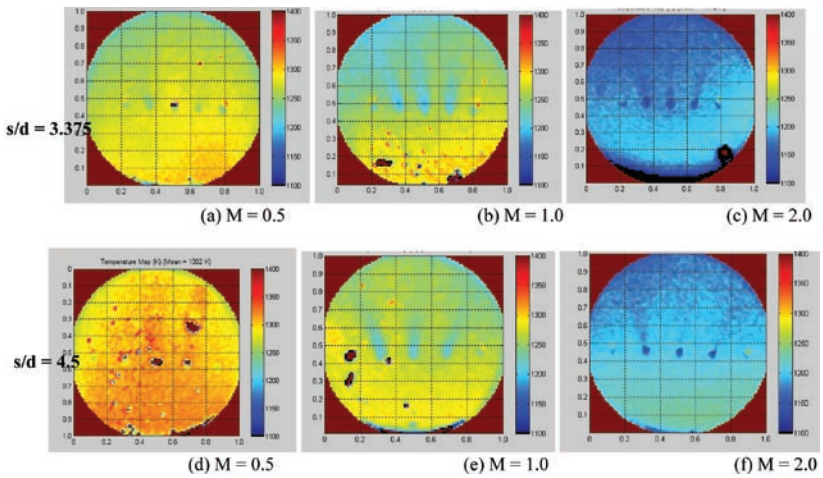

FIGURE 3. Surface temperature maps of metal coupons during deposition for different blowing ratios and hole spacings. Color bar indicates surface temperature in Kelvin. Flow is upward in these figures (three holes blowing).

Scale models (20x) of selected deposits from the TADF experiments were made by sterolithography and used in wind tunnel tests to determine changes in cooling effectiveness and heat transfer coefficients due to the deposits. Figure 5 contains film effectiveness (η) contour maps for smooth and deposit panels at M=1. Perhaps the most obvious alteration is that the s/d=3 deposit panel has higher η levels than any of the other panels (including smooth).

Computational modeling of the deposition process was performed using a Young's modulus approach for the stickiness of particles. A series of adiabatic tests was performed to determine the collection efficiency versus temperature in the TADF, and a temperature-dependent correlation was developed using two-dimensional Fluent calculations. A user-defined function was developed for Fluent to account for adhesion and removal of particles as a function of temperature and particle size. Predictions of collection efficiencies versus blowing ratio for film cooling tests in the TADF compared well with measured data.

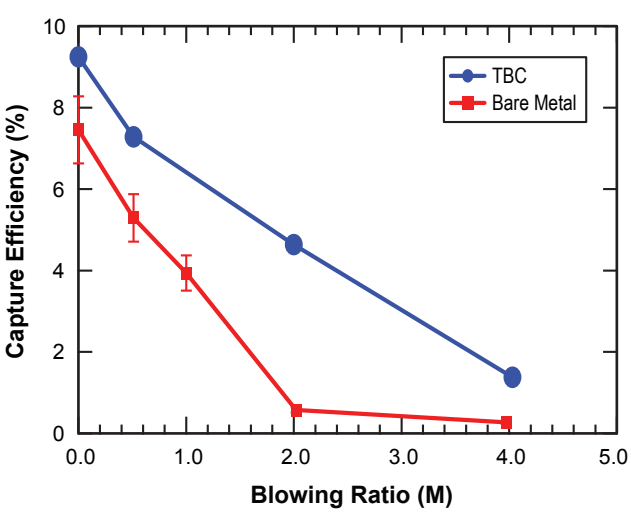

FIGURE 4. Particulate Capture Efficiency vs. Coolant Mass Flow for 13 μm Diameter Coal Particulate (Three Holes, s/d=4.5)

Conclusions and Future Directions

A series of tests were performed in an accelerated deposition test facility to evaluate the influence of film cooling flows on deposit formation from subbituminous coal flyash. Some of the major conclusions from this year are:

- Higher blowing ratios showed less deposition but more nonuniform deposits, with ridges between the coolant flow paths.
- Coupons with TBC showed increased capture efficiencies due to the increased surface temperature of the coupon.
- Deposition was nonlinear in time, so that the deposition rate accelerated once a deposit formed due to increased surface temperature.
- Small particles (4 μm diameter) showed lower capture efficiencies at low blowing ratios in film cooling experiments than larger particles (13 μm diameter), but slightly higher capture efficiencies at higher blowing ratios (M=2).

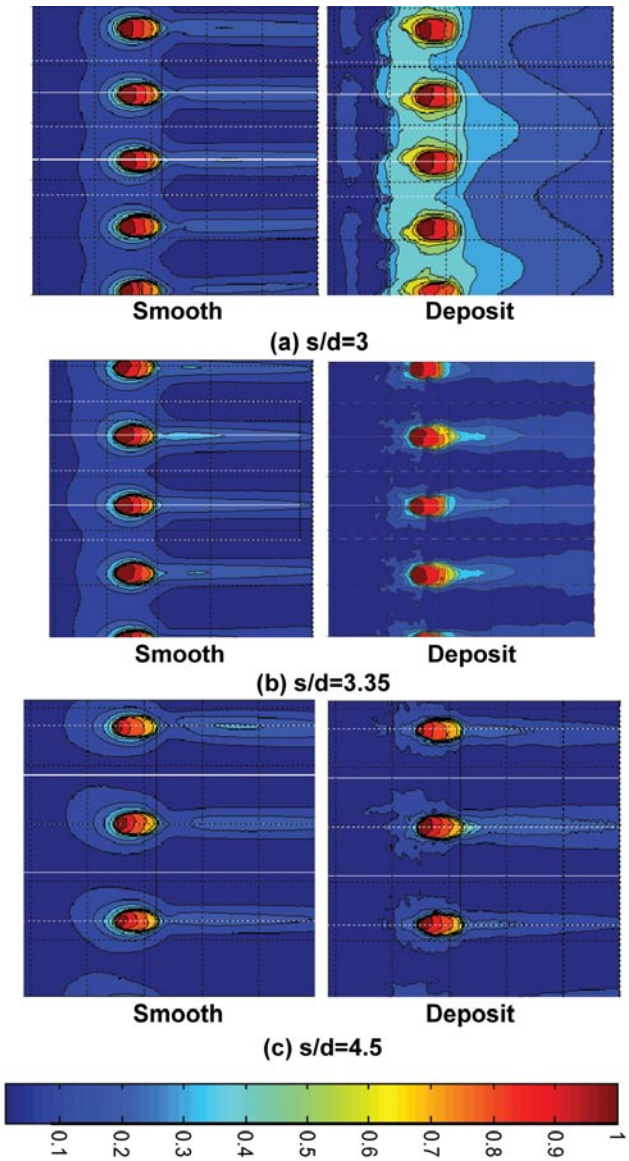

FIGURE 5. Film Effectiveness Contour Maps for Smooth and Deposit Panels at M=1 (flow is left to right)

- Deposition experiments with a trench configuration showed that although the initial cooling effectiveness was enhanced with the trench, particles acculumated in the trench and negated the initial enhanced cooling.
- Scale models (20x) of deposits obtained in film cooling experiments were used to determine cooling effectiveness factors and heat transfer coefficients, and were compared to the smooth base case to illustrate the impact of the deposits.
- A deposition model developed using a temperature-dependent Young's modulus was developed using Fluent, and predictions compared well with capture efficiencies measured as a function of blowing ratio in film cooling experiments.

FY 2009 Publications/Presentations

1. W. Ai and T.H. Fletcher, "Computational Analysis of Conjugate Heat Transfer and Particulate Deposition on a High Pressure Turbine Vane," Paper GT2009-59573, accepted, ASME Turbo Expo, Orlando, Florida (June, 2009).

2. W. Ai, R.G. Laycock, D.S. Rappleye, T.H. Fletcher, and J.P. Bons, "Effect of Particle Size and Trench Configuration on Deposition from Fine Coal Flyash Near Film Cooling Holes," Paper GT2009-59571, accepted, ASME Turbo Expo, Orlando, Florida (June, 2009).

3. W. Ai, N. Murray, T.H. Fletcher, S. Harding, and J.P. Bons, "Effect of Hole Spacing on Deposition of Fine Coal Flyash Near Film Cooling Holes," Paper GT2009-59569, accepted, ASME Turbo Expo, Orlando, Florida (June, 2009).

4. S. Lewis, B. Barker, J. Bons, W. Ai, and T. Fletcher, "Film Cooling Effectiveness and Heat Transfer Near Deposit-Laden Film Holes," Paper GT2009-59567, accepted, Turbo Expo, Orlando, Florida (June, 2009).

References

1. J.W. Jensen, S.W. Squire, J.P. Bons, and T.H. Fletcher, "Simulated Land-Based Turbine Deposits Generated in an Accelerated Deposition Facility," *ASME Journal of Turbomachinery*, Vol. 127, pp. 462-470, July 2005.

V.A.2 Designing Turbine Endwalls for Deposition Resistance with 1,400°C Combustor Exit Temperatures and Syngas Water Vapor Levels

Jeffrey P. Bons (Primary Contact), Ali Ameri
Department of Aerospace Engineering
Ohio State University (OSU)
2300 West Case Rd.
Columbus, OH 43235
Phone: (614) 247-8414
E-mail: bons.2@osu.edu

DOE Project Manager: Mark Freeman
Phone: (412) 386-6094
E-mail: Mark.Freeman@netl.doe.gov

Subcontractor:
Thomas H. Fletcher
Brigham Young University (BYU), Provo, UT

Contract Number: NT0005055

Start Date: October 1, 2008
End Date: September 30, 2011

FY 2009 Objectives

- Select computational framework for deposition modeling initiative.
- Develop and validate particle deposition model.
- Modify BYU's Turbine Accelerated Deposition Facility (TADF) to accommodate 1,400°C gas temperatures.
- Complete OSU's Turbine Reacting Flow Rig (TuRFR) assembly and check-out.
- Conduct hot cascade tests with deposition in OSU's TuRFR facility.

Accomplishments

- Fluent was selected as the computational fluid dynamics (CFD) test bed for deposition studies.
- A particle deposition model was developed incorporating multi-phase particle physics, a deposition capture model, and a deposition removal model. These particle models were incorporated into the Fluent code using user defined functions (UDFs). Model results have been validated using comparisons to experimental deposition data from BYU's TADF facility.
- The acceleration cone and equilibration tube for the TADF were redesigned using silicon carbide – a higher temperature material than the previous Inconel construction. These articles have been received from the manufacturer and tested up to the design flow rates and temperatures. The coupon holder has also been redesigned for higher temperatures.
- The fabrication and initial performance testing of the lower stage of the OSU TuRFR were completed. Stable combustion has been validated with mean exit temperatures of up to 1,150°C at the design mass flow rate.
- The upper section for the TuRFR has been designed and constructed as well. The nozzle guide vane containment section was designed to accommodate two nozzle guide vane (NGV) doublets donated from General Electric (GE). Discussions are underway for additional hardware commitments from Pratt-Whitney, Siemens, and Solar Turbines. The upper section and lower section have been mated and testing is underway.
- The film cooling flow preheater has been selected and installed in the TuRFR facility. This will provide the capability to cool the NGV at representative compressor discharge gas temperatures with up to 5% of the passage throughflow.
- The decision was made to design and build an original particle feeder for the OSU TuRFR. Necessary parts have been ordered and construction has been completed.
- Industrial power generation sources for process ash have been identified. Available ash compounds include: petcoke/coal fuel blends, pure bituminous coal, sub-bituminous coal, and lignite coals among others.

Introduction

Turbine inlet temperatures for large power generation gas turbines have been steadily increasing over the last several decades due to significant advances in materials and cooling technologies. At the same time, political and economic pressures are pushing utilities to consider fuel flexibility using synfuels that have higher concentrations of trace elements and ash compared to "clean" burning natural gas. Current plans to transition from current syngas to high hydrogen fuels produced from coal syngas and oxy-fuels will only exacerbate these challenges with high water vapor levels. The combination of increased engine operating temperatures and synfuel integration

warrant a re-evaluation of current hot gas path design to consider the potential impact of deposition. In the first stage high pressure turbine vane (nozzle), the majority of material system failures occur at the junction of the vane and the passage endwall. Secondary flows in this region create unique challenges for thermal management and efficient cooling design. Recent initiatives of passage endwall contouring and vane leading edge modifications have been developed for use with natural gas fired turbines and thus their compatibility with ash-bearing and/or high steam content synfuels at elevated operating temperatures has yet to be assessed. Clearly, there is a critical need to explore innovative endwall designs that could both increase turbine durability and mitigate the adverse effects of deposition in the endwall.

Approach

This research effort addresses this critical turbine operability and maintainability issue in three distinct phases.

- Phase 1 - Modeling and Experimental Validation: A deposition model will be developed and incorporated in an existing CFD code capable of handling modern turbine geometries. Validation of this new model will be performed using both the OSU and BYU accelerated deposition facilities. The BYU TADF facility will be modified to accommodate higher firing temperatures (up to H-class engine temperatures 1,400°C) and the addition of water vapor. The OSU facility will be used to investigate deposition patterns around real film-cooled turbine hardware at engine relevant conditions. Hardware will be donated from GE, Siemens, and Pratt through collaborative agreements.
- Phase 2 - CFD and Experimental Endwall Design Study: Various endwall design modifications will be evaluated, both experimentally and computationally, to determine their influence on deposition. The objective will be to evaluate each of the design modifications for deposition resistance as well as aerodynamic and heat transfer performance. BYU will perform gas temperature and fuel type test series to determine high temperature extension of deposition data.
- Phase 3 – CFD Design Study with Cooling and Experiments with Water Vapor: BYU will explore the effect of water vapor on turbine deposition. Experiments will be conducted with various thermal barrier coating material systems with water vapor levels up to 15% to simulate levels anticipated with high hydrogen combustion. The effect of film cooling on deposition will also be studied, both at BYU and OSU. Deposition models will be used to determine optimum film flow location to mitigate endwall deposition and improve material system survivability.

Thus, with this aggressive research project, DOE and industry will gain valuable insights into factors affecting the safe, efficient operation of modern industrial turbines with alternative fuels as well as new, innovative endwall designs that are tailored for this more adverse operating environment.

Results

Experimental Facility at BYU

Figure 1 indicates the portions of the TADF that had to be redesigned for high temperature (1,400°C) operation. The original equilibration tube and acceleration cone on the TADF were constructed of alloy 601. The melting range of Inconel 601 is 1,360°C-1,411°C and the current setup has already been known to fail periodically with an operating temperature of 1.183°C, thus necessitating that the cone and tube be replaced. For the current effort, these items must be constructed of a material that can handle higher operating temperatures. Materials that were investigated were fused quartz, alumina, and silicon carbide. Of the three choices, silicon carbide was chosen because it has a greater resistance to thermal shock, thus allowing the combustor to be safely heated up and cooled down at a faster rate without failing.

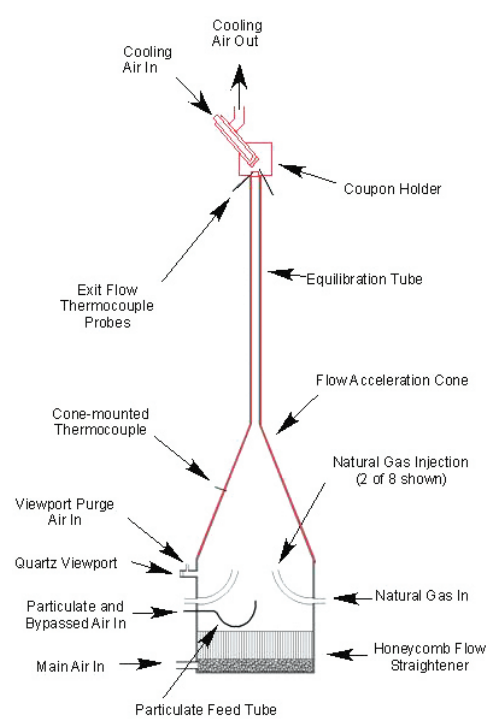

FIGURE 1. TADF at BYU. The red area indicates the portion that must be redesigned for high temperature.

The new cone and tube shell were ordered in January 2009 and finally arrived at BYU in March 2009 (Figure 2). The cone and tube appear to be intact. A primary concern surrounding the use of SiC was thermal shock. While SiC has a greater resistance to thermal shock than other high temperature materials (e.g. alumina), there were concerns that current heating rates after startup and the possible cooling rate in the case of an emergency shutdown would be too great, causing the SiC shell to crack. The manufacturer assured us that there would be no problem with heating the SiC, but that care would have to be taken in the case of cooling. For insurance, a sample of the reaction bonded SiC used for the new shell was obtained and put through a series of tests investigating the possibility of cracking during startup and shutdown. Testing has been successful with the SiC tube sample and now the actual SiC parts have been installed and tested at temperature. This successful result insures that the elevated temperature testing portion of the effort is ready to begin.

Experimental Facility at OSU

The new TuRFR at OSU is modeled after the TADF at BYU, with a natural gas burning combustor and metered particulate injection. The combustor exit flow for the TuRFR must navigate the nozzle hardware before exhausting to ambient. Thus, the combustor will operate at a higher pressure than ambient (approximately 2 atm). The BYU test configuration suspends the target coupon in the hot gas flow. Due to elevated pressures and flowpath constraints, this design was not appropriate for the TuRFR. Instead, the nozzle vanes and associated hardware must form a continuous flowpath from the combustor exit through the nozzle hardware. Because the weight of this exhaust section would pose extreme compressive stresses on the combustor design, the TuRFR employs separate upper and lower sections to complete the gas flowpath. The combined design is displayed in Figure 3. Cold airflow enters from the base and passes through flow straighteners before mixing with the premixed methane gas flow. The reacting flow is controlled through an array of 32 individual flame holders. The hot gas is then accelerated in the conical section to an exit velocity of 150-200 m/s. The lower section was operational before the start of this research effort. A maximum mass flow of 3.5 lbm/sec and gas exit temperatures up to 2,200°F have been confirmed. The order for the upper section was placed in December 2008, but fabrication delays resulted in a delivery date of June 2009. Figure 4 shows the completed assembly of both the lower and upper test sections. With the facility now assembled and operational, deposition testing will ensue in the coming months to complete the Phase 1 project goals.

The film cooling flow preheater has been selected and installed in the TuRFR facility. This will provide the capability to cool the NGV at representative compressor discharge gas temperatures with up to 5% of the passage throughflow. Also, the decision was made to design and build an original particle feeder for the OSU TuRFR. Necessary parts have

FIGURE 2. Silicon Carbide Cone and Tube Shell for BYU TADF

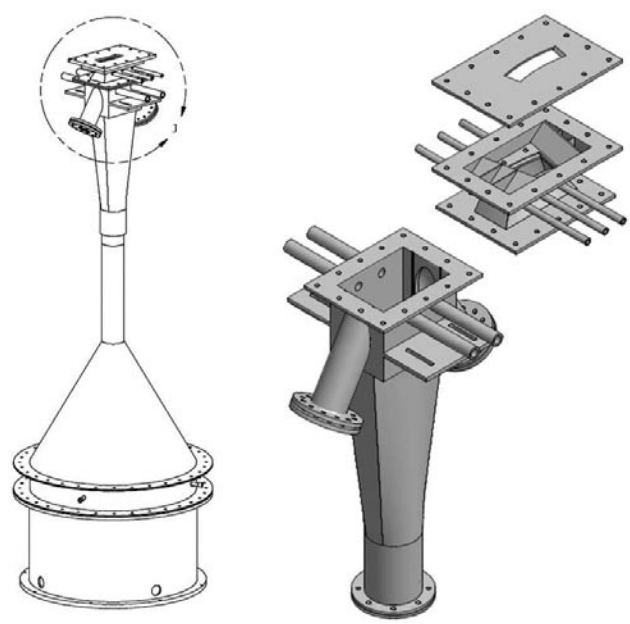

FIGURE 3. Technical Drawing for OSU TuRFR: (a) Showing Upper and Lower Sections (b) Showing Close-Up of Upper Section Only

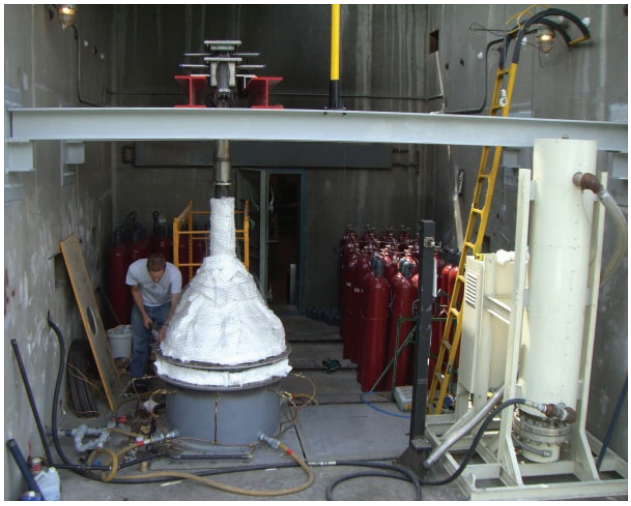

FIGURE 4. Digital Image of OSU TuRFR Showing Upper and Lower Sections Assembled

been ordered and construction has been completed. Finally, industrial power generation sources for process ash have been identified. Available ash compounds include: petcoke/coal fuel blends, pure bituminous coal, sub-bituminous coal, and lignite coals among others.

Computational Methods at OSU

An initial literature survey covering research efforts centered on alternative (syngas) fuels deposition on turbine blades with film cooling was completed. After consulting the literature a methodology for particle tracking and deposition was selected where an Eulerian-Lagrangian approach is to be followed: the Eulerian approach for the continuous phase and the Lagrangian approach for the discrete phase. After considering various options, it was decided that the particle-tracking and deposition models would be developed and implemented with the use of a commercial CFD code, Fluent. Work has been underway to build and validate the deposition model in Fluent using UDF as explained before. Computational results from Ai and Fletcher [1] were used as the comparison parameter for validating the UDF. Ai and Fletcher used a 2-dimensional model in Fluent to calculate the deposition statistics and these have been replicated with the same conditions in a 3-dimensional model. A UDF has been built for the deposition model and incorporated into the Fluent software and initial results look promising.

Conclusions and Future Directions

In summary, the project is off to a great start with healthy progress during the first three quarters. The redesign of the BYU facility is underway with the new high temperature cone delivered at the end of the second quarter. The fabrication and initial performance testing of the lower stage of the OSU TuRFR has been completed and the upper section has been delivered and assembled. Combustion stability at design mass flow has been verified and the film cooling air line and heater have been installed. Hardware and particulate donations are all on schedule. The particle feeder for the OSU TuRFR has also been completed. Finally, significant progress has been made with the computational model development. The commercial CFD code, Fluent, has been exercised and the required UDFs for particle deposition have been developed. Preliminary comparisons with previous studies at BYU appear to be promising. Deposition testing with the BYU and OSU facilities can now begin in earnest. The deposition models will be used to guide the endwall redesign work planned for Phase 2 of the project

FY 2009 Publications/Presentations

1. Presentation of the OSU TuRFR facility construction was made at the Dayton-Cincinnati Area AIAA Section Conference in March 2009.

References

1. W. Ai, T. Fletcher, "Computational Analysis of Conjugate Heat Transfer and Particulate Deposition on a High Pressure Turbine Vane," IGTI, 2009, Florida, United States, GT2009-59573.

V.A.3 Effects of Coating Blockage and Deposits on Film Cooling Effectiveness and Heat Transfer

Minking K. Chyu
Department of Mechanical Engineering
and Materials Science
University of Pittsburgh
Pittsburgh, PA 15261
Phone: (412) 624-9784
E-mail: mkchyu@pitt.edu

Tom I-P. Shih
Department of Aerospace Engineering
Iowa State University
2271 Howe Hall, Room 1200
Ames, IA 50011-2271
Phone: (515) 294-6241
E-mail: tomshih@iastate.edu

DOE Project Manager: Mark Freeman
Phone: (412) 386-6094
E-mail: Mark.Freeman@netl.doe.gov

UTSR Manager of Research: Richard Wenglarz
Phone: (864) 656-2267
E-mail: RWNGLRZ@exchange.clemson.edu

Contract Number: 41431/UTSR 04-01-SR115

Start Date: August 1, 2007
End Date: July 31, 2008

FY 2009 Objectives

- Explore the transport phenomena related to the effects of blockage and surface deposits around film cooling holes in advanced gas turbines.
- Develop advanced concepts incorporating modifications in hole shape and surface profile for more effective film cooling.
- Quantify new film cooling concepts with a combined approach of detailed experimental measurements and computational simulations.
- Provide the turbine manufacturers with fundamental insight that can impact the future designs of turbine cooling systems.

Accomplishments

- Characterized the film cooling performance involving upstream ramp using an infrared (IR) imaging technique.
- Acquired detailed surface thermal data with film cooling for computational fluid dynamics (CFD) validation and benchmarking.
- Obtained optimal operating conditions in terms of coolant blowing ratios and freestream conditions for upstream ramp film cooling designs.

Introduction

The primary goal of this University Turbine Systems Research project is to provide the turbine industry with fundamental insight that can impact the future design of film cooling. The initial phase of the project is to characterize the effects of blockage and surface deposits on the film cooling performance. This will be followed by a systematic approach to explore innovative means to further improve the film cooling performance under realistic turbine conditions. Validation of computational models will use the heat transfer and flow data obtained from the experimental aspect of the project. On the other hand, information gained from the computation will provide the experiment with more detailed insight in data interpretation. A significant portion of the project is to incorporate the change in surface profile, due possibly to unavoidable deposits or intentional modification of thermal barrier coatings for more effective cooling film protection. Several innovative concepts have been developed and fully characterized in this project. This will eventually aid the selection of optimal test geometry and parameters.

Approach

This is a combined effort of experiment and numerical computation for studying the transport phenomena associated with the effects of surface profiles and hole shapes on the performance of film cooling. The research team consists of participants from two universities: University of Pittsburgh (Pitt) and Iowa State University (ISU). The Pitt portion of the combined project is an experimental investigation of the film cooling performance affected by surface features and hole geometry. The specific tasks conducted at Pitt include detailed measurements of surface heat transfer coefficient and film effectiveness. The research focus at ISU is to perform CFD simulation of transport phenomena and providing guidelines for improved designs in film cooling. Validation of computational models use the heat transfer and flow data obtained from the experimental aspect of the project. On the other hand, information gained from the computation provides the experiment

with more detailed insight in data interpretation. This experiment-simulation combined approach has been demonstrated to be very effective for exploring complex aerothermal issues in advanced turbine systems.

Results

A discrete film cooling hole is typically cylindrical or diffusion fan-shaped with a 30°-35° inclination relative to the protected surface along the streamwise direction. Full coverage thermal protection is possible, if the coolant flow stays attached to the protected surface and never penetrates and then dissipates into the hot mainstream. However, such an ideal film cooling performance never occurs. The so-called "kidney vortices", which originate from the flow inside the film cooling hole, always tend to lift the coolant flow off the protected surface. As a result, the coolant flow penetrates and dissipates quickly into the main flow stream, and degraded protection is inevitable. To directly address this issue, there have been studies via either altering the vortices structure or varying the geometry of the film cooling hole or both combined.

In the earlier phase of this project, one of the main efforts of this project is to characterize the film cooling performance of three innovative concepts involving: (1) downstream block aligner, (2) upstream ramp, and (3) transverse trench. Recently, Na and Shih proposed placing a ramp with a backward step upstream of the film cooling holes to modify the approaching boundary layer flow and its interaction with the film cooling flow. Their computational study shows promising results in improved film effectiveness. In this report, the upstream ramp concept is further explored. The purpose is to experimentally examine the efficacy of the concept and possibly the mechanism associated with it. To facilitate the study, the local film cooling effectiveness (η) and heat transfer coefficient (h) are measured simultaneously using an IR imaging technique. The test matrix includes three upstream ramp angles at five different blowing ratios. For each case, the reduced heat flux relative to its corresponding baseline value, i.e. the heat flux without coolant protection, is also determined to assess the overall film cooling performance.

Figure 1 shows the schematic of the test model. The film cooling hole is circular and inclined along the streamwise direction at 30° relative to the tangent surface. The diameter of the injection hole (D) is 6.4 mm (0.25"), and the length to diameter ratio is 10. While this 10-diameter length is significantly longer than that in modern day turbines, this permits a study focused exclusively on the effect of an upstream ramp without much influence from the coolant-inlet condition. Three holes with 3D of pitch form a single row. The upstream ramp with 2D of length is placed

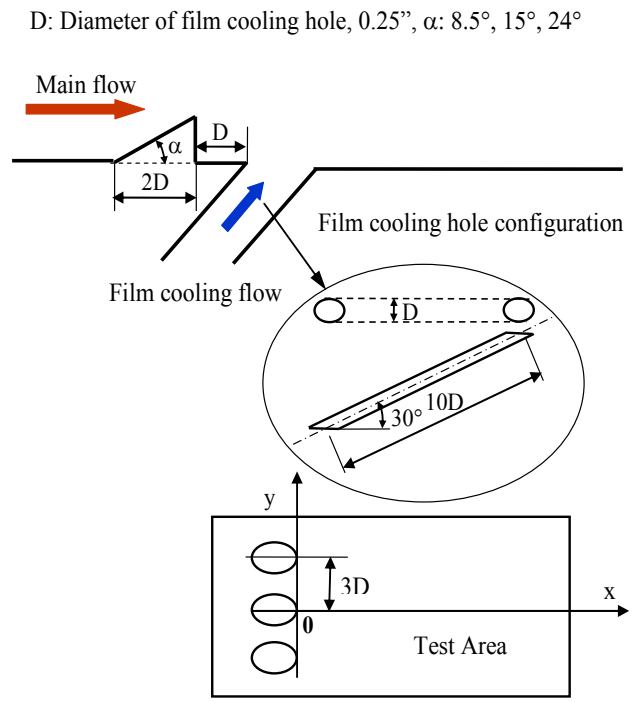

FIGURE 1. Schematic of the Test Model

at a distance D away from the upstream edge of the film cooling holes. Three different angle (8.5°, 15°, and 24°) ramps are studied. The height of the backwards step, determined by the length and angle of the ramp, is different among the three cases.

Film Effectiveness, η

Figure 2 shows the effects of blowing ratio on the spanwise averaged distribution of η. The most distinct feature shown is that a ramp can be effective in producing higher film effectiveness only when the magnitude of blowing ratio is sufficiently high, say $M > 1$. This finding is particularly evident for the case $M = 1.4$, as displayed in Figure 2e, where the ramp is at the steepest angle, 24°. The value of η in this case is about 50% higher than its baseline without a ramp. On the other hand, the presence of a ramp consistently results in an η lower than the value without a ramp when the blowing ratio is low, e.g. $M < 0.6$, (a) to (c) of Figure 2. For the cases with low blowing ratios, say $M = 0.3$, 0.4 and 0.6, the injected coolant which lacks sufficient momentum is overwhelmed by the recirculating flow immediately after it exits the hole. As a result, the film effectiveness is low. In contrast, when the blowing ratio is sufficiently high, e.g., $M = 1.4$, the injectant has higher momentum and is capable of penetrating out of the recirculation zone, making the ramp become useful for enhancing the film effectiveness. The highly turbulent shear layer atop the recirculation zone acts as a cross-flow preventing the

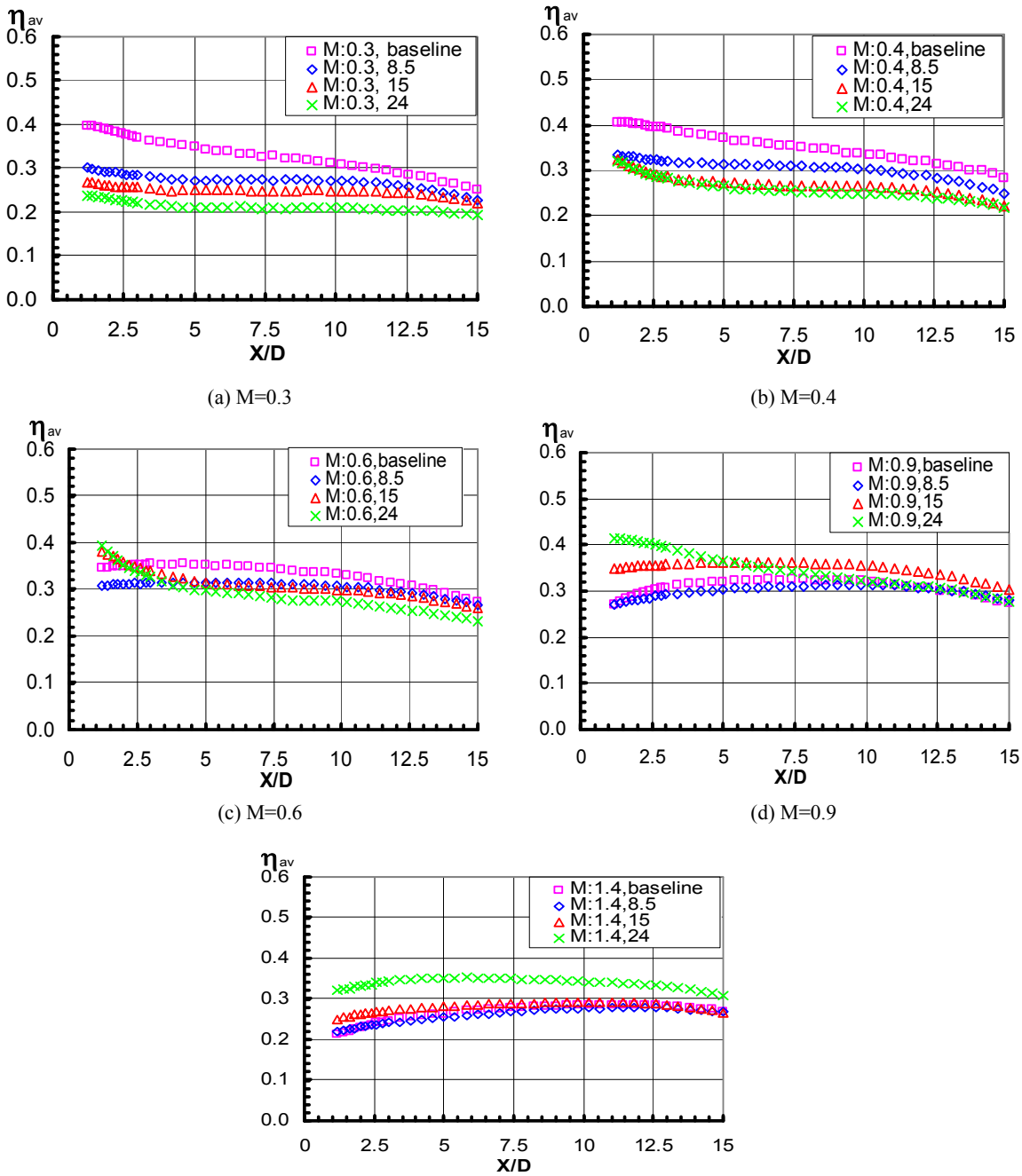

FIGURE 2. Spanwise Averaged Film Cooling Effectiveness for Different Ramp Angles at Various Blowing Ratios

coolant from lift-off, leading to a better film protection in the region. Under this condition, a taller ramp typically strengthens the levels of momentum and turbulence associated with the separated shear layer, which would favor the coolant retention in the region.

Heat Transfer Coefficient

Figure 3 exhibits the measured averaged heat transfer coefficient (h) across the span. The data presented here is the ratio h/h_o, where h_o is the heat transfer coefficient measured over the test plate without coolant injection. As the heat transfer coefficient is by in large a direct measure of the local, near-wall

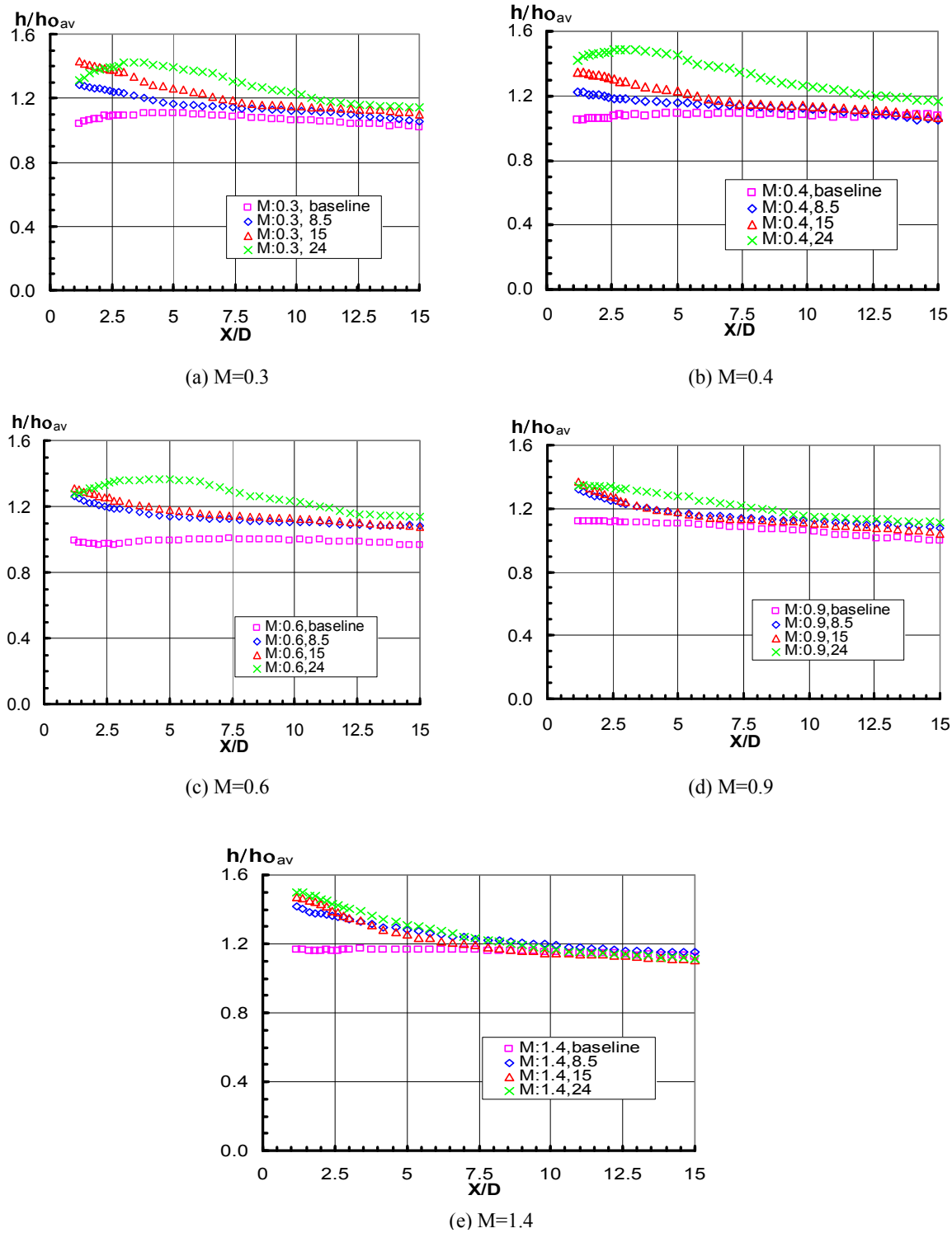

FIGURE 3. Spanwise Averaged Heat Transfer Coefficient for Different Ramp Angles at Various Blowing Ratios

turbulence level, the observation aforementioned overall implies the dominance of ramp-induced flow separation in the regime of low blowing ratios. A higher ramp results in a more turbulent separation, hence a higher heat transfer coefficient. On the other hand, when the blowing ratio is high, the near-wall turbulence, as well as the local heat transfer coefficient, is dominated by the injectant and its interaction with the boundary layer close to the wall. Accordingly, the influence by the ramp presence and its geometry becomes insignificant.

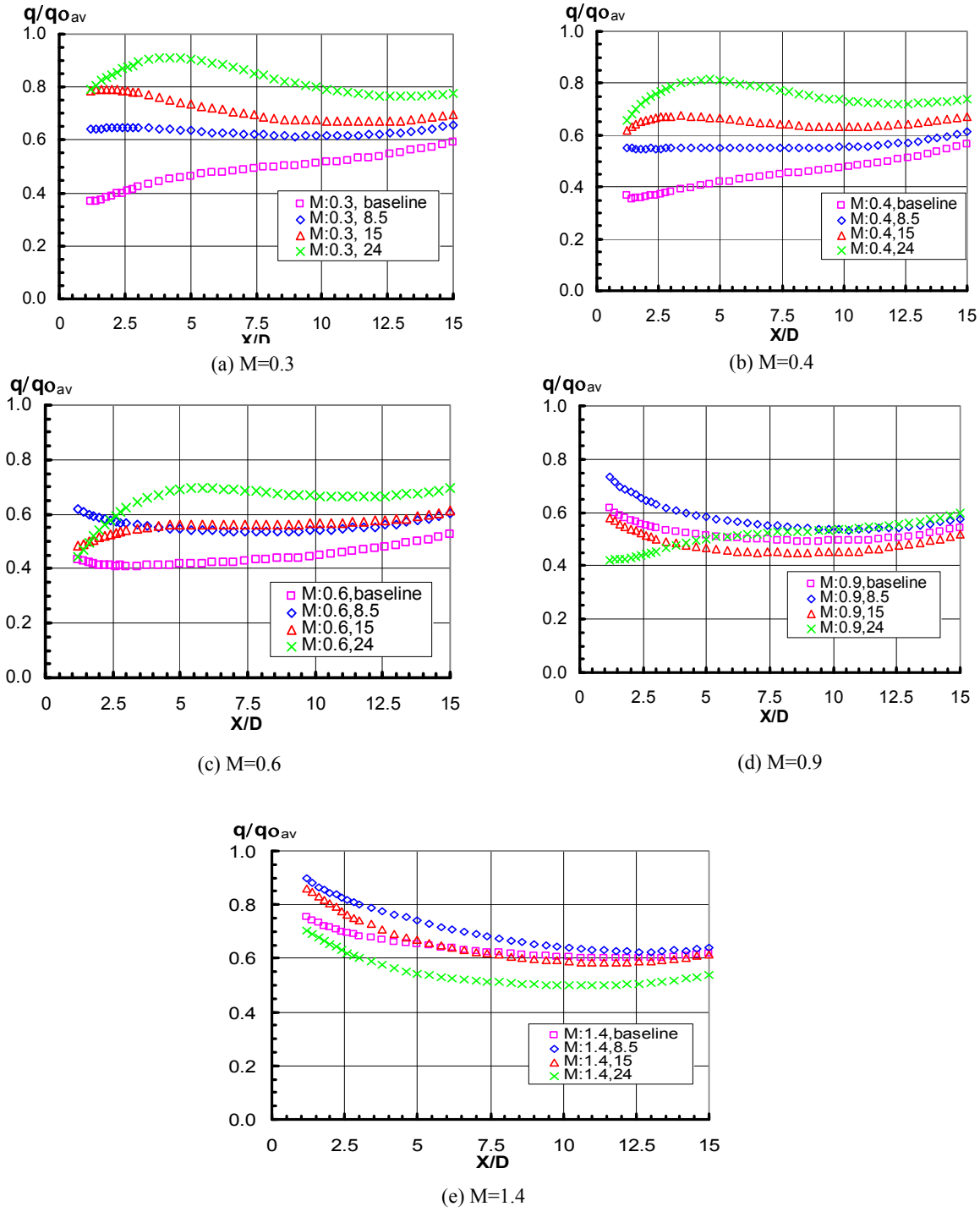

FIGURE 4. Spanwise Averaged Heat Flux Reduction for Different Ramp Angles at Various Blowing Ratios

Reduced Heat Flux

Figure 4 shows the averaged streamwise distribution of q/q_o across the span, respectively. The ramp renders no improvement in overall heat reduction relative to the baseline case without a ramp until the blowing ratio reaches 0.9. According to the data presented earlier, this is fully expected as a ramp present with low blowing ratio leads to higher η and lower η, both of which adversely affect the reduction of heat transfer. However, the trend reverses as the blowing ratio increases. The value of q/q_o improves nearly 20% at the blowing ratio M = 1.4 with a ramp of 24° inclination.

Conclusions and Future Directions

The present study experimentally evaluates the efficacy of the concept of using an upstream ramp to enhance film cooling performance. Three ramp angles, 8.5°, 15°, and 24°, with five blowing ratios ranging from 0.3 to 1.4 are tested. Local film cooling effectiveness and heat transfer coefficient distribution are measured using an IR imaging technique. In general, the presence of a ramp will mildly increase the heat transfer coefficient, due mainly to additional turbulence generated in the system, which, in turn, is detrimental to the overall reduction in surface heat transfer. Therefore, to establish a favorable cooling design with a ramp, the system needs to be operated in a regime that the momentum of injected coolant is sufficiently strong to penetrate out of the recirculation zone, but not overly strong, which can result in the separated shear layer atop the recirculation zone having excessive lift off or coolant detachment.

Special Recognitions & Awards/Patents Issued

Patent Pending

1. Preventing Hot-Gas Ingestion by Film-Cooling Jets Via Flow-Aligned Blockers (Application No.: 60/829,734).

2. Momentum Preserving Film-Cooling Shaped Holes (Application No.: 60/829,712).

3. Increasing Adiabatic Film-Cooling Effectiveness by Using an Upstream Ramp (Application No.: 60/829,737).

FY 2009 Publications/Presentations

1. M.K. Chyu and T.I-P. Shih, "Effects of Coating Blockage and Deposits on Film Cooling Effectiveness and Heat Transfer," DOE-UTSR Peer Review Workshop, October 28, 2008, Anderson, South Carolina.

2. D. Mazzotta, V. Karaivanov, W. Slaughter, M.K. Chyu, and M.A. Alvin, "Gas-Side Heat Transfer in Syngas, Hydrogen-Fired, and Oxy-Fuel Turbines," GT2008-51474, ASME Turbo Expo 2008, Berlin, June 9–13, 2008.

3. M.K. Chyu, "Transport Phenomena in Future Coal-Gas Based Turbine Systems," Pennsylvania State University, Department of Mechanical Engineering, February 14, 2008.

4. M.K. Chyu, "Aerothermal Challenges in Future Coal-Gsa Based Turbine Systems," NASA Propulsion and Power Systems Alliance PPSA, Columbus, August 28, 2008.

References

1. R.S. Bunker, 2002, "Film Cooling Effectiveness Due to Discrete Holes Within a Transverse Surface Slot," Paper GT-2002-30178, IGTI Turbine Expo, Amsterdam, Netherlands.

2. S. Na and T.I-P. Shih, 2006, "Increasing Adiabatic Film Cooling Effectiveness by Using an Upstream Ramp," Proceedings of GT2006, ASME Turbo Expo 2006: Power for Land, Sea and Air, May 8–11, 2006, Barcelona, Spain.

3. S.P. Chen, P.W. Li, M.K. Chyu, F.J. Cunha, and W.A. Messeh, "Heat Transfer in an Airfoil Trailing Edge Configuration with Shaped Pedestals Mounted Internal Cooling Channel and Pressure Side Cutback," Proceedings of GT2006, ASME Turbo Expo 2006: Power for Land, Sea and Air, May 8–11, 2006, Barcelona, Spain.

4. D.E. Metzger, H.J. Carper, and L.R. Swank, 1968, "Heat Transfer with Film Cooling Near Nontangential Injection Slots," J. Eng. Power, 90, pp. 157-163.

5. B. Sen, D.L. Schmidt, and D.G. Bogard, 1996, "Film Cooling with Compound Angle Holes: Heat Transfer," ASME Journal of Turbomachinery, 118, pp. 800-806.

6. Y. Yu, C.-H. Yen, T.I-P. Shih, M.K. Chyu, and S. Gogineni, 2002, "Film Cooling Effectiveness and Heat Transfer Coefficient Distributions Around Diffusion Shaped Holes," Transaction of ASME, 124, pp. 820-827.

V.A.4 Simulating Particle Deposition and Mitigating Deposition Degradation Effects in Film-Cooled Turbine Sections

David G. Bogard (Primary Contact) and
Jason E. Albert
University of Texas at Austin (UT)
Department of Mechanical Engineering
1 University Station C2200
Austin, TX 78712
Phone: (512) 471-3128; Fax: (512) 471-8727
E-mail: dbogard@mail.utexas.edu

DOE Project Manager: Mark Freeman
Phone: (412) 386-6094
E-mail: Mark.Freeman@netl.doe.gov

UTSR Manager of Research: Richard Wenglarz
Phone: (864) 656-2267
E-mail: RWNGLRZ@exchange.clemson.edu

Subcontractors:
Karen A. Thole (Primary Contact) and Seth A. Lawson
The Pennsylvania State University (Penn State)
Department of Mechanical and Nuclear Engineering
136 Reber Building
University Park, PA 16802-1412
Phone: (814) 865-2519; Fax: (814) 865-1280
E-mail: kthole@psu.edu

Contract Number: 41431/UTSR 07-01-SR127

Start Date: August 1, 2007
End Date: July 31, 2010

FY 2009 Objectives

- Develop an experimental methodology to actively simulate the deposition of syngas contaminant particles on film-cooled turbine surfaces, using large-scale turbine vane cascade models;
- Investigate and quantify the effects of deposition on the film cooling of turbine airfoils and endwalls; and,
- Identify and develop features that reduce depositions and/or limit the adverse effects of depositions on film cooling.

Accomplishments

- An existing wind tunnel constructed at Penn State to test various active deposition methodologies was used to simulate deposition using wax in the vicinity of a row of endwall film-cooling holes. Observation of active deposition showed that only large molten particles deposited on the smooth surface. After the surface was roughened by molten deposition, small solid particles then deposited on molten roughness elements.
- The effect of deposition on cooling was quantified using infrared (IR) thermography to measure adiabatic effectiveness at three momentum flux ratios (I=0.23, 0.5, 0.95). Results showed that deposition reduced cooling effectiveness by as much as 25% at I=0.23 and I=0.5 and had a small effect on effectiveness at I=0.95.
- A large-scale turbine vane cascade model is almost completed at Penn State to test the effect of active deposition on various endwall film-cooling geometries.
- A Stokes analysis was performed that shows 100 µm wax particles in the large-scale wind tunnel facility will simulate engine particle trajectories. At Penn State a new wax particle dispersal system was designed and tested with the capability of varying flow rate and particle size distribution independently. Particle size measurements verified that the new dispersal system can produce particles of the necessary size range.
- The new test facility at the University of Texas incorporating a high conductivity vane model was completed and testing has begun. This test facility uses a large scale model of the C3X vane (see Hylton et al. [1] for vane description) which was cast using a high conductivity epoxy selected so that the Biot number for the model matched that for a typical vane at engine conditions. Tests were completed using a model without film cooling in which the surface temperature and heat transfer coefficient distributions were measured.
- Experiments to determine the effects on film cooling from a simulated blade showerhead on the deposition of contaminants were completed. For this experimental project, molten wax particles were used to simulate molten ash particles that are expected to occur at engine conditions. Various operating conditions including mainstream temperature, surface temperature, wax melting temperature, coolant temperature, and coolant blowing rate were investigated. The showerhead film cooling jets were found to significantly inhibit depositions in the immediate vicinity of the jets.

Introduction

A major concern for the next generation of power generation gas turbines is the capability to operate with greater efficiency while using new coal-derived high hydrogen fuels. A major factor when using these fuels is the effects of contaminants on engine operation, particularly the hot section of the gas turbine. In general, contaminants in the main flow can affect the turbine section by causing erosion, corrosion, or deposition to turbine airfoil and endwall surfaces. For higher temperature operation, which is the goal of future designs, the primary degradation effect of contaminants occurs from deposition on turbine surfaces. This deposition results in much rougher surfaces and partial blockage of film cooling holes that seriously degrade the cooling performance. Performing full engine tests to determine where these contaminants deposit and how to mitigate that deposition is cost prohibitive and often results in a lack of detailed information needed to understand the underlying physics of the deposition process. Methods need to be developed whereby accurate deposition simulations can take place in a facility that allows for the underlying physical effects on airfoil heat transfer and aerodynamics to be understood. A major objective of our proposed work is to determine a reliable methodology for simulating contaminant deposition in a low speed wind tunnel facility where testing is considerably less costly.

This project is aimed at developing new cooling designs for turbine components that will minimize the effect of the depositions of contaminant particles on turbine components and maintain good film-cooling performance even when surface conditions deteriorate. Moreover, a methodology will be established that allows controlled laboratory experiments to simulate relevant deposition mechanisms for gas turbines using coal-derived fuels. New film cooling designs for turbine airfoils and endwalls and new endwall contouring designs will result. Reliable and improved film cooling performance for turbine vanes will lead to reduced costs for the user as a result of longer component life.

Approach

Facilities have been constructed at Penn State and UT to develop deposition simulation methodologies. Deposition can be simulated dynamically by dispersing wax particles into the flowfield simulating the hot mainstream flow through a turbine vane cascade. The inertial behavior of particles that exist in engine conditions can be simulated using the appropriate particle size distribution of wax particles. The use of wax also allows for the simulation of the liquid-to-solid phase change that is essential to the primary deposition mechanism.

The performance of shallow trench film cooling configurations for various positions on the suction and pressure sides of a simulated vane with active deposition is being investigated at UT. At Penn State the effect of active deposition on various endwall cooling configurations is being investigated. Preliminary results showed that deposition could be simulated dynamically using wax and that the effects of deposition could be quantified using IR thermography. New endwall and vane surface film-cooling configurations will be developed to minimize deposition and maximize cooling performance under contaminated conditions.

Results

Methods to simulate active deposition using wax were developed at Penn State and UT. At Penn State, wax was injected into the mainstream flow path of a channel with film cooling holes on the bottom endwall. Coolant mass flow was adjusted to test the effects of deposition on cooling at various momentum flux ratios. Wax was injected in 400 g increments over eight cycles. Digital photographs as well as IR images were taken at different stages in the deposition process to determine the qualitative as well as quantitative effects of deposition on cooling.

Figure 1 shows adiabatic effectiveness contour plots and their corresponding surface photographs at $I = 0.23$, where I is ratio of the momentum flux of the coolant to that of the mainstream. In the deposition photographs, deposits resulting from molten particle

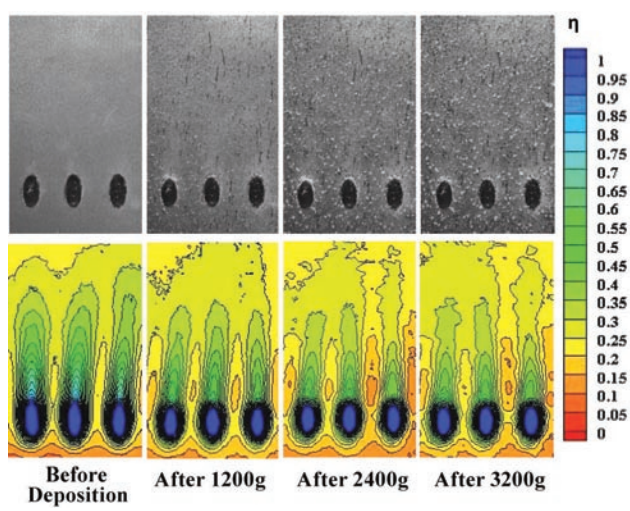

FIGURE 1. Deposition Development Photographs and Corresponding Effectiveness Contour Plots at I=0.23

impaction show up as black streaks while deposits resulting from solid particle deposition show up as white spots. The photographs show that after the first three injection cycles (after 1,200 g), mostly molten particles were depositing on the surface downstream of the film cooling holes. Eventually, the surface became roughened by molten deposits and an increasing amount of solid deposit began to build up on the surface. Close inspection of the surface following testing revealed that very few particles deposited directly downstream of each film cooling hole which implied that coolant jets prevented deposition in near wake regions.

Deposit area coverage was quantified by digitally converting of each surface photograph to a binary image in which black pixels represented deposits and white pixels represented deposit-free surface area. Figure 2 shows area-averaged effectiveness reduction relative to the baseline case with no deposition for each momentum flux ratio tested. The results in Figure 2 show that effectiveness reduction reached an equilibrium state at which further surface deposition no longer reduced effectiveness. At momentum flux ratios of $I = 0.23$ and $I = 0.5$, adiabatic effectiveness was reduced by as much as 25%; however, at $I = 0.95$, adiabatic effectiveness was reduced by only as much as 6%. Adiabatic effectiveness reduction was low at $I = 0.95$ because even without deposition, jet separation resulted in low effectiveness and the addition of deposition actually improved laterally averaged adiabatic effectiveness by enhancing coolant spreading.

One of the experimental projects at UT focused on simulating depositions to the leading edge of a turbine blade. For these experiments a device for spraying molten wax particles of the appropriate size range to match the Stokes number for engine conditions, 8 to 80 μm, was developed. Tests were conducted using models of a typical turbine blade leading edge, one without film cooling and one with three rows of film cooling holes. The leading edge models were cast from a high conductivity epoxy which was selected to match the Biot number for turbine blades operating at engine conditions. Consequently the leading edge surface was cooled to temperatures significantly below the mainstream temperature. This was important because of the need to simulate the molten particles striking a surface which was at a temperature significantly below the melting temperature of the particle.

In these tests the state of the molten particles when they impacted the surface was varied by using varying mainstream temperatures, wax melting temperatures, and coolant temperatures. For the film cooled configuration, blowing ratios of $M = 1.0$ and 2.0 were used. A sample of the results from these tests are provided in Figure 3 showing photographic images of depositions on a leading edge without film cooling and a leading edge with film cooling. These tests showed a maximum deposition thickness of nominally $0.9d$, where d was the coolant hole diameter of 3.1 mm. This maximum thickness occurred along the stagnation line. Although the maximum thickness was similar with and without film cooling, the depositions were significantly reduced in regions covered by the coolant jets. This is evident in Figure 3 where troughs in the deposition pattern are clearly evident at the exit of the coolant holes along the stagnation line.

During these deposition tests, the surface temperature was measured as the depositions were occurring. Since depositions act as an insulating layer,

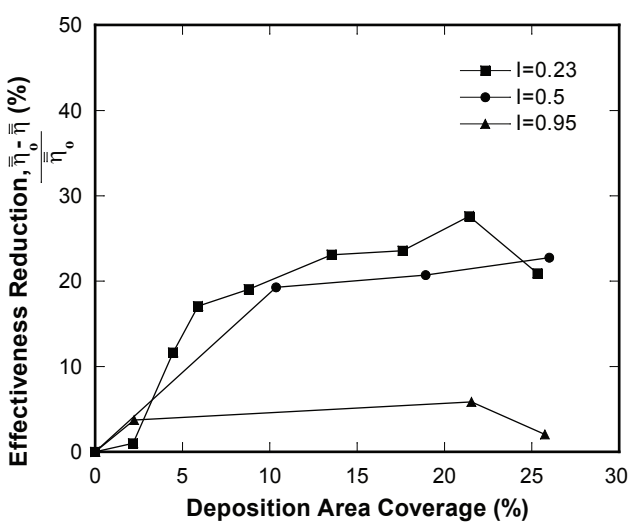

FIGURE 2. Area-Averaged Effectiveness Reduction with Respect to Deposition Area Coverage for All Three Momentum Flux Ratios Tested at Penn State

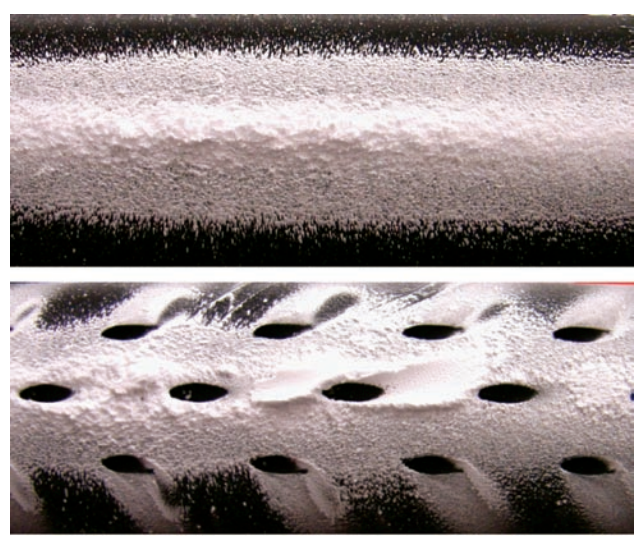

FIGURE 3. Photographic Images of Wax Depositions on a Simulated Leading Edge without Film Cooling (top) and with Film Cooling (bottom)

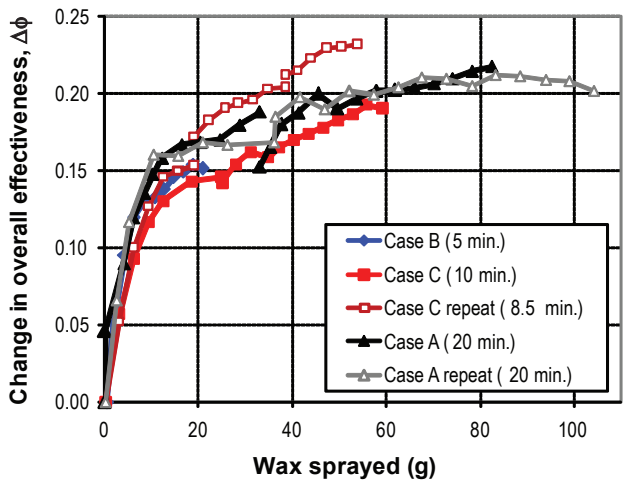

FIGURE 4. Change in Surface Temperature Between Stagnation Row Holes (in terms of ϕ) During Experiments with Varying Spray Durations

the surface temperature was expected to decrease with increasing thickness of depositions. This was found to be the case as shown in Figure 4 where the change in surface temperature is expressed in terms of the dimensionless parameter $\phi = (T_\infty - T_w)/(T_\infty - T_c)$ where T_∞ is the mainstream temperature, T_w is the surface temperature, and T_c is the coolant temperature. The dimensionless ϕ parameter is referred to as the overall effectiveness. Figure 4 shows that an increase in overall effectiveness of $\Delta\phi = 0.2$, indicating a significant reduction in surface temperature due to the insulating effect of the depositions. Also evident from Figure 4 is that the surface temperature reached an asymptotic value after 60 g of molten wax was dispersed from the sprayer. Deposition thickness was also found to remain constant once this mass of contaminant was dispersed.

Conclusions and Future Directions

Depositions tests for the flat surface facility and the leading edge facility showed successful simulation of the deposition of molten particles by use of special waxes with low melting points. Experiments in both facilities showed that coolant flow from film cooling holes mitigated the deposition in regions covered by the coolant.

Work during the coming year will focus on use of facilities which simulate the flow around a turbine vane. At Penn State, experiments will be directed at the effects of depositions on the endwalls, while at UT experiments will be directed on the vane surfaces.

Special Recognitions & Awards/Patents Issued

1. Seth Lawson, IGTI Travel Award to present GT2009-59109.

FY 2009 Publications/Presentations

1. S.A. Lawson and K.A. Thole, 2009, "The Effects of Simulated Particle Deposition on Film Cooling," ASME Paper GT2009-59109, presented at the ASME Turbo Expo, Orlando, Florida and recommended for the *Journal of Turbomachinery*.

References

1. L.D. Hylton, M.S. Milhec, E.R. Turner, D.A. Nealy, and R.E. York, 1983, "Analytical and Experimental Evaluation of the Heat Transfer Distribution over the Surface of Turbine Vanes," NASA CR 168015.

V.A.5 Syngas Particulate Deposition and Erosion at the Leading Edge of a Turbine Blade with Film Cooling

Danesh Tafti (Primary Contact),
Uri Vandsburger, Wing Ng
Virginia Polytechnic Institute and State University
114-I Randolph Hall
Blacksburg, VA 24061
Phone: (540) 231-9975; Fax: (540) 231-9100
E-mail: dtafti@vt.edu

DOE Project Manager: Mark Freeman
Phone: (412) 386-6094
E-mail: Mark.Freeman@netl.doe.gov

UTSR Manager of Research: Richard Wenglarz
Phone: (864) 656-2267
E-mail: RWNGLRZ@exchange.clemson.edu

Contract Number: 41431/UTSR 07-01-SR123

Start Date: August 2007
End Date: July 2010

FY 2009 Objectives

- Investigate deposition in a three-hole leading edge film-cooled geometry at different blowing ratios and particle sizes.
- Investigate the use of polymer materials as a substitute for coal ash for low-temperature experiments.

Accomplishments

- Investigated a three-row leading edge film-cooled geometry with blowing ratios ranging from B.R.=0.5 to 2.0 and ash particle sizes of 5 and 7 microns (Stokes numbers 0.25, 0.49, respectively) using large-eddy simulations.
- Demonstrated that the stagnation row cooling is quite effective in protecting the blade surface locally from deposition by blowing away as well as cooling ash particles below their deposition temperature. Demonstrated that particle Stokes number is an important parameter for deposition. Provided detailed deposition maps.
- Demonstrated experimentally that low melting point polyvinyl chloride (PVC) and Teflon® particles behave similar to ash particles in their scaling with free-stream and surface temperature. Measurements included surface profilometer traces, planer laser induced fluorescence images, and scanning electron microscopy images of the surface with deposits. The result is significant because low-temperature experiments can be used to study deposition at engine conditions.

Introduction

The vision of DOE's Fossil Energy Turbine Program is to provide power generation technology essential to the success of advanced fossil energy power systems in the 2008 to 2015 time frame. One of the key capabilities needed to achieve this goal is coal gasification. One of the issues in achieving this goal relates to the durability of turbine components subjected to a harsh high-temperature, high-pressure, and high-velocity environment in the gas path immediately downstream of the combustor.

Coal gasification and combustion can introduce contaminants in the vapor as well as solid or molten state depending on the gas clean-up procedures used, coal composition and operating conditions. These byproducts when combined with high temperatures and high gas stream velocities can cause deposition, erosion, and corrosion (DEC) of turbine components. Some of the common compounds which lead to DEC are trace amounts of sulphates, chlorides, and hydroxides of alkali metals such as calcium, sodium, potassium, and magnesium. Other metallic compounds of antimony, beryllium, chromium, mercury, selenium and vanadium are also threats for DEC. The extent of damage done by DEC in the gas path is directly dependent on the impaction of solid or molten particulates on surfaces, which lead to erosion and deposition. One surface, which is particularly vulnerable, is the leading edge of vanes and blades in the presence of film cooling.

Approach

The proposed project will be performed at near-engine conditions combining unique computational and experimental equipment and facilities for conditions relevant to the design of systems. A blade with a cylindrical leading edge and a camberless after body in a linear cascade will be tested. The work will use the method of time-accurate large-eddy simulations (LES) as a theoretical tool for simulating particle dynamics and a high temperature experimental facility matched to relevant engine conditions. LES, by accurately representing the unsteady nature of the flow and temperature field and the relevant turbulent

length scales, will leave little uncertainty in modeling the trajectory of particles which will be very sensitive to these factors. By using carefully derived similarity parameters, the high temperature experimental facility will provide an inexpensive and effective testing environment, with much relevancy to industry.

To maintain a high degree of relevancy to industrial design, experimental and computational conditions represent real engine conditions. By using a high temperature test facility (up to 800 K) which can generate velocities up to 200 m/s in a 2"x5" cross-section, engine-like conditions are created in the test section. The use of this facility allows the matching of key similarity parameters relevant to the flow and thermal field and particle dynamics such that experimental and computational observations can be extrapolated to the engine in a straightforward manner.

Results

Computational

The deposition and erosion caused by syngas ash particles in a film cooled leading edge region of a representative turbine vane is investigated. The carrier phase is predicted using LES and two ash particle sizes of 5 and 7 microns are investigated. A threshold ash softening temperature is assumed to determine the state of particles on impact and hence, distinguish between deposition and erosion.

The leading edge with three rows of film cooling holes is shown in Figure 1. One row is located at stagnation and two rows are located at ±4d, on either side of the stagnation line. The lateral pitch spacing (P) between two holes for any given row is 4.5d, and the relative position of the holes on the upper half and lower half are staggered with respect to the stagnation hole. The coolant hole diameter ratio (D/d) is 21.5. The coolant is injected laterally at 45 degrees to the surface with a compound angle of 90 degrees to the mainstream. Table 1 summarizes the leading edge geometry and flow properties. Table 2 shows

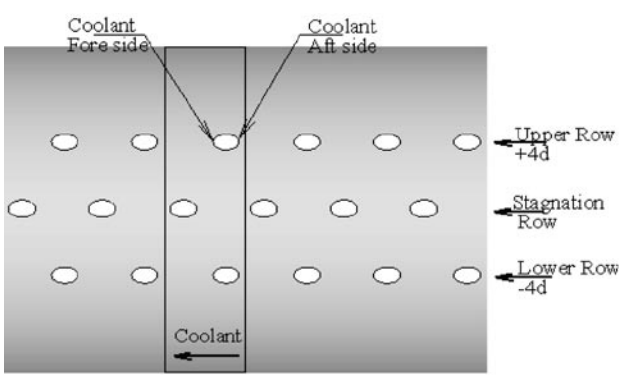

FIGURE 1. Leading Edge Vane Model

TABLE 1. Leading Edge Geometry and Flow Properties

Leading Edge Geometry	
Blade leading edge diameter (D*) [m]	0.01
Coolant jet diameter (d*), [m]	4.65×10^{-4}
Span-wise pitch (p*/d*)	4.5
Flow Properties	
Free stream velocity (U^*_∞), [m/s]	40
Free stream temperature (T^*_∞), [K]	1,600
Free stream pressure (P^*_∞), [atm]	20
Free stream density (ρ^*_∞), [kg/m^3]	4.4
Particle density (ρ^*_p), [kg/m^3]	2,500
Particle Specific heat (c^*_p), [J/kgK]	250
Coolant temperature (T^*_j), [K]	775
Ash softening Temperature, [K]	1,500
Coolant-to-mainstream density ratio	2.071[1]
Coolant-to-mainstream blowing ratio (U^*_j/U^*_∞)	0.5, 1.0, 1.5, 2.0

[1] Computations use a ratio of unity

TABLE 2. Particle Stokes Number

d^*_p (μm)	St_p	St_{conv}	St_{rad}
5	0.25	0.0578	2.24
7	0.49	0.113	3.14

the particle size and Stokes number as related to momentum transfer and heat transfer via convection and radiation.

Figure 2 shows the deposition patterns for two blowing ratios. Increasing blowing ratio decreases the adiabatic effectiveness in the stagnation region. As the blowing ratio is increased to 1.0 and 2.0, the coolant core laterally penetrates further into the mainstream. The penetration is much larger at the stagnation row which has two effects conducive to protecting the surface from deposition. First, the increased momentum of the coolant jets succeed in blowing the particles away from the stagnation region, and second, the particles are in contact with the coolant (albeit mixed with free-stream) long enough to lower their temperature below the softening temperature. In spite of the surface temperature increasing with blowing ratio in the stagnation region (decreasing effectiveness), very few particles reach the surface in the stagnation region. However, immediately downstream of the stagnation hole there is a heavy deposit concentration for B.R.=1.5 and 2.0. This is due to a fountain flow set up in this region [1]. An additional effect which is evident as the blowing ratios increase is that deposition also increases on the aft-side of the off-stagnation jets. This is a region of entrainment of hot freestream fluid, which intensifies

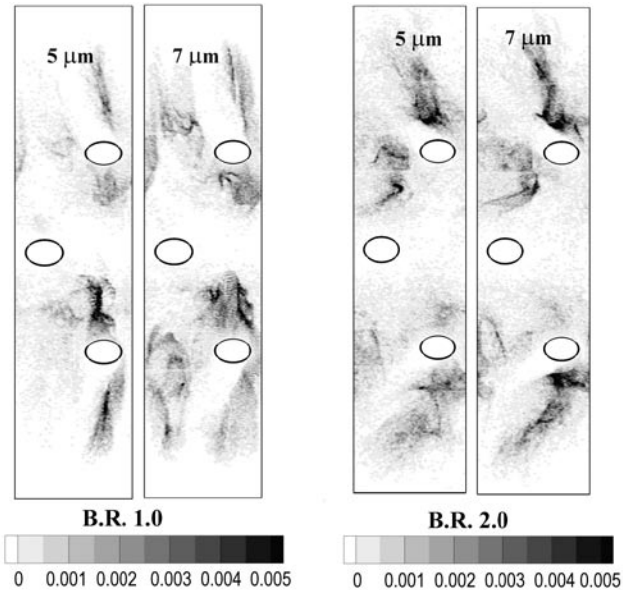

FIGURE 2. Percentage of Particles Depositing on Leading Edge Vane Surface (direction of coolant injection is from right to left)

as the blowing ratio increases and the jet lifts off the surface. The entrained mainstream fluid carries ash particles with it which deposit on the surface. Some particles penetrate into the coolant holes, but they are cooled quickly to below their softening temperature resulting in no deposition.

Experimental

The deposition characteristics of polymer materials, PVC and Teflon®, is investigated as a function of temperatures and compared to actual syngas ash particles. Polymer materials melt at a lower temperature than coal ash, so experiments using polymers can be conducted at more reasonable test conditions. The experiments are directly comparable to experiments by Crosby et al. [2] who had a similar experimental setup and used coal ash particles.

The particles were deposited on a flat plate angled 45 degrees normal to the flow. The particles were injected far upstream of the plate and have reached fluid and thermal equilibrium before arriving at the surface. The surface has a cooling scheme installed so the deposition surface can be maintained at a temperature lower than the free stream. The surface is made from steel and is polished smooth before testing.

Two sets of experiments were conducted; one where the free stream temperature is varied with no cooling and one where the free stream temperature is held constant and the surface is cooled. Figure 3(a) shows the results for the case with no cooling and PVC and Teflon® are compared to syngas ash particles. All particles show the same trend; deposition increases exponentially as free stream temperature is increased. Figure 3(b) shows the case when the surface is cooled and the free stream is held constant. PVC data has yet to be obtained, but Teflon® shows a similar trend as coal ash. Both materials decrease in deposition as the surface is cooled.

Conclusions and Future Directions

It is concluded that ash particle momentum and thermal Stokes numbers and ash softening temperature play a big role in initial deposit formation. It is also shown that polymer particles operating at lower temperatures show similar deposition behavior as

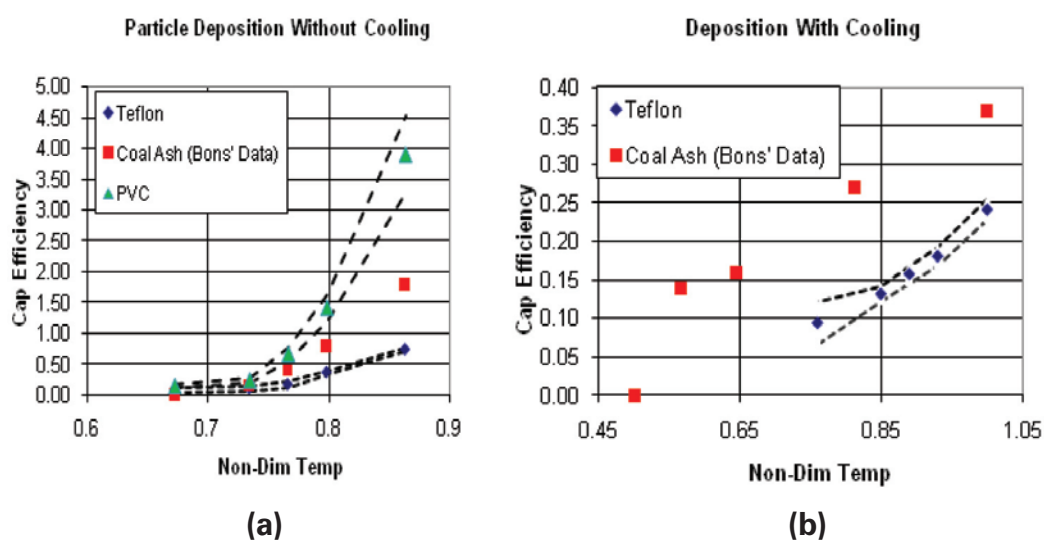

FIGURE 3. (a) Effect of Free Stream Temperature on Deposition; (b) Effect of Surface Temperature on Deposition

ash particles. Future work will focus on developing more elaborate deposition criteria based on critical viscosity and melt fraction of ash constituents which will provide a more accurate model for ash deposition. Experiments using polymer micro particles with a blade and film cooling will be performed and compared to computational results of the same geometry.

FY 2009 Publications/Presentations

1. A. Rozati, D.K. Tafti, and S.S. Sreedharan, "Effect of Syngas Particle Size on Deposition and Erosion of a Film Cooled Leading Edge," *ASME J. Turbomachinery*, accepted December 2008, in press.

2. S.S. Sreedharan and D.K. Tafti, "Effect of Blowing Ratio in the Near Stagnation Region of a Three-Row Leading Edge Film Cooling Geometry Using Large Eddy Simulations," Proceedings of ASME Turbo Expo 2009, June 8–12, Orlando, Florida. ASME Paper No. GT2009-59325. To appear.

3. S.S. Sreedharan and D.K. Tafti, "Effect of Blowing Ratio on Syngas Flyash Particle Deposition on a Three-Row Leading Edge Film Cooling Geometry Using Large Eddy Simulations," Proceedings of ASME Turbo Expo 2009, June 8–12, Orlando, Florida. ASME Paper No. GT2009-59326. To appear.

4. S.S. Sreedharan and D.K. Tafti, "Large Eddy Simulations of a Three-Row Leading Edge Film Cooling Geometry," Proceedings of ASME IMECE2008, November 2–6, Boston, Massachusetts. ASME Paper No. IMECE2008-67019.

References

1. S.S. Sreedharan and D.K. Tafti, "Effect of Blowing Ratio on Syngas Flyash Particle Deposition on a Three-Row Leading Edge Film Cooling Geometry Using Large Eddy Simulations," Proceedings of ASME Turbo Expo 2009, June 8–12, Orlando, Florida. ASME Paper No. GT2009-59326. To appear.

2. J.M. Crosby, S. Lewis, J.P. Bons, W. Ai, and T. Fletcher, 2007, "Effects of Particle Size, Gas Temperature, and Metal Temperature on High Pressure Turbine Deposition in Land Based Gas Turbines from Various Synfuels," Proceedings of GT2007, ASME Paper No. GT2007-27531.

V. UNIVERSITY TURBINE SYSTEMS RESEARCH

B. Combustion

V.B.1 Turbulent Flame Speed Measurements and Modeling of Syngas Fuels

Prof. Jerry M. Seitzman (Primary Contact),
Prof. Timothy C. Lieuwen
School of Aerospace Engineering
Georgia Institute of Technology
270 Ferst Drive
Atlanta, GA 30332-0150
Phone: (404) 894-0013; Fax: (404) 894-2760
E-mail: jerry.seitzman@ae.gatech.edu;
tim.lieuwen@ae.gatech.edu

DOE Project Manager: Mark Freeman
Phone: (412) 386-6094
E-mail: Mark.Freeman@netl.doe.gov

UTSR Manager of Research: Richard Wenglarz
Phone: (864) 656-2267
E-mail: RWNGLRZ@exchange.clemson.edu

Contract Number: 41431/UTSR 07-01-SR122

Start Date: May 15, 2007
End Date: May 14, 2010

FY 2009 Objectives

- Improve understanding of turbulent flame speeds of synthesis gas (syngas) fuels.
- Measure turbulent flame speeds of syngas fuels at conditions relevant to gas turbine combustors.
- Develop predictive flame speed models that can be used by gas turbine manufacturers to develop syngas combustors.

Accomplishments

- Obtained turbulent flame speed data of high H_2 fuel blends over range of conditions of interest, including fuel compositions, velocity, turbulence intensity, preheat temperature, and pressure.
- Demonstrated strong effects of H_2 fuel composition upon turbulent flame speeds at gas turbine realistic velocities and turbulence intensities.
- Developed physics-based correlation model based upon differential diffusion to predict turbulent flame speeds.

Introduction

Turbulent flame speed, S_T, is a key combustion parameter that impacts the performance of low emissions combustion systems. The turbulent flame speed is a measure of how fast (e.g., at what velocity) the fuel and air is consumed. Unanticipated changes in S_T during operation from the expected (design) conditions can therefore alter gas turbine pollutant emissions and combustor operability. While most current ground power gas turbines operate on natural gas fuel, there is great interest in allowing systems to operate on more available and secure sources, such as fuel gas synthesized from coal. These coal-derived syngas fuels contain varying amounts of H_2, CO and diluents, along with some hydrocarbons. The ability to operate on gases with high H_2 content may also permit reductions in CO_2 emissions.

The technical results obtained from this project have important implications on gas turbine design and operation. First, turbulent flame speed has significant impacts upon many of these parameters, such as thermal load, blowoff limits, flashback limits, and combustion instability. In other words, a thorough understanding of any of these issues necessitates understanding of the turbulent flame speed. Second, essentially no data exist for flame speeds of syngas fuels. The turbulent flame speed has a direct impact on the flame length and its spatial distribution in the combustor. This, in turn impacts the thermal loading distribution on combustor liners, fuel nozzles and other hardware. In the same way, the flame's proclivity to flashback is directly a function of how rapidly the flame propagates into the reactants – again, dependent on the turbulent flame speed. In addition, S_T has important impacts on combustion instability.

Unfortunately, little is known about S_T for syngas fuels, in particular at the temperatures and pressures of interest. The measurements that have been obtained were made primarily at atmospheric conditions and are of extremely limited usefulness for gas turbine operations.

The key end work product will be a model and a validating data set that can be used by industry for calculating the turbulent flame speed of syngas mixtures at temperatures and pressures of practical interest. This will allow gas turbine designers to develop systems sufficiently robust to operate on the range of expected syngas fuel mixtures, and for operators to predict changes that may be required to handle new fuel supplies.

Approach

This effort consists of two basic tasks. First is the measurement task. A facility (Figure 1) was developed to make quantitative turbulent flame speed measurements. Due to the definition dependency of the turbulent flame speed, the focus is on obtaining the global turbulent consumption speed, $S_{T,GC}$. Measurements of turbulent flame speeds are being acquired over a broad range of temperatures, pressure, and fuel compositions. The range of operating conditions is being determined in close coordination with gas turbine manufacturers. The second part of this project involves development of physics-based correlations of the turbulent flame speed data and models for predicting the flame speed characteristics of other fuels.

Results

Significant progress was made in two key areas. First, a variable turbulence generator facility was developed (see Figure 2) and characterized with Laser Doppler Velocimetry (LDV). Three-component LDV was performed to characterize the cold flow of the burner at mean flow velocities from 4 m/s to 50 m/s. Representative results are shown in Figure 3 detailing the mean and fluctuating velocity profiles across the burner. Relative turbulence intensities levels of up to 30% were observed, as shown in Figure 4, demonstrating the ability to achieve turbulence intensities seen in gas turbine combustors.

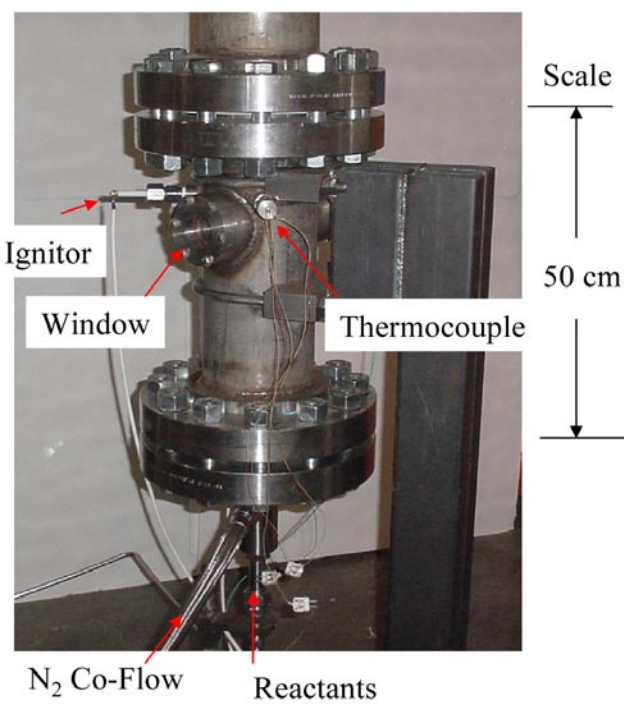

FIGURE 1. Photograph of High Pressure, Preheated Test Facility

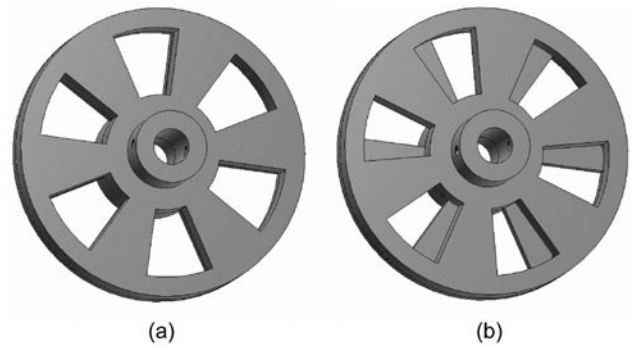

FIGURE 2. Schematic of the Turbulence Generating Plates: (a) Fully Open and (b) Partially Closed

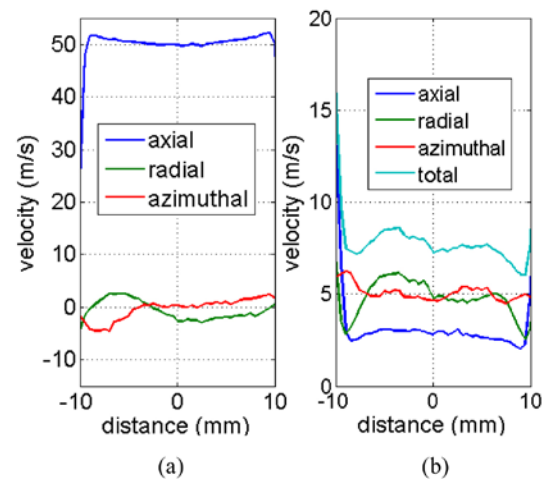

FIGURE 3. Plots of (a) Mean Axial, Radial and Azimuthal Velocities and (b) Fluctuating Axial, Radial, and Azimuthal and Total Fluctuating Velocities as a Function of Radial Distance from Center of the Burner for $\boldsymbol{U}$ = 50 m/s at a Blockage Ratio of 69%

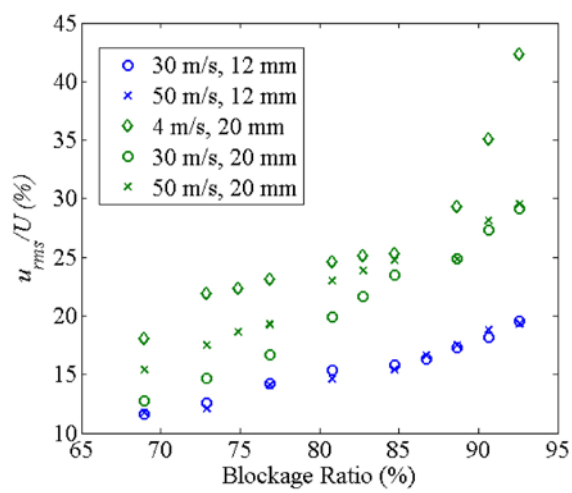

FIGURE 4. Dependence of Burner Centerline Total Turbulence Intensity (i.e., summed over all three fluctuating velocity components) upon Blockage Ratio

Second, turbulent flame speed data was also taken at up to 70 m/s mean flow and turbulence intensities of $u'/S_L = 100$ for burner diameters of 12 mm and 20 mm, at non-preheated and preheated conditions as well as at atmospheric and higher pressures. Data was taken for various H_2/CO ratios at a fixed laminar flame speed, and for various equivalence ratios at fixed H_2/CO ratios.

Figure 5 shows the data for studies where the H_2/CO ratios were varied while keeping the nominal laminar flame speed, S_L, constant at 34 cm/s for a burner diameter of 20 mm with no preheating.

TABLE 1. Legend for Data of Figure 5

		20 mm				12 mm		
		Velocity (m/s)						
		4	10	30	50	20	30	50
H_2 (%)	30	◇	□	○	×	▽	+	△
	50	◇	□	○	×	▽	+	△
	70	◇	□	○	×	▽	+	△
	90	◇	□	○	×	▽	+	△
CH_4		◇	□	○				

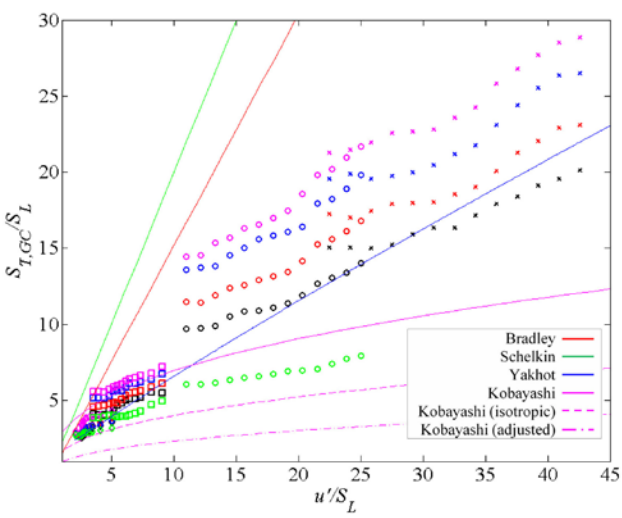

FIGURE 5. Variations of Turbulent Flame Speed, $S_{T,gc}$, with Turbulence Intensity, u', Normalized by S_L at Various Mean Flow Velocities and H_2/CO Ratios

Significantly, the data clearly indicate that the turbulent flame speed monotonically increases with H_2 level in the fuel, even for fuel blends with nominally the same laminar flame speed. This is a significant finding as it shows that the trends observed in prior studies at low turbulence intensities (and previously speculated to disappear at high turbulence intensities), persist to very turbulence intensity flames, where u'/S_L>40. Similar trends were seen with the 12 mm burner diameter, and also when the reactants were preheated to 600 K.

Turbulent flame speed data was also taken at fixed H_2/CO ratios for varying equivalence ratios under the same flow conditions. Under these conditions, the laminar flame speed was no longer a constant 34 cm/s. These results show $S_{T,GC}$ increasing with increasing equivalence ratio and also emphasize the important effects of fuel composition on turbulent flame speed.

Conclusions and Future Directions

Data obtained to date has focused upon high nozzle velocities and turbulence intensities that are representative of realistic systems. These data has allowed us to resolve an issue of whether high H_2 influences observed in low intensity burners persist at very high turbulence intensities. Future work will focus on obtaining further data at high pressure and preheat temperatures, in order to explore the parameter space of most interest to future ultra-low emissions energy systems.

V.B.2 Fundamental Studies in Syngas Premixed Combustion Dynamics

Ahmed F. Ghoniem (Primary Contact),
A. Annaswamy, Zachary A. LaBry,
Raymond L. Speth
Massachusetts Institute of Technology
77 Massachusetts Ave.
Room 3-342
Cambridge, MA 02139
Phone: (617) 253-2295; Fax: (617) 253-5981
E-mail: ghoniem@mit.edu,
zlabry@mit.edu, speth@mit.edu

DOE Project Manager: Mark Freeman
Phone: (412) 386-6094
E-mail: Mark.Freeman@netl.doe.gov

UTSR Manager of Research: Richard Wenglarz
Phone: (864) 656-2267
E-mail: RWNGLRZ@exchange.clemson.edu

Contract Number: 41431/UTSR 05-01-SR121

Start Date: August 1, 2005
End Date: August 1, 2008

FY 2009 Objectives

The primary focus of this project is to develop an understanding of the fundamental physical and chemical processes that give rise to self-sustaining combustion instabilities, and to apply this knowledge to the design of robust and effective passive flame stabilization techniques. In light of the overarching goals of this project and previous accomplishments, the specific project goals for Fiscal Year 2009 include:

- Exploring the use of microjet air injection as a means of suppressing combustion instability; and
- Using advanced diagnostics to explore the mechanistic properties of combustion instability and the unsteady dynamics as the system transitions between stable and unstable modes.

Accomplishments

- Demonstrated secondary flow injection through microjets as a viable, robust means of suppressing combustion instability in the planar combustor;
- Demonstrated potential of microjet air injection for suppressing combustion instability in the axisymmetric combustor;
- Installed advanced optical diagnostics, including high frame-rate chemiluminescence imaging and stereo particle velocimetry; and
- Conducted stereoscopic particle image velocimetry (PIV) experiments in an axisymmetric combustor, looking at primary unstable modes and transient behavior of microjet control.

Introduction

As the demand for clean coal technology for energy and fuel production is expected to expand, the combustion of reformed fuels, of which syngas is one of the most prominent, is gaining more attention. Syngas, produced by coal gasification, is a mixture of carbon monoxide and hydrogen, with the ratio of the two constituents depending on the composition of the feedstock used to produce it. Having been proposed as the fuel of choice for modern, high-efficiency, low-emission power plants, developing an understanding of the dynamics behind lean and ultra-lean syngas combustion has become an important area of research.

Syngas combustion differs from the combustion of complex hydrocarbons in several key aspects, including the high hydrogen content and higher flame speed. The latter attribute makes syngas a candidate for use in lean and ultra-lean combustion systems where lower flame speeds can lead to blow-off. At lean and ultra-lean conditions, the dynamics of syngas combustion exhibits highly unstable regions of the operational parameter space. Such instabilities, which manifest themselves as high amplitude, self sustaining pressure oscillations can cause thermal and mechanical fatigue in gas combustors, and present an obstacle to the effective use of lean premixed syngas combustion technology.

The purpose of this study is to elucidate the fundamental behavior of syngas combustors over a wide range of operating conditions. The understanding gained from this study is important to the development of computational models of combustion and the development of passive flame stabilization environments.

Approach

We have made use of two independent combustors to explore the dynamics of lean and ultra-lean syngas combustion. One combustor is an axisymmetric design with a swirl stabilized flame (Figure 1); the other combustor is a planar design with a flame stabilized by sudden expansion. Systematic measurements of the acoustic field were made in each combustor, varying equivalence ratio, fuel composition, inlet air

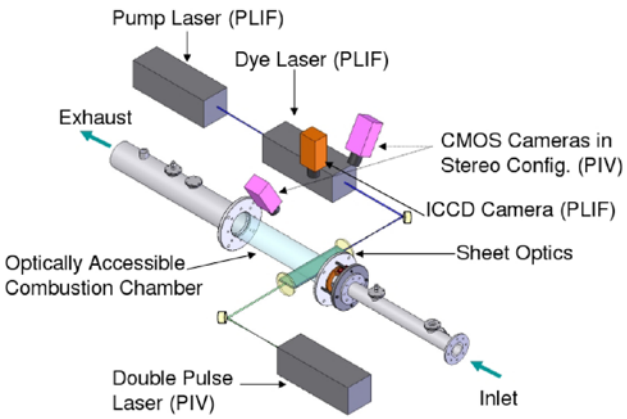

FIGURE 1. Experimental Setup of Axisymmetric, Swirl Stabilized Combustor with Stereo PIV and Planned Planar Laser Induced Fluorescence (PLIF) Systems

temperature and Reynolds number. Stability maps for each combustor under set conditions were made. High speed chemiluminescence imaging and PIV are used to study trends in the integrated heat release and fluid mechanics during stable and unstable operating conditions. Experimental results are used to suggest modifications to the flame stabilization zone and guide the development of reduced order numerical models.

Results

Experimental investigation of streamwise and cross-stream microjet actuation in the planar combustor demonstrated that unstable and high-frequency unstable modes could be suppressed using an optimum secondary air flow rate for each set of conditions. In a paper submitted to *Combustion and Flame*, "Mitigation of Thermoacoustic Instability Utilizing Steady Air Injection near the Flame Anchoring Zone," detailed observations of the interaction between the flame and the modified flow field are made.

High frame-rate chemiluminescence synchronized with pressure measurements enable individual modes of combustion instability to be analyzed. Figure 2 shows a 115 Hz instability mode, observed in the axisymmetric combustor at an equivalence ratio of 0.45 with a syngas fuel mixture of 80% CO and 20% H_2. Each frame represents the average of approximately 10 PIV data sets and chemiluminescence images with a phase difference of no more than 6 degrees, as determined from the pressure signal measured immediately upstream of the flame anchoring zone. Successive frames differ in phase by 90 degrees. The following observations are made about the cycle:

- At the beginning of the cycle, a strong inner recirculation zone exists, propagating upstream of the expansion plane (left edge of each frame).
- As the cycle progresses, the inner recirculation zone weakens, and is replaced by a central jet. The inner recirculation zone exists only down downstream of the expansion plane.
- At the end of the cycle, the inner recirculation zone reforms, and the jets are pushed away from the central axis of the combustor.

Figure 3 shows time-averaged axial velocity fields an inherently stable flame and for an inherently unstable flame, identical to the mode shown in Figure 2, stabilized by the injection of secondary air through axial microjets. The use of PIV for studying the effects of microjet actuation is in its early stages, but these preliminary results demonstrate significant physical differences in the flow field for the these two stable flame cases. We observe that the microjets completely eliminate the inner recirculation zone, replacing it with a strong central jet. A weak outer recirculation zone keeps the flame from blowing downstream of the flame anchoring zone.

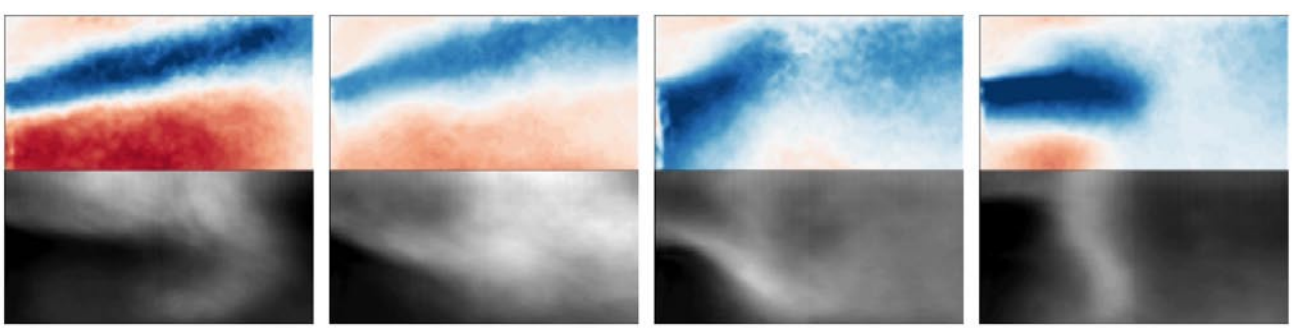

FIGURE 2. Sequence of frames showing axial velocity (top) and chemiluminescence (bottom) at four points in the cycle of the 115 Hz mode of the axisymmetric combustor. Data taken at an equivalence ratio of 0.45 with 80% CO, 20% H_2 fuel composition. Flow direction is left to right. The expansion plane is located at the left edge of each frame. Red indicates reversed flow.

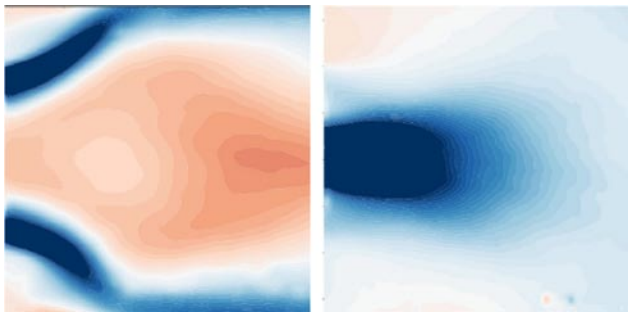

FIGURE 3. Axial velocity of a stable syngas flame (left) and a microjet stabilized flame at an equivalence ratio of 0.45 with a fuel mixture of 80% CO and 20% H_2 and 1.75 g/s of secondary air flow injected parallel to the central axis. Flow direction is left to right. The expansion plane is located at the left edge of each frame. Red indicates reversed flow.

Conclusions and Future Directions

We have conducted a series of experiments in both the axisymmetric and planar combustors to explore the effects of fuel composition, inlet air temperature, equivalence ratio and Reynolds number on lean and ultra-lean syngas combustion. In both combustors, we observe very active dynamics, characterized by coupling between the fluid dynamics in the flame anchoring zone, the acoustic field of the system and the chemistry and heat transport in the combustion zone.

Our studies of microjet actuation have shown that air injection into the flame anchoring zone is a viable and robust way of suppressing combustion instability over a wide range of unstable operating conditions in the planar combustor. Initial experiments with microjets in the axisymmetric combustor have also shown potential for suppressing instabilities.

Future work will focus on using advanced diagnostics, including chemiluminescence and PIV, to develop a better understanding of the effect that microjets have on the fluid mechanics in the flame anchoring zone. The effectiveness of microjets in the axisymmetric combustor is currently under investigation.

Publications

Published, Accepted and Submitted

1. H. Murat Altay, Raymond L. Speth, Duane E. Hudgins, and Ahmed F. Ghoniem, "Flame-Vortex Interaction Driven Combustion Dynamics in a Backward-Facing Step Combustor," *Combustion and Flame* 156 (2009), pp. 1111-1125.

2. Raymond L. Speth and Ahmed F. Ghoniem, "Using a Strained Flame Model to Collapse Model Data in a Swirl Stabilized Syngas Combustor," *Proceedings of the Combustion Institute* 32 (2009), pp. 2992-3000.

3. H. Murat Altay, Raymond L. Speth, Duane E. Hudgins, and Ahmed F. Ghoniem, "The Impact of Equivalence Ratio Oscillations on Combustion Dynamics in a Backward-Facing Step Combustor," *Combustion and Flame*, In Press.

4. H. Murat Altay, Duane E. Hudgins, Raymond L. Speth, Anuradha M. Annaswamy, and Ahmed F. Ghoniem, "Mitigation of Thermoacoustic Instability Utilizing Steady Air Injection near the Flame Anchoring Zone," Submitted to *Combustion and Flame*.

In Preparation

1. Zachary A. LaBry, Raymond L. Speth, Santosh J. Shanbhogue and Ahmed F. Ghoniem, "Instability Suppression in a Swirl-Stabilized Combustor Using Microjet Air Injection," To be presented at the 48th AIAA Aerospace Science Meeting.

2. Santosh J. Shanbhogue, Zachary A. LaBry, Raymond L. Speth, and Ahmed F. Ghoniem, "Investigation into Combustion Instability Control by Microjet Actuation," To be presented at the 48th AIAA Aerospace Science Meeting.

V.B.3 Autoignition Studies of Syngas and Hydrogen (SGH) Fuels

Dr. Robert J. Santoro
The Pennsylvania State University (Penn State)
240 Research Building East/Bigler Road
University Park, PA 16802
Phone: (814) 863-1285; Fax: (814) 865-3389
E-mail: rjs2@psu.edu

DOE Project Manager: Mark Freeman
Phone: (412) 386-6094
E-mail: Mark.Freeman@netl.doe.gov

UTSR Manager of Research: Richard Wenglarz
Phone: (864) 656-2267
E-mail: RWNGLRZ@exchange.clemson.edu

Contract Number: 41431/UTSR 05-01-SR117

Start Date: August 1, 2005
End Date: May 31, 2009

FY 2009 Objectives

- Parametrically quantify the autoignition delay time for CO/H_2 mixtures as function of CO concentration, equivalence ratio, pressure and temperature.
- Quantitatively measure the effect of water concentration on autoignition using mixtures of $CO/H_2/H_2O$.
- Conduct studies at operating pressures up to 3.0 MPa (30 atm) and 860 K (1,100°F) and typical air mass flow rates of 0.5 kg/s (1 lbm/s).

Accomplishments

- Completed assembly of the high-pressure, high-temperature flow reactor for autoignition measurements capable of operation at 3.0 MPa (30 atm) and 860 K (1,100°F).
- Completed the characterization of the the temperature uniformity and mixing characterization of the high-pressure, high-temperature flow reactor showing axial uniformity of ±5 K (±9°F).
- Completed autoignition measurements of syngas showing a highly variable autoignition time for these typical gas turbine conditions.

Introduction

The renewed interest in coal-based integrated gasification combined cycle (IGCC) plants is due to the desire for greater fuel supply flexibility using the large known resources of coal in the United States (U.S.). The use of coal will significantly reduce U.S. dependence on foreign supplies of oil and natural gas currently used to generate electric power. A major technical challenge is to achieve efficient, environmentally clean IGCC technologies that can provide both electrical generation and hydrogen production capabilities. Combustion of syngas produced from the coal gasification process, as well as a broader range of syngas and hydrogen (SGH) fuels, is a key technology research area as syngas is in a sense a new fuel. Furthermore, although syngas is largely composed of CO and H_2, the amount of each of these components in the fuel can vary widely depending on the source of the coal and gasification technology used. Consequently, there is a critical need for fundamental properties such as autoignition time, which is a measure of when a syngas-air mixture will spontaneously ignite. In many gas turbine applications, syngas is premixed with high-temperature air before it burns in the combustion chamber. Thus, knowing the autoignition time for premixed syngas-air mixtures is critical to the operation of gas turbine power systems using lean premixed technology. If this syngas/air mixture autoignites before entering the combustion chamber due to long residence times in the gas turbine inlet section, significant and costly damage can occur to the gas turbine. Measurements of autoignition time are clearly a key issue and are the focus of the present research project. For these measurements to be of use, the autoignition time for syngas-air mixtures must be measured under conditions relevant to gas turbine engines used for power generation. This requires that studies must be done at high pressure (up to 30 atm) and high temperature (up to 860 K [1,100°F]). Such measurements are challenging in terms of the facilities needed to conduct the measurements and the diagnostics required to accurately measure the autoignition time, which can vary from one-thousandth of a second to a few seconds.

Approach

Syngas autoignition experiments conducted at Penn State use a flow reactor based on the design used by Spadaccini and TeVelde [1,2]. A schematic of the flow reactor is shown in Figure 1. Air flow at a

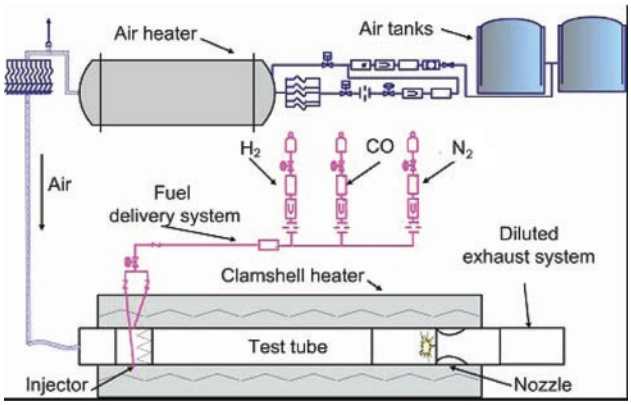

FIGURE 1. Schematic of High-Pressure, High-Temperature Flow Reactor Facility

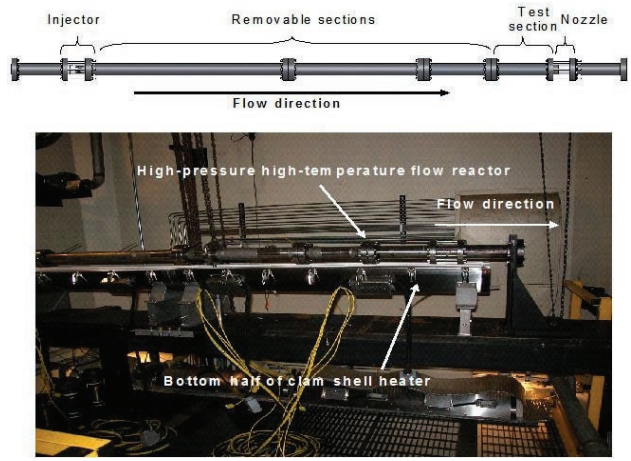

FIGURE 2. Picture of the Assembled Flow Reactor Used for Autoignition Studies of Syngas

maximum flow rate of 2.5 kg/s (5.5 lbm/s) is supplied to an electric resistance-type air heater that can heat 0.5 kg/s (1.0 lbm/s) of air to a maximum temperature of 860 K (1,100°F). The heated air is subsequently mixed with the syngas fuel in the mixer section. The fuel-air mixture then flows through a constant-diameter variable-length instrumented test section that is heated by clam-shell heaters (see Figure 2) followed by a flow nozzle. Once a steady flow has been achieved, the air temperature is slowly increased until a sharp temperature increase is observed in the test section. The variable-length test section with a circular cross section (diameter of 43 mm) provides the capability to determine autoignition times for various syngas and sygas/hydrogen mixtures. The range of ignition delay times that can be measured depends on the length from the injection point to the flow nozzle, *L*, and the average flow velocity, *U*, of the fuel/air mixture. The test conditions can be varied from pressures between 1 and 3 MPa (10 to 30 atm) and mixture temperatures between 700 to 860 K (800°F to 1,100°F), which adequately replicate practical gas turbine inlet operating conditions.

Results

Autoignition times were measured for mixtures of hydrogen (~75% H_2) and carbon monoxide (~25% CO) to simulate syngas at a pressure of 0.96 MPa (9.5 atm) as well as pure hydrogen at a pressure of 2.49 MPa (24.6 atm.). Typically, the flow reactor wall is heated to the target temperature slowly (~2 hours) using the six available zones of the clam-shell heaters (see Figures 2 and 3). Heated air and syngas mix in the injector section at the target mass flow rate and temperature. The air-syngas mixture temperature is measured in the near-wall region using an array of side mounted Type-K thermocouples, labeled T1 through T14 (see Figure 3) that are located 0.51 cm (0.2 in) from wall of the flow reactor.

The uniformity of the centerline temperature in the axial direction was measured using an axial thermocouple rake that was introduced into the flow reactor through the nozzle. These results showed that the air temperature can be controlled to within ±5 K (±9°F) along the length of the flow reactor tube from the injector location to the nozzle. It is also possible to operate the flow reactor under conditions where the reactor walls are heated to the mean temperature of the fuel/air mixture or to a value that is higher or lower than that temperature as desired. This capability is useful in investigating whether ignition is occurring at the wall by operating at lower wall temperatures or to raise the temperature of the fuel/air mixture as it flows through the flow reactor tube. Once stable conditions have been established, the temperature of the air is slowly increased until an autoignition event is observed.

An autoignition event is detected by the series of thermocouples located along the wall of the flow reactor as discussed above and shown in Figure 3. Normally, thermocouple 1 (T1) is used to measure the incoming air temperature, while T2 measures the temperature of the fuel/air mixture 27.25 cm (10.73 in) downstream of the fuel injector. Thermocouples T3 through T13 are used to determine the location in the flow reactor tube where autoignition occurs. Thermocouple T14 measures the temperature downstream of the nozzle. For a valid determination of the autoignition time, the autoignition event should ideally occur between T12 and T13. Then, knowing the distance from the injector to T13 and the mean velocity of the fuel/air mixture, the autoignition time can be calculated as the ratio of that distance divided by the mean velocity of the fuel/air mixture.

Three types of ignition events were observed for the 75% H_2/25% CO mixtures conducted at a pressure

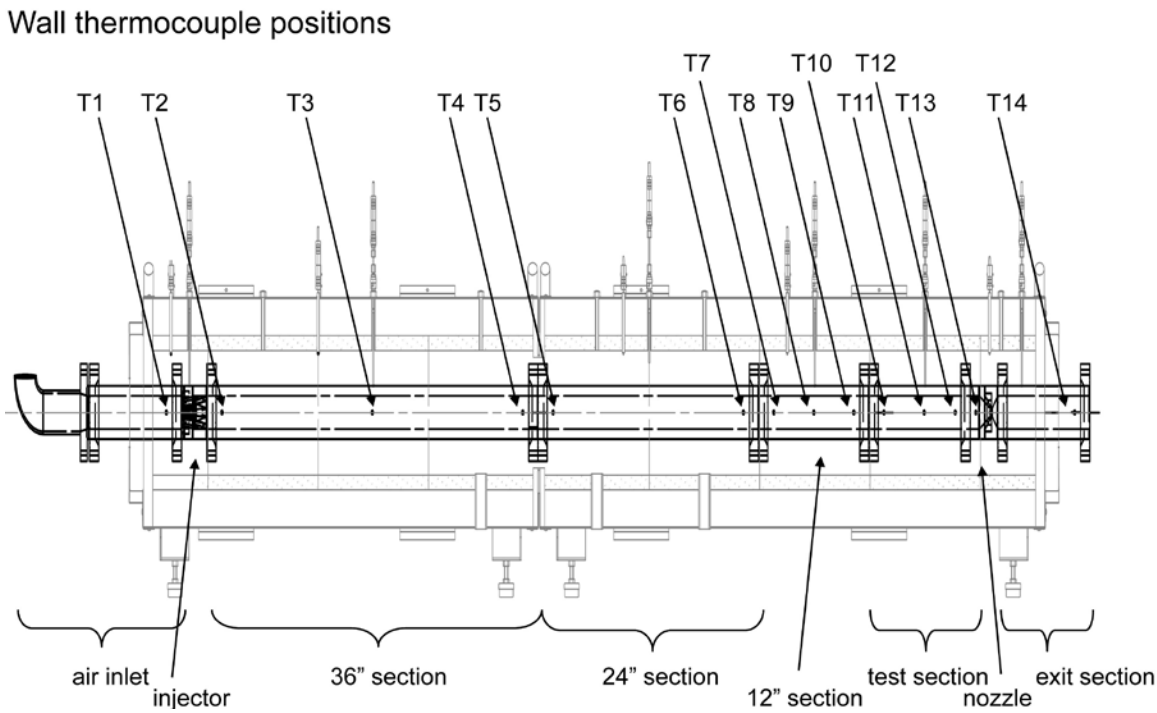

FIGURE 3. A Schematic of the Flow Reactor Tube Identifying the Locations of the Heating Zones for the Clam-Shell Heaters and the Thermocouples Used to Determine the Location of an Ignition Event

of 0.96 MPa (9.5 atm). The most prevalent event was ignition near the injector face as the air temperature is increased from its starting value. More specifically such ignition events occur in the region between the injector face and T2, which is 27.25 cm (10.73 in) downstream of the injector face. In the second type observed, autoignition does occur in the flow reactor tube downstream of the injector. However, the location of the event varies in terms of the position in the flow reactor tube for similar conditions. The third type observed involved cases where no ignition was observed with run times of several seconds or longer. Thus, data obtained for syngas mixture studied does not provide a single value of the autoignition time as should be expected.

This result raises some important questions about the state of understanding of the autoignition behavior of syngas and hydrogen. For example, an interesting point observed in recent experiments has to do with the effect of whether the injector section is inside the clam shell heaters or positioned just upstream of these heaters. All of the experiments initially undertaken were for an arrangement where the injector was inside the clam shell heaters. Ideally, this arrangement is best as it favors a more uniform temperature at the exit of the injector. However, this arrangement nearly always resulted in ignition very near the injector face before the T2 location 27.25 cm (10.73 in) downstream of the injector face. For cases where the injector was placed upstream of the first clam-shell heater, ignition in the flow reactor tube was observed about 50% of the time for cases where the fuel/air mixture temperature was approximately 783 K (~950°F). Of those that ignited in the flow reactor tube, the location of the ignition event occurred at locations between T4 and T10 with about 75% of those events occurring between T8 and T10. The remaining cases either had an ignition event near the injector face (~40%) or no ignition at all (~10%).

Figure 4 shows a plot of the autoignition times measured for 75% H_2/25% CO mixture for those cases where ignition occurred in the flow reactor tube. Results previously reported by other researchers in ref. 3 are shown on this figure as well. Figure 4 also shows an example of a prediction of the autoignition time using a current chemical kinetic model. The significant difference between experiment and modeling is clearly evident.

Dryer and Chaos recently pointed out that the observed autoignition behavior of syngas had been previously observed for pure H_2 oxidation studies [4]. Peschke and Spadaccini also observed that the syngas autoignition time is dominated by the autoignition behavior of hydrogen [2]. Consequently, a study of pure H_2 autoignition was conducted at a pressure of 2.49 MPa (24.6 atm) using the flow reactor described earlier. The results of those studies are also plotted in Figure 4 and are very similar to the results observed for

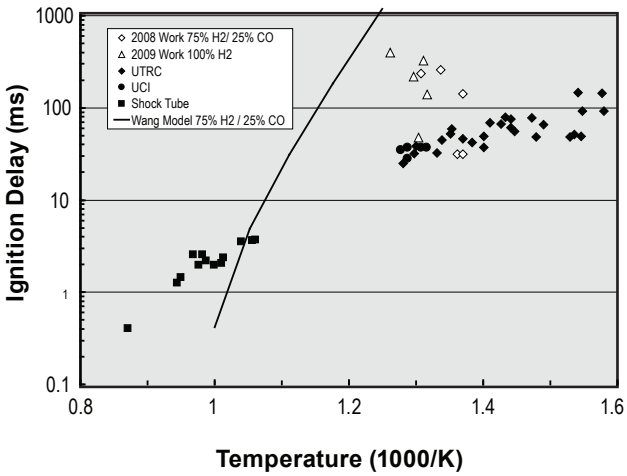

FIGURE 4. Plot of the measured autoignition time as function of temperature along with a comparison with previously reported results. Note all results reported are for a pressure corrected to 20 atm as described in Ref. 3.

the 75% H_2/25% CO mixtures as suggested by Dryer and Chaos [4] and Peschke and Spadaccini [2].

Recently, Beerer and McDonnel using a similar flow reactor apparatus have reported autoignition times for hydrogen and air that show similar variations with respect to whether ignition occurred or not [5]. Their study reported cases where hydrogen/air mixtures with the same equivalence ratio and mixture temperatures within ±5 K (9ºF) of each other sometimes ignited and other times did not ignite. At the present time, there is a significant controversy on-going about the autoignition of syngas and hydrogen. Recently, measurements reported by Petersen et al. have shown that autoignition time for syngas measured in shock tubes and flow reactors deviate significantly from current chemical kinetic models [3]. Dryer and Chaos in their paper attribute the deviation observed to result from catalytic reactions with the wall material of the apparatus used in these autoignition studies [4].

Conclusions and Future Directions

Experimental studies conducted in Fiscal Year 2009 to measure the autoignition time for syngas were completed under conditions similar to actual gas turbine operating conditions. A study of the autoignition of pure hydrogen was also completed that showed results very similar to the earlier 75% H_2/25% CO studies. Thus, confirming the work of other researchers that syngas autoignition was dominated by the behavior of hydrogen in the syngas. Furthermore, both the syngas and the hydrogen studies revealed that the autoignition process for syngas and hydrogen is intrinsically variable under the pressure and temperature conditions studied in terms of the time and conditions at which autoignition is observed. The source of this unexpected variability is not yet understood, but does present a major challenge for the use of syngas under lean premixed conditions.

FY 2009 Publications/Presentations

1. Autoignition Studies of Syngas and Hydrogen (SGH) Fuels, Semi-Annual Report For August 1, 2008 to January 31, 2009.

2. Autoignition Studies of Syngas and Hydrogen (SGH) Fuels, Final Report, 2009.

References

1. L.J. Spadaccini and J.A. TeVelde, *Combust. Flame*, Vol. 46, 1982, 283:300.

2. W.T. Pescheke and L.J. Spadaccini, "Determination of Autoignition and Flame Speed Characteristics of Coal Gases Having Medium Heating Values," EPRI AP 4291, November 1985.

3. E.L. Petersen, D.M. Kalitan, A.B. Barrett, S.C. Reehal, J.D. Mertens, D.J. Beerer, R.L. Hack, and V.G. McDonell, *Combust. Flame*, Vol. 149, 2007, 244:247.

4. F.L. Dryer and M. Chaos, *Combust. Flame*, Vol. 152, 2008, 292:299.

5. D.J. Beerer and V.G. McDonell, *J. Engineering for Gas Turbines and Powe*r, Vol. 130, 2008, 051507-1:051507-8.

V.B.4 Combustion Dynamics in Multi-Nozzle Combustors Operating on High-Hydrogen Fuels

Dom Santavicca
The Pennsylvania State University
Research Bldg. East, Bigler Road
University Park, PA 16802
Phone: (814) 863-1863; Fax: (814) 865-3389
E-mail: das8@psu.edu

DOE Project Manager: Mark Freeman
Phone: (412) 386-6094
E-mail: Mark.Freeman@netl.doe.gov

Subcontractor:
Tim Lieuwen, Georgia Institute of Technology, Atlanta, GA

Contract Number: NT0005054

Start Date: October 1, 2008
End Date: September 30, 2011

FY 2009 Objectives

- Design multi-nozzle test rig with transverse forcing.
- Fabricate and construct multi-nozzle test rig with transverse forcing.
- Initiate transverse forced response tests in multi-nozzle annular configuration.
- Design multi-nozzle test rig with longitudinal forcing.
- Fabricate and construct multi-nozzle test rig with longitudinal forcing.
- Initiate longitudinal forced response tests in multi-nozzle can configuration.
- Initiate formulation of flame response model for transverse forcing.
- Initiate formulation of flame response model for longitudinal forcing.

Accomplishments

- Demonstration of experimental design development based on commercially available finite element method software.
- A detailed map of the acoustic structure in the transverse forcing combustor has been developed over a wide range of frequencies.
- The existence of strong flow/flame response to acoustic excitation in the transverse forcing combustor has been verified.
- A comprehensive particle image velocimetry (PIV) study has been performed of the flow behavior in the transverse forcing combustor under both cold flow and reacting conditions.
- Fabrication of the components and partial assembly of the multi-nozzle can combustor for the longitudinal air and fuel forcing tests has been completed.

Introduction

Combustion dynamics [1,2] is one of the biggest technical challenges in efficient, low emission gas turbines. High frequency, transverse modes are particularly dangerous and can cause severe structural damage within seconds. The goal of this research is to use a synergistic research approach to understand the underlying physics of the coupling mechanism between catastrophic acoustic resonances and the flame dynamics that fuel them. The use of a multiple-nozzle experimental facility recreates the flow conditions in an actual gas turbine and allows for specific attention to be paid to the complicated interactions between flames that can aggravate the combustion dynamics problem. To date, this research has focused on understanding the fluid instabilities and flame dynamics in a single nozzle, as a building block to understanding dynamics in the multi-nozzle combustors that are used in actual power generation turbines. Strong evidence of a coupling between the transverse acoustic field and axial velocity motions has been established. These axial velocity perturbations create large vortices that deform the flame and cause bursts of heat release that feed back into the acoustic field. Understanding the vortex dynamics is also important in the multi-nozzle problem, since the paths of the convecting vortices of each nozzle intersect, allowing for vortex and flame interaction. This phenomenon has been seen at several operating conditions and acoustic frequencies, showing that this problem can be pervasive in several different gas turbine geometries and operating conditions. The knowledge garnered in this phase of the investigation will allow for better understanding of this important problem.

Approach

A physics-based, flexible, and synergistic approach is the key to successfully studying the response of a multi-nozzle combustor to longitudinal and

transverse acoustic excitation. The test rigs that have been designed and constructed specifically for this study are shown in Figure 1. A main thrust of the research is accomplished with the use of PIV [3], a technique that measures two dimensional velocity fields. This technique is used to capture phase-resolved measurements of the velocity field and flame shape under different acoustic forcing conditions. The phase-resolved measurements reveal the effect of the acoustic forcing on an average basis. At eight phases throughout the acoustic cycle, 512 velocity fields are recorded and information about the flow field can be found by investigating the ensemble average of these images at each phase. In the next phase of this project, time-resolved measurements will be made which will allow for more detailed inspection of vortex formation, flame movement, and adjacent flame interaction. This approach will reveal more of the detailed physics that are not available using the phase-resolved system.

Results

The first task in the transversely-forced multi-nozzle test rig was to establish the existence of bulk transverse motion. This was done to examine the influence of the transverse sound field on the flow over the course of an acoustic cycle. Strong transverse motions were found throughout the flow at all three test frequencies, 400 Hz, 750 Hz, and 1,200 Hz.

The second task was to determine the regions of the flow that responded most to the transverse forcing by measuring the ratio of the transverse velocity fluctuation to the total velocity fluctuation magnitude. An example of this result is shown in Figure 2, where the contour plot on the bottom of the image is an average picture of the axial flow field, and the lines with height on the Z-axis show the ratio of transverse velocity to total velocity fluctuations. It is evident from the contours of the ratio that the shear layers and the center recirculation bubble respond well to the transverse acoustic excitation, as the ratio of transverse velocity to total velocity is near one. This ratio drops

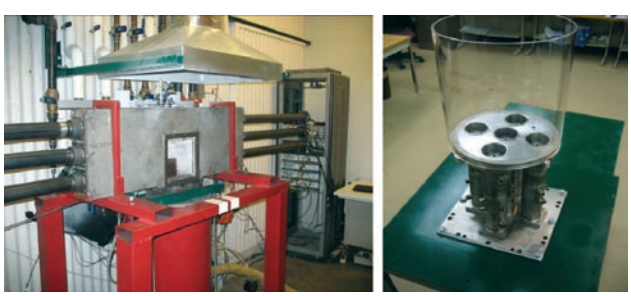

Transverse forcing, multi-nozzle experimental facility.

Multi-nozzle can combustor experimental facility.

FIGURE 1. Multi-Nozzle Experimental Facilities for Transverse and Longitudinal Forcing

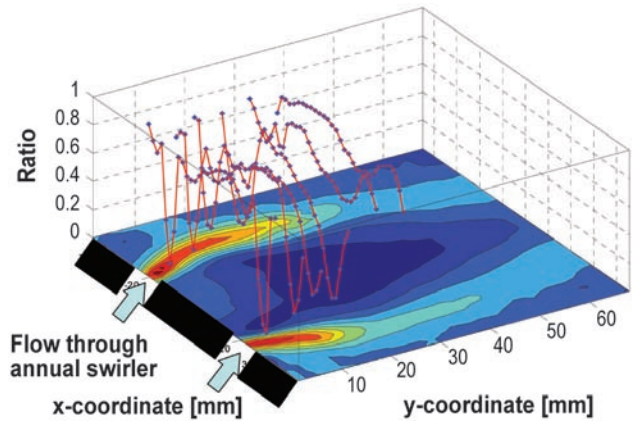

FIGURE 2. Ratio of Transverse Velocity to Total Velocity for 400 Hz in Reacting Flow

in the region of the jets, particularly near the dump plane, as would be expected due to the highly axial velocity emanating from the jet source.

Conclusions and Future Directions

The goal of this study is to understand the coupling between a resonant acoustic field inside a multi-nozzle combustor, the fluid mechanic instabilities in the combustor, and the flames whose unsteady heat release feeds energy into a destructive feedback loop. The expected results fall into three categories of understanding: acoustic behavior, fluid mechanic behavior, and flame behavior.

The key to understanding the acoustic behavior will be to measure and model the complex acoustic field near the flame stabilization point. The cavity of the annular jet creates a locally two-dimensional acoustic field that can trigger vortex formation at the corners of the dump plane and center body, which then deform the flame.

The unstable fluid mechanic behavior, particularly in the two shear layers of each flame, is not only the most important part of understanding this phenomenon, but also the most difficult. The behavior of the shear layers will dictate the flame behavior due to the flame stabilization points at the origins of these shear layers.

Finally, the flame behavior will be studied from two directions. First, the flame/flow interaction will be important to understanding the coupling between the acoustics and the flame behavior on a single flame. Second, interaction of adjacent flames will be studied. Interactions both in terms of the shear layers and the flames themselves are important to understanding how the dynamics of this multi-component system feeds the energy of combustion dynamics.

References

1. S. Ducruix, et al., "Combustion Dynamics and Instabilities: Elementary Coupling and Driving Mechanisms," *Journal of Propulsion and Power*, Vol. 19, pp. 722-726, 2003.

2. G. Staffelbach, et al., "Large Eddy Simulation of Self Excited Azimuthal Modes in Annular Combustors," *Proceedings of the Combustion Institute*, Vol. 32, No. 2, pp. 2909-2916, 2009.

3. J. Westerweel, "Fundamentals of Digital Particle Image Velocimetry," *Meas. Sci. Technol.*, Vol. 8, pp. 1379-1392, 1997.

V.B.5 Numerical and Experimental Study of Mixing Processes Associated with Hydrogen and High Hydrogen Content Fuels

Vincent G. McDonell (Primary Contact), Amin Akbari, Scott Hill, and Patrick Randall
University of California, Irvine (UCI)
UCI Combustion Laboratory
Irvine, CA 92697-3550
Phone: (949) 824-5950 x121; Fax: (949) 824 7423
E-mail: mcdonell@ucicl.uci.edu

DOE Project Manager: Mark Freeman
Phone: (412) 386-6094
E-mail: Mark.Freeman@netl.doe.gov

Contract Number: NT0006551

Start Date: October 1, 2009
End Date: September 30, 2011

FY 2009 Objectives

- Define experimental/numerical test matrix.
- Define/quantify diagnostics for measuring H_2 mixing.
- Design and fabricate test hardware needed for the test matrix.
- Initiate acquisition of experimental data.
- Initiate numerical studies with grid development and some simulations.

Accomplishments

- A test matrix to systematically vary fuel composition, swirl strength, fuel jet penetration, fuel jet location, and quarl type was developed and reviewed with DOE. Matrices comprising 48 combinations and 106 combinations were developed. The total number of cases to be run will be defined as testing proceeds.
- All test hardware required for the test matrix was fabricated and received in-house. This consists of a new quarl part and a new centerbody with interchangeable end caps to change fuel jet location and numbers. These parts compliment existing hardware and all configurations called for in the test plan can be run as desired.
- The planned laser Raman scattering diagnostic was established and assessed for capability of providing the desired spatially and temporally resolved information. The applicability proved to be mixed with the equipment available. A backup strategy involving microsampling probes will be relied upon as a result as work on getting the Raman method proceeds in parallel. An alternative strategy for time resolved information will also be pursued, namely planar laser induced fluorescence.
- Two-dimensional (2D) computational fluid dynamics (CFD) simulations were carried out for an axisymmetric co-flowing hydrogen/air jet arrangement as an initial demonstration of the sensitivity of mixing to the selection of models available in most codes.

Introduction

Efficient design and optimization of combustion hardware requires a combination of engineering experience and skill with effective tools to help evaluate design strategies. The development of lean premixed combustion strategies have resulted in significant advances in low emission, high efficiency gas turbines for operation on natural gas. These advances have been made possible in part by the use of advanced simulation tools like CFD. However, for high hydrogen containing fuels, the applicability of modeling strategies that worked well for natural gas may not be as accurate. As a result, (and as stated by the DOE's funding opportunity notice) research is needed to better characterize, understand, and model the fuel profile and unmixedness using turbine appropriate pre-mixer approaches for operation with low molecular weight, high mass diffusivity fuel mixtures containing high hydrogen levels. The outcomes will (1) help more efficiently design advanced fuel injection/combustion systems, (2) provide better understanding of the way in which new fuels mix with air/oxygen, and (3) provide a basis for better modeling approaches for the mixing behavior of fuels of interest.

In the present case of hydrogen, detailed measurements of fuel/air mixing for a systematic variation in a generic premixer geometry with controlled swirl, air side pressure drop, air turbulence levels, fuel injection location, fuel injection momentum, fuel/air density ratios, and fuel type. In addition, the details of the premixer aerodynamic field will be measured and calculated using CFD (large eddy simulation [LES]).

The proposed research is directed at evaluating methods for characterizing fuel profiles and unmixedness and applying these methods to provide detailed fuel concentration profile data that can be

used to develop and/or validate modeling approaches for determination of the fuel distribution produced by typical premixing strategies. The objectives of the proposed project are to (1) establish and apply reliable, accurate measurement methods to establish the instantaneous and time averaged fuel distribution at several locations downstream of the point of injection and (2) evaluate how CFD software model coefficients and approaches within affect the overall accuracy of the numerical simulations.

Approach

To accomplish the objectives of the project, two major tasks will be carried out. The first task is associated with the experimental study of fuel/air mixing. This task will require minor modifications to existing test hardware to configure it for the experiments planned. This consists of fabricating 12 axisymmetric parts that will interface with existing hardware. This task will also involve the preparation of the planned diagnostic techniques that will provide a critical evaluation of the accuracy and ability of each technique to measure the necessary quantities (e.g., time resolved/time averaged concentration of individual fuel species). With the developed hardware and diagnostics, measurements will be made systematically for a number of hardware geometry configurations which will result in detailed data for fuel concentration as a function of swirl, turbulence levels, injection location, injection type (e.g., centerline, radial, from spokes), fuel-to-air density ratio, and fuel type. In addition, the aerodynamic flow field produced by the test hardware will be delineated using an LES modeling approach coupled with detailed velocity measurements as validation. Using the results obtained, analysis will be carried out to establish physics-based design guides for the fuel/air behavior (e.g., rules for penetration vs. momentum flux ratio, rules for fuel plume spread vs appropriate non-dimensional groups).

The second major task is the application of different CFD modeling techniques to evaluate their ability to match the measured data over a wide range of conditions. Both Reynolds averaged Navier-Stokes (RANS) and LES will be used. For RANS, sensitivity to different turbulence models and model coefficients (e.g., Schmidt number) will be carried out to determine if a tuned RANS approach can be used. LES will be used as well and the results will establish the required CFD approach for correctly simulating mixing of a wide range of fuel types.

To the extent possible, UCI will work closely with the National Energy Technology Laboratory and original equipment manufacturer researchers relative to parametric simulations.

Results

Table 1 summarizes the plans for the initial testing/simulation geometries and conditions with a goal of varying the key phenomena associated with mixing processes. Two basic methods, radial and axial fuel injection, are being considered and for both methods a combination of parameters are being considered. For context, Figure 1 shows the test hardware which is based on a combination of existing and new components. Table 1 summarizes the parameters that are being varied for both experimental and numerical studies.

TABLE 1. Experimental Design

Factor	Levels	Comment
Swirl	– 0 (no swirl) – 45 deg axial vanes	
Quarl	– Straight Barrel (see Figure 1) – Tapered	
Injection Type	Radial Jets outward Axial at Centerline	
Injection Momentum	Low High	Defined based on jet to crossflow momentum flux ratio
Fuel Type	H_2/CO/Diluent blends	Could include as a mixture subdesign or select 3-4 discrete fuels

To get started with simulations in parallel with the development of hardware, effort has been directed at computations for a simplified 2D axisymmetry geometry for which existing data were available in the literature [1]. This study was the only one found with full measurements of flow field and hydrogen concentrations. The geometry associated with this study is shown in Figure 2. With this straightforward 2D geometry, a refined structured grid was applied

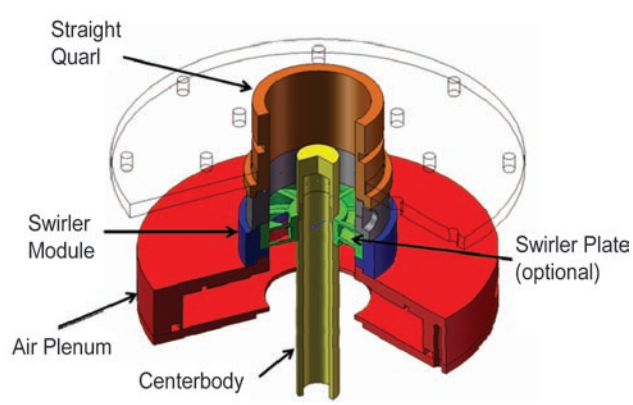

FIGURE 1. Test Hardware Sectioned View

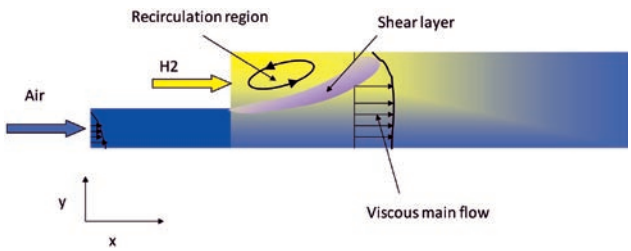

FIGURE 2. 2D Hydrogen-Air Mixing Experiments of Smith, Giel & Catalano, 1980

in order to gain some experience working with the different modeling approaches to help guide the three-dimensional (3D) simulations.

Table 2 summarizes the turbulence models considered in this exercise along with the "standard" arguments for their development and purported applicability. In reality, these models have evolved over the past four decades, and although it may be evident that they fulfill identified weaknesses in earlier models, the general overall improvement in performance must be fully assessed.

TABLE 2. Summary of Turbulence Models Considered

Turbulence Model	Purported Characteristics and Applications
Realizable k-epsilon model	Improved performance for swirling flow and recirculation, as low cost as the standard k-epsilon model.
Standard k-epsilon model	Common, low cost, good for simple high speed turbulent flows; poor performance in complex 3D, anisotropic turbulence such as swirl, recirculation, flow separation.
Renormalization group (RNG) k-epsilon model	Use RNG method; add analytic formulation for turbulent Prandtl number, improved performance for swirling flow and recirculation, slightly higher cost and harder to converge than the standard k-epsilon model.
Reynolds stress model (RSM)	Relatively complex and advanced, in principal can account for non-isotropic turbulent flows with swirl and recirculation.

Figure 3 shows a comparison of the axial velocity at the centerline of the flow using different turbulence models typically applied within commercial software codes. In addition, a radial profile of hydrogen concentration is also shown. The results illustrate the sensitivity of the velocity and concentration fields to the modeling approach chosen. The velocity profile is relatively insensitive to the modeling approach used, and the simulations, regardless of modeling approach applied, capture the basic trends shown by the measured profiles. Some discrepancies still exist however. Perhaps ironically, the "standard k-ε" model (i.e., one of the earliest turbulence closure models conceived) shows the best performance, illustrating the need to take care when interpreting the relative merit of "new and improved" models. Another issue that needs to be more rigorously addressed in the casual use of "acceptable agreement" when comparing simulations with measurements. In the current project, care will be taken to avoid this and to work to establish bounds for overall simulation accuracy that can be expected for the different premixer classes studied.

Also shown in Figure 3, the sensitivity of the hydrogen concentration to modeling approach is

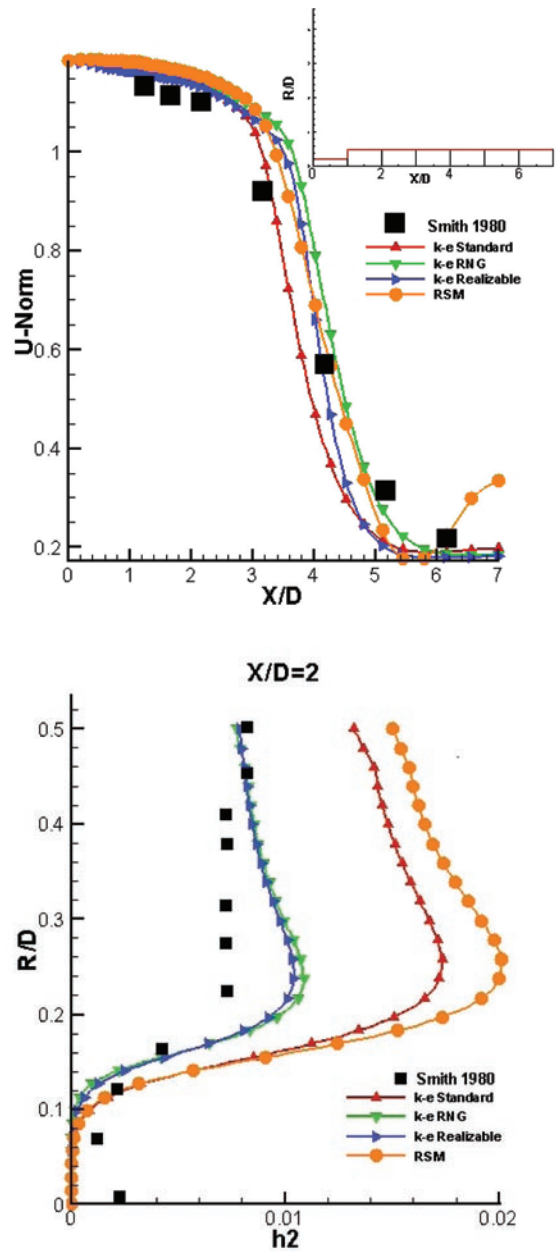

FIGURE 3. Example Velocity and Hydrogen Concentration Comparisons

much greater than is the velocity field. In this case, the simulation approach selected can result in factor of 3 variations from the measurements, whereas other approaches exhibit variation of 50%. Hence, the application of generally accepted simulation approaches for hydrogen/air mixing can generate highly varying results and thus great care must be taken with using these simulation methods for design screening, etc.

This is further illustrated by comparing contours of the hydrogen concentration as shown in Figure 4. Two basic patterns are shown depending on the modeling approach used, which is perhaps good as it illustrates two "classes" of simulation. What is needed is understanding and an explanation as to why the simulation approaches result in the differences shown. Generally speaking, the performance of the models strongly depends on geometry, conditions, flow fields, etc. Hence in the planned geometry and simulations for the present work, flows and features found within typical gas turbine premixers are included to help ensure the relevance of the findings to gas turbine systems.

Conclusions and Future Directions

Thus far, the experimental apparatus has been largely completed and various strategies for quantification of the hydrogen concentration evaluated. It is evident that multiple measurement methods will be required to obtain the information required for the validation of simulations and these are being applied now. The simulation approaches have been established and demonstrated and work has been done to reaffirm the challenge with effectively simulating the behavior of hydrogen/air systems in terms of fuel/air mixing. In the coming months, significant progress will be made towards completion of the systematic parametric study and conclusions will begin to be generated regarding recommended simulation approaches for the different premixer classes being evaluated.

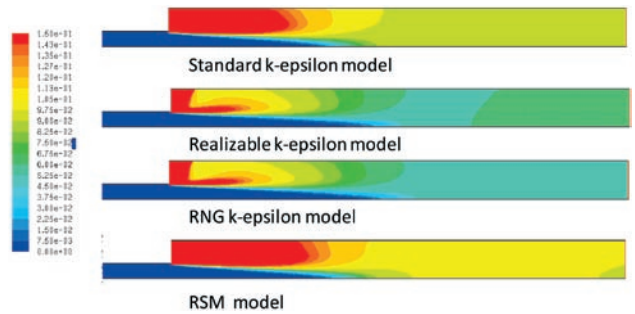

FIGURE 4. Comparison of Hydrogen Concentration Fields

FY 2009 Publications/Presentations

1. Quarterly Progress Report (October 2008 – December 2008), January 2009.

2. Quarterly Progress Report (January 2009 – March 2009), April 2009.

References

1. G.D. Smith, T.V. Giel, and C.G. Catalano (1980), "Measurements of Reactive Recirculating Jet Mixing in a Combustor," *AIAA Journal*, Vol. 21 (2), pp. 270-276.

V.B.6 High Pressure Kinetics of Syngas and Nearly Pure Hydrogen Fuels

Professor John W. Daily, Director
Center for Combustion and Environmental Research
Department of Mechanical Engineering
University of Colorado at Boulder (UC)
Boulder, CO 80309-0427
Phone: (303) 492-7110; Fax: (303) 492-3498
E-mail: john.daily@colorado.edu
Web site: http://spot.colorado.edu/~daily

DOE Project Manager: Mark Freeman
Phone: (412) 386-6094
E-mail: Mark.Freeman@netl.doe.gov

UTSR Manager of Research: Richard Wenglarz
Phone: (864) 656-2267
E-mail: RWNGLRZ@exchange.clemson.edu

Contract Number: 41431/UTSR 07-01-SR126

Start Date: May 15, 2007
End Date: May 14, 2010

FY 2009 Objectives

- Develop the necessary chemical kinetics information to understand the combustion of syngas and nearly pure hydrogen fuels at conditions of interest in gas turbine combustion.
- Explore high pressure kinetics by making detailed composition measurements of combustion intermediates and products in a flow reactor using molecular beam/mass spectrometry (MB/MS) and matrix isolation spectroscopy (MIS).
- Compare experimental data with calculations using existing mechanisms.
- Use theoretical methods to improve the predictability of existing mechanisms.

Accomplishments

Task I. "Select existing reaction mechanisms most likely to form a firm basis for extension to high pressure and carry out sensitivity and rate of production analysis to identify critical reactions and species."

Current chemical kinetic mechanisms do a poor job of predicting important combustion characteristics such as ignition delay at the low temperatures and high pressures found in gas turbine combustor inlets. Discrepancies of nearly three orders of magnitude in ignition delay exist between the theoretical predictions and experimental results at 700 K and 20 bar. Several paths were explored whereby gas phase reactions could explain the observed discrepancy. Reaction rate uncertainties for several modern mechanisms were first examined. Then, a chemometric approach was used to explore whether any important species and/or reactions were overlooked in the mechanisms. In particular, ozone and longer polyoxides were examined to see if they might produce additional chain branching. The possible role of sensitizers, in particular NO and NO_2, was investigated due to their known ability to induce chain branching reactions at lower pressures. Sensitivity to perturbations in the local thermodynamic state was also explored. These gas phase pathways seem extremely unlikely, and other explanations such as catalytic wall effects should be explored.

Task II. "Carry out experiments for conditions pertaining to gas turbine operation using both syngas and nearly pure H_2 fuels burned with air and oxygen. Measure species concentrations as a function of temperatures and pressure."

As described in previous reports, this task is being approached with a changed objective. Since it has been concluded that gas phase reactions cannot explain discrepancies between experiments and computations for properties such as ignition delay, focus has been shifted to catalytic wall reactions. To explore these experimentally, a high temperature micro nozzle flow reactor assembly has been designed and built. The flow reactor is designed to be able to change out reactor wall materials. Experiments are currently underway.

Task III. "Compare experimental results with predictions to identify shortcomings in reaction mechanisms. In particular identify, if any, important intermediate species not previously included in existing mechanisms."

A detailed computational fluid dynamics (CFD) analysis of the flow in the micro nozzle has been carried out to support interpretation of the experimental results. Density functional theory (DFT) is being used to explore the physical details of surface reactions.

Introduction

The objective of this project is to develop the necessary chemical kinetics information to understand the combustion of syngas and nearly pure hydrogen fuels at conditions of interest in gas turbine combustion. Syngas is the product of the gasification

of coal and/or biomass. The composition of syngas can vary considerably, but typically contains mostly hydrogen, CO and CO_2 with smaller amounts of CH_4, O_2, N_2, other hydrocarbons and water vapor. With further processing, the hydrogen content can be increased to fairly high levels. Both syngas and nearly pure H_2 mixtures can be oxidized either with air, or with pure oxygen, or any combination thereof. The use of any particular fuel/oxidizer combination in gas turbines will require an ability to predict important combustion properties such as laminar flame speed, autoignition conditions, flammability limits and NOx formation rates.

Approach

Combustion properties depend on the chemical kinetics of the fuel/oxidzer combination. Existing reaction mechanisms do a satisfactory job of predicting these properties at pressures close to atmospheric and below, but are less well tested at higher pressures in the range of 15-20 bar, especially at lower temperatures. The initial approach of this project was to explore the high pressure kinetics by making detailed composition measurements of combustion intermediates and products in a high pressure flow reactor using MB/MS and MIS. The data would then be compared with calculations using existing mechanisms. However, since concluding that gas phase reactions are not the cause of observed discrepancies between experiments and computation, the focus has shifted to catalytic wall reactions. An interesting aspect of wall reactions is that they are sensitive to pressure only through the concentration of gas phase species adjacent to the wall. This is unlike the gas phase, where high pressure amplifies the importance of tri-molecular reactions leading to the unusual explosion limit behavior of H_2/O_2 combustion. Thus, the experiments to explore reaction mechanisms do not need to be carried out at high pressure.

The approach of this project is to carry out experiments in a specially designed high temperature (hyperthermal) micro nozzle flow reactor in which surface material can be changed. (There is extensive experience in using these types of reactors at CU.) The flow reactor is shown in Figure 1. The assembly to the left of the gold flange is a solenoid activated valve. The nozzle/reactor is the small tube seen at the right end of the white insulating shield to the right of the gold flange. The tube can be manufactured using different materials of engineering and scientific interest. To date, tubes have been fabricated using alumina, which is inert, silicon carbide, which is known to be catalytically active, and stainless steel, which simulates current gas turbine premixed inlet materials. The tube can be heated electrically to controlled temperatures. Molecular beam/photoionization mass spectrometry (PIMS) and matrix isolation infrared (IR) spectroscopy are still being used for diagnostic purposes.

The complete experimental configuration (with IR diagnostics) is shown in Figure 2. Cold reactant gases are fed into the reactor where they pass over the heated surface. Both the diagnostics used require that the reactor tube exit into vacuum conditions. There is a practical limit to the mass flow rate that can be handled by the vacuum pumps. Therefore, the reactor is operated in a pulsed mode. In the case of PIMS the pulsed operation is also required to match the duty cycle of the pulsed laser ionization light source. The matrix diagnostic could be run continuously except for the pumping limitations just mentioned.

The experiments result in measurements of the compounds exiting the reactor, although not all products can be detected. When using PIMS, only species whose ionization potential is below 10.8 eV are detectable. This excludes H and O atoms, OH, and water. When using IR, only polyatomics and heterogeneous diatomics can be detected. Thus, H_2 and O_2 cannot be seen, but OH, water, CO and CO_2, etc. can be seen easily. Hydrogen-rich syngas is mainly composed of H_2 and CO. The products expected to

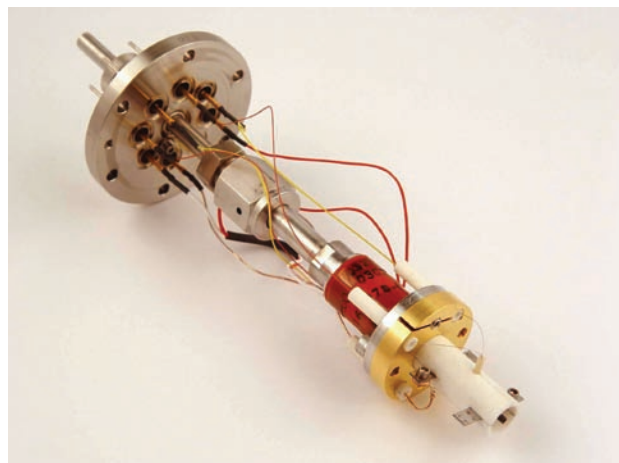

FIGURE 1. Hyperthermal Nozzle Assembly

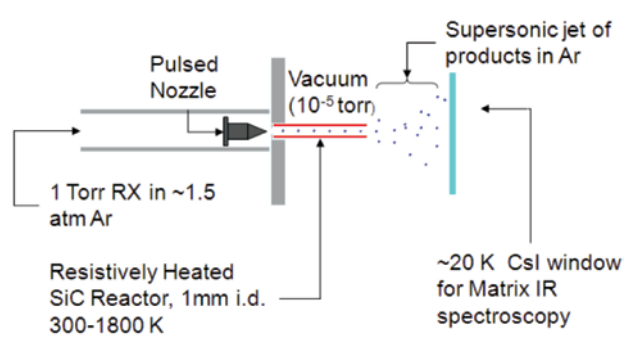

FIGURE 2. Experimental Configuration

if catalysis is present are OH, H_2O and CO_2. For this reason, efforts are presently focused on using the IR diagnostic.

Results

Reactor Simulations

It is necessary to have some understanding of the fluid and thermodynamic states within the reactor. Since the reactor is very small, it is impractical to carry out direct measurements within it. CFD was used to model the flow through the inlet system and reactor. The CFD results can be compared with flow rate measurements and with calibration kinetic measurements. Figure 3a shows the pressure distribution through the system when the inlet pressure is 2 atm. Figure 3b shows velocity profiles within the reactor. Temperature and pressure distributions are also calculated. Knowing the fluid and thermodynamic states within the reactor, one can also perform kinetic calculations. Figure 4 shows an example CHEMKIN simulation of the reactor flow assuming catalytic wall reactions. The inlet flow consisted of 2% H_2, 1% O_2 and the remainder the argon carrier gas. The Princeton gas phase and the Deutschmann surface mechanisms

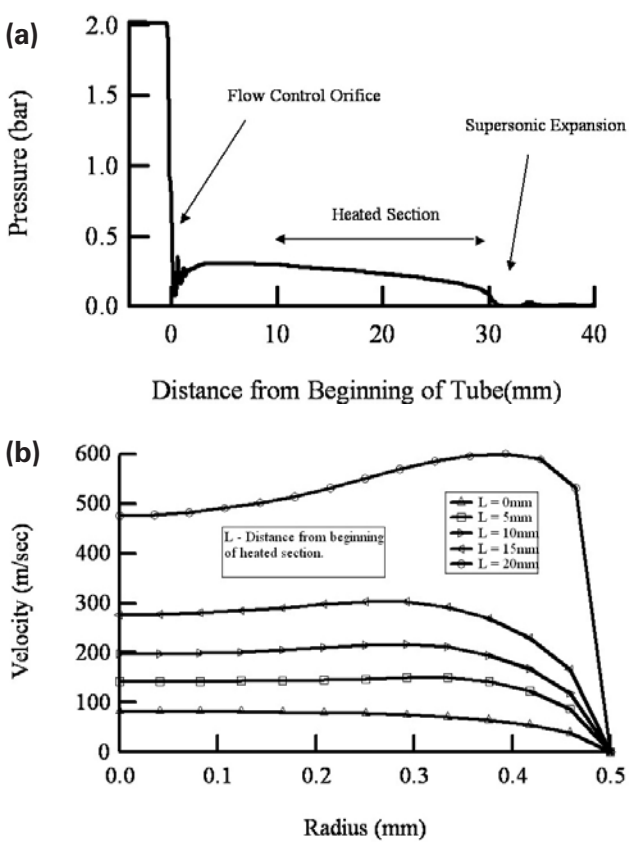

FIGURE 3. (a) Pressure Distribution Through Reaction from CFD Simulation and (b) Velocity Profiles in Reactor from CFD Simulation

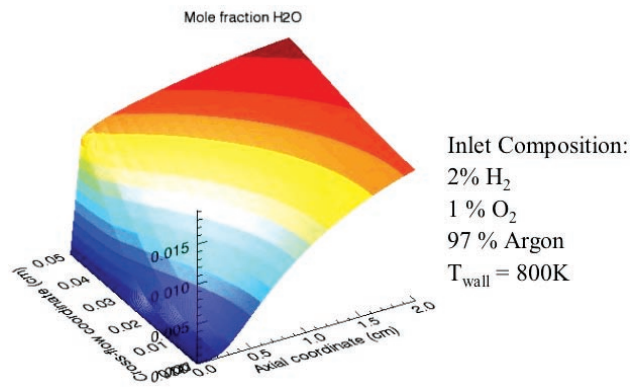

FIGURE 4. Water Distribution in Reactor when Wall Reaction Present

were used in the simulation. The surface mechanism probably respresents the upper limit for wall reaction rates and thus helps define the experimental range of conditions that need to be explored.

Calibration Experiments

Experiments with the new reactors are just beginning. To date, a few calibration runs have been completed. Figure 5a shows the IR spectra for a run of pure argon. The spectra illustrates the necessity to account for background amounts of water vapor and CO_2. Figure 5b shows the IR spectra for a run with 1/2/70 mixture of CO, O_2 and argon. Here the CO_2 and water background recede in comparison to the much larger CO spectrum. Figure 5c shows the IR spectra for a run with 1/70 mixture of CO_2 and argon. Here the CO_2 spectrum is prominent with background water receding.

These types of runs allow calibration of the IR signal levels with respect to gas concentration at the exit of the reactor. It appears that there will be ample signal to noise ratios to detect significant levels of reaction products when operating with various syngas compositions. In the production experiments, various mixtures of $H_2/CO/CO_2/O_2$ diluted in argon at concentrations sufficient to observe any meaningful chemical conversion will be run. In addition, the effect of hydrocarbon contaminants in the syngas will be explored.

Conclusions and Future Directions

Concluding that gas phase reactions are not the cause of observed discrepancies between experiments and computation has led to the exploration of catalytic wall reactions. Task II experiments are underway using a high temperature micro nozzle flow reactor facility. CFD simulations have been developed to assist in data interpretation. Preliminary calibration

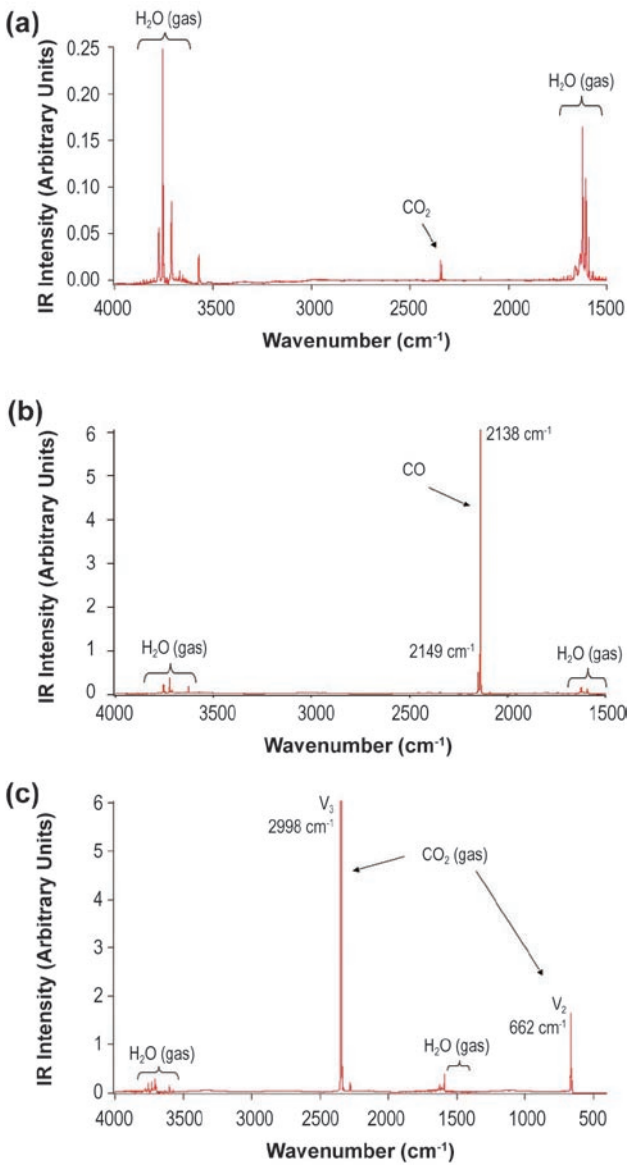

FIGURE 5. (a) IR Spectra for Argon Calibration Run at Room Temperature; (b) IR Spectra for Calibration Run with ($CO:O_2:Ar$) = (1:2:70) at Room Temperature; (c) IR Spectra for Calibration Run with ($CO_2:Ar$) = (1:70) at Room Temperature

experiments have demonstrated that the apparatus is working properly.

During the next reporting period, runs will be carried out using various syngas mixtures, including those with hydrocarbon contaminants. Each mixture will be run in reactors with each of the available wall materials and at a range of temperatures. At least one additional reactor will be fabricated from an advanced hastelloy type material with high nickel content. DFT quantum calculations to understand wall chemistry will continue to be explored.

FY 2009 Publications/Presentations

1. "Ignition Delay in High Pressure-Low Temperature Hydrogen Rich Syngas Combustion: Discrepancies between Experiment and Prediction," Poster presented at the International Combustion Symposium, Montreal, Canada, August 3–8, 2008.

2. "High Pressure Kinetics of Syngas and Nearly Pure Hydrogen Fuels," Talk presented at the UTSR Workshop October 28–29, 2008.

3. "High Pressure Kinetics of Syngas and Nearly Pure Hydrogen Fuels," Semi-annual report, November 15, 2008.

V. UNIVERSITY TURBINE SYSTEMS RESEARCH

C. Materials

V.C.1 Degradation of Thermal Barrier Coatings from Deposits and Its Mitigation

Prof. Nitin P. Padture
Ohio State University (OSU)
Department of Materials Science & Engineering
2041 North College Road
Watts Hall, Room 480
Columbus, OH 43210
Phone: (614) 247-8114; Fax: (614) 292-5241
E-mail: padture.1@osu.edu

DOE Project Manager: Mark Freeman
Phone: (412) 386-6094
E-mail: Mark.Freeman@netl.doe.gov

Contract Number: NT0006552

Start Date: October 1, 2008
End Date: September 30, 2011

FY 2009 Objectives

- To understand the thermal barrier coating (TBC) damage mechanisms due to deposits in integrated gasification combined cycle (IGCC) engines.
- To apply an approach that we have used to mitigate attack by calcium-magnesium-alumino-silicate (CMAS) in aero engine TBCs to IGCC engine TBCs.
- To provide a comprehensive understanding of degradation of TBCs from deposits and attendant mitigation approaches.

Accomplishments

During the last eight months different fly ash samples were collected from power plants and their morphology and composition were examined. Fly ash samples were applied to 7 wt% Y_2O_3 stablized ZrO_2 (7YSZ) air plasma spray (APS) TBCs and heat treated at 1,200 or 1,250°C. Some findings are given:

- Powder River Basin (PRB) and lignite fly ash samples have 6 wt% and 16 wt% of Fe_2O_3, respectively, apart from CMAS composition and other trace elements.
- Lignite and PRB fly ash have a broader particle size distribution, 5-50 μm.
- Deposits collected from turbine blades have up to 80 wt% Fe_2O_3 with traces of Ni, Co, Cr oxides.
- Powder River Basin fly ash composition has an intermediate phase between Ca_2SiO_4-$Ca_2Si_3O_7$-$CaAl_2O_4$-$Ca_2Al_2SiO_7$ on the ternary phase diagram, while lignite's phase is psuedowollastonite-gehlenite-anorthite.
- Fly ash samples completely diffused through the 7YSZ compositions APS TBCs when treated at 1,200°C or 1,250°C.
- A new TBC composition, $Gd_2Zr_2O_7$, is being tested to study the effect of CMAS and Fe_2O_3 interaction.
- A flame rig is being built at Ohio State University to study the thermal gradient response of TBCs with simultaneous injection of deposits and water.

Introduction

TBCs [1] are being used to protect and insulate hot-section metallic components in IGCC gas turbine engines. There is growing evidence that the use of syngas in IGCC engines results in different types of TBC degradation compared to TBCs in engines using conventional fuels. Owing to the use of syngas, deposits have been found to accumulate on the TBC surfaces in IGCC engines. The nature and mechanisms by which these deposits degrade IGCC TBCs is not clear at this time, but this could turn out to be a critical issue limiting the performance and durability of IGCC engines. In the proposed research we will use an approach that we have used to mitigate attack by CMAS in aero engine TBCs. The basic idea behind this approach is to have the TBCs serve as reservoirs of tailored chemical species that will interact with the deposits, and render the deposits benign by altering their chemical/phase makeup [2].

New TBCs will be fabricated using the APS method, which will be thoroughly characterized. The new TBCs will be coated with simulated deposits and tested under isothermal conditions with various levels of water vapor in the environment. The TBCs will also be tested under thermal gradient [3] conditions. The tested TBCs will be thoroughly characterized to understand the mitigation mechanisms. These results will be analyzed for a comprehensive understanding. The optimized compositions and microstructures will be transferred to original equipment manufacturer companies for further development and possible commercialization.

Approach

Two fly ash samples namely, PRB and lignite were collected from power plants. These powders were ball milled for three days to get uniform particle size distribution. A scanning electron microscope (SEM) equipped with energy dispersive X-ray spectroscopy (EDS) facility available at Campus Electron Optics

Facility, OSU was utilized to probe the sample morphology and chemistry. PRB, lignite and the TBC deposit samples were analyzed on a Rigaku ZSX-101e wavelength dispersive X-ray fluorescence (XRF) spectrometer and on a Perkin Elmer Optima 3000 inductively coupled plasma optical emission spectrometer at OSU. Thermal analysis was performed on a SDT Q 600 differential scanning calorimetry system. A predetermined fly ash sample was brush coated onto air APS TBCs and heat treated at 1,200 or 1,250°C in air for 24 hrs to examine the diffusion of fly ash elements into the TBC layer.

Results

Two fly ash samples, namely PRB and lignite were subjected to SEM/EDS analysis to understand size and elemental composition. Size analysis on as procured samples revealed a broader size distribution from 5-50 mm. The mean particle diameter is observed to be 2-5 microns after 3 days of ball milling. Powder X-ray patterns showed a complex composition with huge silica/quartz and other compounds involving silicon, calcium, magnesium, aluminum, potassium, iron oxides, chlorides and phosphates.

EDS studies showed Si, C, Al, Ca, and O as major constituents, and Fe, Mg, Na, P, S in trace amounts, with 5-30 micron size distribution. Lignite powder has a large size distribution from 10-50 micron. It is found that lignite is mainly Si, C, O, Al, and Ca, and has Fe, Ti, Mg, Na, K, F, P, S in small quantities.

The elemental analysis on PRB and lignite fly ash is primarily composed of CaO, Al_2O_3, SiO_2, Fe_2O_3 and MgO with low concentrations of other elements. However, the deposits collected from turbine blade are constituted with 80% of Fe_2O_3 along with traces of other magnetic elements. Table 1 presents the composition for PRB and lignite derived from XRF analysis. Both lignite and PRB samples have CMAS composition along with excess Fe_2O_3 phase. Differential thermal analysis (Figure 1) showed a large weight loss around 500°C, which is the attributed to organic compound decomposition.

TABLE 1. Elemental Composition (wt%) of PRB and Lignite Fly Ash Derived from XRF Analysis

	SiO_2	CaO	Fe_2O_3	Al_2O_3	Cr_2O_3	MgO	SO_3
Lignite	29.1	24.9	16.1	14.4	5.02	3.48	1.74
PRB	22.1	42.2	6.13	10.5	-	6.92	5.74

	TiO_2	SrO	MnO	K_2O	Na_2O	NiO	P_2O_5
Lignite	1.09	0.96	0.85	0.78	0.59	0.5	0.15
PRB	2.24	0.31	-	0.5	1.77	-	1.74

Figure 2 illustrates the intermediate phase composition of PRB and lignite fly ash samples on a redrawn ternary phase diagram. Fly ash composition is calculated from the elemental analysis performed with XRF spectroscopy. Mole fraction of three major constituents SiO_2, Al_2O_3 and CaO are considered to determine the phase composition. It is very important to notice that the lignite composition points to the glassy psuedowollastonite-gehlenite-anorthite intermediate phase; and PRB has Ca_2SiO_4-$Ca_2Si_3O_7$-$CaAl_2O_4$-$Ca_2Al_2SiO_7$ intermediate phase. Based on the previous results [2] it is essential to transform the phase glassy composition to crystalline anorthite, which could arrest the advancement of CMAS into TBCs.

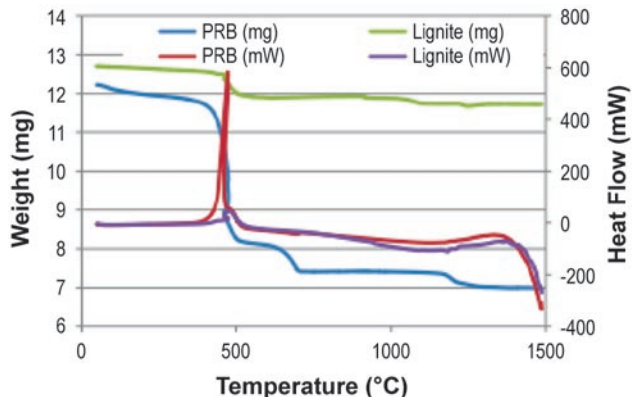

FIGURE 1. Thermogravimetric analysis on the PRB and lignite fly ash samples shows the decomposition of organic content at 450°C.

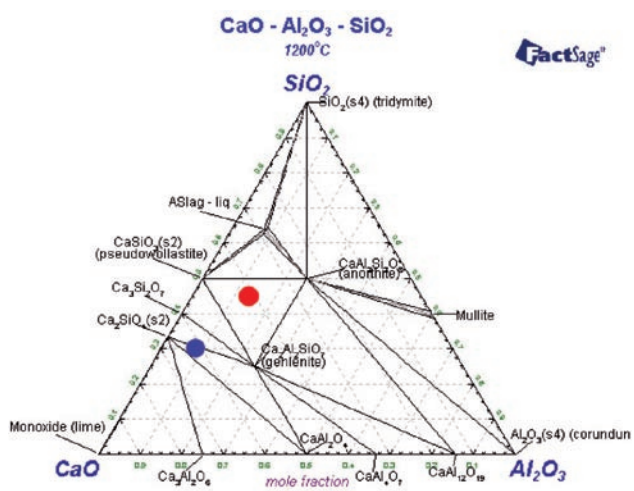

FIGURE 2. The redrawn ternary phase diagram at 1,200°C showing an intermediate Ca_2SiO_4-$Ca_2Si_3O_7$-$CaAl_2O_4$-$Ca_2Al_2SiO_7$ phase for PRB (blue circle) and psuedowollastonite-gehlenite-anorthite phase for lignite (red circle) when considering the CaO-Al_2O_3-SiO_2 in appropriate mole percentage. The mole percentage composition is estimated using the XRF analysis.

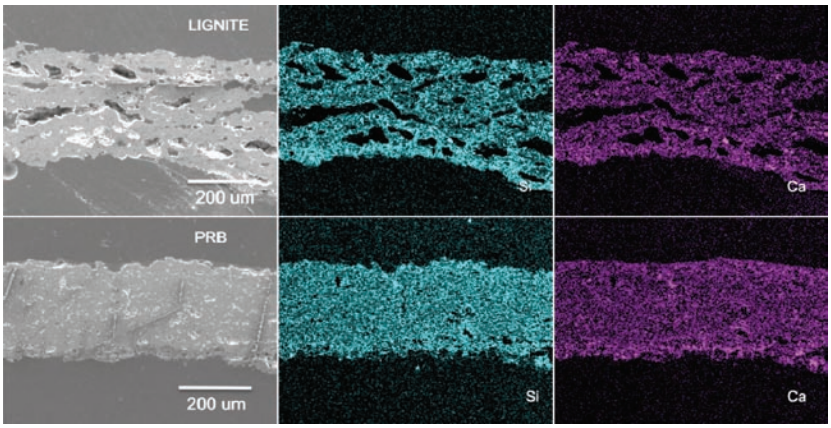

FIGURE 3. SEM image and elemental mapping on cross-sectional samples of TBCs treated with lignite and PRB at 1,200°C for 24 hrs in air. It is obvious that Si and Ca are diffusing through the TBC.

7YSZ composition APS TBCs were treated with PRB and lignite fly ash samples and heat treated at 1,200°C or 1,250°C for 24 hrs in air. Cross-sectional images were obtained using SEM. Elemental mapping on these samples demonstrated the complete ingestion of fly ash samples into the TBCs. Fly ash samples completely destroyed the TBCs as shown by the representative elemental mapping images (Figure 3, cross-sectional view).

Conclusions and Future Directions

Preliminary studies on PRB and lignite fly ash samples were performed to identify the morphology and composition. PRB and lignite samples were found to have CaO, SiO_2, Al_2O_3, Fe_2O_3, MgO in major proportions. PRB composition has an intermediate phase between Ca_2SiO_4-$Ca_2Si_3O_7$-$CaAl_2O_4$-$Ca_2Al_2SiO_7$ on the ternary phase diagram while lignite's phase is psuedowollastonite-gehlenite-anorthite. Fly ash samples completely diffused through the 7YSZ compositions APS TBC when treated at 1,200°C or 1,250°C. New TBC compositions, such as $Gd_2Zr_2O_7$, which are resistant to the fly ash composition, are being designed and tested in the coming months. The TBCs with and without the fly ash deposits will be tested under isothermal conditions (furnace) in environments containing different water vapor contents (0 to 20%). This will enable us to study the effect of temperature and water vapor on the chemical attack of TBCs. Selected TBCs will also be tested under thermal-gradient conditions. A thermal gradient flame-rig is being built in the laboratory at OSU to perform these tests.

Special Recognitions & Awards/Patents Issued

1. The principal investigator, Prof. Nitin P. Padture, was elected Fellow of the American Association for the Advancement of Science (AAAS) in February 2009 for "outstanding contributions to the field of advanced ceramics and nanomaterials, particularly for understanding of processing and mechanical behavior of ceramic composites and coatings." AAAS is the largest general scientific society in the world serving over 10 million individuals, and it publishes the journal *Science*.

FY 2009 Publications/Presentations

1. J. Drexler, A. Aygun and N.P. Padture, "Novel Thermal Barrier Coatings That Are Resistant to Molten Deposits Attack," Presentation at PACRIM 2009 Conference, The American Ceramic Society, Vancouver, Canada, June 2009.

2. N.P. Padture, "Novel Thermal Barrier Coatings," Colloquium presented at the Case Western Reserve University, Cleveland, Ohio, February 2009.

References

1. N.P. Padture, M. Gell and E.H. Jordan, "Thermal Barrier Coatings for Gas-Turbine Engine Applications," Science, 296, 280-84 (2002).

2. A. Aygun, A.L. Vasiliev, N.P. Padture and X. Ma, "Novel Thermal Barrier Coatings That Are Resistant to High-Temperature Attack by Glassy Deposits," Acta Mater., 55, 6734-45 (2007).

3. A.G. Evans and J.W. Hutchinson, "The Mechanics of Coating Delamination in Thermal Gradients," Surf. Coat. Technol., 201, 7905-16 (2007).

V.C.2 Evaluating Coatings for Current and Future Service

Associate Prof. Ted Bennett
University of California, Santa Barbara
Department of Mechanical Engineering
Santa Barbara, CA 93106
Phone: (805) 893-8115; Fax: (805) 893-8651
E-mail: bennett@engineering.ucsb.edu

DOE Project Manager: Mark Freeman
Phone: (412) 386-6094
E-mail: Mark.Freeman@netl.doe.gov

UTSR Manager of Research: Richard Wenglarz
Phone: (864) 656-2267
E-mail: RWNGLRZ@exchange.clemson.edu

Contract Number: 41431/UTSR 07-01-SR125

Start Date: October 1, 2007
End Date: September 30, 2009

FY 2009 Objectives

- Provide quantitative nondestructive measurements of the thermal protection offered by coatings on servable engine parts.
- Understand how individual elements of service related change effects the thermal protection provided by a coating.
- Monitor the complex physical changes that precede coating failure.

Accomplishments

- Validation measurements demonstrating 2% agreement in thermal diffusivity, 5% agreement in thermal conductivities, and 7% agreeement in volumetric heat capacity on a well characterized sample.
- Investigated the relationship between coating density and thermal conductivity on an actual engine blade.
- Investigation into the changing thermal characteristics of coatings exposed to isothermal high temperature.

Introduction

Thermal barrier coatings (TBCs) must demonstrate many favorable characteristics to perform satisfactorily. In addition to providing thermal protection, coatings must survive cyclic heating to high temperatures, and offer good resistance to mechanical and chemical forms of degradation [1-4]. The standard metric of thermal performance, with which coating materials are evaluated, is thermal conductivity. Although thermal property measurements are routinely reported in the literature, such measurements are not straightforward.

Prior to our work, the quantitative nondestructive measurement of the thermal protection offered by a coating was not among the measurements one could employ on serviceable engine parts (or even on many experimental specimens). Our research concerns a first-principle measurement for quantifying thermal properties of coatings without specialized sample preparation. These measurements carry sufficient quantitative value to make meaningful assessments and comparisons of different coating materials, and can be richly descriptive of the multifaceted nature of service related change over the lifetime of a coating.

Approach

The principle of Phase of Photo-Thermal Emission Analysis (PopTea) is to determine coating thermal properties from indirect interrogation of the temperature phase established in a coating by periodic heating. The experimental measurement is shown schematically in Figure 1. A CO_2 laser is used as a heat source because of its good intrinsic ability to couple energy to zirconia-based coatings. An external opto-acoustic modulator creates a harmonic laser intensity used to heat the coating. An analytic model has been developed to calculate the transient temperature in the

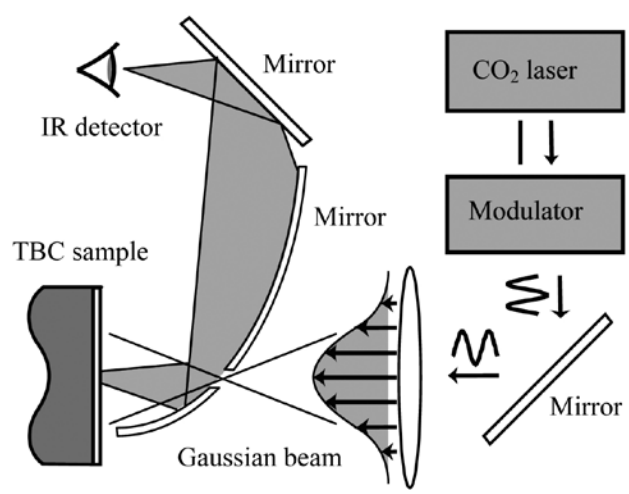

FIGURE 1. Schematic of PopTea Measurement Tool

TBC as a function of unknown material properties and known geometric parameters [5].

Thermal emission from the coating in the near infrared is measured with an indium antimonide detector. The peak sensitivity of the detector is at 5 μm. Because zirconia-based coatings are translucent in the near infrared [6], emission originates from a volume of the coating, and does not correspond to the temperature conditions at one specific location (e.g., the surface). With knowledge of the temperature field, a description of the radiative field is created to predict the phase of the thermal emission evolving from the coating [7]. The calculated phase of thermal emission is compared with experimental measurements to evaluate candidate solutions to the coating properties. A set of measurements consists of recording the phase of thermal emission as a function of laser heat frequency. The phase of thermal emission lags behind the phase of laser heating. This phase difference is the primary measurement that is performed over frequency space. Laser frequencies are selected such that a wide range of thermal penetration depths are achieved in the measurement: from a small fraction of the coating thickness to greater than the coating thickness.

Results

The PopTea measurement is validated by comparison with diffusivity measurements obtained by thermal flash. Thermal flash measurements were performed in Ref. [8] on a thin free-standing Corning 0211 Microsheet. To make comparative measurements, the 185 μm thick Corning 0211 Microsheet was bonded to a superalloy-based metal with Pelco™ Colloidal Silver Liquid and measured by the PopTea method. PopTea measurements were conducted at a temperature of 70°C. Table I shows the comparison of thermal properties obtained by the two methods. Thermal diffusivities agree within 2%, the thermal conductivities agree within 5%, and the volumetric heat capacity agrees within 7%. It should be noted that for the thermal conductivity to be measured by the flash method, two addition measurements were required to obtain the glass density and the specific heat. In contrast, the PopTea measurement was the sole measurement used to determine all the thermal properties in the current investigation. As an additional data point, the manufacturer reports a thermal conductivity of 0.96 W/m/K for Corning 0211, but the temperature at which this measurement was made is uncertain.[1]

[1] Corning 0211 Microsheet Product Information sheet specifies that the thermal conductivity value is for 0°C, which seems unlikely in light of the measurements made here and in Ref [8].

TABLE I. Measured Corning 0211 Thermal Properties

	PopTea (at 7°C)	Ref. [11] (at 70°C)
α (mm^2/s)	0.418	0.426
k_z (W/m/K)	0.938	0.90
pC (J/cm^3/K)	2.25	2.1

Recent measurements were made on an actual turbine blade, provided by Siemens Power Generator, Inc. The coating on this blade is a 7 wt% yttria-stabilized zirconia air plasma spray (APS) that has seen no service. The blade base metal is a single crystal Ni-based superalloy (IN939). PopTea measurements were made at 17 locations on the blade and the thermal properties analyzed. The thickness of the coating was determined using the eddy current technique. PopTea can be used to measure the porosity of the blade coating, since both the specific heat and the theoretical bulk density of the coating material are well known. As a consequence, an investigation can be made into the relationship between coating thermal conductivity and coating porosity from the blade measurements. Figure 2 shows the thermal conductivity measurements plotted against porosity, as determined from the density measurements. The data indicates a trend in which the thermal conductivity of the coating decreases with increasing porosity. This makes physical sense, since increasing porosity means increasing the content of air gaps and interfaces in the microstructure. These results are in agreement with an independent study

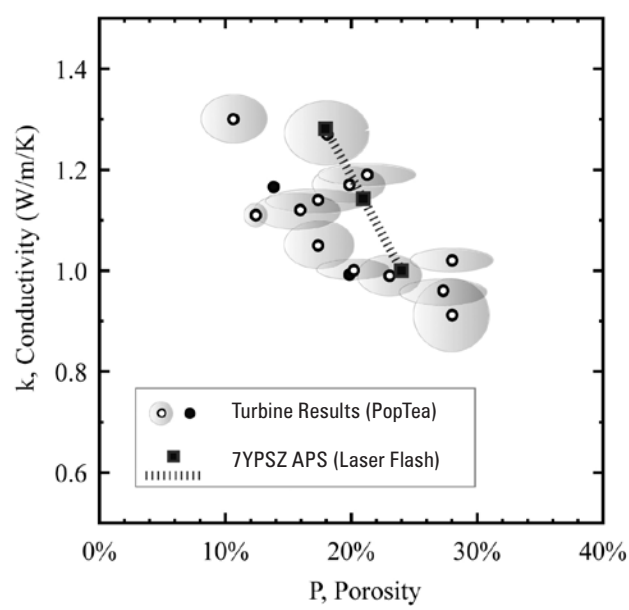

FIGURE 2. Relationship between thermal conductivity and porosity of the coating on a turbine blade. Uncertainty is related to the hollow circles which represent multiple measurements. Solid circles identify single measurements. Solid square symbols are data from Ref. [9].

(also shown in Figure 2) [9]. In that work, the thermal properties of the coatings were evaluated with laser flash and the porosity was determined from the weight to volume ratio. This measurement procedure would be impossible to perform on actual engine hardware. Both studies have nearly the same median value of coating porosity, and show the same trend with respect to decreasing thermal conductivity with increasing porosity. The current results suggest that a larger spread in porosity is supported by the APS coating on the blade than the coating investigated in Ref. [9]. The earlier studies suggest that thermal conductivity has a steeper dependency on porosity than the current study. For example, a linear extrapolation of their results suggests that the coating thermal conductivity goes to zero at a porosity of 47%. However, it is known that such factors as pore orientation, in addition to pore fraction, influence the thermal conductivity of a coating [10]. Therefore, it is reasonable to argue that the relationship between thermal conductivity and porosity alone could be nonlinear. These measurements demonstrate the utility of PopTea for characterization of coatings on serviceable engine hardware.

The development of new coating systems is reliant on studies that investigate thermal performance under service conditions. An important area of study investigates the coating response to high temperature exposure. The thermal properties of coatings can change as interfaces within the coating material evolve with high temperature exposure. Additionally, the mechanical integrity of the coating interface with the substrate system (bond-coat/superalloy) can be compromised by reactive chemistry and stresses caused by thermal expansion mismatch. To illustrate, we investigated two new coating systems "A" and "B", both deposited on the same superalloy/bond-coat system. After one hour heat treatment in argon, the coating systems were exposed to 100 hours of isothermal furnace heating at 1,150°C in air. Thermal property measurements were performed three times: after an initial one hour heat treatment in argon, after 10 hours heat treatment in air, and after 100 hours heat treatment in air. Infrared images of the coatings were also taken at the time of the PopTea thermal property measurements. These images are taken when the back surface of the sample substrate is held at 65°C. When the interface between the coating and the superalloy substrate material is disrupted, the infrared camera images show increased grayscale contrast caused by regions of cooler coating material (overlying the delaminated areas) and by changes in the optical properties of the interface (since the coating is translucent in the near infrared). Therefore, such images are useful in qualifying the state of the interface between the coating and the substrate system.

Figures 3 and 4 show contrasting behavior for the two different coating systems to isothermal aging at

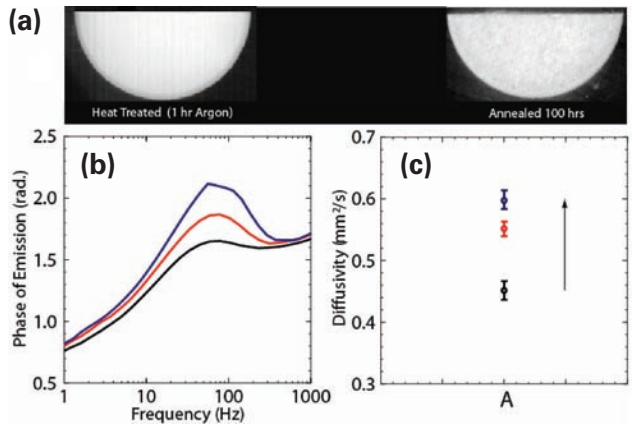

FIGURE 3. Isothermal aging of system "A." a) Infrared images of the coating; b) raw phase of thermal emission data; c) coating thermal diffusivity measurements.

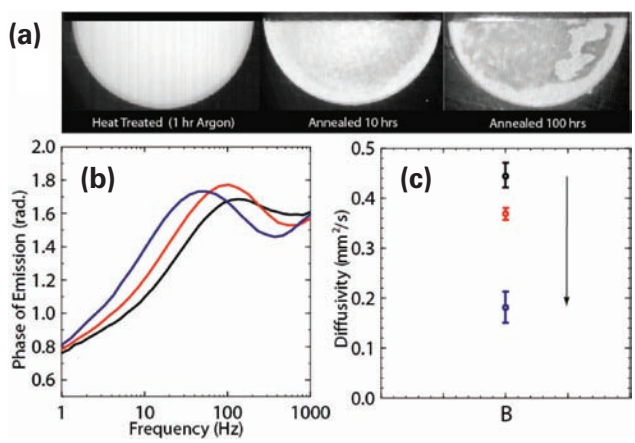

FIGURE 4. Isothermal aging of system "B." a) Infrared images of the coating; b) raw phase of thermal emission data; c) coating thermal diffusivity measurements.

1,150°C in air. Each figure shows the results of thermal diffusivity measurements, the infrared camera images, and the raw phase of thermal emission data from the PopTea measurement. For system A, isothermal aging drove the thermal diffusivity higher with lengthening exposure time. Most of the change occurred in the first 10 hours, but the measurement made after 100 hours still showed higher thermal diffusivity over the 10-hour measurement. For system A, the infrared images of the coating shows little change, indicating that the integrity of the interface after 100 hours is still good. However, the raw phase of thermal emission data shows marked rise in the peak phase of emission. This trend can be explained with the observation that the phase of thermal emission is influenced by the percentage of emission coming from the coating versus the underlying interface with the substrate system. As the thermal diffusivity of the coating rises, enhanced

heat transfer to the interface causes its contribution to increase. Because the heat transfer to the interface is over a greater distance, the phase lag of this contribution is greater. Because of the combination of these effects, the peak in the phase of emission spectra grows, as seen in Figure 3.

Figure 4 shows the contrasting behavior of coating system B. The infrared images show a marked increase in grayscale contrast with isothermal aging time. This indicates a failure at the interface between the coating and substrate system. Additionally, the diffusivity is seen to decrease with isothermal exposure time, which is the opposite trend from system A. In these measurements, the influence of the coating resistance to heat transfer is not distinguished from the interfacial thermal contact resistance between the coating and the substrate system. Therefore, the fall in thermal diffusivity is caused by the dominant effect of a rising thermal contact resistance at the interface. The raw phase of thermal emission data from the PopTea measurement also reveals an interesting contrast between system A and B. Although system A exhibited a growth in the peak phase of thermal emission value, system B reveals the peak shifting out to lower laser heating frequencies. The peak does not grow because the degrading thermal contact between the coating and substrate system does not allow for greater emission from the substrate. The peak shifts out to lower frequencies as a consequence of the overall rise in resistance for heat transfer to the substrate.

Conclusions and Future Directions

In this report, the quantitative success of the PopTea measurement was demonstrated by the accurate measurement of a Corning 0211 glass cover slip, having known thermal properties, that was bounded to a superalloy. Agreement in thermal diffusivity is within 2%, the thermal conductivities within 5%, and the volumetric heat capacity within 7%. We also demonstrated the ability to perform fundamental studies of coating applied to actual engine hardware. In this report, the relationship between coating porosity and thermal conductivity was investigated. Finally, we have demonstrated the utility of the PopTea measurements for investigating the high temperature performance of new coatings under development. Contrasting behaviors of coating systems can be understood, and quantitatively addressed, with PopTea measurements.

Future work will look at the further quantification of changes in the thermal contact resistance when a coating debonds from the substrate system. In the current analysis, the rising thermal contact resistance between the coating and the substrate convolutes the measured thermal properties of the coating. Therefore, it is desirable to deconvolute changes in the intrinsic properties of the coating material from changes in the thermal contact resistance between the coating and the substrate system.

FY 2009 Publications/Presentations

1. Ted D. Bennett, Tyler R. Kakuda, and Anand Kulkarni, "Front Surface Thermal Property Measurements of Air Plasma Spray Coatings," Journal of Applied Physics 105 (2009) 083501-1.

2. Tyler R. Kakuda, Andi M. Limarga, Ted D. Bennett, and David R. Clarke, "Evolution of Thermal Properties of EB-PVD 7YSZ Thermal Barrier Coatings with Thermal Cycling," Acta Materialia 57 (2009) 2583–2591.

3. Ted D. Bennett and Tyler Kakuda, "The Nondestructive Measurement of Thermal Barrier Coatings Thermal Properties," Proceeding of the 55th International Instrumentation Symposium, June 1–5, 2009, South Shore Harbour Resort & Conference Center, League City, Texas.

References

1. M.Y. Ali, "Creep Effects on Early Damage Initiation in a TBC System," Journal of Materials Science 39 (2004) 3383-3390.

2. B. Baufeld, "Life Time Dependency on the Pre-Coating Treatment of a Thermal Barrier Coating under Thermal Cycling," Surface and Coatings Technology 201 (2006) 2667-2675.

3. A. Feuerstein, "Technical and Economical Aspects of Current Thermal Barrier Coating Systems for Gas Turbine Engines by Thermal Spray and EBPVD: A Review," Journal of Thermal Spray Technology 17 (2008) 199-213.

4. S. Marinetti, "Thermographic Inspection of TBC Coated Gas Turbine Blades: Discrimination Between Coating Over-Thicknesses and Adhesion Defects," Infrared Physics & Technology 49 (2007) 281-285.

5. T.D. Bennett, T. Kakuda, and A. Kulkarni, "Front Surface Thermal Property Measurements of Air Plasma Spray Coatings," Journal of Applied Physics 105 (2009) 083501-1.

6. R. Siegel and C.M. Spuckler, "Analysis of Thermal Radiation Effects on Temperatures in Turbine Engine Thermal Barrier Coatings," Materials Science & Engineering A (Structural Materials: Properties, Microstructure and Processing) A245(2) (1998) 150-9.

7. T.D. Bennett, "Complex Combination Solution for Radiation-Conduction Transport with Periodic Boundary Conditions," International Journal of Heat and Mass Transfer 46(13) (2003) 2341-2351.

8. R. Ikkawi, N. Amos, A. Lavrenov, A. Krichevsky, D. Teweldebrhan, S. Ghosh, A.A. Balandin, D. Litvinov, and S. Khizroev, "Near-Field Optical Transducer for Heat-Assisted Magnetic Recording for Beyond-10-Tbit/in^2 Densities," Journal of Nanoelectronics and Optoelectronics 3 (2008) 44–54.

9. Y. Sohn, "Microstructural Characterization of Thermal Barrier Coatings on High Pressure Turbine Blades," Surface & Coatings Technology 146 (2001) 132-139.

10. G. Bertrand, "Low Conductivity Plasma Sprayed Thermal Barrier Coating Using Hollow psz Spheres: Correlation Between Thermophysical Properties and Microstructure," Surface & Coatings Technology 202(10) (2008) 1994-2001.

V.C.3 Materials for Oxy-Fuel Turbomachine Conditions

Professor Gerald H. Meier and
Professor Frederick S. Pettit
Department of Mechanical Engineering and Materials Science
848 Benedum Hall
University of Pittsburgh
Pittsburgh, PA 15261
Phone: (412) 624-9720; Fax: (412) 624-8069
E-mail: ghmeier@pitt.edu; pettitfs@pitt.edu

DOE Project Manager: Mark Freeman
Phone: (412) 386-6094
E-mail: Mark.Freeman@netl.doe.gov

UTSR Manager of Research: Richard Wenglarz
Phone: (864) 656-2267
E-mail: RWNGLRZ@exchange.clemson.edu

Contract Number: 41431/UTSR 06-01-SR124

Start Date: July 15, 2007
End Date: July 14, 2010

FY 2009 Objectives

The overall objective of this investigation is to evaluate the durability of turbine materials at the temperatures and oxygen pressures typical of those in the high steam and CO_2 levels expected in coal-based oxy-fuel systems. Specific objectives include:

- Evaluating the performance of candidate alloys and coatings in environments starting with 85% steam and 15% CO_2 (by volume) and then for reduced levels of steam to accommodate up to 5% O_2, which may represent excess oxygen needed to assure complete oxy-fuel combustion.
- Advancing the existing knowledge of how steam (water vapor) affects the selective oxidation of high temperature alloys.
- Investigate the effects of carbon and hydrogen on the oxidation and ductility of alloys exposed to H_2O-CO_2 mixtures.
- Examine the effects of contaminants such as SO_2 and alkali deposits ($(Na, K)_2 SO_4$, CaO) on the degradation of alloys in H_2O-CO_2 gas mixtures.

Accomplishments

This project is in the second year of a three year effort. Accomplishments achieved since the initiation of this project are as follows:

- Alloys to be studied in this project, namely René N5, IN 738, and GTD 111 have been obtained and specimens have been coated with a platinum aluminide coating. Specimens of the NiCoCrAlY have been obtained.
- An apparatus has been constructed whereby coupon specimens can be exposed to gas mixtures containing 85% H_2O-15% CO_2 at temperatures from 700°C to 1,100°C.
- Oxidation data existing in the literature for the alloys and coatings being studied in this project have been tabulated to compare with results generated in this project.
- Specimens of René N5, IN 738, GTD 111, and platinum aluminide coated René N5 have been exposed in dry air, 10% H_2O-90% air and 85% H_2O-15% CO_2 at 900°C and 950°C. Severe attack of these alloys and coatings was not observed in any of these gas environments. Such results indicate that these alloys will not be severely degraded in the high steam and CO_2 levels expected in coal-based oxy-fuel systems.

Introduction

In order for coal-based oxy-fuel systems to be used, it is necessary to investigate the effects of combustion gases containing 85% steam and 15% CO_2 on the degradation of gas turbine alloys and coatings at temperatures between 700°C (1,292°F) and 1,100°C (2,012°F). The upper temperature limit has been selected since the adverse effects produced by these gaseous species may be more obvious at the higher temperatures. The experimental approach for this investigation consists of exposing relevant alloys and coatings to controlled gas mixtures containing H_2O, CO_2, and O_2 at temperatures of interest. The presence of oxygen in some of the gas mixtures is necessary because when oxygen is added to the gas mixture of H_2O and CO_2, the attack may not be as severe as when it is absent. The degradation of the exposed specimens will be documented by using weight change versus time measurements, X-ray diffraction, scanning electron microscopy, and optical metallography.

Approach

To achieve the project objectives the alloys René N5, GTD 111 and IN 738 as well as these alloys with a platinum modified aluminide and a NiCoCrAlY coating will be exposed to gas mixtures containing

85% H_2O-15% CO_2 and 80% H_2O-15% CO_2-5% O_2 at temperatures between 700°C and 1,100°C. The exposed specimens will be examined using optical metallography, scanning electron microscopy, and X-ray diffraction to document the attack of these alloys. As the degradation of these alloys induced by the two gas mixtures becomes understood, additional experiments will be performed to examine the effects of contaminants (i.e., SO_2, CaO, $(Na, K)_2 SO_4$). This work is to be performed over two years. In a third year of this project, the performance of thermal barrier coatings exposed to the conditions described above is to be studied.

Results

Specimens of the three alloys have been obtained and specimens of these alloys have been coated. An existing cyclic oxidation apparatus has been modified such that gas mixtures of 85% H_2O-15% CO_2 can be obtained. Finally, data that is available on these alloys and coatings for exposure in air with water vapor at pressures of 10.13 kPa (0.1 atm) and 50.65 kPa (0.5 atm) at the temperatures of interest have been obtained and will be used to compare with the data to be generated in the H_2O-CO_2 gas mixtures.

The alloys, René N5, IN 738, GTD 111, a platinum aluminide coating on René N5 have been exposed at 900°C and 950°C in dry air, air with 85% H_2O, and in a gas mixture containing 85% H_2O-15% CO_2. Scanning electron micrographs of some of these specimens after exposure for 340 cycles (1 cycle: 10 minutes heat, 45 minutes at temperature and 10 minutes cool to room temperature) are presented. Figures 1, 2, and 3 where the amount of oxidation of the uncoated alloys in air and 85% H_2O-15% CO_2 are compared. The amount of oxidation of the alloys is not significantly different when air and the gas mixture are compared.

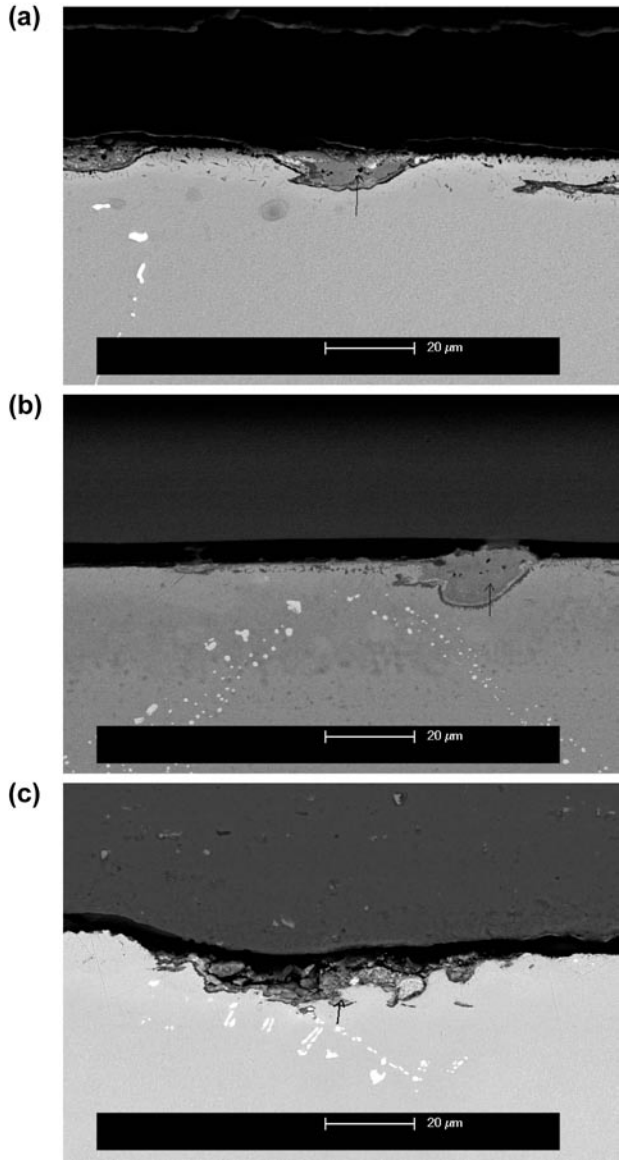

FIGURE 1. Scanning electron micrographs of René N5 metallographic cross-sections after exposure for 30 cycles (a) at 950°C in dry air, (b) in air with 85% H_2O, and (c) at 900°C for 340 cycles in 85% H_2O-15% CO_2. Transient oxides (arrows) have developed on all three specimens.

Conclusions and Future Directions

The uncoated superalloys, René N5, IN 738, and GTD 111, as well platinum aluminide and NiCoCrAlY coatings have been exposed at 900°C in an 85% H_2O-15% CO_2 gas mixture. The amount of oxidation of all of these alloys and coatings was comparable to that observed for oxidation at 900°C in air. Testing must still be done in this gas mixture at temperatures of 700°C and 1,100°C, but at present it appears that the degradation of these alloys and coatings is similar to that in air. The oxygen partial pressure in this gas mixture is lower than in air and protective oxides consisting of α-Al_2O_3 or Cr_2O_3 are formed. The carbon or hydrogen activity established in this gas mixture does not affect the oxidation characteristics of these alloys. Future work will involve testing Ni-8Cr-6Al and Fe-10Cr. The oxidation of these alloys may be different in 85% H_2O-15% CO_2 compared to air since a substantial amount of oxygen is consumed by these alloys during the initial stages of oxidation. Such a condition may cause carbon and hydrogen activities to reach levels sufficient to influence the oxidation behavior and mechanical properties of these two alloys.

During the third year of this project, testing of selected alloys and coatings will be performed to determine the temperature dependence of the oxidation

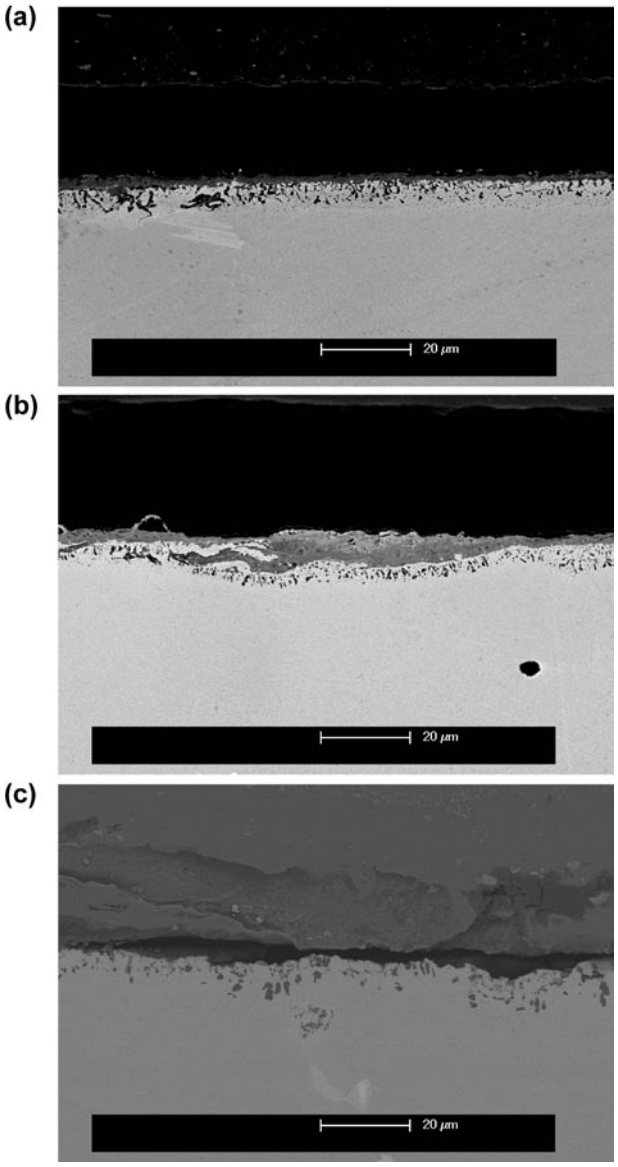

FIGURE 2. Scanning electron micrographs of GTD 111 metallographic cross-sections after exposure for 30 cycles (a) at 950°C in dry air, (b) in air with 85% H_2O, and (c) at 900°C for 340 cycles in 85% H_2O-15% CO_2. External scales of Cr_2O_3 can be seen on (a) and (b) and internal zones of alumina particles have developed on all three specimens.

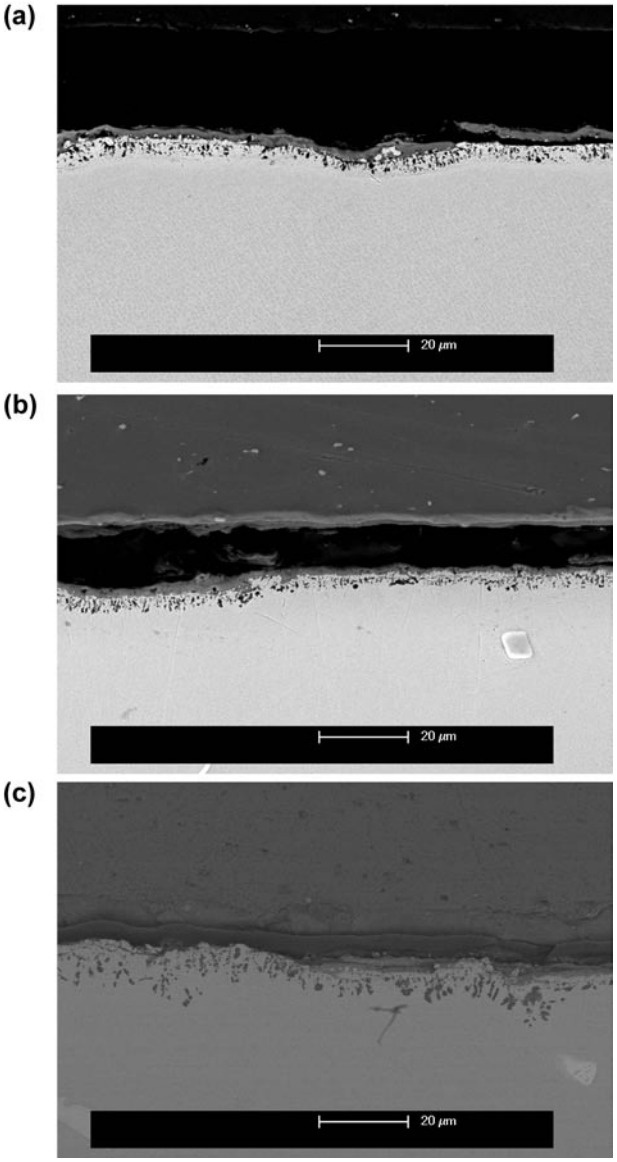

FIGURE 3. Scanning electron micrographs of IN 738 metallographic cross-sections after exposure for 30 cycles (a) at 950°C in dry air, (b) in air with 85% H_2O, and (c) at 900°C for 340 cycles in 85% H_2O-15% CO_2. External scales of Cr_2O_3 with alumina subscales have developed on all three specimens.

process in 85% H_2O-15% CO_2. The influence of contaminants such as SO_2 will also be studied. Finally, the effects of gas mixtures containing H_2O and CO_2 on the oxidation behavior of thermal barrier coatings will be examined.

FY 2009 Publications/Presentations

1. Review Presentation, "Materials for Oxy-Fuel Turbomachine Conditions," Clemson University, October 28, 2008.

VI. Acronyms and Abbreviations

°	Degree
°C	Degree(s) Celsius
°F	Degree(s) Fahrenheit
@	At
Δ	Change (delta)
ΔP	Change in pressure
Φ, ϕ	Equivalence ratio, ratio
η	Effectiveness
μm	Millimeter(s), micron(s)
~	Approximately
<	Less than
>	Greater than
2D, 2-D	Two-dimensional
3D, 3-D	Three-dimensional
7YSZ	7 wt% yttria-stabilized zirconia
AAAS	American Association for the Advancement of Science
A&WMA	Air and Waste Management Association
AC	Alternating current
AIAA	American Institute of Aeronautics and Astronautics
Al	Aluminum
AL	Alabama
ANSYS	An engineering simulation and modeling company
APS	Air plasma spray
Ar	Argon
ASME	American Society of Mechanical Engineers
ASU	Air separation unit
atm	Atmosphere(s)
Ave.	Avenue
BFW	Boiler feed water
Bi	Biot number
B.R.	Blowing ratio
Btu	British thermal unit
BYU	Brigham Young University
C	Carbon
C	Celsius
Ca	Calcium
CA	California
CCD	Charge-coupled device
CES	Clean Energy Systems
CFD	Computational fluid dynamics
CH_4	Methane
Cl	Chlorine
cm	Centimeter(s)
cm^2	Square centimeter(s)
cm^3	Cubic centimeter(s)
CMAS	Calcium-magnesium-alumina-silicate
CMOS	Complementary metal oxide semiconductor
Co	Cobalt
CO	Carbon monoxide
CO	Colorado
CO_2	Carbon dioxide
Cr	Chromium
CT	Connecticut
d, D	Diameter
D.C.	District of Columbia
DEC	Deposition erosion and corrosion
deg	Degree
DETE	Discrete error transport equation
DFT	Density functional theory
DLN	Dry low NOx
DNS	Direct numerical simulation
DOE	U.S. Department of Energy
E	East
EB-PVD	Electron beam physical vapor deposition
ed.	Editor
EDS	Energy dispersive spectroscopy
e.g.	*Exempli gratia*: for example
Eng.	Engineering
EPD	Electrophoretic deposition
ESEM	Environmental scanning electron microscope
F	Fahrenheit
F	Fluorine
FCL	Fundamental Combustion Laboratory
Fe	Iron
FE	Fossil Energy
Fe_2O_3	Ferric oxide
FFB	Fuel fired boiler
FIG.	Figure
FL	Florida
FOV	Field of view
FTT	Florida Turbine Technologies
FY	Fiscal year
g	Gram(s)

GA	Georgia
g/cm^2	Gram(s) per square centimeter
g/cm^2s	Gram(s) per square centimeter second
GE	General Electric
GFY	Government fiscal year
g/s	Gram(s) per second
GT	Gas turbine
GTI	Gas Technology Institute
h	Hour(s)
H	Hydrogen
H_2	Diatomic hydrogen
H_2O	Water
hp	Horsepower
HP	High pressure
hr	Hour(s)
Hz	Hertz
I	Current
IA	Iowa
ICCD	Intensified charge coupled device
ICEPAG	International Colloquium on Environmentally Preferred Advanced Power Generation
ICF	Inner City Fund
IGCC	Integrated gasification combined cycle
IGTI	International Gas Turbine Institute
IL	Illinois
in	Inch(es)
IN738	A nickel-based alloy
IN939	A nickel-based alloy
Inc.	Incorporated
IP	Intermediate pressure
IPT	Intermediate pressure turbine
IR	Infrared
ISU	Iowa State University
J	Joule(s)
J.	Journal
$J/cm^3/K$	Joule(s) per cubic centimeter per Kelvin
K	Conductivity
K	Potassium
K	Kelvin
kg	Kilogram(s)
kg/m^3	Kilogram(s) per cubic meter
kPa	Kilo Pascal(s)
KPP	Kimberlina Power Plant
kW	Kilowatt(s)
lb/h, lb/hr	Pound(s) per hour
lbm	Pound(s) mass
lbm/s	Pound(s) mass per second
LBNL	Lawrence Berkeley National Laboratory
LCF	Life cycle fatigue
LDV	Laser Doppler velocimetry
Le	Lewis number
LES	Large eddy simulation
LHV	Lower heating value
LLC	Limited liability company
LP	Low pressure
LSB	Low-swirl burner
LSI	Low-swirl injector
m	Meter(s)
MA	Massachusetts
MB/MS	Molecular beam/mass spectrometry
mg	Milligram(s)
Mg	Magnesium
MGM	Modified Global Mechanism
MI	Michigan
MIS	Matrix isolation spectroscopy
mK	Milli-Kelvin(s)
mm	Millimeter(s)
mm^2	Square millimeter(s)
MΩ	Mega-ohm
$MΩ/cm^2$	Mega-ohms per square centimeter
MPa	Megapascal(s)
m/s	Meter(s) per second
ms	Millisecond(s)
m/sec	Meter(s) per second
MTS	Multi-timescale
mW	Milliwatt(s)
MW	Megawatt(s)
MWe	Megawatt(s) electric
MW_{th}	Megawatt(s) thermal
N	Nitrogen
N_2	Diatomic nitrogen
Na	Sodium
NASA	National Aeronautics and Space Administration
NETL	National Energy Technology Laboratory
NGV	Nozzle guide vane
Ni	Nickel
NIST	National Institute for Standards and Technology
NJ	New Jersey
NO	Nitrogen oxide
No.	Number
NOx	Oxides of nitrogen

NY	New York
O	Oxygen
O_2	Diatomic oxygen
OEM	Original equipment manufacturer
OH	Ohio
OH*	Chemiluminescence
OH	Hydroxyl radical
OH-PLIF	Planar laser-induced fluorescence imaging of OH radicals
OR	Oregon
ORNL	Oak Ridge National Laboratory
OSU	Ohio State University
p.	Page
P	Phosphorus
P	Pressure
Pa	Pascal
PA	Pennsylvania
PACRIM	Pacific Rim Conference on Ceramic and Glass Technology
PCI	Precision Combustion, Inc.
Penn	Pennsylvania
PIMS	Photoionization mass spectrometry
PIV	Particle image velocimetry
PLIF	Planar laser induced fluorescence
P.O.	Post office
POGT	Partial oxidation gas turbine
POR	Partial oxidation reactor
pp.	Pages
ppm	Part(s) per million
ppmv	Part(s) per million by volume
ppmvd	Part(s) per million by volume dry
ppmw	Part(s) per million by weight
pps	Pulse repetition rate
PRB	Powder River Basin
psia	Pound(s) per square inch absolute
Pt	Platinum
PVC	Polyvinyl chloride
Q	Quarter
Q1	First quarter
Q2	Second quarter
Q3	Third quarter
Q4	Fourth quarter
RANS	Reynolds-averaged Navier-Stokes
RCL®	Rich catalytic lean-burn
RCM	Rapid compression machine
R_{CO}	Ratio of carbon monoxide
Rd.	Road
RD&D	Research, development, and demonstration
RDS	Research and Development Solutions
Ref.	Reference
REFPROP	Reference Fluid Thermodynamic and Transport Properties Database
s	Second(s)
S	Sulfur
SBIR	Small Business Innovation Research
SC	South Carolina
Sci.	Science
SCR	Selective catalytic reduction
SDT	Simultaneous differential scanning calorimeter and thermalgravimetric analyzer
SEM	Scanning electron microscopy
SGH	Syngas and hydrogen
SGT	Siemens Gas Turbine
Si	Silicon
SimVal	Simulation and validation
SMR	Steam-methane reformer
ST	Stokes
SV7	Low swirl injector configuration number 7
SV8	Low swirl injector configuration number 8
Syngas	Synthesis gas
T	Temperature
T1 . . . T14	Thermocouple 1 . . . thermocouple 14
TADF	Turbine Accelerated Deposition Facility
TBC	Thermal barrier coating
$Tbit/in^2$	Terabits per square inch
TGO	Thermally grown oxide
Ti	Titanium
TN	Tennessee
TSS	Thermal Spray Society
TuRFR	Turbine reacting flow rig
TX	Texas
U.	University
UC	University of Colorado
UCI	University of California, Irvine
UFD	User defined functions
U.S.	United States
USA	United States of America
UT	University of Texas at Austin
UT	Utah
UTSR	University Turbine Systems Research
VA	Virginia

Vol.	Volume
W	West
W	Watt(s)
W/m/K	Watt(s) per meter per Kelvin
w/o	Without
wt%	Weight percent
WV	West Virginia
X-45	A cobalt-based alloy
XRF	X-ray fluorescence
Y	Yttrium
Y_2O_3	Yttria
YSZ	Yttria-stabilized zirconia
ZEPP	Zero Emission Power Plant
Zr	Zirconium
ZrO_2	Zirconia

VII. Primary Contact Index

A

Alvin, Mary Anne 82
Anderson, Reed 15

B

Bennett, Ted 160
Bischoff, Ronald 55
Bogard, David 123
Bons, Jeffrey 113

C

Casleton, Kent 37
Cheng, Robert 33
Chyu, Minking 117

D

Daily, John 150
Downs, James 75

E

Etemad, Shahrokh 46, 104

F

Fadok, Joseph 18
Fletcher, Thomas 109

G

Ghoniem, Ahmed 136

H

Harvey, Allan 96
Haynes, Joel 30
Hebbar, Mohan 51
Holcomb, Gordon 93

J

Ju, Yiguang 100

L

Lieuwen, Tim 78

M

Mansour, Adel 42
McCrabb, Heather 71
McDonell, Vincent 146
Mehta, R.S. 68
Meier, Gerald 165

P

Padture, Nitin 157

R

Rabovitser, Joseph 21

S

Santavicca, Dom 143
Santoro, Robert 139
Seitzman, Jerry 133
Shih, Tom 61
Sung, Chih-Jen 64

T

Tafti, Danesh 127

VIII. Organization Index

A

Ames Laboratory 61

B

Brigham Young University. 109

C

Case Western Reserve University 64

CFD Research Corporation 68

Clean Energy Systems, Inc. 55

F

Faraday Technology, Inc. 71

Florida Turbine Technologies, Inc. 75

G

Gas Technology Institute 21

GE Energy 15

GE Global Research 30

Georgia Institute of Technology 78, 133

L

Lawrence Berkeley National Laboratory 33

M

Massachusetts Institute of Technology. 136

N

National Energy Technology Laboratory 37, 82, 93

National Institute of Standards and Technology. . . . 96

O

Ohio State University 113, 157

P

Parker Hannifin Corporation 42

Pennsylvania State University (The). 139, 143

Precision Combustion, Inc. 46, 104

Princeton University. 100

S

Siemens Energy, Inc. 18, 51

T

The Pennsylvania State University 139, 143

U

University of California, Irvine 146

University of California, Santa Barbara. 160

University of Colorado at Boulder 150

University of Pittsburgh 117, 165

University of Texas at Austin 123

V

Virginia Polytechnic Institute and
State University 127

IX. Contract Number Index

41431/UTSR 04-01-SR115 117
41431/UTSR 05-01-SR117 139
41431/UTSR 05-01-SR120 109
41431/UTSR 05-01-SR121 136
41431/UTSR 06-01-SR124 165
41431/UTSR 07-01-SR122 133
41431/UTSR 07-01-SR123 127
41431/UTSR 07-01-SR125 160
41431/UTSR 07-01-SR126 150
41431/UTSR 07-01-SR127 123
41776 30
41817 82
42643 15
42644 18
42645 55
42646 51
42647 46
42648 42
42649 21
42716 100
42717 64
42957 96
43069 78
84202 71
84668 75
85007 68
85015 104
220623-3 37
220682-2/a 93
678402 33
AL05205018 61
NT0005054 143
NT0005055 113
NT0006551 146
NT0006552 157

NATIONAL ENERGY TECHNOLOGY LABORATORY

1450 Queen Avenue SW
Albany, OR 97321-2198
541-967-5892

2175 University Avenue South
Suite 201
Fairbanks, AK 99709
907-452-2559

3610 Collins Ferry Road
P.O. Box 880
Morgantown, WV 26507-0880
304-285-4764

626 Cochrans Mill Road
P.O. Box 10940
Pittsburgh, PA 15236-0940
412-386-4687

Granite Tower, Suite 225
13131 Dairy Ashford
Sugar Land, TX 77478
281-494-2516

Richard A. Dennis
Technology Manager, Turbines
304-285-4515
richard.dennis@netl.doe.gov

Visit the NETL website at:
www.netl.doe.gov

Customer Service:
1-800-553-7681

U.S. DEPARTMENT OF ENERGY

DOE/NETL-2009/1378

November 2009